



Pilkington Library

Author/Filing Title MERMELSTEIN

Vol. No. Class Mark T

**Please note that fines are charged on ALL
overdue items.**

FOR REFERENCE ONLY

0402805569



**ASPECTS OF THE DESIGN OF A
CIRCULAR WARP KNITTING
MACHINE**

by

Sylvia P. Mermelstein


**A doctoral thesis submitted in partial
fulfillment of the requirements for the degree
of**

**PhD in Mechanical Engineering of
Loughborough University**

July 15, 2002

**Supervisors: Dr. Memiş Acar
Dr. Mike R. Jackson**

by Sylvia P. Mermelstein, 2002

 Loughborough University 2000
Date Aug 03
Class
Acc No. 040280556

Abstract

The warp knitting machine market has long been dominated by large-scale flat models, which have been steadily developed. Tubular fabrics are generally made in a special version of flat warp knitting machines containing two needle bars, one for each side of the tube, joined on the sides by yarns knitting alternatively on each bar. Warp knitting technology has failed to enter the circular knitting industry, dominated by weft knitting, due to its complexity in achieving warp knit structures in circular form. This thesis presents the design, synthesis, manufacture and test of an innovative method of producing tubular warp knitting fabrics, using a circular format rather than flat needle bars. This novel concept opens up many industrial applications from medical textiles to fruit packaging.

The new warp knitting machine concept uses an innovative circular disposition of the needles to perform the two required motions in one movement of the needles. The needle-cone concept was invented after a thorough research into warp and weft knitting principles and mechanisms. By using a slotted ('tricked') truncated cone instead of a cylinder, the needles slide simultaneously in radial and vertical directions to collect the yarns from eyelets in patterning rings and then make a stitch. The tricked cone concept deployed for the knitting/swinging mechanism and its interaction with the patterning rings' shogging movement is undoubtedly unique.

The interaction between the patterning and knitting mechanism of a warp knitting machine is paramount to maximise the machine production. The movements performed by needles and guide bars in a flat warp knitting machine are mainly rectilinear and therefore, the calculation of the amplitude of the shogging movements is simple. In a circular machine, on the other hand, geometric parameters such as the radius of the patterning rings and the distance between the patterning and the needles can improve or reduce the patterning capabilities of the machine. This research describes an approach

to modelling the yarn and needle paths in a circular machine using a conical needle bed in order to optimise its performance.

A prototype machine has been designed, built and successfully tested to prove the knitting mechanism and its interaction with the patterning mechanism, using an optimum cam profile design for the reciprocation of the needles at high speeds and desired knit structure patterns.

A method of synthesising the knitting cam profiles based on the use of Piecewise Polynomials together with an optimisation technique is presented as part of this research. Special cases and limitations are discussed and illustrated, making the procedure complete and systematic for any cam design requirements.

Various different knit structures using different patterning cams with enclosed cam followers have been successfully produced. The new machine also enables changing the diameter of the knitted tube by controlling the yarn feed rate, offering new fabric formation opportunities.

The patterning cams also require a mechanical linkage to transmit the motion from the patterning cam to the patterning rings, which is prone to vibration. In the second part of the research, electronically controlled patterning mechanisms replace the patterning cams and hence increase the patterning possibilities. This enables features such as changing fabric pattern during knitting without requiring machine stoppages and cam changes.

The new generation design replaces the mechanical cam and linkage with high-speed, AC brushless servomotors, enabling limitless, precision patterning possibilities. A method of selecting servomotors based on minimising the power required to perform the fastest motion required for a given application is reported. This method ensures cost minimising by selecting the smallest servomotor suitable for a given application. A second circular warp-knitting machine using servomotor drives selected using the method reported has been designed, built and successfully tested.

Table of Contents

ABSTRACT.....	I
TABLE OF CONTENTS	III
TABLE OF FIGURES	VI
ACKNOWLEDGEMENTS	X
CHAPTER 1. INTRODUCTION	1
1.1 BACKGROUND	1
1.2 DEFINITION OF THE PROBLEM.....	1
1.3 AIMS AND OBJECTIVES	3
1.4 STRUCTURE OF THE THESIS.....	4
CHAPTER 2. INTRODUCTION TO WARP KNITTING MECHANISMS.....	8
2.1 WARP KNITTING BASIC TERMINOLOGY AND DEFINITIONS.....	9
2.1.1 <i>Knitting Elements.....</i>	<i>9</i>
2.1.2 <i>Warp and Weft Knitting.....</i>	<i>11</i>
2.1.3 <i>Raschel Knitting.....</i>	<i>11</i>
2.1.4 <i>Tricot Machines.....</i>	<i>11</i>
2.2 WARP KNITTING CYCLES	12
2.3 KNITTING MECHANISMS.....	14
2.3.1 <i>Bearded Needle Machine Mechanisms.....</i>	<i>14</i>
2.3.2 <i>Compound Needle Machine Mechanisms.....</i>	<i>18</i>
2.3.3 <i>Raschel (Latch Needle) Machine mechanisms.....</i>	<i>21</i>
2.4 WARP LET-OFF MECHANISMS.....	21
2.4.1 <i>Tension controlled let-off mechanisms.....</i>	<i>22</i>
2.4.2 <i>Constant Yarn Speed Let-Off.....</i>	<i>27</i>
2.5 TAKE-UP MECHANISMS.....	32
CHAPTER 3. LITERATURE SURVEY AND PATENT SEARCH.....	35
3.1 LITERATURE SURVEY.....	35
3.1.1 <i>Needle Fatigue.....</i>	<i>35</i>
3.1.2 <i>New Developments in Warp Knitted Fabric Structures</i>	<i>36</i>
3.1.3 <i>Warp Let-off Systems and Tension Control</i>	<i>38</i>
3.1.4 <i>Calculations of the yarn run-in length per knitted course.....</i>	<i>41</i>
3.1.5 <i>Mathematical Models of Loop Formation.....</i>	<i>43</i>
3.1.6 <i>Other Developments in Knitting Machine Accessories</i>	<i>46</i>
3.2 PATENT SEARCH.....	48
3.2.1 <i>Circular Machines.....</i>	<i>49</i>
3.2.2 <i>Flat Machines.....</i>	<i>51</i>
3.2.3 <i>Fabrics.....</i>	<i>53</i>

CHAPTER 4. MACHINE SPECIFICATION AND CONCEPT EVALUATION	55
4.1 INTRODUCTION	55
4.2 CIRCULAR WARP KNITTING MACHINE DESIGN SPECIFICATION.....	55
4.2.1 PDS Database.....	55
4.2.2 PDS Design Decisions.....	57
4.3 CONCEPT EVALUATION	59
4.3.1 Main Mechanisms: Knitting and Patterning.....	60
4.3.2 Secondary Mechanisms	82
4.4 CONCLUSIONS.....	89
CHAPTER 5. KNITTING MECHANISM.....	90
5.1 INTRODUCTION	90
5.2 CAM AND FOLLOWER DESIGN SOLUTION	90
5.3 KINETIC ANALYSIS	99
5.3.1 Needles and Strengthening Inserts.....	99
5.3.2 Reciprocating Shafts and Needle Support Plate.....	102
5.3.3 Cam Followers.....	104
5.3.4 Knitting Cams.....	106
5.4 EFFECT OF ELASTICITY	113
5.5 CAM AND PROFILE DESIGN.....	115
5.5.1 Cam Profiles.....	116
5.5.2 Pressure Angle.....	125
5.5.3 Static and Dynamic Balance.....	126
5.6 EXPERIMENTAL MEASUREMENT OF CAM FOLLOWER DISPLACEMENT AND MACHINE VIBRATION.....	131
5.6.1 Experiment Description.....	132
5.6.2 Results and Analysis.....	137
5.6.3 Experimental Measurements Conclusions.....	153
5.7 CONCLUSIONS.....	154
CHAPTER 6. OPTIMISED CAM MOTION BASED ON PIECEWISE POLYNOMIALS.....	156
6.1 INTRODUCTION	156
6.2 PIECEWISE POLYNOMIALS	157
6.2.1 Boundary Conditions.....	160
6.2.2 Continuity Conditions.....	162
6.2.3 Polynomial Order.....	164
6.2.4 Solving for the Polynomial Coefficients.....	166
6.2.5 Dwells.....	171
6.3 OPTIMISATION	174
6.3.1 Procedure	174
6.3.2 Proof of Minimum.....	185
6.3.3 Case Study 4. Incorrect Boundary Conditions Specified.....	190
6.4 OPTIMISATION METHOD APPLIED TO THE WARP KNITTING CAM.....	193
6.5 CONCLUSIONS.....	200
CHAPTER 7. PATTERNING MECHANISM.....	202
7.1 INTRODUCTION: PATTERNING MECHANISM OVERVIEW.....	202
7.2 SYSTEM REQUIREMENTS	204

7.3	MECHANICAL SOLUTION	206
7.4	SERVO-CONTROLLED SOLUTION.....	217
7.5	MOTOR SELECTION.....	223
7.5.1	<i>Selection Optimisation.....</i>	223
7.5.2	<i>Measurement of Motor and Drive Response</i>	228
7.6	CONCLUSION	232
CHAPTER 8. MODELLING THE PATTERN CREATION PROCESS		234
8.1	INTRODUCTION	234
8.2	DESCRIPTION OF THE MATHEMATICAL MODEL	236
8.3	UNDERLAP AND OVERLAP IN OPPOSITE DIRECTIONS.....	240
8.3.1	<i>Underlap.....</i>	242
8.3.2	<i>Overlap.....</i>	250
8.4	UNDERLAP AND OVERLAP IN THE SAME DIRECTION.....	250
8.4.1	<i>Overlap.....</i>	252
8.4.2	<i>Underlap.....</i>	253
8.5	SHOG ANGLE CALCULATION ALGORITHM.....	253
8.5.1	<i>Underlap and Overlap in the Same Direction.....</i>	254
8.5.2	<i>Underlap and Overlap in Opposite Directions</i>	256
8.6	CIRCULAR WARP KNITTING CASE.....	258
8.7	CONCLUSIONS.....	261
CHAPTER 9. CONCLUSIONS AND SUGGESTIONS FOR FUTURE WORK		262
9.1	ACHIEVEMENTS	262
9.2	SUGGESTIONS FOR FUTURE WORK	265
9.2.1	<i>Fabric Development</i>	265
9.2.2	<i>Electronic Control of Patterning.....</i>	265
9.2.3	<i>Cam Design</i>	266
9.2.4	<i>Warp Knitting Machine Design.....</i>	266
REFERENCES		269
APPENDIX A. WARP KNITTING TERMINOLOGY.....		274
APPENDIX B. PATENTS SUBCLASS INDEX.....		283
APPENDIX C. PDS DATABASE RECORDS.....		290
APPENDIX D. PROGRAM FOR PIECEWISE POLYNOMIALS CASE STUDY NO 2		310
APPENDIX E. PROGRAM FOR CAM OPTIMISATION CASE STUDY NO 3.		319
APPENDIX F. PROGRAM FOR WARP KNITTING CAM OPTIMISATION CASE STUDY.		338
APPENDIX G. PROGRAM FOR GEOMETRIC MODEL OF THE SHOG MOVEMENTS.....		351

Table of Figures

FIGURE 1-1. THESIS STRUCTURE *	4
FIGURE 2-2. BEARDED NEEDLE KNITTING CYCLE. AFTER REICHMAN (1964).	13
FIGURE 2-3. NEEDLE BAR MOTION; CAM DRIVE. AFTER PALING (1965) ⁷ ,	15
FIGURE 2-4. NEEDLE BAR MECHANISM; ECCENTRIC DRIVE. AFTER RAZ (1987).	16
FIGURE 2-5. SINKER BAR MOTION; CAM DRIVE. AFTER PALING (1965).	17
FIGURE 2-6. SINKER BAR MECHANISM; ECCENTRIC DRIVE. AFTER RAZ (1987)	18
FIGURE 2-7. COMPOUND NEEDLE BAR MECHANISM. AFTER GROSBERG (1968).	19
FIGURE 2-8. SINKER BAR MOTION. AFTER PALING (1965) ⁷	20
FIGURE 2-9. BRAKE DRUM LET-OFF. AFTER REISFIELD (1966).	22
FIGURE 2-10. EXPANDING BRAKE LET-OFF. AFTER REISFIELD (1966).	24
FIGURE 2-11. ELECTRICAL LET-OFF. AFTER FROM REISFIELD(1966).	25
FIGURE 2-12. HYDRAULIC LET-OFF. AFTER REISFIELD (1966).	26
FIGURE 2-13. FNF LET-OFF. AFTER REISFIELD (1996) ⁸	27
FIGURE 2-14. DISC UNIT. AFTER REISFIELD (1996) ⁸	28
FIGURE 2-15. ELECTROMAGNETIC CLUTCH. AFTER REISFIELD (1996) ⁸	29
FIGURE 2-16. READING LET-OFF.	30
FIGURE 2-17. MAYER LET-OFF. AFTER SPENCER (1989).	31
FIGURE 2-18. CONTINUOUS TAKE-UP SCHEMATIC. AFTER PALING (1965).	32
FIGURE 2-19. INTERMITTENT TAKE-UP. AFTER PALING (1965).	33
FIGURE 2-20. TAKE-UP WITH PIV.	34
FIGURE 3-1. FABRIC MOVING CIRCULAR WARP KNITTING MACHINE.	50
FIGURE 3-2. CIRCULAR MACHINE WITH TRICKED TORUS SINKER AND GUIDE RINGS.	51
FIGURE 4-1 PDS DATA RECORD FORMAT	56
FIGURE 4-2. NEEDLE MOTION WITH DWELLS	61
FIGURE 4-3. ECCENTRIC SCHEMATIC	62
FIGURE 4-4. ECCENTRIC MOTION GEOMETRY	63
FIGURE 4-6. SINGLE ECCENTRIC DISC MOTION EXAMPLE.	68
FIGURE 4-7. DOUBLE ECCENTRIC MECHANISM SCHEMATIC.	69
FIGURE 4-8. SIMULATED DOUBLE ECCENTRIC MOTION, EXAMPLE 1	70
FIGURE 4-9. SIMULATED DOUBLE ECCENTRIC MOTION, EXAMPLE 2	71
FIGURE 4-10. CYLINDRICAL CAM WITH TRANSLATING ROLLER FOLLOWER. (AFTER ERDMAN, 1991).	72

FIGURE 4-11. SPIDER THREADER.....	75
FIGURE 4-12. PNEUMATIC THREAD DISPLACEMENT.....	76
FIGURE 4-13. CAMERA LENS SHUTTER.....	76
FIGURE 4-14. TRICKED CONE CONCEPT.....	77
FIGURE 4-15. PIVOTED NEEDLES CONCEPT.....	78
FIGURE 4-16. THREE RINGS DRIVEN BY SERVOMOTORS.....	80
FIGURE 4-18. VIEW OF THE LET-OFF CHANGE GEARS.....	86
FIGURE 4-19. LET-OFF YARN SUPPLY PLAN VIEW.....	86
FIGURE 5-1. SCHEMATIC ASSEMBLY OF KNITTING MECHANISM COMPONENTS.....	91
FIGURE 5-2. CONICAL NEEDLE BED WITH NEEDLES (DOWN) AND YARNS.....	92
FIGURE 5-3. NEEDLES AT THEIR HIGHEST POSITION.....	93
FIGURE 5-4. PICTURE OF CASTING FOR KNITTING MECHANISM.....	95
FIGURE 5-5. DETAIL OF ROLLER FOLLOWER IN CAM TRACK.....	96
FIGURE 5-6. FORCES ON NEEDLE AND STRENGTHENING INSERTS.....	99
FIGURE 5-7. FORCES ON RECIPROCATING SHAFTS AND THE NEEDLE SUPPORT PLATE RING.....	102
FIGURE 5-8. FORCES ON THE CAM FOLLOWER.....	104
FIGURE 5-9. FORCES ON ONE OF THE KNITTING CAM PAIR.....	106
FIGURE 5-10. REACTIONS FOR A SAMPLE CYCLOIDAL PROFILE.....	112
FIGURE 5-11. ELASTIC MODEL OF THE SYSTEM.....	113
FIGURE 5-12. EFFECT OF BODIES' ELASTICITY.....	115
FIGURE 5-13. DISPLACEMENT, VELOCITY, ACCELERATION AND JERK RELATIONS FOR PARABOLIC MOTION.....	117
FIGURE 5-14. DISPLACEMENT, VELOCITY, ACCELERATION AND JERK RELATIONS FOR SIMPLE HARMONIC MOTION.....	118
FIGURE 5-15. DISPLACEMENT, VELOCITY, ACCELERATION AND JERK RELATIONS FOR CYCLOIDAL MOTION.....	120
FIGURE 5-16. MOTION CHARACTERISTICS OF POLYNOMIAL PROFILE.....	124
FIGURE 5-17. STATIC UNBALANCE.....	127
FIGURE 5-18. SIMPLIFIED VIBRATION AMPLITUDE.....	129
FIGURE 5-19. DYNAMIC UNBALANCE.....	131
FIGURE 5-20. KNITTING MECHANISM.....	132
FIGURE 5-21. CYCLOIDAL CAM.....	134
FIGURE 5-22. POLYNOMIAL CAM.....	134
FIGURE 5-23. MACHINE SIGNATURE WITH CYCLOIDAL CAM RUNNING AT 5Hz.....	137
FIGURE 5-24. CYCLOIDAL CAM RESPONSE AT 18.06Hz.....	139

FIGURE 5-25. DETAIL OF DISPLACEMENT SIGNAL FOR UNDERLAP DWELL AT 18.06HZ	140
FIGURE 5-26. DETAIL OF DISPLACEMENT SIGNAL FOR CYCLOIDAL UNDERLAP DWELL AT 18.06HZ	140
FIGURE 5-27. POLYNOMIAL CAM RESPONSE AT 12.12HZ.....	141
FIGURE 5-28. DETAIL OF DISPLACEMENT SIGNAL FOR POLYNOMIAL OVERLAP DWELL AT 12.12HZ	141
FIGURE 5-29. POLYNOMIAL CAM RESPONSE AT 24.02HZ.....	142
FIGURE 5-30. DETAIL OF DISPLACEMENT SIGNAL FOR POLYNOMIAL OVERLAP DWELL AT 24.02HZ	142
FIGURE 5-31. THEORETICAL VS. MEASURED DISPLACEMENT COMPARISON	144
FIGURE 5-32, POLYNOMIAL CAM RESPONSE AT 18.93HZ.....	145
FIGURE 5-33. THEORETICAL ACCELERATION SUPERIMPOSED TO THE RISE PORTION OF THE CYCLOIDAL CAM'S RESPONSE AT 18.06 HZ.....	146
FIGURE 5-34. THEORETICAL ACCELERATION SUPERIMPOSED TO THE RISE PORTION OF THE POLYNOMIAL CAM'S RESPONSE AT 18.93 HZ	148
FIGURE 5-35. POLYNOMIAL CAM RESPONSE AT 26.01HZ.....	150
FIGURE 5-36. POLYNOMIAL CAM RESPONSE WITHOUT COUNTERBALANCING WEIGHTS	151
FIGURE 5-37. POLYNOMIAL CAM RESPONSE WITH COUNTERBALANCING WEIGHTS ..	151
FIGURE 6-1. DISPLACEMENT DERIVATIVES OF CAM PROFILE USING PIECEWISE POLYNOMIALS.	170
FIGURE 6-2. DISPLACEMENT DERIVATIVES OF PROFILE WITH INCORRECT DWELL BOUNDARY CONDITIONS	173
FIGURE 6-3. DISPLACEMENT DERIVATIVES FOR OPTIMISED CASE STUDY	184
FIGURE 6-4. DISPLACEMENT DERIVATIVES USING REPLACEMENT VALUES FOR DESIGN VARIABLES	186
FIGURE 6-5. PROOF OF MINIMUM. JERK IN TERMS OF EACH OF THE DESIGN VARIABLES.	187
FIGURE 6-6. DISPLACEMENT DERIVATIVES FOR MODIFIED BOUNDARY CONDITIONS	189
FIGURE 6-7. CASE STUDY 4. DISPLACEMENT DERIVATIVES	192
FIGURE 6-8. CASE STUDY 4. JERK IN TERMS OF THE DESIGN VARIABLES.....	193
FIGURE 6-9. WARP KNITTING DISPLACEMENT DERIVATIVES WITHOUT OPTIMISING..	198
FIGURE 6-10. WARP KNITTING DISPLACEMENT DERIVATIVES AFTER OPTIMISING....	199
FIGURE 7-1. A PATTERNING RING AND NEEDLES ON A CIRCULAR WARP KNITTING MACHINE	205
FIGURE 7-2. MECHANICAL PATTERNING MECHANISM.	207
FIGURE 7-3. CAMS FOR 8-COURSE PATTERNS.....	208
FIGURE 7-4. CAMS FOR 6-COURSE PATTERNS.....	208

FIGURE 7-5. MECHANICAL DESIGN PATTERNING MECHANISM	210
FIGURE 7-6. LEVER PIVOTS SLIDE IN SLOTS TO PROVIDE AMPLIFICATION OF THE CAM MOVEMENTS.	211
FIGURE 7-7. POSITION OF YARN AFTER A COURSE.....	212
FIGURE 7-8. EXAMPLE OF STROKE CALCULATION USING GRAPHICAL METHOD.....	213
FIGURE 7-9. 6-COURSE HEXAGON FABRIC STRUCTURE.	215
FIGURE 7-10. EXF FILE EXAMPLE FOR A 6-COURSE PATTERN	215
FIGURE 7-11. CAM FOLLOWER RUNNING ON A PATTERNING CAM WITH NO EXCESSIVE VIBRATION OR WEAR.....	216
FIGURE 7-12. VIEW OF PATTERNING MECHANISM WITH TWO RINGS THREADED.....	219
FIGURE 7-13. VIEW OF THE YARNS THREADED IN THE TOP PATTERNING RING.....	219
FIGURE 7-14. YARN PATHS FROM LET-OFF UNITS TO THREE RINGS	220
FIGURE 7-15. EXPLODED PATTERNING RINGS ASSEMBLY.....	221
FIGURE 7-16. SERVOMOTOR CONTROLLED PATTERNING MECHANISM.....	221
FIGURE 7-17. PATTERNING MECHANISM CONTROL AND DRIVES	222
FIGURE 7-18. MOTOR REQUIREMENTS	224
FIGURE 7-19. TIME REQUIRED TO REACH THE MAXIMUM ANGULAR VELOCITY.....	225
FIGURE 7-20. TORQUE REQUIRED TO REACH THE MAXIMUM ANGULAR VELOCITY.....	226
FIGURE 7-21. POWER VS. MAXIMUM ANGULAR VELOCITY.....	227
FIGURE 7-22. MINIMUM POWER REQUIREMENT.	228
FIGURE 7-23. BEST RESPONSE FOR AN 80° MOTION - WITHOUT LOAD.....	231
FIGURE 8-1. EXPLODED ASSEMBLY OF TRICKED CONE AND PATTERNING RINGS.	235
FIGURE 8-2. ASSEMBLED PATTERNING RINGS AND YARNS	236
FIGURE 8-3. NEEDLE RISE AFTER A TWO-NEEDLE UNDERLAP.....	237
FIGURE 8-4. CONE SECTION USING PLANE THROUGH TARGET NEEDLE.....	239
FIGURE 8-5. OVERLAP AND UNDERLAP	240
FIGURE 8-6. UNDERLAPPING YARN.....	241
FIGURE 8-7. ILLUSTRATION OF ACCEPTABLE REGION FOR INTERSECTION POINT.....	243
FIGURE 8-8. YARN VECTOR CONSTRUCTION.....	244
FIGURE 8-9. THREAD VECTOR PROJECTIONS.....	245
FIGURE 8-10. NEEDLE PLANE FOR GEOMETRICAL ANALYSIS.....	247
FIGURE 8-11. ACCEPTABLE AREA OVERLAP INTERSECTION.....	252
FIGURE 8-12. FLOWCHART FOR OVERLAP AND UNDERLAP IN THE SAME DIRECTION .	254
FIGURE 8-13. FLOWCHART FOR OVERLAP AND UNDERLAP IN OPPOSITE DIRECTIONS	256
FIGURE 9-1. MECHANICAL PATTERNING CIRCULAR WARP KNITTING M/C.....	267
FIGURE 9-2. ELECTRONICALLY CONTROLLED CIRCULAR WARP KNITTING M/C	268

Acknowledgements

This thesis would not have been written without the patience and support of all my family, especially Jim, who served as proof-reader, cook and motivator with admirable selflessness in the countless late nights and weekends writing up. Thank you.

My gratitude goes also to my supervisors, Memiş Acar and Mike Jackson, for, without Memiş' guidance and motivation in the (very long) final period of thesis, I might not have finished

Finally, I am also indebted to Tritex International Ltd., especially Kevin Roberts, Peter Denman and the assembly and manufacturing technicians, who made the project and the machines possible.

Chapter 1. Introduction

1.1 Background

In the textile world, warp knitting is deemed to be a small but growing industry.¹ It is also the youngest of the three main fabric forming processes; while the invention of weaving cannot be traced in history, mechanical weft knitting was invented by Reverend William Lee in 1589. It took a further 200 years for Crane of Nottingham to invent warp knitting by supplying warp yarns to each needle in Lee's knitting frame.

In warp knitting, each needle is supplied with one or more yarns so all the loops in one course are produced simultaneously, this basic warp knitting principle is what makes it faster than weaving or weft-knitting.² It also has a wider scope for variation of fabric structure, because the guide bars that feed the needles with yarns, are independently shogged sideways.

Amongst all textile materials produced by weaving and knitting, it is within the industrial or technical fabrics sector where the fastest growth has occurred in recent years.³

However, tubular fabrics are still mainly produced by circular weft knitting machines since traditional weft knitting has dominated the market.

1.2 Definition of the Problem

Many tubular fabrics, especially those in the technical textiles sector, could benefit from the advantages of warp knitting in both structural flexibility and faster production rates.

The warp knitting industry is almost synonymous with large-scale flat bed machines, as recent investment in research and development has focused on modernising and increasing their efficiency.

For that reason, tubular fabrics are still manufactured with flat bed double-needle-bar machines; where each needle bed produces half of the ground fabric. To produce the ground fabrics at least 4 patterning bars are used and between these bars, further bars are used to knit the necessary connections required to form the tube.

In addition, there are no large manufacturers of either circular or flat bed warp knitting machines currently in Great Britain, although the market for these machines at the beginning of this project was calculated at over ECU 300'000,000⁴, and growing. This supports the argument that there is commercial potential for the manufacturing of circular warp knitting machines.

In order to achieve a design solution with the efficiency and versatility of the flat bed machines used in the production of tubular fabrics, research into the design of machines with circular needles beds is required.

An immediately noticeable benefit for implementing a circular needle bed, is that it will greatly reduce the patterning capabilities required to produce tubular fabrics, as it does not require patterning bars for connecting the two sides of the fabric.

Also, it would improve the quality of the knitted fabric, as it will no longer have inconsistent wales (columns of stitches) on the sides; (a critical factor for medical applications such as artificial arteries, where the consistency of the knitted structure is paramount in its performance).

After some consideration of the circular warp knitting concept, it is clear that it could use existing designs and ideas from both the circular weft knitting industry as well as the flat bed warp knitting industry. But it will be different in the way it creates two of the most critical motions of a warp knitting machine; firstly, in the radial 'swing' of the yarn from the front to the back of the needles; and secondly, in the tangential 'shog' of the yarns around the needles. These two are especially affected by the circular positioning of the needles.

1.3 Aims and Objectives

The research project's main aim is defined as:

To prove how modern approaches; to design methodology, mechanism analysis and mechanism synthesis; can lead to an innovative design solution for a new type of warp knitting machine with commercial potential.

Further objectives, identified as being conducive to achieving the main aim of the research, were to:

- i. Investigate the current trends in warp knitting mechanism design and research.
- ii. Identify potential applications for a circular warp knitting machine and the requirements that their fabric structures impart on the machine design.
- iii. Generate, compare and select original design concepts for each of functional subsystem of the machine.
- iv. Identify the critical functions or mechanisms of the machine and the research required to provide an optimum design solution for them.
- v. Design and implement innovative solutions addressing the critical function problems in the circular warp knitting machine process.
- vi. Carry out experimental tests or additional research related to the critical areas identified in (iv), to demonstrate that the solutions reached are the most advantageous.

1.4 Structure of the Thesis

The structure of the thesis is illustrated in Figure 1-1.

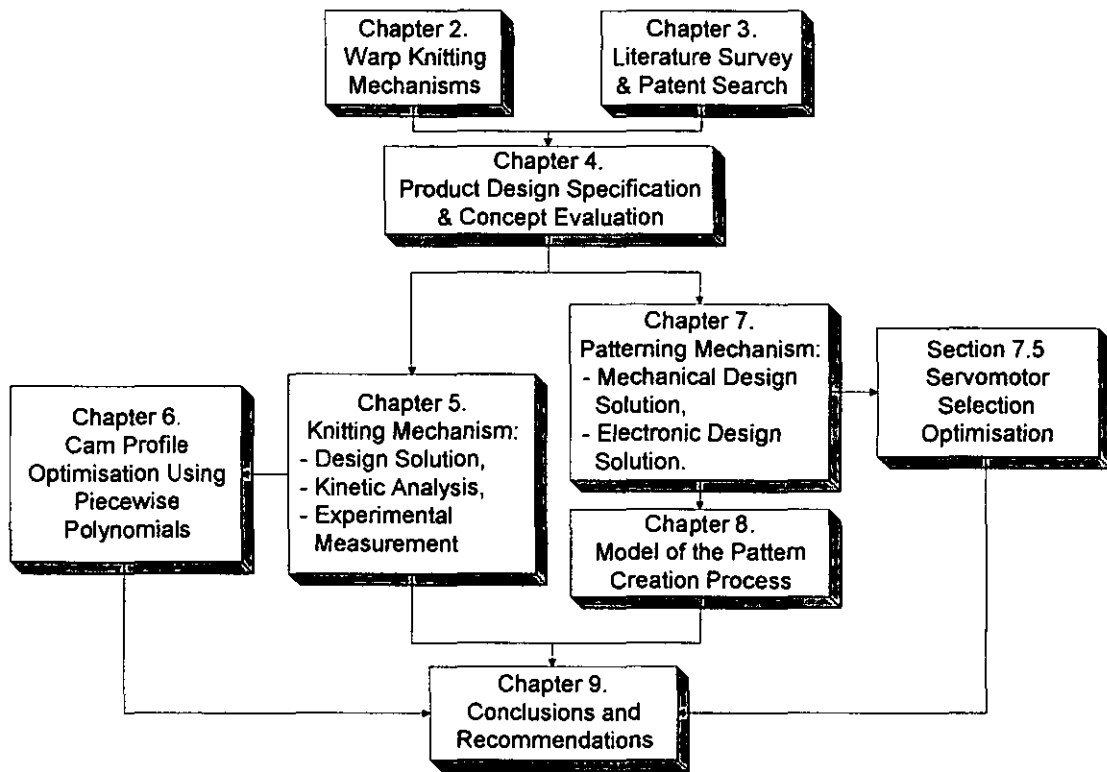


Figure 1-1. Thesis Structure

The structure unfolds following this introductory Chapter 1 as follows.

Chapters 2 and 3 establish the background knowledge required to undertake the research project; Chapter 2 summarises the range and development of mechanisms currently used in the warp knitting industry; while Chapter 3 reviews the current research trends and patents in subjects related to warp knitting machine design in two sections; 3.1 Literature Survey, where the findings are reviewed from a thorough search of the leading engineering and textile journals about circular warp knitting machine design; while 3.2 Patents discusses the results of a patent survey for the subject area.

In Chapter 4, the main design concepts are characterised and the direction of the research is defined as follows:

Section 4.1 explains the methodology used to conceive the initial Product Design Specification (PDS), also including the results of the PDS for a framework of design decisions, on which to base the ultimate design for the machine mechanisms. It is clear from the research in Chapter 1 and 2 and from the analysis the PDS database, that the two critical mechanisms in a circular warp knitting machine are the knitting and patterning mechanisms. Consequently the direction for the rest of this research is defined.

Section 4.2 Concept Evaluation is sub-divided into:

- i. The Main Mechanisms sub-section where design concepts are analysed and evaluated in order to choose the best solutions, (as discussed in more detail in Chapters 5 to 8).
- ii. The Secondary Mechanisms sub-section which summarises the requirements of the let-off and takedown systems with descriptions of the solutions implemented.

From this chapter onwards (see Figure 1-1), the research follows two subject areas. One area encompasses those research subjects affecting the design of the knitting mechanism (Chapters 5 and 6), while the other area encompasses those subjects affecting the design of the patterning mechanism for a circular warp knitting machine (Chapters 7 and 8).

Chapter 5 is structured as follows: Section 5.1 describes the knitting mechanism design solution proposed and its main innovative features. Then Sections 5.2, 5.3 and 5.4 analyse the kinetic interactions between the different parts of the mechanism and the factors affecting the interactions such as cam profile design and parts elasticity. Finally Section 5.5 compares the theoretical analysis, from the previous sections of this chapter, with experimental measurements of cam follower displacement and vibration, as tested on the manufactured machine.

In chapter 6, an optimisation method based on piecewise polynomials is proposed. This was necessary having ascertained that the cam profile design is a critical factor in the performance of the machine, and that existing cam motion synthesis techniques are not sufficiently developed to optimise a cam profile for a specific application. Several case studies are discussed in the chapter, including the circular warp knitting machine design, to demonstrate its effectiveness.

Chapter 6 in Figure 1-1 is shown to the left of Chapter 5. This is to clearly indicate that, although it stemmed from the design of the knitting mechanism, it is applicable to the design of a cam regardless of the application. Its contents on cam profile optimisation, in conjunction with the servo motor optimisation of Chapter 7 section 7.5, are both contributions to the thesis for more general mechanical engineering research fields, these are therefore not confined to the subject of warp knitting research.

Chapter 7 is the first of the two chapters dedicated to the patterning mechanism design in detail. The first two sections of the chapter introduce the patterning mechanism and its design requirements; the following two sections describe the two design solutions proposed and implemented; one mechanical the other electronically controlled. In these sections both their main innovative features and comparative advantages are described and discussed. Finally, Section 7.5 proposes a new method for the selection of servomotors; its findings can be applied to servomotor selection for any application. For that reason, as explained for Chapter 6, it is shown to the side of Chapter 7 in Figure 1-1.

Chapter 8 describes an approach to modelling the yarn and needle paths in a circular warp knitting machine to optimise its performance. This is significant because in a circular warp knitting machine certain geometric parameters can either enhance or hinder the patterning capabilities of the machine. For instance, (i) the taper angle of the needle bed, (ii) the diameter of the patterning rings and (iii) the distance between the patterning rings and the needles.

The importance of this model is that it enables the designer to select the dimensions and geometric constraints of the patterning mechanism according to the fabric patterns required.

This reflects the principles guiding the design methodology throughout this thesis whose premise is to drive the machine design by end-product fabric requirements.

Chapter 9 draws conclusions from the research and gives recommendations for future work.

Chapter 2. Introduction to Warp Knitting Mechanisms

Due to the complexity and the scale of warp knitting machines in general, the first task undertaken by the author was to establish a basic understanding of warp knitting; its terminology and the mechanisms currently in use. Most of this chapter is devoted to that task; it summarises in its findings the range and development of mechanisms currently used in the warp knitting industry. More specific current developments and research areas are discussed in Chapter 3.

For study purposes, it is better to divide a warp knitting machine into sections defined by the function they perform, although these sections are not independent from each other;

1. Frame or carcass - support.
2. Control and drive system - power for drive and mechanisms
3. Yarn supply - yarn package, tensioning devices carriers, guides and let-off mechanisms.
4. Knitting system - knitting elements, main knitting mechanisms.
5. Patterning -guides and pattern mechanisms for swing and shog motions.
6. Fabric takedown - fabric tensioning and wind up mechanism.
7. Quality control system -stop motions, fault and needle detectors, automatic oilers, dirt removers.

The chapter covers mainly items 3 through 6 above, as these are thought to be the most relevant areas in the subject of warp knitting machine design. An initial subsection is intended to familiarise the reader with the basic terminology used in warp knitting The ones not covered, namely the frame,

drive and quality control system will be largely dependant on the mechanisms used.

A summary of the main terminology used in this thesis is presented below. A more detailed discussion on warp knitting basic terminology and definitions is presented in Appendix A.

2.1 Warp Knitting Basic Terminology and Definitions.

2.1.1 Knitting Elements.

Needles

A knitting needle must have some method of closing its hook to retain the new loop and exclude the old loop.

The most common types of needles are; bearded needles, latch needles and compound needles. See Figures 1, 2 and 3 in Appendix A. In all cases the fabric draw off will be from the side remote from their hooks and a variation of the depth of descent will alter the yarn tension.

Latch needles are self acting while bearded needles need a force on their hook and compound ones need separate tongue and stem motions in order to produce a new loop.

Other needles include specially designed ones to facilitate rib loop transfer by selective lifting and double sided purl needles, that can knit from opposing beds by sliding through the old loops and knitting with each side of the needle alternatively.

Sinkers

A sinker can perform up to three different functions;

- i. Loop formation; only on bearded needle weft knitting.
- ii. Holding down; which enables to produce tighter structures, the knitting to be commenced on empty needles and minimum draw-off tension.

- iii. Knocking over; when the sinker holds the fabric while the new loop is being formed. On latch needle machines the verge performs this function.

Patterning Guides

Guides are the knitting elements that position the threads on and around the needles.

Trick Plate

A grooved plate supporting the needles in Raschel machines.

Overlap

The motion of the guide bars across the open side of the needle hook during the forming of a new loop; it is normally limited to one needle space.

Underlap

The patterning motion of the guides across the closed side of the needle hook that takes place when the needles are at their lowest position. The number of needle spaces of the underlap is only restricted by the patterning mechanism characteristics.

Open Loop

Knitted loops whose legs do not cross; the overlap and the following underlap must be performed in the same direction in order to produce an open loop.

Closed Loop

Knitted loops whose legs do cross; the overlap and the next underlap must be performed in opposite directions in order to produce a closed loop.

Fabric Take-up or Takedown

The mechanism charged with maintaining a constant fabric tension at the needles while knitting. The take-up rate, the speed at which the mechanism rotates, is calculated from the courses per inch (cpi) of fabric.

Let-off

A mechanism to feed yarn to the knitting elements at the required rate.

Run-in

The length of yarn used in a RACK (480 courses) of a given fabric.

2.1.2 Warp and Weft Knitting

The main difference between warp and weft knitting is that in warp knitting every needle being used is supplied with at least one yarn end. Ends supplied by the same warp sheet normally have identical lapping movements. These movements are timed and configured by the patterning mechanism in the form of overlaps and underlaps.

2.1.3 Raschel Knitting

Raschel warp knitting machines can be defined as those with latch needles.

2.1.4 Tricot Machines

Tricot fabrics are generally the lighter of the apparel and furnishing fields. They comprise those made using bearded or compound needles.

2.2 Warp Knitting Cycles

The latch needle knitting cycle is shown schematically in Figure 2-1. At stage 1, the needle has the old loop round its stem and the yarns swing to the front of the needles, a thread is laid under the hook of the needle at stage 2. This is the overlap shog motion. The yarns then swing to the back of the needle (stage 3) and then start to move downwards, the old loop is caught under the latch and closes the hook (stage 4). It continues down until the old loop reaches the top of the needle and it is cast-off and pulled by fabric tension. At this point, the underlap shog is performed (stage 5), moving the yarns behind the needles to the position where they will make a new stitch. As the needle rises again to the starting position, the thread in the hook opens the latch and becomes the next old loop.

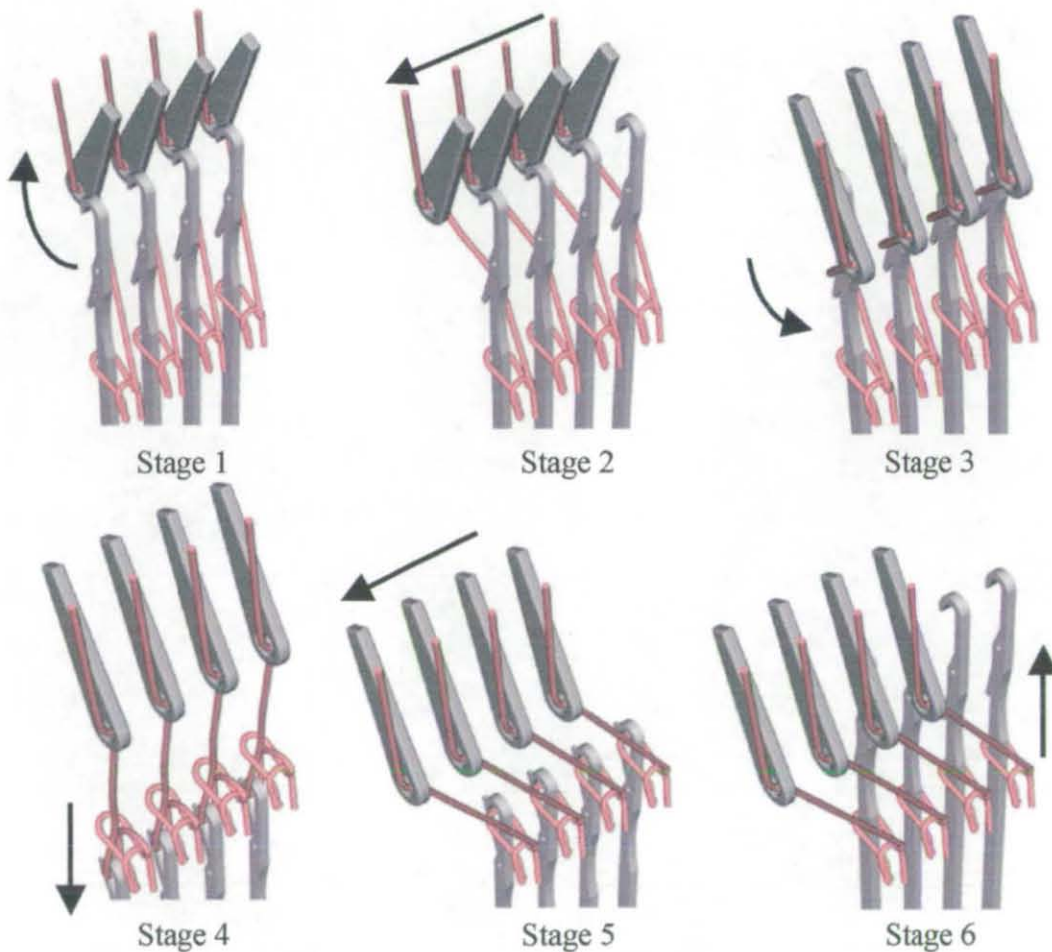


Figure 2-1. Latch needle Knitting Cycle.

When knitting, the needles move in a trick plate and the fabric is pulled down its front. Its top edge, called the verge, defines the level of the old loops on the shanks. The old loops are prevented from moving upwards along with the needles by the downward pull of the fabric and the sinkers between the needles.

Figure 2-2 shows the cycle for a bearded needle. The principle is the same as that of a latch needle but since the needle is not self acting, a presser is required to close the hook. Also, due to the length of the beard, a thread cannot be laid directly into the hook, it is put across over the beard. As the needle rises, the thread falls on to the stem and the needle then drops to bring it inside the hook. Before the old loop reaches the beard tip, the presser closes the hook and the old loop slides on the outside of the beard.

In bearded-needle machines, the sinker performs the functions of both, the verge and the sinker of the Raschel machines.

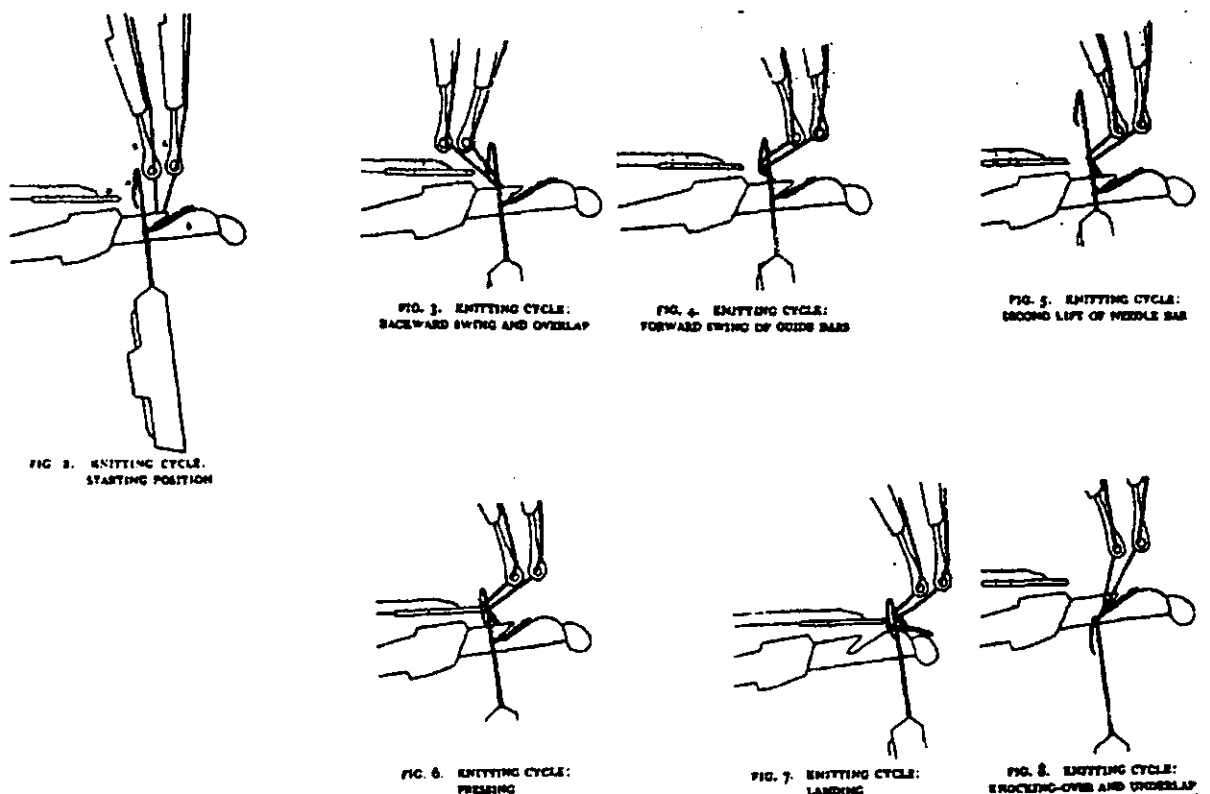


Figure 2-2. Bearded Needle Knitting cycle. After Reichman (1964)⁶.

The knitting cycle for a compound needle is very similar to that of the latch one, but as the needles retract towards cast-off the tongues retract at a lower speed until the hooks are closed.

2.3 Knitting Mechanisms.

2.3.1 Bearded Needle Machine Mechanisms

Warp knitting machines using bearded needles provide a high rate of production and a very flexible dimensional stability, that is, fabrics can be made as stable as woven cloths or as elastic as weft knitted ones.

Widths and gauges can vary greatly, although the most common are 84 and 168 inches and 28 needles per inch respectively.

The guides, attached to a horizontal bar in flat machines, control the warp threads throughout the knitting cycle. They are given a compound motion during the knitting action, derived from two separate sources. A swinging motion is obtained from cams on the main camshaft and lateral movement (shog) is obtained from pattern wheels or chains.

Bearded needles are inserted almost vertically in the needle bar. The latter obtains its motion from the main camshaft of the machine; it can be considered to be taking place in a straight line and at a slight angle to the vertical.

Sinkers function only as web holders and knocking over bits (and take no part in the actual sinking of the loop).

Some external means of closing the needles beards must be provided. This takes the form of a horizontal plate or presser.

2.3.1.1 Needle bar motion using Cam Drive.

Refer to Figure 2-3. Needle bar (F) is driven by a needle bar rocking shaft (D) and connected to it by a long arm (G). The rotation of shaft (D) will produce an almost vertical oscillation of needle bar (F), according to the

length of arm (g). The shaft rotational movement is transmitted from a forked arm (H), attached to trucks or cam followers (T and T1). Each truck follows a separate cam, one being complementary to the other, and therefore giving positive control of the needle bar in both directions.

The trucks are adjustable in slots, which are held in position by locking nuts. Adjusting the setting screws allows to alter the position of the needle bar, relative to the other knitting elements.

The depth to which the needle descends does not have a direct effect on the stitch length or the quality of the fabric.

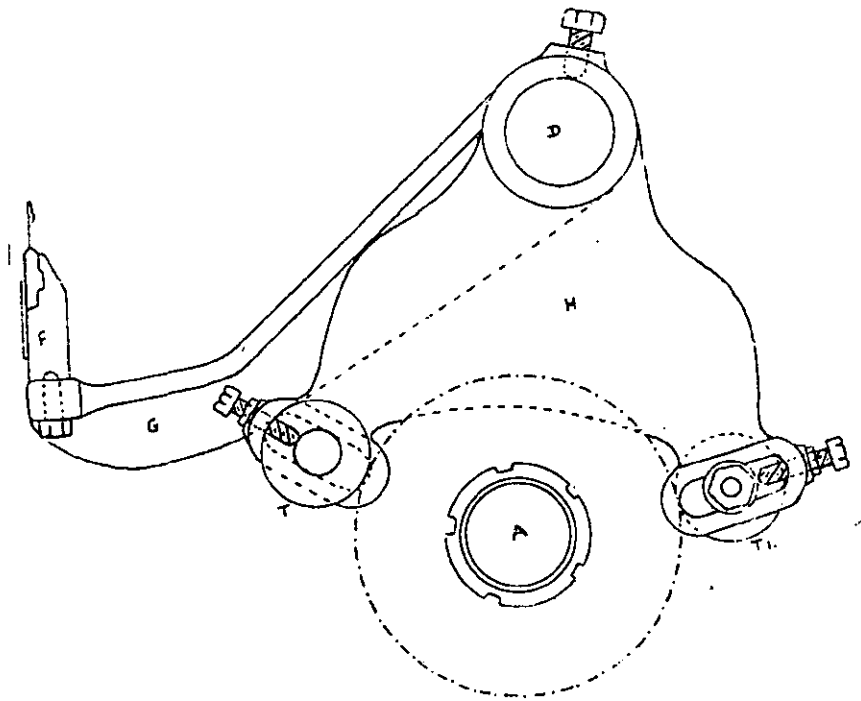


Figure 2-3. Needle Bar Motion; Cam drive. After Paling (1965)⁷,

2.3.1.2 Needle bar motion using Eccentric Drive.

Refer to Figure 2-4, The needle bar (A) is held in place by arm B, which is free to rotate around roller bearings carried on shaft C.

The main shaft of the machine (D) produces a vertical motion on rod Q through eccentric E and a compound system of linkages (F-G and J-K-M)

that are simultaneously actuated from two sources of output of eccentric E separated by 85 deg.

Push rod Q contains adjusting pieces R. Locking cap S and Screw cap T can be slackened to lengthen or shorten the push rod.

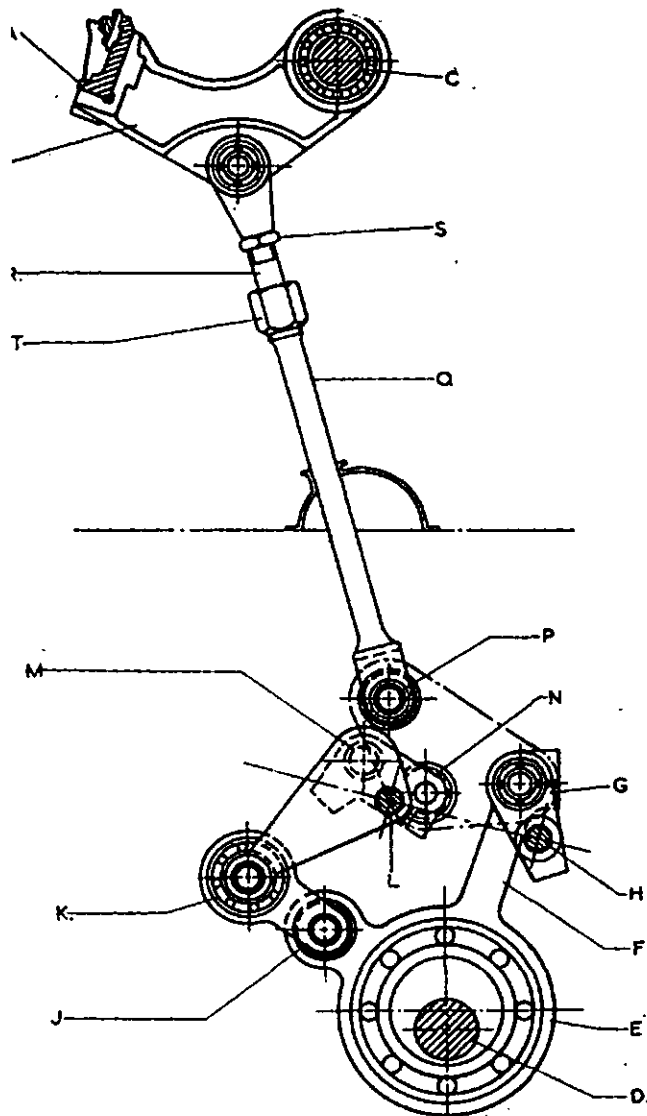


Figure 2-4. Needle Bar Mechanism; Eccentric Drive. After Raz (1987)

2.3.1.3 Sinker bar motion using cam drive

In Figure 2-5, the sinker bar (M) is mounted on an upright arm (J) attached to the sinker-rocking shaft (C). The motion of the rocking shaft is given by arm K and L, which are attached to the followers T2 and T3. The main shaft of the machine drives the cams.

The amount of forward movement of the sinker bar controls the position taken up by the previous course of loops as the needles are rising to the starting position.

The sinker bar should be adjusted to bring the sinker throats further through the needles when knitting a slack quality fabric and dropped back when knitting a tight quality.

The height of the sinker bar can also be adjusted (not in the diagram) using setscrews, increasing or decreasing the depth of knockover.

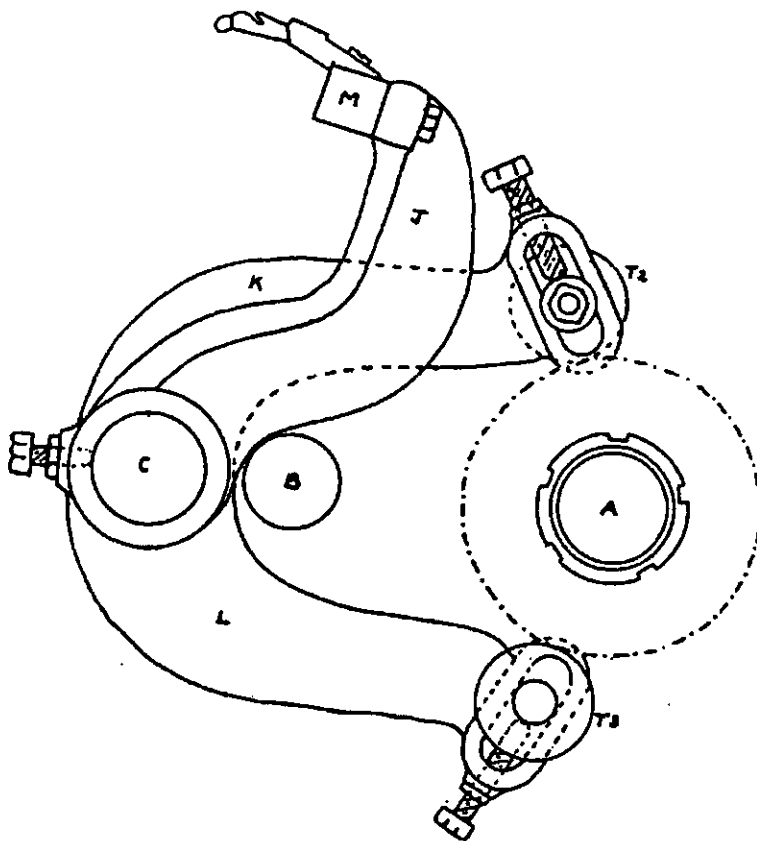


Figure 2-5. Sinker Bar Motion; Cam Drive. After Paling (1965)⁷.

2.3.1.4 Sinker bar motion using eccentric drive.

Refer to Figure 2-6. The sinker bar (A) is mounted on an upright arm (B). It can be adjusted vertically using setscrew C once the main fixing screw (D) is slackened. The arm (B) is free to rotate on shaft E.

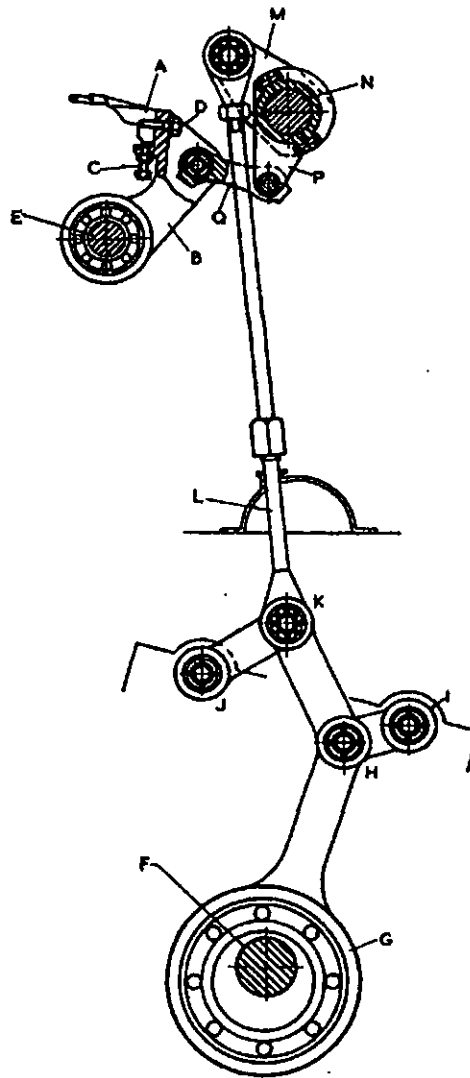


Figure 2-6. Sinker Bar Mechanism; Eccentric Drive. After RAZ (1987)

2.3.2 Compound Needle Machine Mechanisms

In this type of machines, the motions of the needle bar, the tongue bar, the sinker bar and one of the components of the guide bar movements are derived from double eccentrics.

The advantages of this system over the previously described were:

- Less vibration
- Less movement
- Less acceleration

During the knitting cycle it is not necessary to raise the needle after the lapping movements are completed, neither is it necessary to stop the downward movement for the landing of the fabric loops.

The motions (see Figure 2-7) derive from two parallel crankshafts in the base of the machine (A&B). The secondary (A) is driven at 2000rpm and, by means of a 2:1 reduction gears drives the primary at 1000rpm.

The movements are obtained by connecting rods C&D and their bearings. The movements produced are combined into a single compound motion at the centre of the cross-link E.

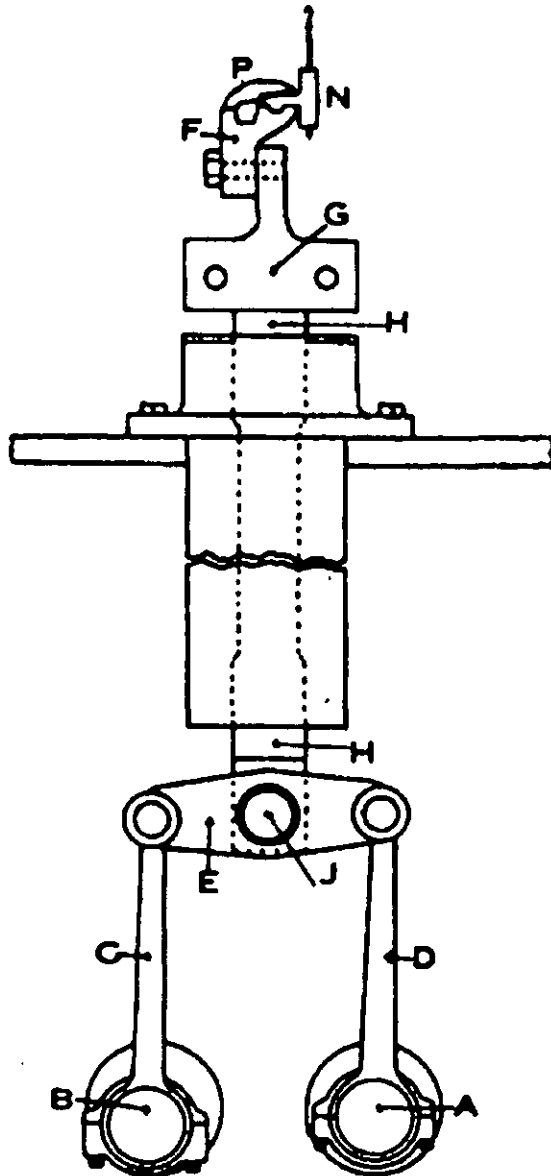


Figure 2-7. Compound Needle Bar Mechanism. After Grosberg (1968)⁶.

The throw of the crankshaft and the relative timing of the cranks have to be varied to obtain different results for the movements.

i. Needle Bar Motion.

The resultant movement of the link is applied directly to the needle bar through push rod H.

ii. Tongue Bar Motion

Tongues are located in tricks on the tongue bar in a similar way to the needles. The vertical movement is transmitted through a push rod.

iii. Sinker Bar Motion.

Sinkers (S) are held on bar B (See Figure 2-8). The motion from the eccentrics is transmitted through pusher tube to the linkage brackets L, in turn connected to the sinker shaft A. The oscillatory motion of shaft A is conveyed to the sinker through the linkage bracket F and actuating arm C.

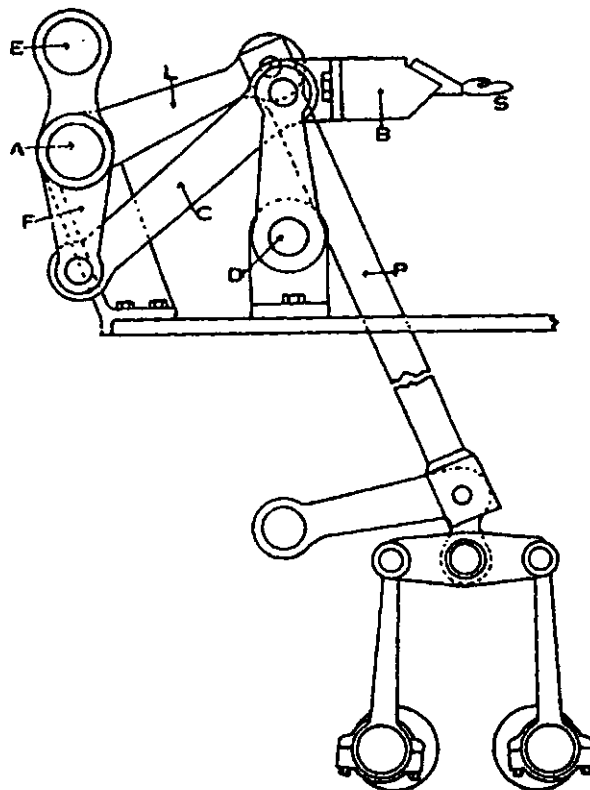


Figure 2-8. Sinker Bar Motion. After Paling (1965)⁷.

2.3.3 Raschel (Latch Needle) Machine mechanisms.

These machines are generally used as single-bed ones, with multiple guide bars, and can produce almost all the fabrics the bearded needle machines make. However, they do not normally compete with bearded needle machine because of the slower running speeds (usually due to having more guide bars and therefore requiring a longer swing motion to carry all the guides through the needles), and the fact that they are, generally, coarser in gauge⁷.

Raschel machines are therefore employed almost exclusively on fancy fabrics with effects difficult to achieve with bearded needles. One bed models produce banded laces, curtain nets, elasticated nets for corsetry, outerwear fabrics, hairnets, veilings, nets and meshes, which usually involve more guides than those available in bearded needle machines or lapping movements which require each thread to continue lapping on the same needle.

Other raschel models are used to produce structures which need special mechanisms, such as, fall plate, plush and crepe.

2.4 Warp Let-Off Mechanisms

"The function of let-off motion is to feed the warp to the knitting elements at a rate commensurate with the stitch construction while imposing minimum strain on the yarn and least loop distortion"⁸. It requires to;

- i. Deliver the warp sheet at a rate consistent with the fabric construction whether the structure has uniform length of lapping movements or not.
- ii. Impose on the yarn less strain by maintaining the warp sheet under the minimum possible tension.
- iii. Have an effective provision for blind lapping.

There are two main factor governing let-off control; warp tension and linear speed. The former is simpler in construction and activates its let off mechanism only when a tension build up occurs in the warp sheet. The latter

is usually more complex since it must include a mechanism to check and correct the linear velocity of the warps.

2.4.1 Tension controlled let-off mechanisms

2.4.1.1 Brake Drum Let-Off

This is simplest let-off mechanisms (see Figure 2-9) and consists of a brake drum (1) keyed to a beam shaft (2) and a friction rope (3) loaded with weights. The beam shaft carries a warp beam (5); the warp sheet unwound (6) is taken around a tension bar (10) and to the guides (11).

The beam shaft will only turn when $R \times T$ equalises $r \times F$. Since R is constantly changing (decreasing), tension T would have to increase to satisfy the condition. To maintain T constant weights are periodically removed from the friction rope.

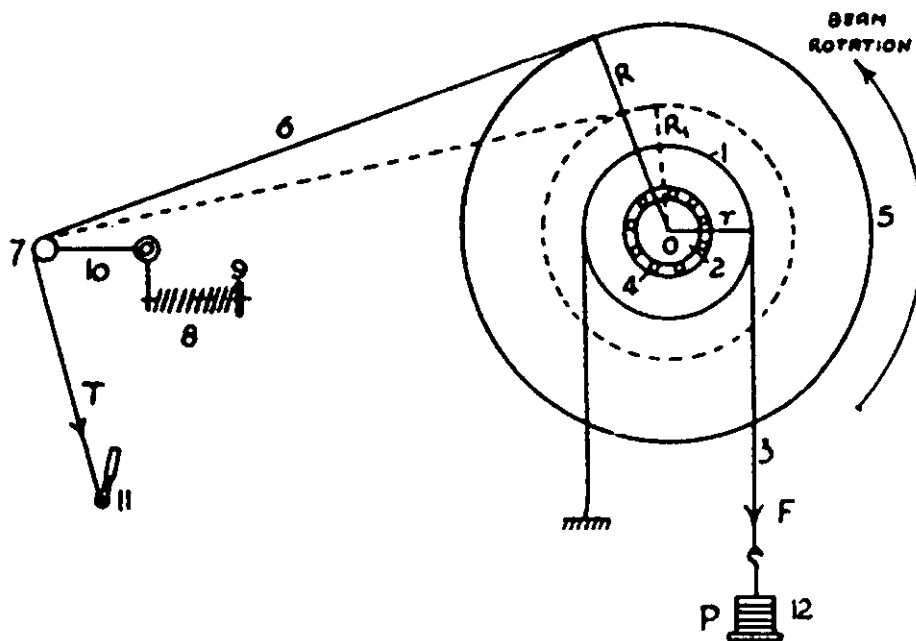


Figure 2-9. Brake Drum Let-off. After Reisfield (1966)⁸.

The warp is subjected to two tension peaks throughout a knitting cycle. They occur at the knock over stroke and at the lapping movement. These peaks should be taken into account to avoid overstrained threads. However they

are too short to produce movement of the beam on their own. It is then the average tension, the one that governs over the motion of the beam.

This type of let-off has the advantage of its simplicity and low cost. Since it releases yarn only on demand, there is no need for special mechanisms for tucks and other blind lapping and no danger of sudden tension loss or increase. It also allows for delivery of very short runners, just by substantially increasing the weights on the rope.

It has, however other major drawbacks, the main being the need for periodical removal of weights. It will also produce, generally, high average tensions and large tension amplitude, making it difficult to handle weak yarns at high speeds.

2.4.1.2 Expanding Brake Let-Off .

In this intermittent, negative let-off system, the warp sheet (3) (see Figure 2-10) is released from the beam mounted on shaft 2 and passed around guide rod (4) and tension bar (5). Beam shaft (2) rests on coupling (6) fixed on shaft (7). This shaft is driven by spur gears (8 & 9) keyed on shaft 10. Brake drum (11) is mounted on the same shaft. Brake shoes (12) are mounted on arms (14 & 15), pivoted on pins 16 & 17 and connected with cross spring 18. Compression spring (24) exerts an upward pressure on lever 23 and, through axle 22, on lever 19 as well. This pressure counteracts that of the warp beam attempting to depress the tension bar (5) and lever 19.

When the tension of the warp sheet increases, tension bar 5 is rotated against the pressure of spring 24 to position 30. The clockwise movement of lever 19 will make axle 22 turn, engage anvils 21 and force arms 14 and 15 apart against the pull of spring 18. This will remove pressure off brake shoes (12) and allow the beam to turn and release yarn.

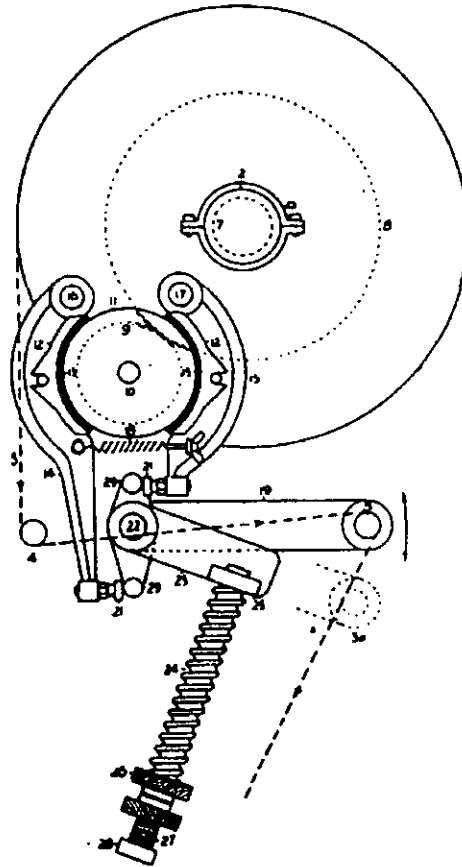


Figure 2-10. Expanding Brake Let-Off. After Reisfield (1966)⁸.

2.4.1.3 Variable-Speed Let Off Systems.

Mechanical Let-Offs

In general, mechanical variable speed transmission let-offs have two major drawbacks:

- i. The response to the signals from the tension bar is delayed for a number of courses.
- ii. The tension bar performs a mechanical function of actuating speed regulatory linkages.

Electrical Let-Offs

Most electrical let-off systems designed after World War II used sensitive limit switches energising an electromagnetic clutch driving the beam and an auxiliary motor compensating for the decrease in beam diameter. The actuation of the switches, however, was still performed by the tension bar.

In Hobbley's Albion machine (photo below) all three units are driven from the main camshaft. Each beam (4) is turned by transmission 5 through gears 6, governed by the magnetic clutches energised by microswitches (7). These are operated by tension bar linkage (8).

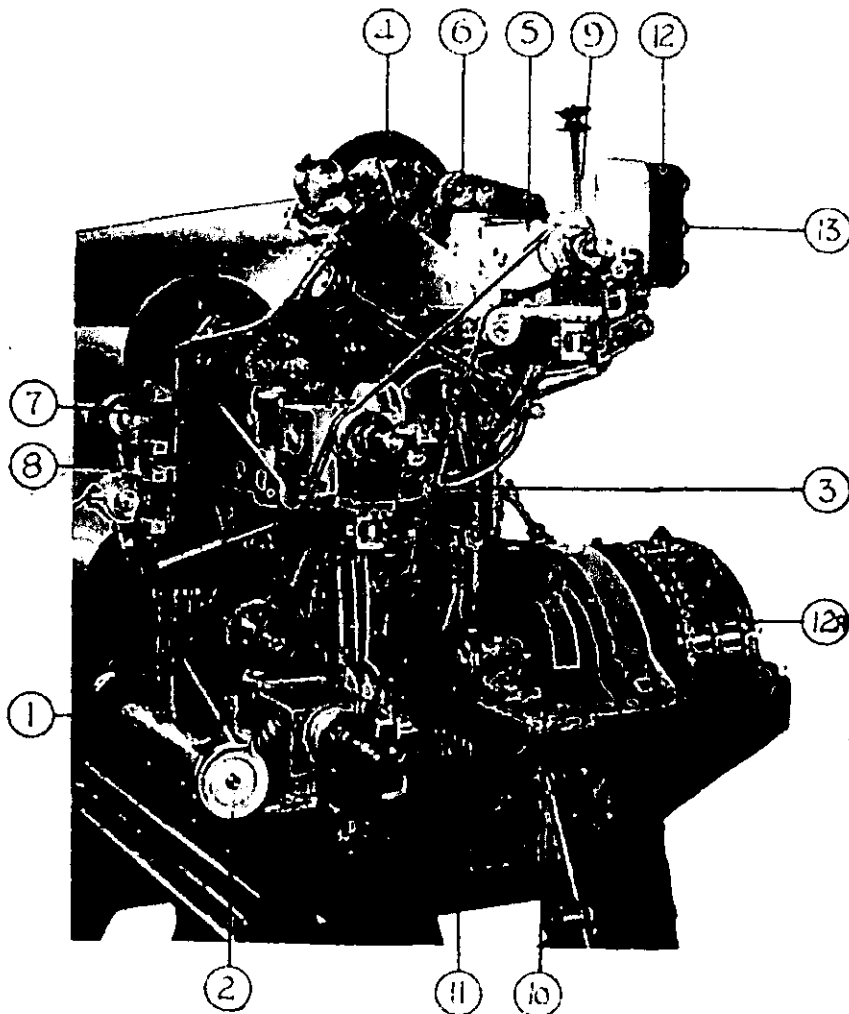


Figure 2-11. Electrical Let-off. After From Reisfield(1966)⁸.

Hydraulic Let-Off

This system uses small hydraulic motors, the output which is regulated by oil pressure to vary the speed of the beam drive. (See Figure 2-12 below). The fluid pressure is generated by a continuously rotating pump. The beam speed is altered by regulating the amount of fluid circulating through the motor. This is done by means of a valve actuated from the tension bar.

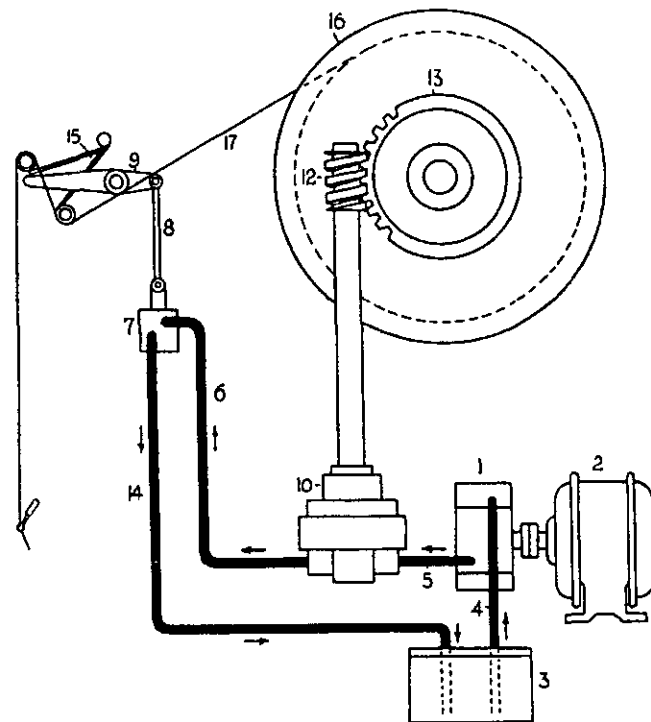


Figure 2-12. Hydraulic Let-off. After Reisfield (1966)⁸.

In the figure, spur gear pump (1) continuously driven by electric motor (2) sucks oil from a reservoir (3) and sets pressure in pipes 5 and 6. Valve 7 regulating the flow is operated from plunger 8, connected to lever 9 of the tension bar arrangement.

Tension on the warp sheet will cause the plunger to rise, opening valve 7 and thus turning the hydraulic motor (10) rotating the beam. Once the tension is relieved the plunger comes down again, closing the valve (7) and stopping the action of the motor (10). Tension let-off mechanisms have several drawbacks, which led manufacturers into the design of new speed controlled systems;

- i. Difficulty in obtaining a satisfactory average tension across the warp sheet.
- ii. b. Variability of yarn lots meant differences in tension, which meant problems with the let-off.
- iii. c. Variation of tension throughout the loop forming cycle.

2.4.2 Constant Yarn Speed Let-Off

A constant yarn speed let off mechanism must feature;

- i. Yarn speed monitoring mechanism.
- ii. Variable speed transmission driving the beam.
- iii. Compensating motion to produce the pre-set yarn speed, by adjusting the beam's variable speed transmission.

2.4.2.1 F.N.F. Let-Off mechanism.

This system was the first one to use speed control rather than tension control over the warp let-off.

A "slave thread" (A) in Figure 2-13 is taken from cone (B) and wound round the circumference of a freely mounted rotary yarn disc (C). It is then taken twice round the beam and knitted. The rate at which disc C rotates provides a comparative mechanism with a datum speed corresponding to the beam speed.

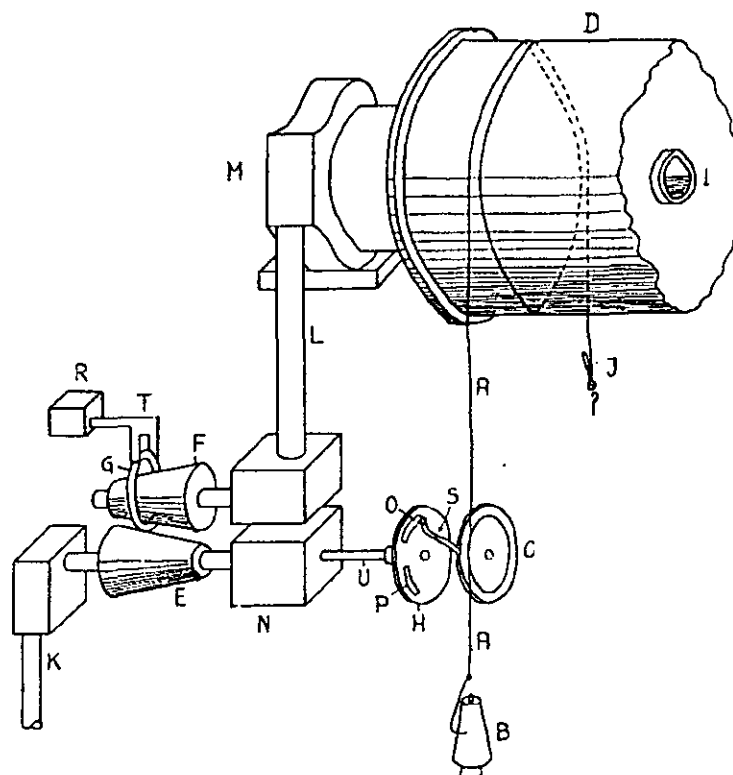


Figure 2-13. FNF Let-Off. After Reisfield (1996)⁸.

The beam is driven by the main shaft of the machine through a variable speed drive composed of cones E & F and ring G. Shaft K transmits the input drive from the main shaft, while L transmits the output drive from the variable speed unit to the beam through gears in M.

Shaft K drives, through reduction gearbox N and via shaft U, a constant speed disc (H) mounted in the same plane as C. By the use of change gears, gearbox N can drive disc H at the speed corresponding to any runner required. Disc H has two contact segments (O & P) connected electrically to the speed adjustment mechanism R.

When the linear speed equivalent to the runner value is equal to the linear velocity of warp A, discs H and C will be synchronised and finger S will rest between segments O and P and no change will occur. Any deviation of the yarn speed from the pre set value will make the two discs de-synchronise and finger S will make contact with O or P (depending on whether the speed needs to be increased or decreased), causing shipper T to alter its position and hence accelerate or decelerate the beam. The photograph below shows the disc unit more in detail, and the following one shows the electromagnetic clutch energised by finger S making contact with one of the segments on disc H.

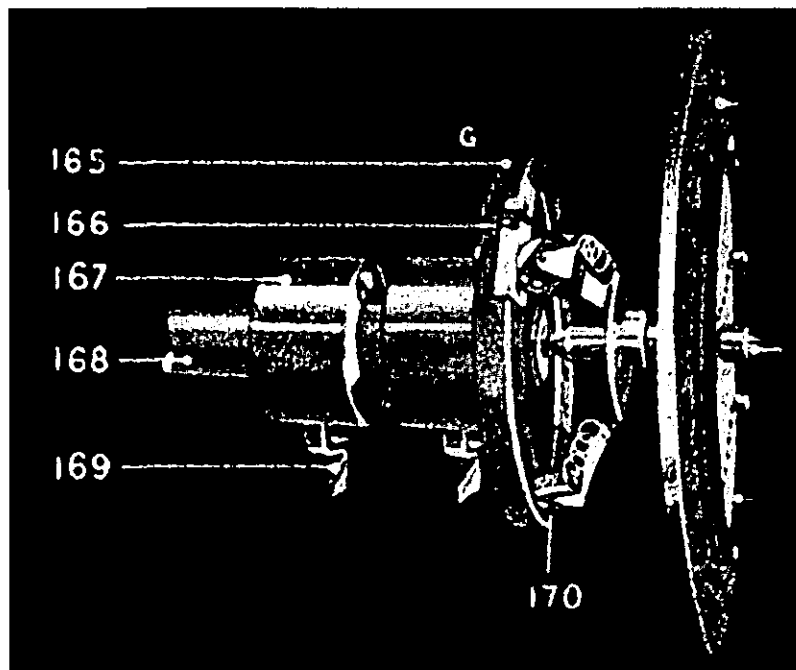


Figure 2-14. Disc Unit. After Reisfield (1996)⁸.

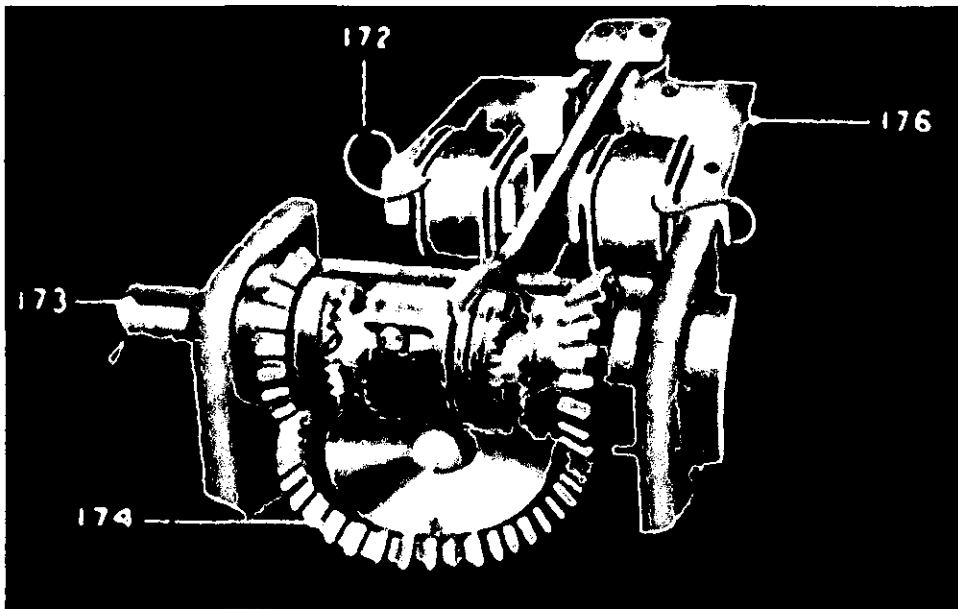


Figure 2-15. Electromagnetic Clutch. After Reisfield (1996)⁸.

The main drawback of the FNF system was that adjustment and tuning needed higher skills than for other let-offs.

2.4.2.2 Reading Let-Off

This system is entirely mechanical and uses the principles of two identical infinitely variable speed transmissions combined with a differential unit.

Figure 2-16 shows the system schematically. Shaft J is driven from the main shaft of the machine. The yarn speed transmission is set according to the runner and the output is transmitted through shaft K. Shaft K drives the warp speed transmission, whose output is transmitted directly to the beam. The decreasing beam diameter is the governing factor for the setting of the warp speed transmission. Shaft is driven by shaft K through worm and wheel gears, and these drive the shaft that holds gear M. On the other hand, the signal rolls drive gear N directly from the beam. If the speeds of gears M and N are different, bracket P will rotate making the hemisphere tilt.

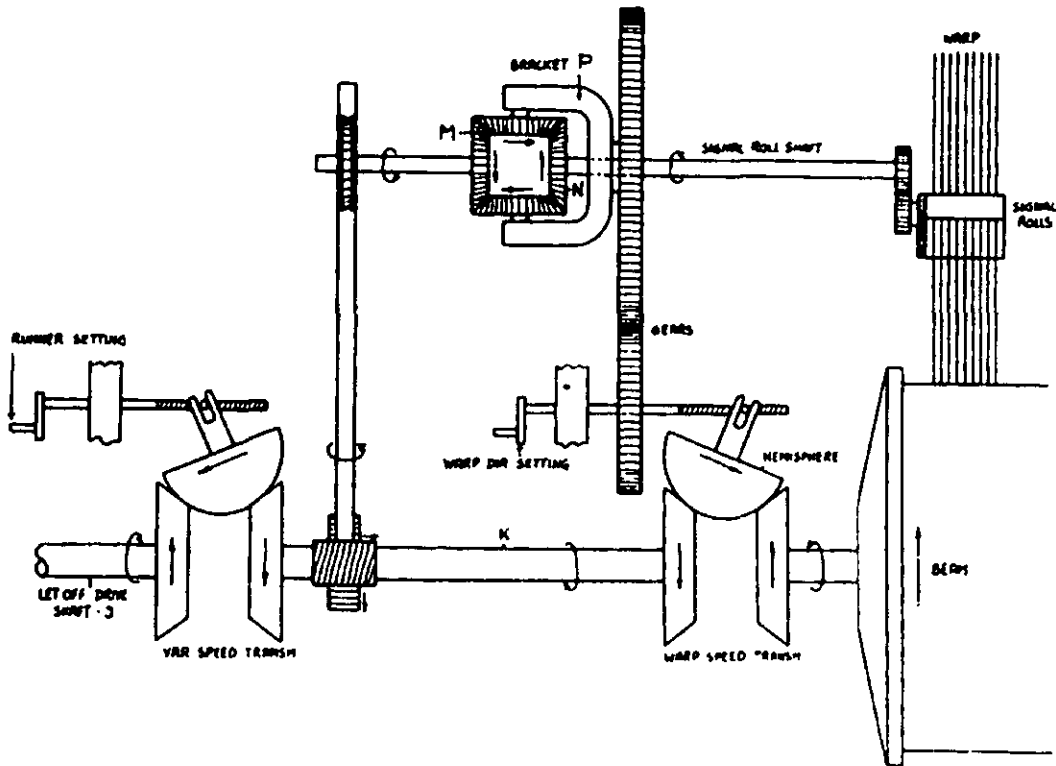


Figure 2-16. Reading Let-Off

2.4.2.3 Mayer Let Off.

This let off mechanism operates entirely on a mechanical basis, and its construction is similar to that of the F.N.F. machine. See Figure 2-17. PIV box 5 drives cone 1 through chain 6 and sprocket 7. Cone 1 drives cone 2, which turns the beam 8 through bevel gears 10&11 and worm and wheel gears 12. Fixed on cone 1's shaft (13) is worm 14, which drives wheel 15. Wheel 16 is coaxially mounted with wheel 15 and cam 18. The cam imparts an up and down motion to the clawker mounting block 19, while the wheel drives another wheel (20). Wheel 20 has a worm thread (21) in its centre, which fits into a worm shaft (22) operating clawkers 23 & 24. The worm shaft is driven from signal rollers in contact with the beam through pulleys 26 and 27. Collars 30 and 31 can only move axially on worm shaft 22, moving levers 32 and tilting the clawker.

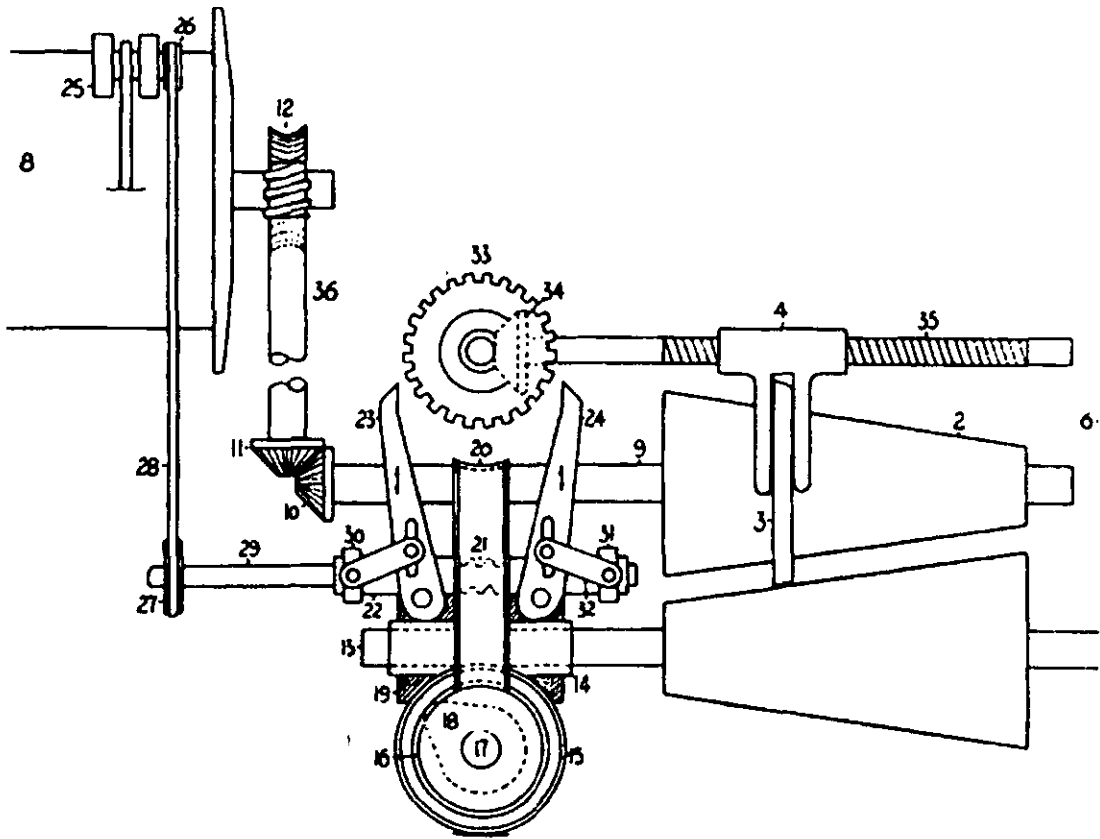


Figure 2-17. Mayer Let-Off. After Spencer (1989)⁹.

The PIV drives cone 1 at a constant speed according to the runner required. Cone 2 drives the beam increasing gradually its speed to ensure that the warp unwinds at a constant linear velocity. Worm shaft 22 and wheel 20 are the basis of the speed comparing mechanism. Wheel 20 is driven at a constant speed by cone 1, while the shaft (22) is driven from rollers 25 on the beam (i.e. directly indicate the linear speed of the yarn).

As long as the runner value remains equivalent to the rpm's of shaft 22, there will be no axial movement of the latter. However, when that balanced is disturbed, shaft 22 will move axially producing one of the collars (30) to move inwards and tilt its clawker towards gear 33. The upward movement of cam 18 will lift both clawkers and make the tilted one engage with and turn gear 33, which will in turn rotate a pair of bevel gears (34). These gears drive screw shaft 35 and shipper 4. The re-positioning of shipper 4 and its ring 3 will modify the speed of cone 2 and hence that of the beam.

2.5 Take-up Mechanisms.

Although the quality of a warp knitted fabric is not determined primarily by the rate of take up, it should be adjusted to give an adequate fabric tension.

The take up mechanism should be positive in action. Designs have been developed for intermittent and continuous mechanisms. The former rotate a fixed angle at every machine cycle. The latter is constructed either using a train of gears to give an appropriate relation from the main shaft to the quality rollers or using a PIV. While PIV boxes are easier to adjust, change-gears are accurate and reproducible.

A continuous fabric take up mechanism is shown in Figure 2-18. The drive is derived from the main shaft M to a gearbox (S, S1 & J). Its output is taken to the quality roller A through worm & worm wheels W, W1, X & X1. The quality roller drives disc G, which in turn drives disc F ensuring a constant speed of the batching roller D.

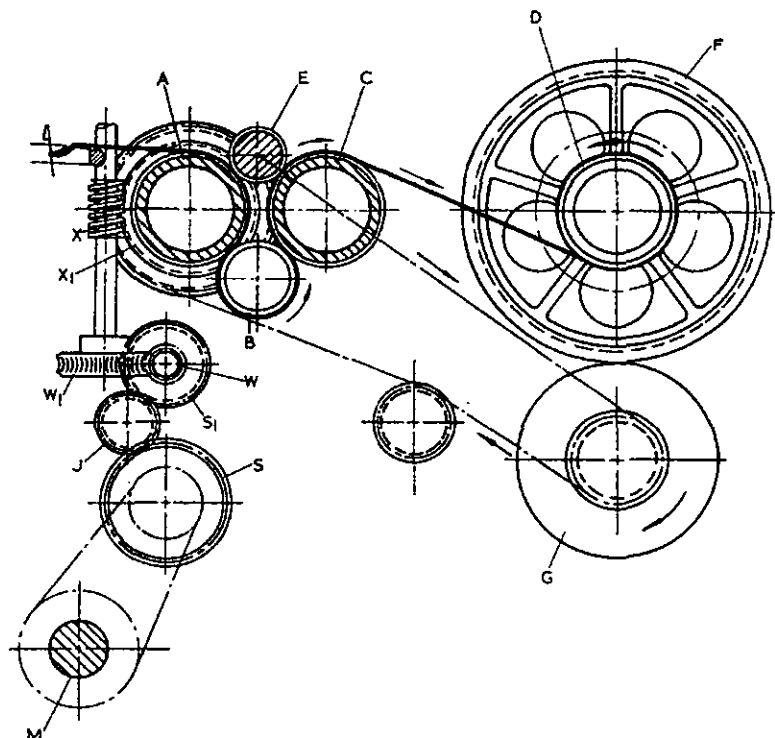


Figure 2-18. Continuous Take-up Schematic. After Paling (1965)⁷.

The fabric is passed around quality roller A, diverting roller B and exit roller C. B is pressed against A and B with an adjusting spring, while a clamp roller E is situated above the level of the fabric.

Figure 2-19 shows an old-type intermittent take up mechanism. Sprocket B is chain driven at a ratio of 2:1 from the main shaft of the machine, A. The rod C, eccentrically connected to the sprocket moves twice during each machine cycle and operates the pawl D upon the teeth of the ratchet wheel once for every knitted course. Movement is transmitted to sprocket H through pinions F and G. This sprocket is interchangeable and drives the emery-covered rollers N and P via sprockets J, K, L and M.

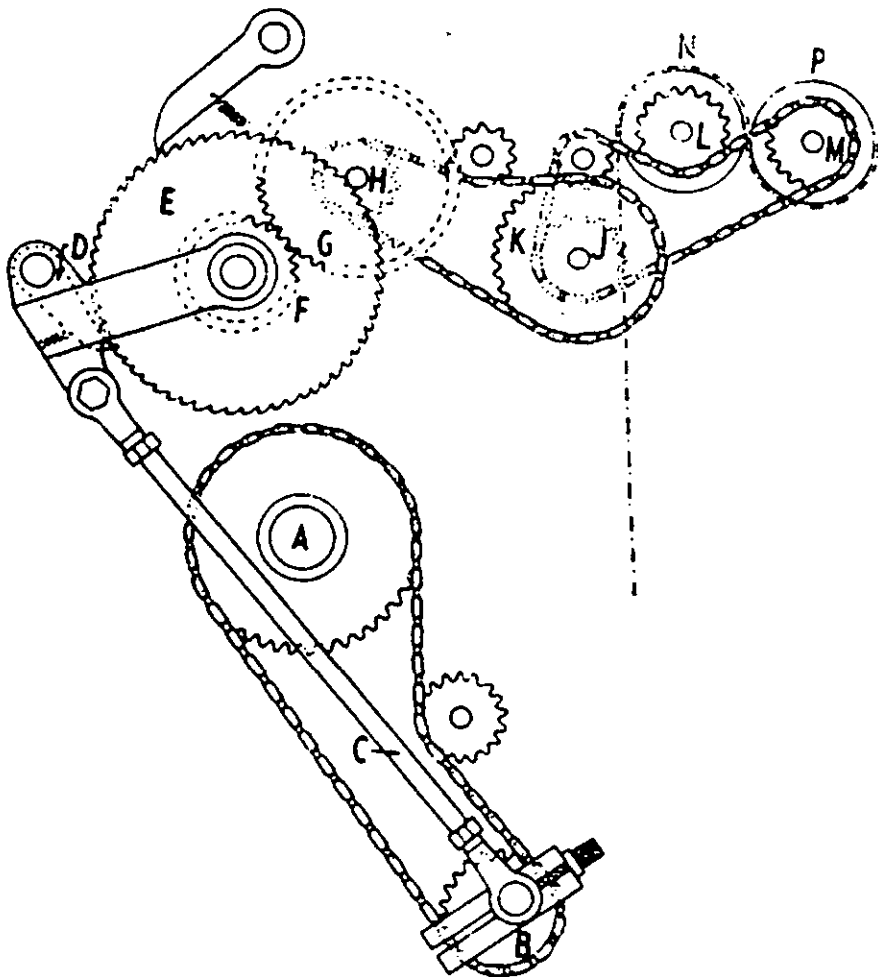


Figure 2-19. Intermittent Take-up. After Paling (1965)⁷.

Varying the eccentricity of rod C and/or changing sprocket H sets the fabric quality.

Figure 2-20 shows a take up mechanism using a PIV. Here, quality rollers C and D are geared together at a 1:1 ratio and covered with a material with a high coefficient of friction with the fabric. Tension roller F is loosely mounted between the quality rollers, usually felt covered and is pulled against the quality rollers under the tension of the fabric, thus increasing the pressure on the fabric and the contact area between the rollers and the fabric. The hand wheel J can be rotated manually after the taking safety pin K out.

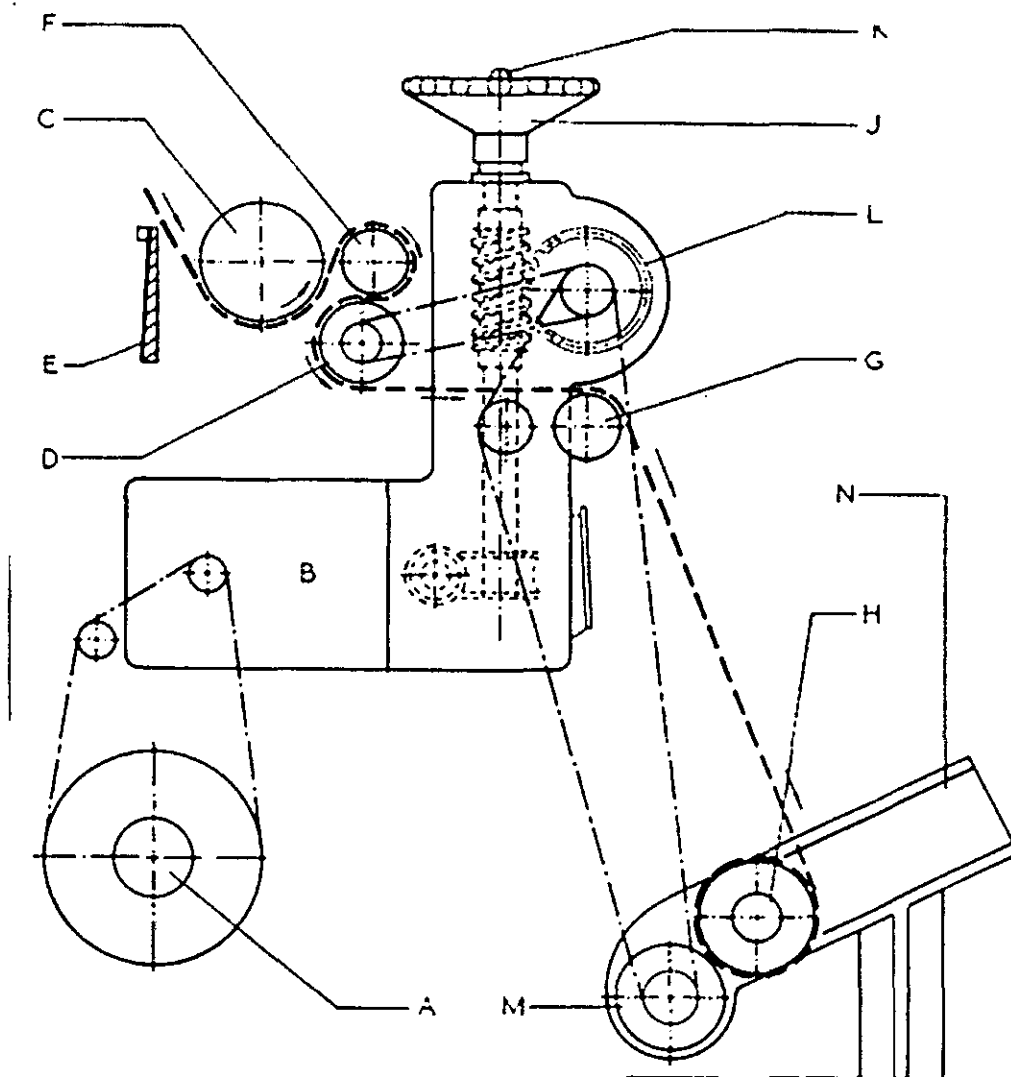


Figure 2-20. Take-up with PIV.

Chapter 3. Literature Survey And Patent Search

3.1 Literature Survey.

A thorough search in the leading engineering and textile journal compendia shows that very little is published specifically dealing with issues that would affect circular warp knitting machine design. There is, however, some research publications in related areas that can aid the above-mentioned design. The most relevant papers found can be described in six categories;

3.1.1 Needle Fatigue

A paper submitted by Lyon and Malinin¹⁰ to the 1995 Design Engineering Conference describes several techniques developed to apply Finite Element Analysis software to estimate the fatigue life of the needles, and to understand what the critical features of their design were. Although the paper does not give specific recommendations for design modifications and it considers only weft knitting machine needles, a similar analysis could be of use in the optimisation of the knitting elements for the warp knitting case.

Weft knitting cam-driven needles travel vertically on a slot in the machine cylinder following the movements given by a cam, that rotates around the cylinder. With the warp knitting case on the other hand, all needles slide inside the cylinder slots simultaneously, driven by a vertical force created by a cam, which is not moving around the cylinder. Nevertheless, the analysis described by the Lyon and Malinin paper is useful as a warp knitting model because it does not take into account the tangential force which the weft knitting cam would transmit onto the needles as it rotates around the cylinder.

Another line of research was undertaken by Smith et al¹¹ in 1974 to analyse the frictional forces present during knitting between the yarns and weft-knitting elements. The authors concluded from the study that previous

equations derived to calculate these forces were not accurate after carrying out relevant experimental work, and proposed a modified equation that predicts the relation between the yarn tension going in to the needle hook and the yarn tension after the needle. This study was later followed and expanded in a series of papers by Wray and Burns (1976) to analyse the dynamic forces present in weft knitting. The most relevant one for a warp knitting machine analysis is Part II ¹² of the series, where "a method for the analysis of yarn tension is demonstrated, and the theoretical results derived from this are compared with experimental results".

3.1.2 New Developments in Warp Knitted Fabric Structures

Circular warp knitting machines will produce tubular warp knitted fabrics, which are now made on double needle bar flat warp knitting machines. Developments in the structures that can be made by the latter are always relevant to the design of a circular machine. In an article in the Indian Textile Journal, Venkatraj (1997)¹³ describes new developments in the fabrics that can be produced in double needle bar machines.

With regards to tubular fabrics, Venkatraj describes methods of production of seamless pantyhose and branched arteries. For the former, a minimum of 6 guide bars was required; two for the base fabric (one the front, the other the rear fabric), two to produce the pattern and the remaining two to knit the selvedge. Although a circular machine would have the advantage requiring only two rings to produce the same fabric, it would be impossible to produce two tubes and join them on a single circular machine.

Venkatraj explained that shaping of the fabric was achieved by varying the stitch length along the garment, and that for this purpose the let-off and takedown systems were essential. The effect of let-off and takedown variation on the dimensions of the fabric produced are envisaged to be an important part of the testing to be performed on the circular knitting machine prototype.

Other researchers such as Mary et al (1997)¹⁴ have also reported on the use of warp knitted structures for arterial prosthesis. In this specific study, a well

known warp knitted structure, 'sharkskin', was compared with others that had been previously used in medical applications, and proved it to have superior dimensional stability and improved dilatation resistance. This paper is of special interest to the circular knitting machine design as the circular disposition of the needles could further improve the quality of the prosthesis fabric. It is in technical textile developments like this one, where the consistency of the fabric structure is critical, that the advantages of a circular warp knitting machine could make a difference. A flat bed, double needle bed machine will always produce a tubular fabric with a minor defect on each side, while a circular machine can produce a perfectly consistent fabric.

In the technical textiles sector, Anand (1991)^{15,16}, and (1995)¹⁷ has produced a series of general publications for trade magazines and conferences summarising the latest improvements in Karl Mayer and Liba's technologies in particular and in the industry as a whole which "demonstrate the unique flexibility and versatility of the warp knitting process" that ensure its dominance in the elastic fabrics market. In addition, the properties and production of the main types of warp knitted structures used in composites were discussed.

Understanding the trends in the technical textiles industry is important for any development of textile machines, as technical textiles are regarded as the fastest growing sector within the textile industry. David Rigby Associates¹⁸ prepared a report in 1997 which aimed to forecast global technical textile consumption by end use and by geographical region to 2005.

The report suggested that despite the fact that the growth of the technical textile industry is proportionally higher than the overall growth in the textile industry, consumption rates of increase in most application areas will be lower in the decade from the year 2000 than in the 90's.

The report also concluded that more strategic developments are required to compete in the market this decade, as the fastest period of (unplanned) expansion of the industry is already over. Their growth prediction was that of 4% per year to the year 2005.

Table 1. End use consumption forecasts from David Rigby Associates

'000 tonnes	1985	% total	1995	% total	2005	% total	% cagr ¹ 85-95	% cagr 85-95
Transportation (automobiles, ships, railways & aerospace)	1408	23%	1918	21%	2483	18%	3.1%	2.6%
Filtration, cleaning and other industrial	980	16%	1523	16%	2344	17%	4.5%	4.4%
Furnishing component, household & floor cov.	854	14%	1439	15%	2259	17%	5.3%	4.6%
Medical & hygiene	703	12%	1177	13%	1652	12%	5.3%	3.4%
Building and construction	508	8%	849	9%	1266	9%	5.3%	4.1%
Agriculture, horticulture & forestry	554	9%	741	8%	1021	7%	3.0%	3.3%
Technical components of shoes and clothing	505	8%	647	7%	824	6%	2.5%	2.5%
Packaging textiles	278	5%	423	5%	658	5%	4.3%	4.5%
Geotextiles and civil engineering	99	2%	251	3%	574	4%	9.7%	8.6%
Sport and leisure	127	2%	237	3%	390	3%	6.5%	5.1%
Environmental protection	88	1%	167	2%	305	2%	6.6%	6.2%
Personal and property protection	45	1%	117	1%	215	2%	10%	6.3%
Totals	6062	100%	9321	100%	13688	100%	4.4%	3.9%

David Rigby Associates divided the technical textiles industry into 12 application areas and showed consumption from 1985 to their 2005 prediction. Their findings are summarised in table 2.3 of the report, which is reproduced above.

David Rigby Associates predicted in the report, as it can be seen from Table 1, that the smaller sectors are the ones that will show the higher growth in the future.

3.1.3 Warp Let-off Systems and Tension Control

Porat et al (1994)¹⁹ described the differences between the developments of let-off systems in warp knitting and weaving. Mainly, that warp knitting

¹ cagr = compound annual growth rate

developments have led to positively driven mechanisms where the length and speed of yarn supplied is controlled, and the tension of the yarn is relegated to a less important role. Weaving let-off systems, on the other hand, have remained largely negative, making the tension the constant parameter and disregarding the amount of yarn supplied.

They stressed the importance of using the expertise from the knitting industry in weaving and vice versa, although acknowledging that the reasons for the diverging evolution of the two let-off systems were due to the differences in the structures of the two products. While the length of warp required by a loom in most cases is quite similar to that of the fabric produced, the warp length required to produce a warp knitted structure will vary greatly and it can be several times the length of the fabric produced. Therefore, the critical parameter in weaving let-off systems is the warp tension; it is irrelevant to the operator whether the rate of warp feed is constant or not. On the other hand, warp knitting let-off systems have been developed to ensure a constant warp feed delivery leaving the tension as a less important parameter (this is true of tricot machines; some raschel machines have maintained negative let-off mechanisms).

Tension control, however, should not be relegated to this situation as it does play an important role in the building of warp knitted structures, and could restrict the development of the warp knitting machine as a whole. In a positive let-off system, the average yarn tension of the warp sheet is controlled by the amount of yarn supplied, but the relative movements of the knitting elements bring about oscillation of the warp tension.

To overcome this, a tension rail, mounted on leaf springs is used. The low inertia of the rail allows it to react rapidly to tension fluctuations. It will supply yarn into the knitting zone, when required, and retract to take back the slack created by the knitting elements.¹

Within the design of let-off systems, Xunwei and Guangting (1993)²⁰ examined what effect the relative position of a spring rail to the knitting elements and their displacement had on tension variation. Researchers have long acknowledged that the control of warp tension variation during a warp

knitting cycle is a difficult task²⁰. Different authors investigating the subject have found tension peaks at different points within the cycle. Reisfield's⁸ experiments indicated that the maximum tension occurred at the knock-over position, while Xunwei and Guangting's experimental data suggested that the maximum tension occurred at the end of the overlap motion, with another smaller tension peak at knock over.

Xunwei and Guangting claimed that the tension fluctuations would vary greatly by positioning an extra guide rod in between the tension rail and the guide bar. Their work stopped short of recommending a given position for the extra rod, and instead showed the different tension graphs obtained. The paper does not state whether the experiment was successful in reducing the average tension within the cycle, or if it merely distributed the tension peaks better.

In weft knitting, Endou et al (1994)²¹ addressed the control of both tension and positive feed speed and "ascertain the control characteristics of yarn tension and yarn speed in the knitting machine, and the interaction between them."

An example of a mechatronic development in yarn-feed mechanisms is described by Kennon et al²² (2000). The design presented was based on feeding the yarn to a flat bed weft knitting machine through a servo controlled delivery drum that delivered precise lengths of yarn to the knitting head. The yarn tension was permanently monitored by transducers that fed the tension information to a PC which, in turn, calculated the length of yarn required by the knitting process.

This development is driven by the thesis that "stitch length is the most important parameter governing the dimensions of a knitted fabric and it is the primary factor in the determination of the fabric quality"²². Accuracy and repeatability of the stitch length throughout a knitted fabric will produce even stitches and reliable dimensions. In warp knitting, the importance of accurate yarn length supply is even more critical because the stitch length changes for each course.

Since warp let-off mechanisms are generally more complex due to the number of yarns in a warp sheet, designs like the one presented in this paper can provide insights on practical problems or breakthroughs in a smaller scale that may be applied to the warp knitting case. The use of a delivery drum for each yarn in a warp sheet is probably impractical. However, the tension measuring devices may be used to monitor a few of the yarns in a warp sheet, and send the information to a PC that can average the inputs and adjust the rotation of the warp beam. In cases where yarns are fed directly to a warp knitting machine from cones (rather than from a warp beam), the system proposed could be modified to connect several supply drums. This might be of special interest for complex patterning designs.

The paper concluded on the effects on yarn delivery of varying the yarn properties, the delivery speed and the wind-on tension.

3.1.4 Calculations of the yarn run-in length per knitted course

The calculation of the run-in length per knitted course is seen in several publications as a critical factor in the quality of the fabric as well as the reduction of unnecessary waste created by excess warping in one or more of the beams.

Hallos and Sun (1997)²³ compared the actual yarn run-in required to produce 12 different fabrics on a specific raschel knitting machine (which uses a negative let-off mechanism) with the expected values obtained using three theoretical prediction methods. They claimed that Sun's model gives the best approximation to the actual values. The three models use equations including a combination of the following parameters to calculate the run-in value;

- Distance between wales
- Distance between courses
- Number of wale spaces that underlap crosses
- Loop inclination
- Yarn diameter

There was no discussion in the paper about how the models were developed. It is also stated in the introduction that the type of let-off device used (i.e. positive or negative) would affect the run-in value, therefore this experiment was by no means complete.

Although weft-insertion is not one of the immediate design goals for this research, a paper by Zhuo et al (1991)²⁴ is of specific relevance, since it used chain stitch and tricot ground structures for their analysis, both of which will be produced by the circular knitting machine prototype. Like Hallos and Sun, the equations they derived related the total run-in per course with the yarn radius, the machine gauge and the courses per unit length in the machine state. However, this paper does describe in detail how the system was modelled to derive the equations mentioned.

After deriving the run-in equations from the geometry of the fabric, assuming that all yarns have circular cross sections and they are incompressible and inextensible, Zhuo et al ²⁴ used them to calculate the run-in for a range of values of all the parameters involved and deduced from them some empirical regression equations.

The validation of the equations found was the subject of Part II²⁵ of this series of papers. In it, an experiment producing 58 different fabric structures on a weft-insertion warp knitting machine was carried out to compare the actual run-in with that calculated from the equations derived in Part I. Two types of yarns were used for the warp and three others for the weft.

Also relating to the let-off system, Roy et al (1995)²⁶ described a new system designed to reduce the tension variations within a knitting cycle of compound and bearded needle warp knitting machines to one third of the variation created when using traditional tensioning systems. The yarn demand in the knitting zone changes very rapidly during the different stages of the knitting cycle, and the let-off mechanism cannot cater for those changes. The conventional spring loaded tension bar was still a source of tension peaks.

Roy et al acknowledged that let-off mechanisms have moved on from negative to positively driven to supply the right amount of yarn without

creating the tension peaks of tension-controlled (negative) ones. The spring-loaded tension bar (being tension driven) could also be superseded by a positively driven one. However, they claimed that given the speed of these machines, 1000rpm with three peaks in a cycle, the response must be better than 250Hz and the cost of such a low-inertia device would probably be prohibitive.

Instead, their design is based on the concept of tensioning the yarn with air pressure, by positioning a rubber tube filled with compressed air underneath the conventional cantilever springs that hold the tensioning bar. It is claimed this reduced the movement of the cantilever spring substantially and maintained the tension in the yarn nearly constant.

3.1.5 Mathematical Models of Loop Formation

Various researchers have tried to model the knitting process in order to develop electronically controlled systems. However, this is only true in the weft knitting industry and there is a distinctive lack of research in this field for the warp knitting case. Grishanov et al. (1996)²⁷ insisted that a standardisation of these models is needed, in order to develop a universal electronic control system, which could then be applied to any type of knitting machine, using a standard PC platform.

In the Grishanov model, the needle has two automata operating together; one being the butt and the other the latch. The former receives information from a given cam track specifying what function to perform. The latter, the “operational automaton”, provides the storage of the knitted structural elements under the needle hook. The stack memory comprises the structural elements situated on the needle stem, under the hook.

One of the most interesting applications for mathematical models is that of a pattern recognition system, capable of ‘reading’ a knitted pattern from a fabric and/or programming a knitting machine from a given set of symbols. Again, only in weft knitting is this research to be found, probably because the structure of weft knitted fabrics is far more homogenous than that of warp knitted ones, and therefore the former are easier to analyse than the latter.

Nevertheless, and for the same reason, there is a wide scope for the development of a 'computer aided warp-knit design'.

Miyazaki et al (1995)²⁸ proposed to represent a basic stitch from a knitting pattern image with a unique stitch symbol that is easy to read. The "Stitch Symbol Generating System (SSGS)" is aimed at aiding beginners to identify knitted structures and others to design new ones. The method used to detect the structure from each knitted pattern image is based on the levels of brightness from each pixel in the picture. First, all the background pixels are discarded by setting a background pixel brightness threshold. Any pixel with brightness above the threshold will be part of a yarn, while any pixel with brightness below the threshold is part of the background.

The model assumed an almost round yarn, where the brightness of the pixels located in the middle of a yarn is greater than that of the ones located on its sides. This was used to determine the main paths followed by the yarns, while the cross between two pieces of yarn were found by applying a set of continuity rules that a yarn path should follow. This provides with a picture of the outline of the yarns, with the information about disconnected portions of the yarn (i.e., where a yarn passes under another).

The outline was thinned into a wire-frame image using Hilditch's thinning algorithm reported in Mizayaki's research. Crossing points were then found through another iterative algorithm, which again is based on geometrical constraints set by the researchers to decide whether two unconnected yarns are actually the same one passing under another. The resultant picture contains all the necessary information about yarn paths and crossings.

The final part of the process comprised the generation of the stitch symbols from the information of the knitted pattern image produced before. The method proposed has been called *Axis-Loop* representation. Every stitch symbol is defined by the state of a loop in relation to its neighbouring loops; the type of loop, the loop where it is hung on, the loop(s) over it and the loop(s) that pass through it.

Once a list of states to include all loops has been created, the information is replaced with the appropriate stitch symbols. The method is successful in cases where the stitch density is not great or where there are no crossed yarns at the back of the fabric, totally out of sight. The researchers also concluded that by using this method, a long time is required to produce the outline of the fabric.

This type of research would be invaluable in warp knitting, where fabric analysis and design is a longer process than in weft knitting. The use of brightness levels to identify the outline of the fabric and the method to find yarn crossings seems to be as suitable for warp knitting as it is for weft knitting, although, as in the latter case, fabrics with high stitch density would be very difficult to analyse. The third step, the stitch symbol generation, will not be portable to warp knitting mainly because the structure of warp knitted fabrics makes them less homogenous and the method of axis-loop representation, whereby an imaginary grid is superimposed on the fabric to locate the loops, is not likely to give reliable results. Warp knitted loops tend to be moved out of their grid-like positions by the action of tension from yarns that will be joined to loops several needles away.

The prediction of the appearance of a warp knitted structure before it is knitted is arguably the most needed research, as the current method of pattern design does not depict the real shape of the fabric after it is knitted. Again, research in this area is limited to weft knitting, where the analysis is made easier by the homogeneity of the structure.

The introduction of mechatronic systems in knitting machines that allow visualisation of designs on a computer screen has stimulated the research to understand and predict the physical appearance of knitted structures. This, however, requires an underlying mathematical model describing the geometry of the structure. Demiroz and Dias²⁹ investigated the design of a software program to generate 3-D graphical representation of plain weft knitted structures that have not actually been produced in a knitting machine.

The initial objective system should take yarn and structure parameters (such as yarn diameter, course and wale spacing and stitch length) as inputs and

fit a 3-D cubic spline representing a stitch (or unit cell). Their main contributions to this area of research are the ability to generate the geometric parameters to display 3-D models on screen and the proposition that the stitch length is an important factor on the geometrical features of a stitch within a knitted structure.

The importance of the stitch length as a crucial factor in the appearance of a warp knitted fabric has long been accepted. On the other hand, it is not clear whether the use of mathematical models based on 3-D cubic splines is applicable to describing and predicting the appearance of warp knitted fabrics.

3.1.6 Other Developments in Knitting Machine Accessories

Warp knitting machine accessories are generally to aid in the quality control of the fabric produced or preventive stop-motions that will halt the machine before the malfunction of one of the knitting elements or when a yarn breakage causes a defect on the fabric.

The development of these devices has been fuelled by the increasing productivity of machines coupled with rising labour costs. The International Textile Bulletin (1994)³⁰ reported on the optoelectronic monitoring of filament yarns, which claimed is replacing the former mechanical means of overseeing large warp sheets, especially in fine filaments processing. Four types of devices were described, two of which have special relevance in the case of the circular knitting machine; one for monitoring yarn breaks before they enter the knitting mechanism, and another to control defects on the knitted fabric.

The former consisted of a photoelectric barrier, the transmitting head of which sends a beam below the warp sheet to the receiving head, at the same time that a high-pressure fan targets an air stream on to the warp sheet. The air stream blows broken ends into the monitoring beam and the signal generated stops the machine.

The fabric monitoring system is based on a scanner that moves across the surface of the fabric at a constant rate. It stores the information of a faultless

section of the fabric and compares it with newly acquired data as it sweeps from one side to the other of the machine. This system was preferred over the beam of light used to monitor warp sheets because the latter would only report a fault when a loose yarn enters the beam of light. The scanner, on the other hand will also identify faults where a yarn has been knitted by an adjacent needle.

This system seems appropriate for adapting to a circular knitting machine because although the scanner would have to rotate around the knitted fabric (not a difficult mechanism as a change of direction is not needed), the amount of information that the scanner needs to store is reduced to a small portion of faultless fabric, so the processing requirements to compare with incoming data are greatly diminished.

An interesting research area that has been undertaken in other textile applications is that of using image processing of fabrics either for pattern recognition or fault-finding, i.e. quality control. Xu (1996)³¹ explored the use of Fast Fourier Transforms (FFT) in image processing used for weaving pattern recognition. Weaves' repetitive units are particularly suitable for this type of analysis, and in his study, Xu attempted to use the FFT techniques to identify basic weave patterns and to measure structural characteristics such as fabric counts and skewness.

Warp knitted fabric analysis is a difficult task, especially because the yarns are distorted after knitted according to the fabric structure. Although warp knitted products would not show such a high periodicity in their structure, the use of FFT and image processing could represent an interesting area of research. It would be very useful if it could be developed to the point where changes to the spectrum generated after applying a FFT could be translated into the necessary modification to the fabric structure to achieve a given characteristic, by applying inverse FFT.

Image processing using FFT and other methods for measuring fibre orientation have also been investigated in the case of nonwovens by Pourdeyhimi et al (1996)³², while Tsai et al (1995)³³ used an artificial neural

network to construct a pattern recognition system for inspecting fabric defects.

With regards to warp knitting thread velocity measurement, Seeger et al (1996)³⁴ developed a velocity meter with a high dynamic response to incorporate features that the conventional speed meters lacked; namely, coping with high momentary velocities, distinguishing the direction of travel and reacting to fast changes in magnitude and direction.

The solution presented is based on a hollow 20mm diameter capstan roller, (light weight, low moment of inertia and minimum friction) around which a thread is wrapped several times to avoid slippage and dissipate the effect of thread tension. The rotational movement of the roller is converted into electrical pulses by a miniature pulse generator. The design of the circuit controlling the processing of the output of the pulse generator makes the speed meter reliable both at high and low speeds.

Measurements taken by the researchers show how the speed of threads fed into a warp knitting machine varied within a stitch forming cycle. This occurs as a consequence of the movements of the tension rail explained earlier. Interestingly, this is the only research paper found in which the analysis of variations within the cycle focuses on the yarn speed rather than the tension.

3.2 Patent Search.

This section of the chapter outlines the major findings of a patent survey using the facilities of the British Science Reference Library, London and the CD ROM database of European patents available at Loughborough University's Library. The survey has been continuously updated through abstracts published in the Knitting International Magazine.

The great majority of warp knitting patents have been granted to the major manufacturers of flat machines; Karl Mayer, Liba, etc., and contain details of recent developments, which are not relevant for this research. This section will outline some of the more relevant patents found and provide a summary of the classification of patents for warp knitting machines for further consultation.

Warp Knitting Patent Classification

Braiding, lace making, knitting, trimmings and nonwoven machines are all classified under Volume 4 Section D (Abbreviated as “D 04”) of the International Patent Classification Index. Within that section, subsection D 04 B relates to knitting machines. A copy of the full subclass index can be found in Appendix B. There is no specific class for circular warp knitting machines; flat bed ones are included in the subclass D 04 B 23/00 & 25/00 and circular (weft) ones in D 04 B 9/00 & 13/00. There is however, a subclass 25/02: Tubular machines under the category “Warp knitting machines not otherwise provided for”.

Under “Miscellaneous knitting processes, apparatus, or machines...” there is an interesting subclass labelled D 04 B 39/04: “... adapted for combined weft and warp knitting”.

The subclass indexes for D 02 H: Warping, beaming or leasing is also included in the Appendix B.

3.2.1 Circular Machines

Only two patents for circular warp knitting machines were available for inspection in the British Library, which holds European and British patent applications only. The first one (Borenstein, 1986)³⁵ is a European patent application filed by an Israeli company. The second one is a UK Patent Application filed by a Russian company (Vyacheslavovich Ragosa, 1990)³⁶.

The former was a design for a circular warp knitting machine with two patterning rings, introducing an innovative way to make a stitch. The drive makes the tube holding the knitted fabric reciprocate vertically, while the needles remain stationary. The movement of the fabric (rather than the needle cylinder) produces the stitch. See Figure 3-1.

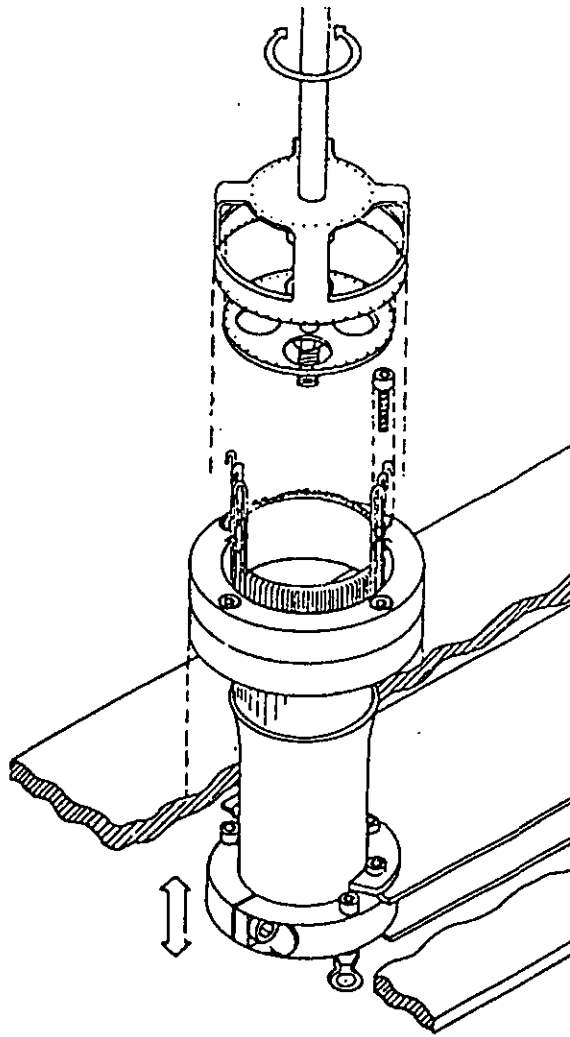


Figure 3-1. Fabric Moving Circular Warp Knitting Machine.

Inside the cylinder, a tube reciprocates vertically moving the knitted fabric with it from the stem of the needles upward to clear the hooks of the needles. The patent claims that in this way an increased speed can be achieved and the needles are subjected to less wear, splitting and breaking. Tritex International Limited has put this type of mechanism into production in their model NE150.

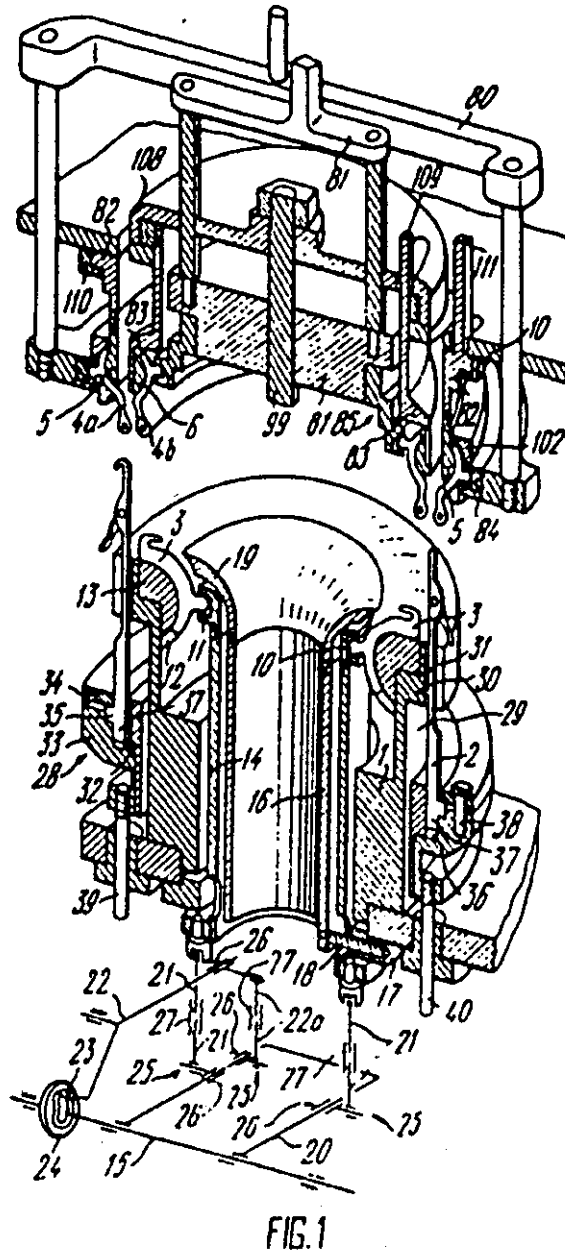


FIG. 1

Figure 3-2. Circular Machine with Tricked Torus Sinkers and Guide Rings

The latter³⁶ is also a design for a machine with two patterning rings. Its main improvements are a set of radially moving sinkers, two sets of guide needles (also radially moving) and two concentricly arranged annular guide bars. See Figure 3-2.

3.2.2 Flat Machines

A much larger number of patent applications have been filed for flat warp knitting machines. Only a few of the patents are described here.

Within the broad subject of flat warp knitting machines, patterning mechanisms are probably the ones that have been studied in greater detail recently, as it is shown by the large percentage of patent applications filed in this subject. Large companies have modified the traditional chain-link for electronically controlled patterning bars or hybrid mechanisms. European patent application EP 0 511 580 (LIBA, 1992)³⁷ claimed the invention of a 'Warp Knitting Machine with a Weft Inlay Bar Provided with Individually Movable Thread Guides', in which the patterning drives 'are designed as servomotors which are controlled electrically by a program control.

The latest developments in the patterning mechanisms of large-scale flat warp knitting machines are related to individual guide control with piezoelectric actuators. Several patents have been applied for, mainly by the larger players in the warp knitting machine manufacturing market, with regards to these types of mechanisms. UK Patent Application GB 2 290 310 A (Karl Mayer, 1995)³⁸ is a good example of one of the various patent applications filed by Karl Mayer Textilmaschinenfabrik GMBH, Germany, probably the largest flat warp knitting machine manufacturer. This one in particular claimed to have simplified the replacement of the bending transducers, which individually control each guide through a control device. The applicability of similar piezo actuators to the circular machine should be investigated further.

A related Patent Application (Karl Mayer, 1994)³⁹ filed by the same manufacturer to claim the invention of a "Warp Knitting Machine With Jacquard Control" relates the use piezoelectric transducers arranged on the guide bar and which displace the associated plating needles by applying a control voltage. The ones used by the German manufacturer are flexural transducers with a plate-shaped carrier and at least one layer of piezoelectric material applied to it. One end region of the plate is clamped firmly onto a holder that is then secured to the guide bar, while the other end carried the plating needle.

Nippon Mayer Co. (1995)⁴⁰, filed a relevant application, patenting a "Guide Bar Driving Force Control Apparatus Provided with Selective Overlapping

Mechanism". The invention claimed to provide a the driving force control for the patterning bar of a Warp Knitting machine with a thumbing mechanism using a gauge piece. The force can be transmitted to all the guide bars or selectively to any of them.

Some advancements have also been made on the let-off mechanisms of flat warp knitting machines; in particular efforts have focused on the control of the warp beam speed. The German machine manufacturer, Liba Maschinenfabrik, has patented both the beam speed control circuit (EP 0 457 322, Liba Maschinenfabrik, 1991)⁴¹ and the device to measure digitally the length of yarn being fed into a warp knitting machine circuit (EP 0 457 323, Liba Maschinenfabrik, 1991)⁴². The control circuit invented was based on a pressing roller on the warp beam, which provides an actual momentary thread draw-off speed. The pressing roller is pivoted on an arm, whose angular position produces a pivot signal. This signal, together with that of a nominal value, is fed to a comparator that provides a control signal to an amplifier. The degree of amplification increases as the warp beam diameter decreases and vice-versa.

Although the patent mentioned in the paragraph above will only be of use if using warp beams as the basis of the let-off mechanism, the "Device for Digital Measuring the String Yarn length from a Warp Beam of a Warp Knitting Machine" can be implemented on any type of roller from which yarn is being drawn. It comprised a tension roller that bears against the yarn on the warp beam and drives a pulse generator for transmitting yarn length pulses. The number of pulses is a measure of the yarn length drawn off from the warp beam.

3.2.3 Fabrics

There are numerous patents for warp knitted fabrics, in particular for so-called technical textiles, which are thought to be an important potential application for the circular warp knitting machines. For instance, European patent No. EP 0561710 A1 (Laboreau Jaques Phillippe, 1993)⁴³: "Artificial Ligament" claimed inventing an artificial ligament formed by rolling or folding two intra-osseous parts, both being warp knitted fabrics of technical fibres

with a weft inserted filament. This type of application could be improved by using a circular machine that would make the rolling step unnecessary.

Other relevant warp knitted fabric patent applications include; European patent No. EP 0630997 A1 (Marumiya Shoko Kabushiki Kaisha , 1994)⁴⁴, “Resilient Material Comprising Warp Knitted Fabrics and Warp Knitted Composite fabric” and World patent application WO 9424510 (Barracuda Technologies, 1997)⁴⁵: ‘Warp Knitted Camouflage Material’.

Another application for a circular warp knitting machine is the production of bandages; one of the patents claiming to have invented a “Warp Knit Casting Bandage Fabric” (Lohmann Gmbh. & Co, 1997)⁴⁶ summarised the most common structure used in this type of fabrics. It described the fabric comprising one group of continuous multi filament fibreglass yarns forming lengthwise extending chains of spaced-apart loops and a second group of the same yarns together with a group of thermoplastic yarns forming a width-wise inlay.

Tubular warp knitted mesh has also been patented as fish bait. “Intended mainly for use in long line fishing [a fish bait] comprises bait material such as shellfish, fish offal, ... and/or fish oil enclosed in a porous casing” (Morton, Peter, 1992)⁴⁷. The casing is made of a collagen based semi-permeable membrane and a tubular reinforcing knitted mesh, preferably made from cotton.

Chapter 4. Machine Specification and Concept Evaluation

4.1 Introduction

The wide range of potential features and capabilities to design for a warp knitting machine is so vast, that a means of deciding which are required for a circular warp knitting machine them is essential. The first section of the chapter (4.2) explains the methodology used to conceive an initial Product Design Specification (PDS). It then includes the results of this PDS, which define the mechanisms in which the rest of this research is focused on.

Then, in section 4.3, concepts for the different functional sections of the machine are discussed. The concepts selected as best solutions for the two main mechanisms (knitting and patterning) will be discussed in more detail in Chapters 5 to 8. The solutions implemented for the takedown and let-off mechanisms, on the other hand, are discussed in section 4.3.2.

4.2 Circular Warp Knitting Machine Design Specification

4.2.1 PDS Database

An efficient approach to create a PDS for the circular warp knitting machine was to build a database, using data received from the answered questionnaire of potential users selected from various warp knitting contact sources; e.g. industry literature (trade press, magazines, journals), warp knitting machine manuals, mechanism patents and knitting samples.

The database format was intended to emphasise the link of a given feature or sub-assembly to each of the 3 end products likely to have the most potential for a circular warp knitting machine; (i) packaging and other nets, (ii) ladies stockings and (iii) bandages and medical textiles.

The information encapsulated in the PDS database includes:

- i. Specific end products that define a machine requirement; e.g. to knit ladies stockings 4-inch diameter cylinders are required, whereas packaging nets can be produced using 0.5-inch to 6-inch diameter cylinders.
- ii. Existing machine features which determine the fabric structure capabilities; e.g. "Standard Pattern guide bars" refer Appendix C, Section 3.

The PDS database is divided into 11 sections broadly encompassing the main design decisions. Each database record is divided into 5 data boxes as illustrated Figure 4-1 below.

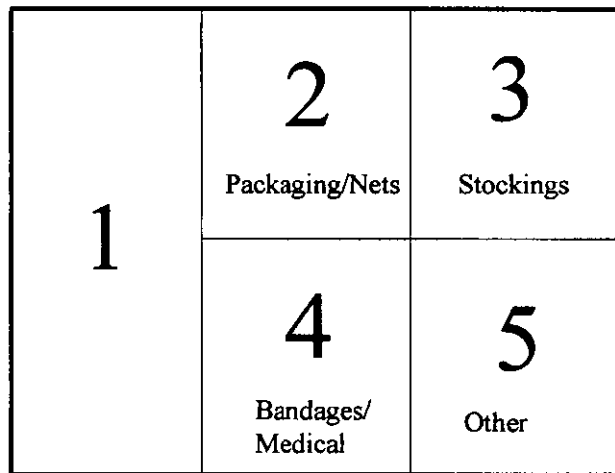


Figure 4-1 PDS Data Record Format

The Box contents of the PDS database format are (refer Appendix C):

Box 1 contains: (i) section heading, (ii) specific fabric structure or machine feature discussed in the database record and (iii) information not specifically relevant to any particular end product.

Boxes 2, 3 and 4 have data relevant to the record topic and the respective end product.

Box 5 contains information relevant to the record topic and an end product different to the 3 main end products.

Therefore, the database represents an organised set of requirements, used to define the PDS document; a design brief for the development of the circular warp knitting machine.

4.2.2 PDS Design Decisions

From analysing the information contained in the PDS database, there are five key decisions to be considered.

4.2.2.1 Needle Type

Most of the fabric structures in the three target end products have been traditionally manufactured on raschel machines. Tricot machines (which traditionally use bearded needles) rely on the sinker for the stitch forming process, while raschel ones would only use them as web holders, to prevent the fabric from rising with the needles. This gives raschel machines more flexibility in the stitches formed, which is useful especially for net type fabric structures.

Many of the modern flat-bed warp knitting machines use compound needles, especially those manufactured by Karl Mayer GmbH, due to the reduction in stroke they allow for, coupled with their improved comparative hook strength. However, the improvements in productivity of compound needles might be outweighed by the more complex design needed for the tongue mechanism. The double needle bar machines used in the production of tubular fabrics have maintained the use of latch needles.

The circular warp knitting machine should therefore work in the manner of a raschel machine.

4.2.2.2 Number of Guide Rings

For most fabrics, the ground structure is simple in construction and requires one or two guide bars. This is probably because the flat-bed warp knitting machine manufacturers had to develop special machines to produce tubular fabrics (with two needle bars, and many guide bars dedicated solely to joining the two sides of the fabric together). Therefore, it would be possible to

produce most of the current warp knitted products ground structure in a machine with two guide rings.

The number of extra guide rings required varies according to the application:

- i. Packaging end products generally will not require extra patterning rings, as netting structures are symmetrical and rely entirely on the two guide rings knitting the ground structure.
- ii. Medical bandages will require at least one patterning guide ring, generally with the elastic material, but normally not more than two.
- iii. Stockings can use as many patterning rings as there are available, as each one will give more versatility in the pattern design. Alternatively, two jacquard patterning guide rings will give a great deal of patterning possibilities.

4.2.2.3 Needle Gauge

Flat-bed machine needle gauges range from 4 to 44 needles per inch (npi). However, the finest gauge required for a circular warp knitting application is 18 npi for stockings. It is therefore reasonable to fix a needle gauge range for the circular warp knitting machine from 4 npi to 20.

4.2.2.4 Cylinder Size

The cylinder size range in circular warp knitting machines is dependent upon the application.

- i. For bandages it varies from approx. 0.5" to 6" diameter and because of the types of structures used the cylinder size is an important factor in the quality of the finished fabric.
- ii. In the case of packaging nets, the cylinder size is not a crucial characteristic of the machine. A very loose symmetrical structure use for most nets implies that the actual fabric diameter will depend solely on the number of needles, the stitch length and the hole depth (defined by the fabric structure).

- iii. Ladies stockings will only require cylinder sizes between 3" and 4" in diameter.

4.2.2.5 Let-off and Takedown mechanisms

The let-off and takedown mechanisms should provide the means of controlling: (i) the stitch length, (ii) the finished fabric tension and (iii) the yarn supply tension. From previous experience of flat-bed manufacturers, it is clear that a positively driven yarn supply is crucial to the consistency of the finished fabric quality. Provided that the let-off mechanism is positive in action, the takedown mechanism becomes less critical.

The design brief for these five critical issues, affecting the design of the main mechanism of a circular warp knitting machine, can now be used as the basis for the concept evaluation stage described in the next section. Further references to the findings of the PDS are made in the concept evaluation section below.

4.3 Concept Evaluation

The warp knitting machine can be divided into four functional sections in addition to the structural elements, namely: let-off, takedown, patterning and knitting mechanisms. However, it is clear from the research and the Product Development Specification (PDS) that the two critical mechanisms in a circular warp knitting machine are the knitting and patterning ones. For this reason this research concentrates in the design and synthesis of the two critical systems. However, in order to have a fully functional design, the secondary mechanisms must also be designed. Therefore, the section is comprised of two parts.

Main Mechanisms (4.3.1) where design concepts for these are analysed and evaluated; here although patterning and knitting mechanisms are closely interdependent, both are analysed independently and interdependently. The aim of this part is to provide a comparative analysis of the different concepts for each mechanism. The mechanisms selected as best solutions for the two main functions will be discussed in more detail in Chapters 5 to 8.

Secondary Mechanisms (4.3.2) aims to summarise the driving requirements of the let-off and takedown systems, derived from the PDS, and to describe the solutions implemented. The let-off and takedown mechanisms can be thought of as related but independent design projects and are therefore analysed separately.

4.3.1 Main Mechanisms: Knitting and Patterning.

The design of the knitting mechanism is closely linked to that of the patterning one, as the motion described by the needles will depend on the motion of the patterning bars/rings to ensure the yarns are wrapped around the hook of the appropriate needle at the right time. This is especially true of circular machines.

In most flat machines the swing and shog movements are performed by the patterning mechanism, while the knitting mechanism is solely dedicated to reciprocate the needles nearly vertically in order to make a stitch. A circular machine has the intrinsic advantage in the underlapping movement that, as a threaded patterning ring is rotated to produce the underlap, the rotated threads will also move radially relative to the needle where they last made a stitch; i.e. they will perform part of the swing movement. Positive as it might seem, this can also be a disadvantage in the overlap movement as after a long underlap, the threads may be too far inside from the needles intended to wrap.

4.3.1.1 Needle Motion

The following concepts investigate different ways of achieving the optimal relative motion between the needles and the yarn threads.

Most of the mechanisms used to reciprocate flat warp knitting needles vertically produce sinusoidal profiles. This has two undesirable results; firstly that the shogging has to take place while the needles are in motion, and secondly, that there is very little control over the proportion of the cycle devoted to underlapping or overlapping.

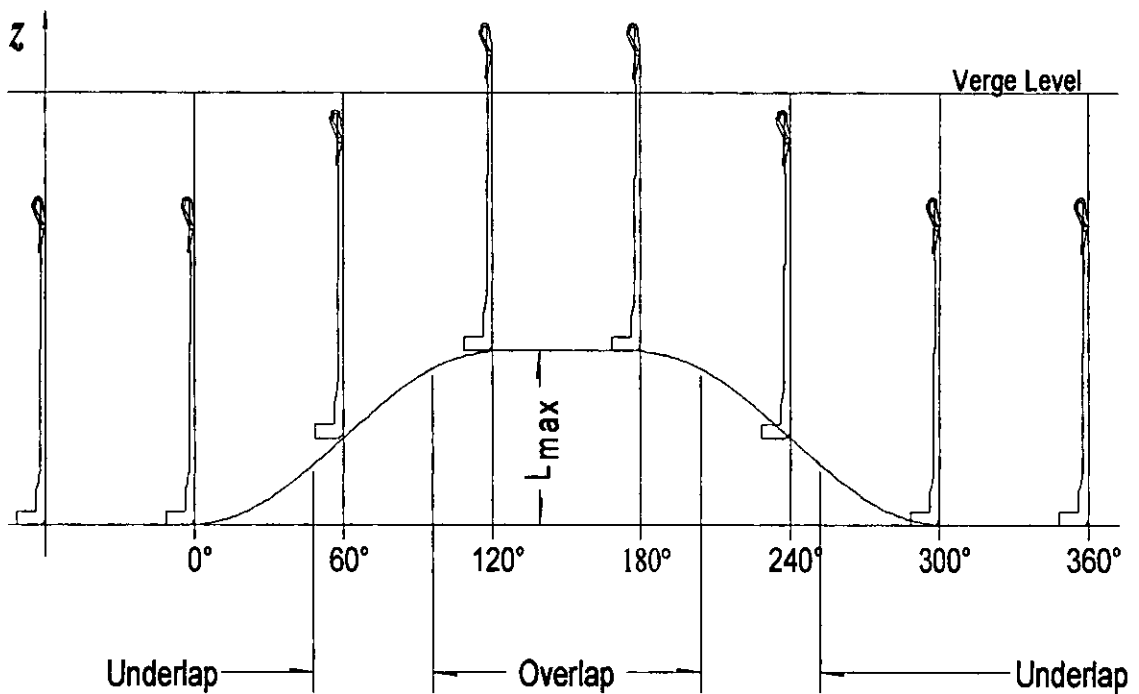


Figure 4-2. Needle Motion with Dwells

Moreover, symmetrical designs such as a pure sinusoidal one do not reflect the needs of a warp knitting cycle because the underlap can generally be longer than the overlap, and therefore a larger proportion of the cycle time should be allocated to perform it.

Sinusoidal patterning mechanisms must allow for this shortcoming by: 1) making faster movements when longer underlaps are required, and 2) allowing excessive time to perform short overlaps.

A new design concept was thought to benefit from including dwells in the needle motion, thus allowing for the patterning mechanism to wrap the yarns around them while stationary (Figure 4-2), as well as from making the underlap longer than that for the overlap.

The benefits of implementing this innovation into the knitting mechanism of warp knitting machines should not be outweighed by the complexity of the mechanism required.

4.3.1.2 Needles Reciprocation

Single Eccentric (Slider-Crank) Mechanism

This is a common mechanism to produce a vertical reciprocation of the needles. It consists of a circular disc rotating about a point at a distance from its centre. Its importance in the context of this research is that by altering the relation between the physical length of the crank, the value of the eccentricity and the radius of the disc, a needle motion incorporating dwells can be achieved.

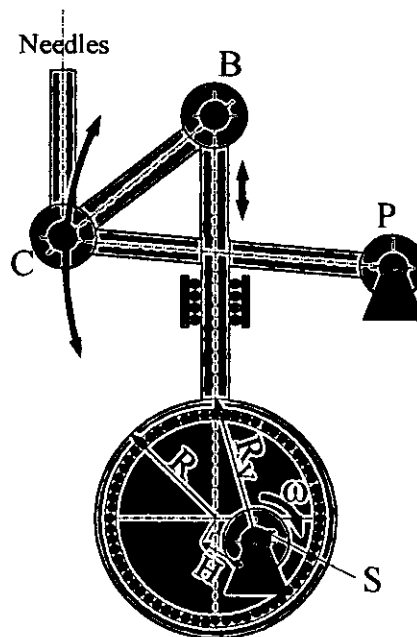


Figure 4-3. Eccentric Schematic

As the motion is dependent on the geometrical features of the mechanism, it is important to understand the possibilities given by this type of mechanism. The following analysis shows the relationships between the critical geometrical variables and the final needle movement.

Figure 4-3 shows a schematic diagram of a single eccentric mechanism design. The shaft S rotates around its centre at $\omega(s^{-1})$, making the lever to B

move vertically guided by linear bearings. This movement provides the driving motion for the oscillation of lever PC about P, to which the needles are attached at C.

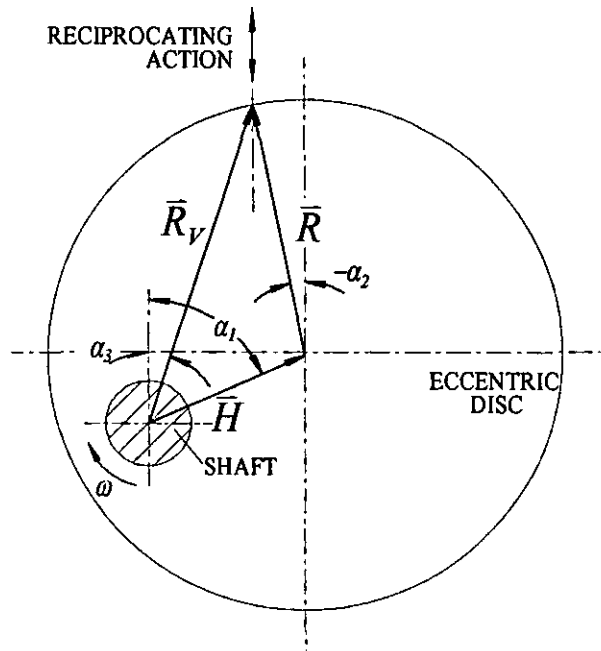


Figure 4-4. Eccentric Motion Geometry

The motion of the vertical reciprocating lever (Figure 4-4) can be described at any instant by the vector addition:

$$\vec{R}_v = \vec{H} + \vec{R}$$

(4-1)

The magnitude of \vec{H} and \vec{R} are constant. Also, at least the horizontal component of \vec{R}_v is known and constant. If the centre of shaft S is aligned with the centre of the vertical lever, then the direction of \vec{R}_v will be known and constant.

In addition, at any given $\alpha = \omega \cdot t$, the direction of \vec{H} is also known. Therefore, at a given α , there are only two unknowns in the system; namely, the magnitude of \vec{R}_v and the direction of \vec{R} . The system can therefore be solved.

In order to solve the system, polar complex numbers can be used and each vector can be expressed as

$$\vec{V} = V \angle \theta = V \cdot e^{j\theta} \quad (4-2)$$

The original system equation (4-1) becomes

$$R_V \cdot e^{j\alpha_3} = H \cdot e^{j\alpha_1} + R \cdot e^{j\alpha_2} \quad (4-3)$$

Where α_1, α_2 and α_3 are measured clockwise from the vertical; this convention illustrates the fact that the motion of R_V starts with a vertical position and rotates clockwise,

$$\alpha_1 = \omega \cdot t,$$

H, R, α_3 are constant.

Dividing equation (4-3) by $e^{j\alpha_3}$,

$$R_V = H \cdot e^{j(\alpha_1 - \alpha_3)} + R \cdot e^{j(\alpha_2 - \alpha_3)} \quad (4-4)$$

Applying Euler's trigonometric equation, we obtain,

$$R_V = H \cdot (\text{Cos}(\alpha_1 - \alpha_3) + j \hat{\text{Sin}}(\alpha_1 - \alpha_3)) + R \cdot (\text{Cos}(\alpha_2 - \alpha_3) + j \hat{\text{Sin}}(\alpha_2 - \alpha_3)) \quad (4-5)$$

which, when separated into complex and real parts becomes the following system:

$$\begin{cases} R_V = H \cdot \text{Cos}(\alpha_1 - \alpha_3) + R \cdot \text{Cos}(\alpha_2 - \alpha_3) \\ 0 = H \cdot \text{Sin}(\alpha_1 - \alpha_3) + R \cdot \text{Sin}(\alpha_2 - \alpha_3) \end{cases} \quad (4-6)$$

From the second equation in the system above,

$$\alpha_2 = \text{Sin}^{-1}\left(\frac{-H \cdot \text{Sin}(\alpha_1 - \alpha_3)}{R}\right) + \alpha_3 \quad (4-7)$$

Substituting α_2 into the first equation, an expression for R_V (the position of the follower) as a function of $\alpha_1 = \omega \cdot t$ is obtained. That is, the position of the follower as a function of time:

$$R_V = H \cdot \text{Cos}(\omega \cdot t - \alpha_3) + R \cdot \text{Cos}\left(\text{Sin}^{-1}\left(\frac{-H \cdot \text{Sin}(\omega \cdot t - \alpha_3)}{R}\right)\right) \quad (4-8)$$

From the motion of the follower, the motion transmitted to the needles can also be analysed using vectors.

$$\overline{PB}^{\text{x}\cdot\text{x}} = \overline{PC}^{\text{x}\cdot\text{o}} + \overline{CB}^{\text{x}\cdot\text{o}} \quad (4-9)$$

Where the signs on top of each vector represent whether their respective direction and magnitude are known (x) or unknown (o).

Both magnitude and direction of vector \overline{PB} are known at each moment in time. On the other hand, only the magnitude of the other two vectors is known. Therefore, the two unknowns in the system are the direction of \overline{PC} and \overline{CB} .

Let γ_1 , γ_2 and γ_3 be the anti-clockwise angle from the horizontal to \overline{PC} , \overline{CB} and \overline{PB} respectively. (4-9) can then be re-written as;

$$\begin{aligned} |\overline{PB}| \cdot e^{j\gamma_3} &= |\overline{PC}| \cdot e^{j\gamma_1} + |\overline{CB}| \cdot e^{j\gamma_2} \\ \Rightarrow |\overline{PB}| &= |\overline{PC}| \cdot e^{j(\gamma_1 - \gamma_3)} + |\overline{CB}| \cdot e^{j(\gamma_2 - \gamma_3)} \\ \Rightarrow |\overline{PB}| &= |\overline{PC}| \cdot e^{j(\gamma_1 - \gamma_3)} + |\overline{CB}| \cdot e^{j(\gamma_2 - \gamma_3)} \end{aligned} \quad (4-10)$$

Squaring and adding together, we obtain;

$$|\overline{PC}|^2 = |\overline{PB}|^2 + |\overline{CB}|^2 - 2 \cdot |\overline{CB}| \cdot |\overline{PB}| \cdot \text{Cos}(\gamma_2 - \gamma_3) \quad (4-11)$$

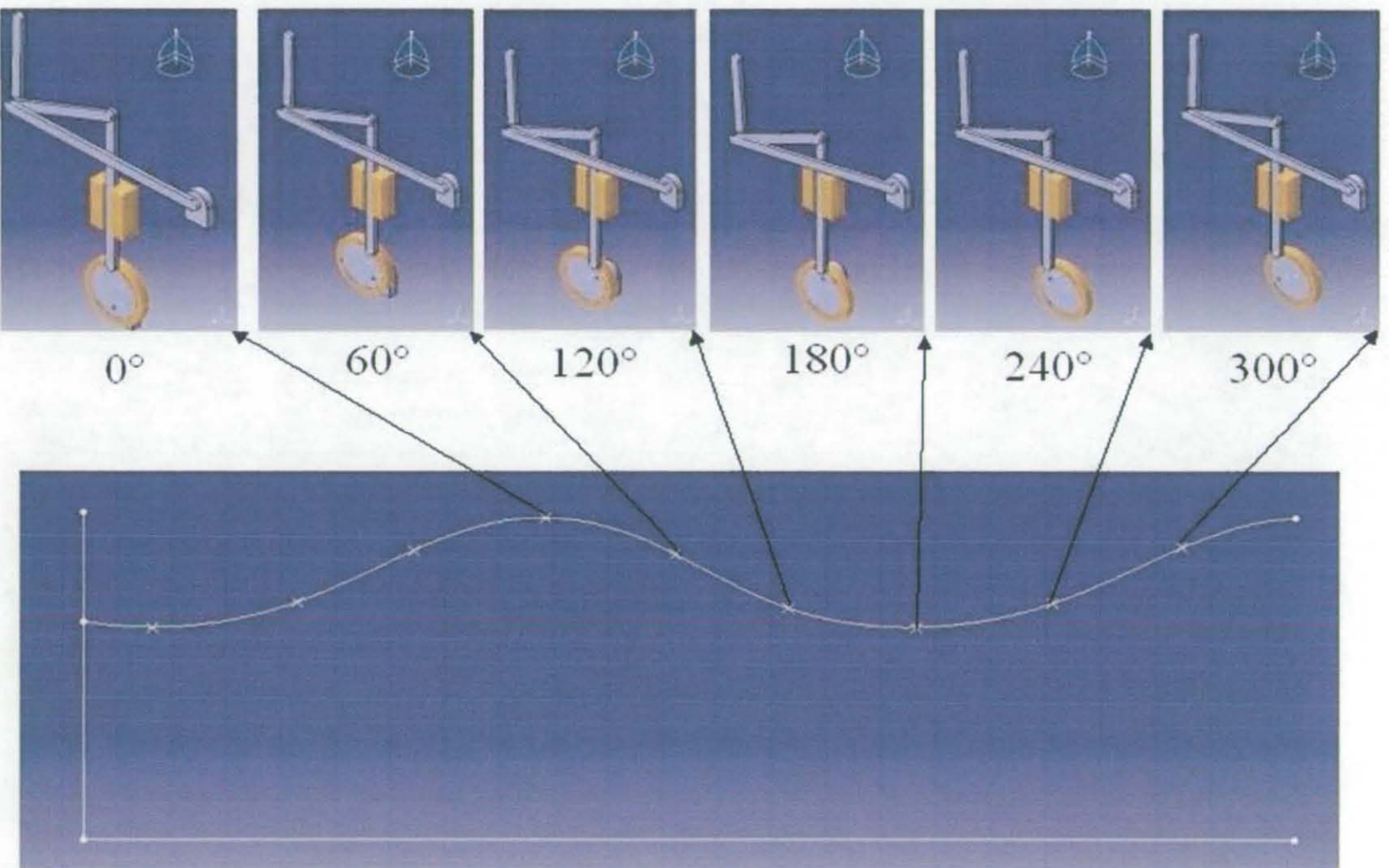


Figure 4-5. Simulation of Single Eccentric Mechanism

Applying the cosine law,

$$\gamma_2 = \gamma_3 \pm \text{Cos}^{-1} \left(\frac{|\overline{PB}|^2 + |\overline{CB}|^2 - |\overline{PC}|^2}{-2 \cdot |\overline{CB}| \cdot |\overline{PB}|} \right) \quad (4-12)$$

Similarly,

$$\gamma_1 = \gamma_3 \pm \text{Cos}^{-1} \left(\frac{|\overline{PB}|^2 + |\overline{PC}|^2 - |\overline{CB}|^2}{-2 \cdot |\overline{PC}| \cdot |\overline{PB}|} \right) \quad (4-13)$$

The needles' movement (offset from point $C(x, y)$) is given by

$$\begin{aligned} C_x &= |\overline{PC}| \cdot \text{Sin} \gamma_1 + P_x \\ C_y &= |\overline{PC}| \cdot \text{Cos} \gamma_1 + P_y \end{aligned} \quad (4-14)$$

The mechanism was modelled using 3-D modelling software (CATIA ® Solutions, version 5), adding kinematics constraints to the joints. The motion was then simulated. A trace of the point to which the needles would be attached is shown in the bottom part of Figure 4-5. The top section of the same figure shows snapshots of the model simulation at 60° intervals. From the figure, it can be seen that in this type of mechanism the sinusoidal shape is modified elongating the valley and shortening the peak or vice versa.

The length $|\overline{PC}|$ should be kept as large as possible to avoid large horizontal movements. The eccentric motion -equation (4-8)- will largely depend on the proportion between R and H; a longer dwell can be obtained by making them very similar, as shown in Figure 4-6.

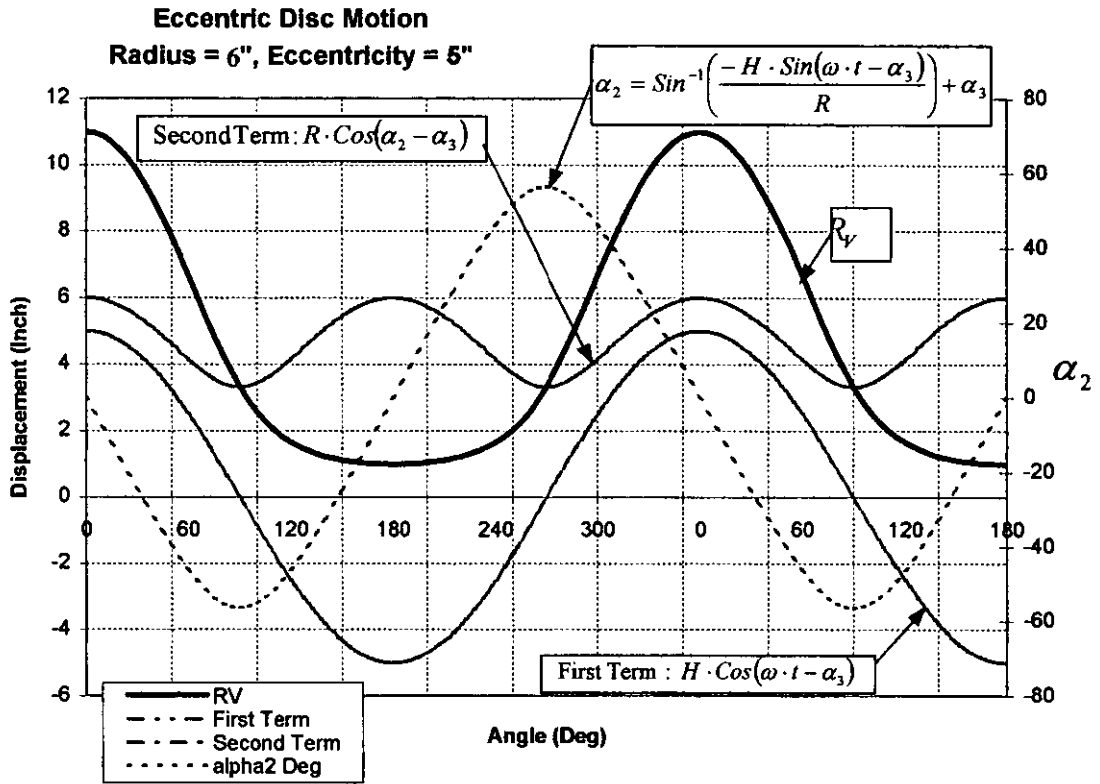


Figure 4-6. Single Eccentric Disc Motion Example

Double Eccentrics.

The double-eccentric mechanism concept is based on the FNF Limited, knitting machine model developed in the 1940's. In this mechanism (Figure 4-7) either needles, or the knitted fabric (as in the case of Figure 4-7), are reciprocated vertically through rods that are linked to two independent eccentric camshafts.

A suitable action for the needles can be achieved by combining the right eccentric motions, as appropriate dwell periods, rises and falls can be obtained by varying different geometrical parameters of the eccentric discs.

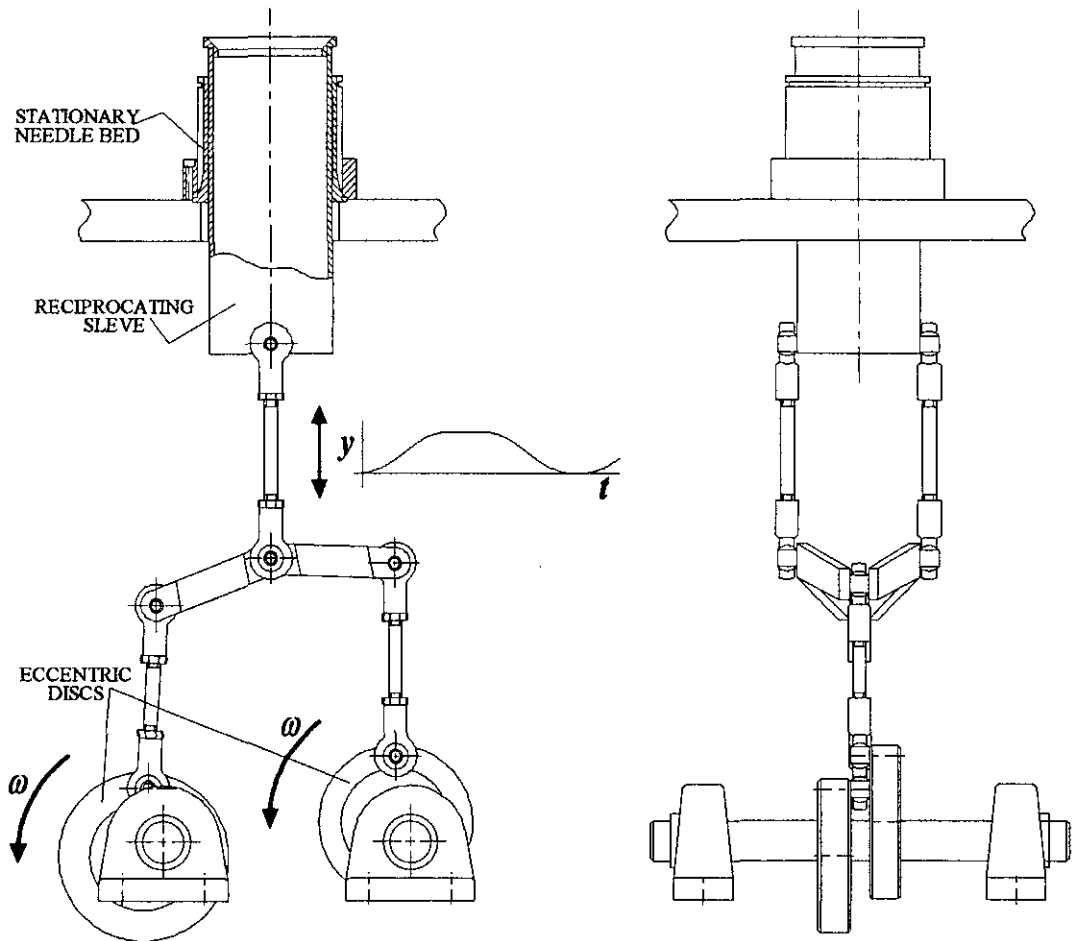


Figure 4-7. Double Eccentric Mechanism Schematic

The motion for the central rods that would drive the needles up and down will depend on the motion of each of the eccentrics as well as the phase between them. equation (4-8) was used to calculate the motion of each of the eccentric discs. Meanwhile, the movement at the central pivot is equal to

the sum of each disc's displacement value at that instant in time, divided by 2; that is, the average of the two instantaneous displacement values. Figure 4-8 illustrates one of the possible combinations.

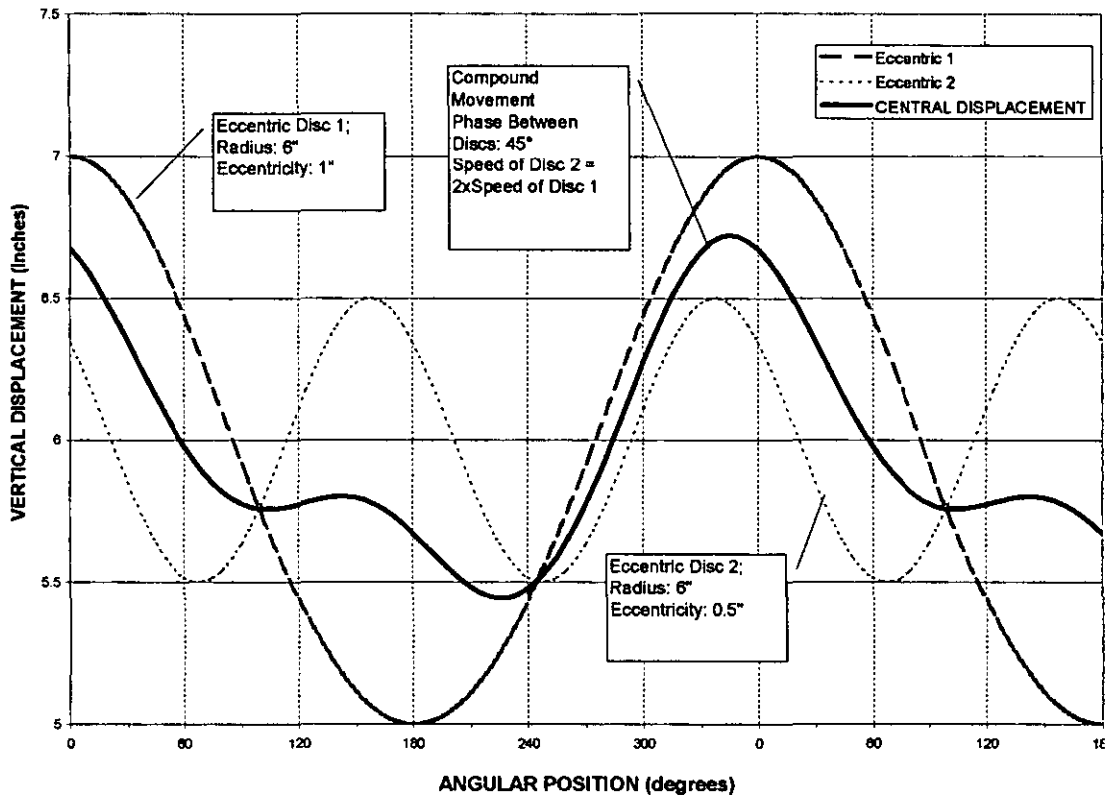


Figure 4-8. Simulated Double Eccentric Motion, Example 1

The longest needle dwell found (by trial and error) with this type of mechanism was created by using two equally sized discs, with similar eccentricity values, and running with no phase or 180° between them.

With a 45° phase angle, every other valley of the motion of the faster disc coincides with a peak of the slower disc and the compound motion produced approximates a dwell (Figure 4-9). The eccentricity of the fast disc should be smaller than that of the slow disc, to ensure that the amplitude of the peaks and valleys of the former are smaller than the latter, and that the second valley does only cancel out the slow disc's peak without creating an unwanted downward movement (a 'mini-valley') in the compound motion.

There are two possible approaches toward this concept. Firstly, the motion could be simulated on a PC until a suitable combination of parameters is found, producing the required rise-dwell characteristic for a general warp knitting requirement and is also appropriate with the geometrical constraints of the machine. The chosen discs are then manufactured with no in-built allowance for alteration, which will reduce the cost of manufacture.

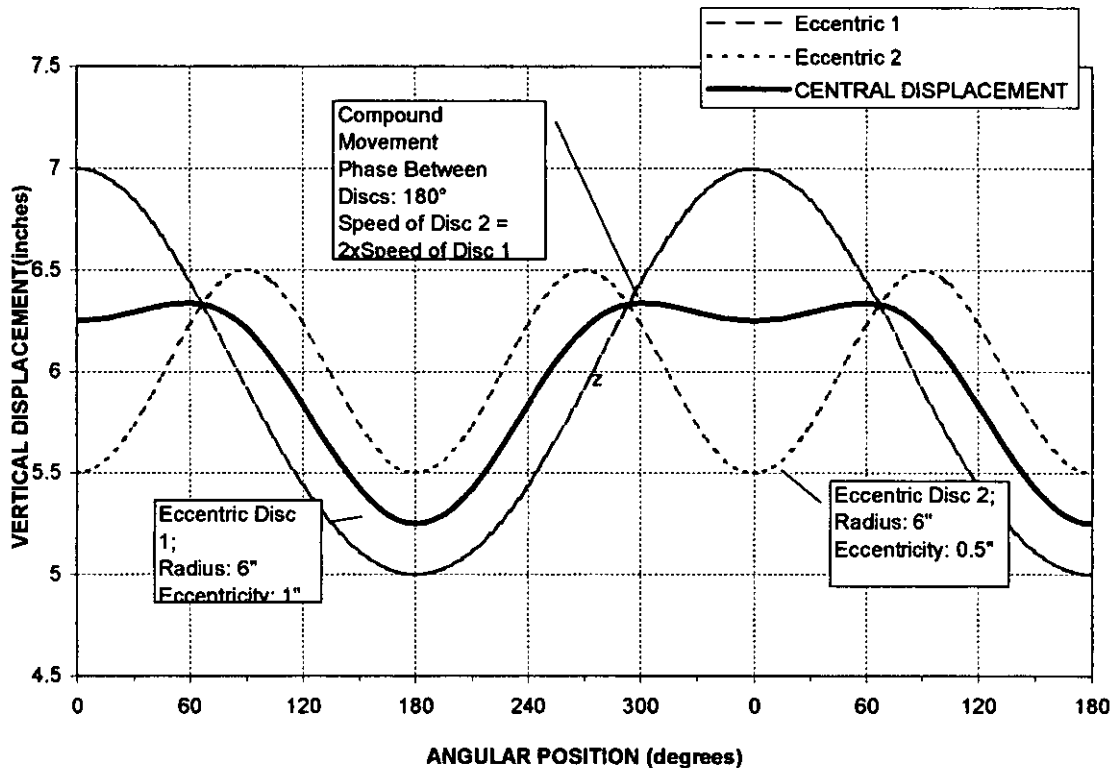


Figure 4-9. Simulated Double Eccentric Motion, Example 2

On the other hand, the concept could be developed to produce a flexible mechanism where the parameters mentioned above could be altered according to the requirements of a specific fabric to be knitted. For example, the long dwell shown in Figure 4-9 would not be necessary in the case of the production of a fabric with short underlaps. If the mechanism can be altered to shorten the dwell, there could be an increase in the machine speed and therefore in its production. This option has the added difficulty that the patterning mechanism (which needs to be synchronised with the knitting) would have to include the same capacity for modifications.

Cam and Follower.

Cams are convenient devices for transforming usually rotational motion to reciprocating or oscillating motion⁴⁸. The curved or grooved surface of the cam imparts the desired motion to the follower. In the warp knitting machine application, the rotating motion imparted by the main motor of the machine needs to be transformed into a translating one at the follower.

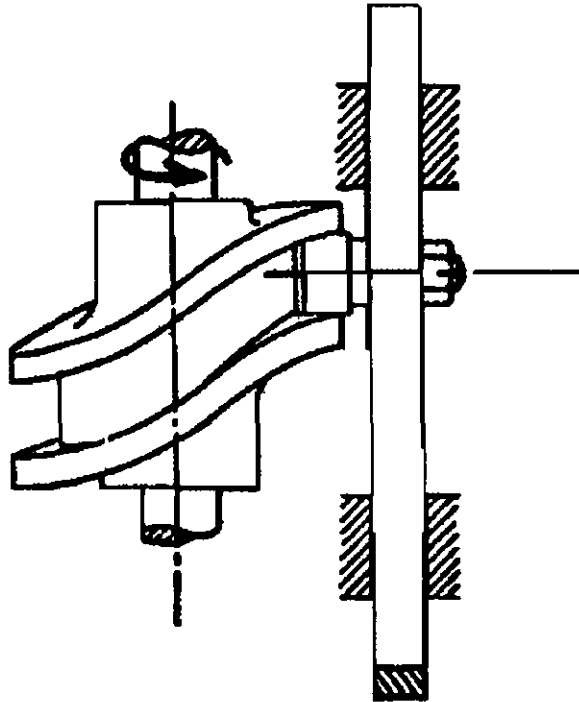


Figure 4-10. Cylindrical Cam with Translating Roller Follower. (After ERDMAN, 1991⁴⁹)

A flat disc shape for the cam was thought to be the most suitable, since the motion required is restricted to a single plane. The three-dimensional cams studied require a more complex profile in 3D space to produce similar planar reciprocating motions (see Figure 4-10).

Given the high speed of rotation of a warp knitting machine, a face cam (that is a disc where the cam track is milled out on a face of the cam) would be preferred to a simple disc cam and spring. At high speeds it is difficult to control the motion of the roller follower at the end of a rise when using a simple disc cam, as the follower tends to leave the disc and can only be prevented from doing so by the spring. In the case of the face cam, the roller

follower is enclosed and it can only move to the outside track at the end of the rise. Thus reducing the deviation from the desired motion to the value of the clearance between the track's width and the follower's diameter.

It should be noted, however, that bouncing from one side of the track to the other will force the roller follower to change its direction of rotation and will create an impact force on the cam. These effects can be analysed in more detail when the parts are manufactured.

The cam and roller follower option has the advantage over the eccentric-based options, in that the most suitable profile for the needle motion can be milled out. It has the disadvantage that it cannot be adjusted for the underlap requirements of different fabrics. It is thought to be the optimal design solution for machines aimed at producing a small range of fabrics only. The requirements of these fabrics, known in advance, will determine the shape of the cam.

The ease of manufacture and the simplicity of a cam-based mechanism makes it the best solution for the needle reciprocation in a warp knitting machine.

The cam profile design procedure will therefore be analysed in more detail in Chapter 5.

4.3.1.3 Yarns Swing

The swing motion can be described as the relative transverse movement of the yarns and the needles that occurs while the needles are moving up or down. The swing positions the yarns behind or in front of the needles' hook before the shogging movement makes an overlap or an underlap. In most flat-bed warp knitting machines there is a separate mechanism that swings the whole guide bar from the front to the back of the needle bar and vice-versa. In a circular machine this would not be possible, since the swing movement becomes a radial one, unless each yarn is swung individually.

To perform the overlap, the yarn guides on a circular machine will form a ring with a diameter just greater than that of the needles. They will have to swing

in radially to form a smaller ring (of diameter just smaller than that of the needles) to perform the underlap.

The issues from the product design specification that affect the swinging mechanism design include:

- i. If swinging the guides on a ring, it should be capable of rotating about its centre (shogging motions) after swinging. This is because the same ring will perform the shogging movement after swinging.
- ii. At least two guide rings are to be mounted on the machine. If the rings are stacked vertically, the higher the ring relative to the needles, the larger the angle required to position the yarn in front or behind the needles.
- iii. The machine should be capable of knitting with a maximum gauge of 20npi, which reduces greatly the space from one guide to the next (depending on the machine's diameter).
- iv. The machine should be designed for a maximum speed of 1000rpm. The machine speed and the proportion of the knitting cycle given to raise and lower the needles determine the speed at which the swinging movement should be performed.
- v. Guides and needles are envisaged to be the most prone to wear and breakage, making it a design priority to allow for their easy replacement.

The following is a summary of ideas generated to solve the swinging mechanism using three different approaches: 1. Swinging the guides on their rings (i.e. the swing as part of the shogging mechanism), 2. Manipulating the threads independently of the guide rings, and 3. Moving the needles radially. (i.e., the swing as part of the knitting mechanism).

1. Swinging the guides on their rings

Among those where the guides were swung on the rings, the most notable was the use of a contracting ring named a spider threader, shown in Figure 4-11.

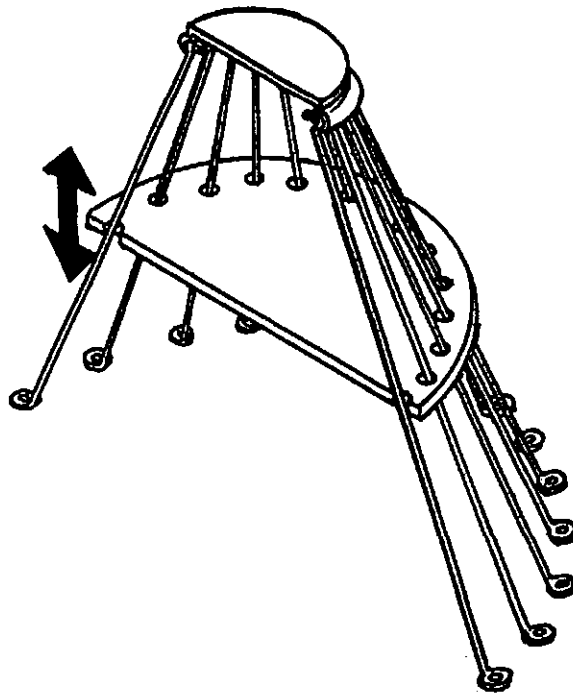


Figure 4-11. Spider Threader

The main advantage of a mechanism of this type is that the driving force is purely vertical, and therefore can easily be coupled to that created by the knitting mechanism (as it will require the same dwells and rises). Its main potential disadvantage being that due to its shape, it might be difficult to fit more than one of them onto a machine.

Another concept envisaged making radial slots on the rings in which the guides, thought of as small tubes inside the slots, would slide in when compressed air was let into the slotted ring. Although air could be an ideal solution to the problem of space (i.e. it would not increase the height of the rings as the previous concept did), the speed of movement required might not be achievable. In addition, a means of synchronising with the other mechanisms needs to be designed, and special attention must be paid to the

design of the air pipes to ensure all the guides move radially in and spring back to their outer positions. See Figure 4-12.

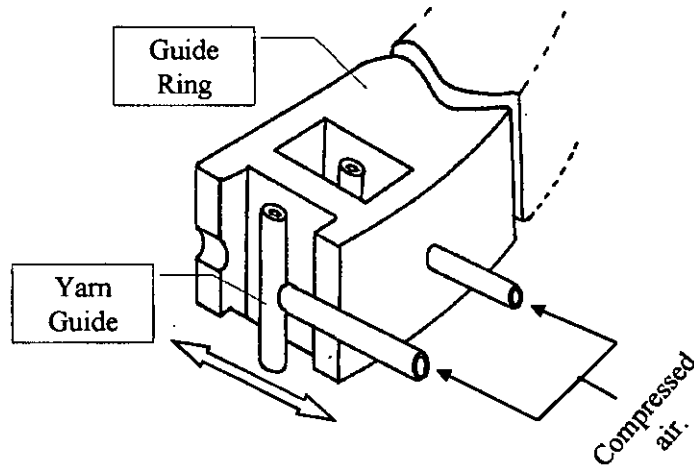


Figure 4-12. Pneumatic Thread Displacement

A third concept, based on an existing sinker ring, was that of a slotted torus. The shape of the slot makes it possible for the vertical driving force to be translated into radial movement.

Again, the vertical drive would be ideal, as it can be taken almost directly from that of the needles, and therefore no extra synchronisation is required. The main disadvantage of this concept is the manufacturing complexity of the slotted torus.

2. Manipulating the threads independently of the guide rings.

Another concept where the shogging motion would be independent from the swinging one involved the development of a mechanism based on the camera lens shutter shown in Figure 4-13.

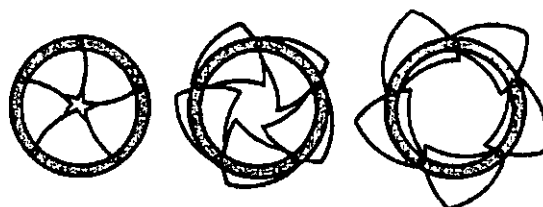


Figure 4-13. Camera Lens Shutter.

The main advantage of this mechanism being that this technology has already been proven to work at high speeds (generally up to 1/1000 of a second), although with no load on it. It would be, however, very difficult to implement it when four patterning rings are required, since all the threads would be taken inwards at the same time.

3. Moving the needles radially.

These ideas were based on the needles moving radially in and out as they were reciprocated vertically.

The best concept involved the needles sliding on a cylinder, each of them enclosed inside a 'trick' cut along its outer face. These tricked cylinders are the standard in weft knitting machines.

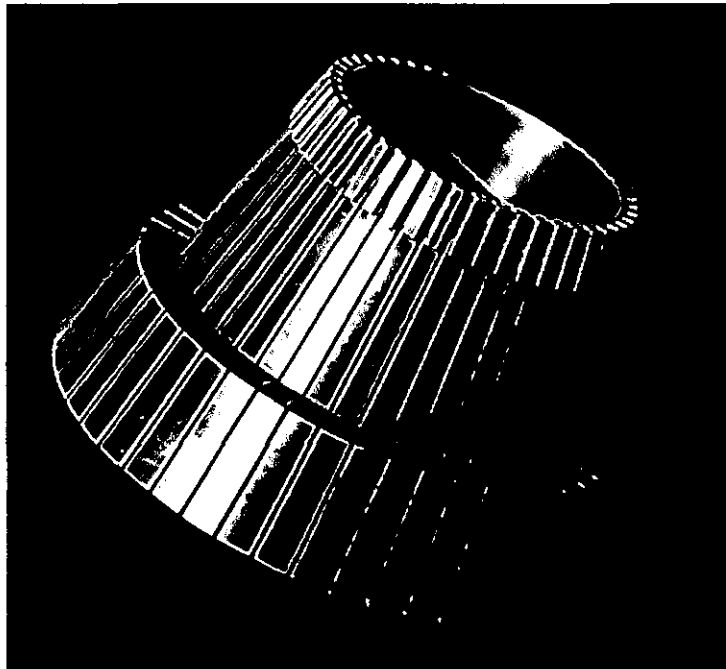


Figure 4-14. Tricked Cone Concept

In order for the needles to move radially, the cylinder could be tapered (making a cone instead Figure 4-14). The needles, sliding at an angle to the vertical, would be moving inward as they are driven up and outward as they

fall. The appealing advantage of this concept is that there is no need for an extra mechanism to perform the swinging movement.

However, the means of transmitting the vertical force from the main knitting mechanism into the set of angled needles without creating excessive bending moments is not straightforward.

Finally, and following the idea of moving the needles radially rather than the guides, a concept involving the needles being pivoted at their bottom was also developed (Figure 4-15). This concept is very similar to that of the contracting guide ring described earlier. It does not have the problem of lack of space, as there will always be a single set of needles, regardless of the number of patterning rings. It has however a drawback; there are no standard needles that would easily lend themselves to pivoting around a ring, and therefore special ones would have to be designed thus increasing the cost.

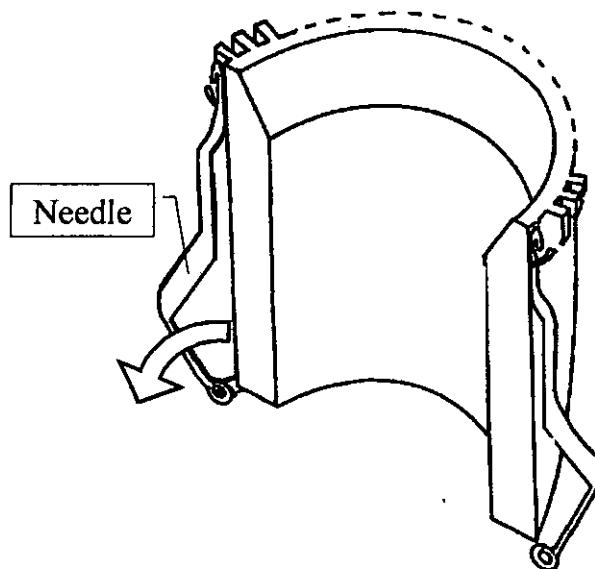


Figure 4-15. Pivoted Needles Concept

If this concept was to be developed, special attention must be paid to the synchronising of the swing motion with the needles reciprocating vertically. Both movements should be carried out simultaneously to: 1) make the

mechanism more efficient; and 2) reduce the variation in yarns tensions that would probably cause faults in the knitting process.

The fact that the tricked cone is the only concept where the whole swinging mechanism can be avoided, as it combines both the swing and the vertical reciprocation in the same movement, made it an excellent solution to the problem, outweighing all of the other concepts mentioned. It can not only increase the speed at which a stitch is produced, but more importantly it simplifies the yarns movement, that will now only involve the tangential motion of threads relative to the needles.

4.3.1.4 Yarns Shog

The shogging mechanism could be seen as the most important mechanism in a warp knitting machine. This is because it limits the machine's patterning flexibility. Having isolated the swinging problem from the shogging one, the latter is now simplified to designing a means to rotate threaded rings about their centre in the smallest possible space, but allowing for easy threading of the rings.

Minimising the space used is emphasised because the angle that a ring needs to be rotated in order to shog over a given number of needle spaces increases with the vertical distance between the ring and the needles. Therefore, in order to minimise the amount of rotation required, all rings need to be as close as possible to the needles.

Concepts for the physical means of driving the patterning rings generally reverted to a combination of pulleys and gears, given the restriction of space. Room for innovation in the patterning mechanism lies in the way the fabric design is transmitted to the threaded rings.

This part of the patterning mechanism has evolved throughout the years. Currently, a common mechanical flat warp knitting machine patterning mechanism is based on coupling a series of different sized links either onto a drum or to make a chain. The size of each link will determine the amplitude of the shog for a given guide bar. Electronic machines use controllers to

rotate eccentric discs, which in turn will shorten or lengthen the travel of a guide bar.

For the implementation of a mechanical design, a chain link system similar to that already in use by flat machine manufactures could be adapted to work for a circular machine. However, a cam-based mechanism was thought to be preferable. The advantage of the latter being a reduction in cost. Its main disadvantage is the lack of flexibility (each fabric will require a new cam manufactured).

A much more flexible and innovative design, for an electronically controlled machine, was based on the use of servomotors driving each of the patterning rings. The servomotor controllers can store programs with the series of movements required by a given fabric design.

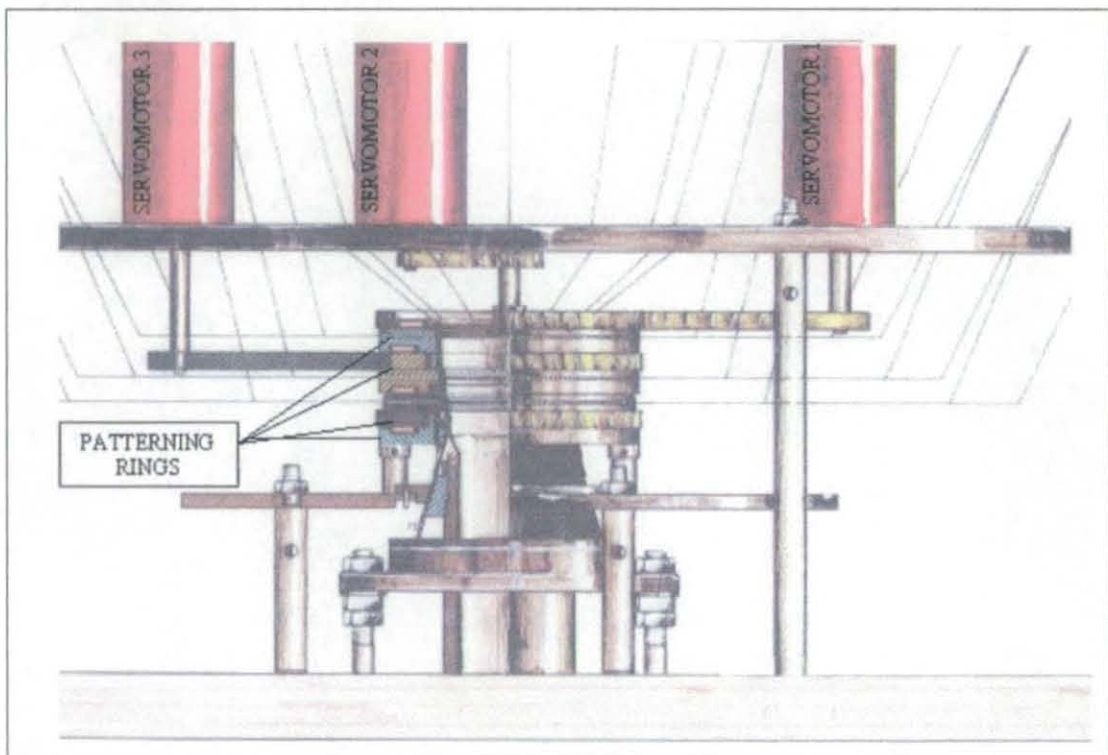


Figure 4-16. Four Rings Driven by Servomotors

It was decided to use three rings as a first design option in order to substantiate the concepts discussed. The design of the location of the rings and the rings themselves depend largely on the way they are intended to be driven. Figure 4-6 shows the three rings stacked vertically and separated by

thrust bearings. This concept is possible because the rings are driven by three spur gears, each one connected to a servomotor.

A mechanism like the one illustrated in Figure 4-16, has the added cost of the design of the servomotor controllers and the development of a user interface to program them. The cost of the servomotors will also increase the cost according to the power required. However, an electronically controlled shogging mechanism will give the machine the maximum patterning flexibility, and therefore makes it the best solution concept.

An adjustable let-off mechanism based on cones and not warping beams, would be ideal to complement a flexible patterning mechanism, as it would not pose any obstacle for the creation of new and different fabrics. A means of synchronising the two should be developed.

The servomotor program should include the appropriate dwells in the ring rotation when the needles are being raised or lowered, and a means for synchronisation between the shogging movement and the knitting mechanism should be devised.

One of the main difficulties with compact systems like this one is that the threading can become painstaking and time-consuming. Depending on the machine diameter and the number of rings, hundreds of yarns need to be threaded through very small holes and linked to the right needles. This must be taken into account during the detail design of this mechanism.

4.3.2 Secondary Mechanisms

4.3.2.1 Let Off Mechanism

There are mainly two ways of feeding in the threads coming into a knitting machine; using warping beams or feeding directly from cones. The former is the most common method in the warp knitting industry while the latter is mostly used for weft knitting machines. The basic deciding factor is the number of threads required by the machine. This is because the overhead costs incurred when using warping beams can only be justified when used with a large number of threads.

In both cases, the primary function of the let-off mechanism is to feed the warp threads into the knitting elements at a rate consistent with the fabric construction. In weft knitting this is generally achieved ensuring a constant velocity of the threads by using positive feed units. This mechanism is very effective when a small number of threads are needed. However, it is not thought to be feasible for large scale warp knitting machines where the warp sheet is made up of thousands of threads.

The most common warp beam let-off mechanisms have been explained in Chapter 2.

In the case of the circular warp knitting machine, the number of threads will not generally be large enough to justify a warp beam mechanism but not sufficiently small either to use a weft knitting positive feed system. An intermediate solution had to be devised. The design brief for this mechanism can be summarised as follows;

- i. The Let-off mechanism should be positive in action, that is, the yarns should be fed to the knitting elements at an appropriate speed to maintain consistent tension rather than the let-off mechanism being activated only when a tension build-up on the warp sheet occurs.
- ii. The threads should be fed from cones (to avoid the extra investment) but the mechanism to ensure an appropriate speed and tension of the yarns should be a common one for the whole warp sheet. Using a

positive feed device for each yarn requires too much space and becomes very expensive.

- iii. Generally, a warp knitting machine should have as many warp sheets (and thus let-off mechanisms) as patterning rings. This is because the required feeding speed and tension will vary from ring to ring according to the fabric structure. The exception to this rule being symmetrical fabric structures (such as netting) where two rings will require the same feeding speed and tension, as the laps performed by both rings are exactly the same and opposite and therefore can share the same let-off unit.
- iv. The feeding speed should be maintained constant (relative to the speed of the machine). Although the fabric structures do require different amounts of yarn throughout the knitting process (e.g. more yarn is required for longer underlaps), it is thought feasible to maintain constant feeding speed and regulate the tension with tension springs placed as close as possible to the knitting elements. This assumption will simplify the design. This decision was based on the present mechanisms used in warp knitting machines, where constant linear speed designs have superseded tension-controlled ones.
- v. The mechanism should be easily adjustable to different linear feeding speeds as each fabric structure will require a different setting. Moreover, the quality of the fabric (that is, the number of courses per knitted inch of fabric) is largely dependent on the let-off speed, and therefore feeding speed may be altered to increase or decrease the quality of a given fabric while in production.
- vi. The let-off mechanism drive should be dependant on the main drive of the machine, as the let-off speed must vary proportionally to that of the machine.

The let-off mechanism concept used for building the circular warp knitting machine comprised a standard creel, a stand-alone eyelet board, a driving unit, an adjustable speed drive and a set of yarn detectors (Figure 4-17). The

driving unit is based on the design of a standard weft knitting take-down unit with the fabric being driven through rubber covered rollers pressed together with compression springs at their ends. The let-off is connected through pulleys and belts to the main shaft; the speed of the feeding rollers controlled with an adjustable gearbox, which drives one of the rubber covered rollers via timing belt and pulleys. The second roller is driven by a spur gear and extra pressure to ensure that the yarns do not slip is achieved with the use of compression springs at each end of the driven roller.

Relative speed ratios between the different let-off units (there will be one for every patterning ring) are also altered using change-gears, the assembled mechanism and the change gears in particular, are shown in Figure 4-18.

The yarns are fed from the roller into the patterning rings via a series of rings with ceramic eyelets (see Figure 4-19). Connected to each eyelet is a spring with a second eyelet attached through which the yarns are also threaded. This spring helps to compensate for the tension variation throughout the knitting cycle.

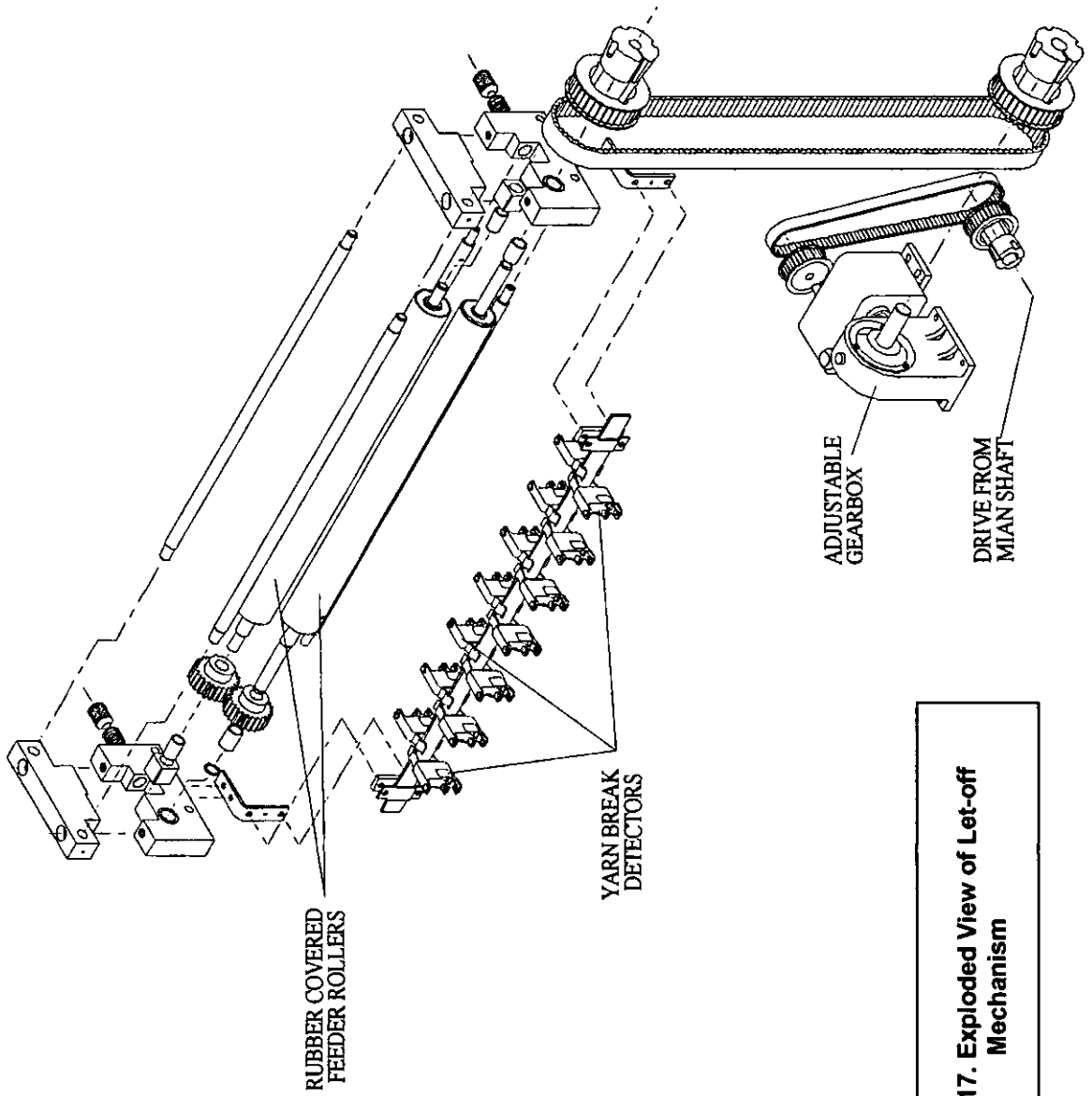


Figure 4-17. Exploded View of Let-off Mechanism



Figure 4-18. View of the Let-off Change Gears.

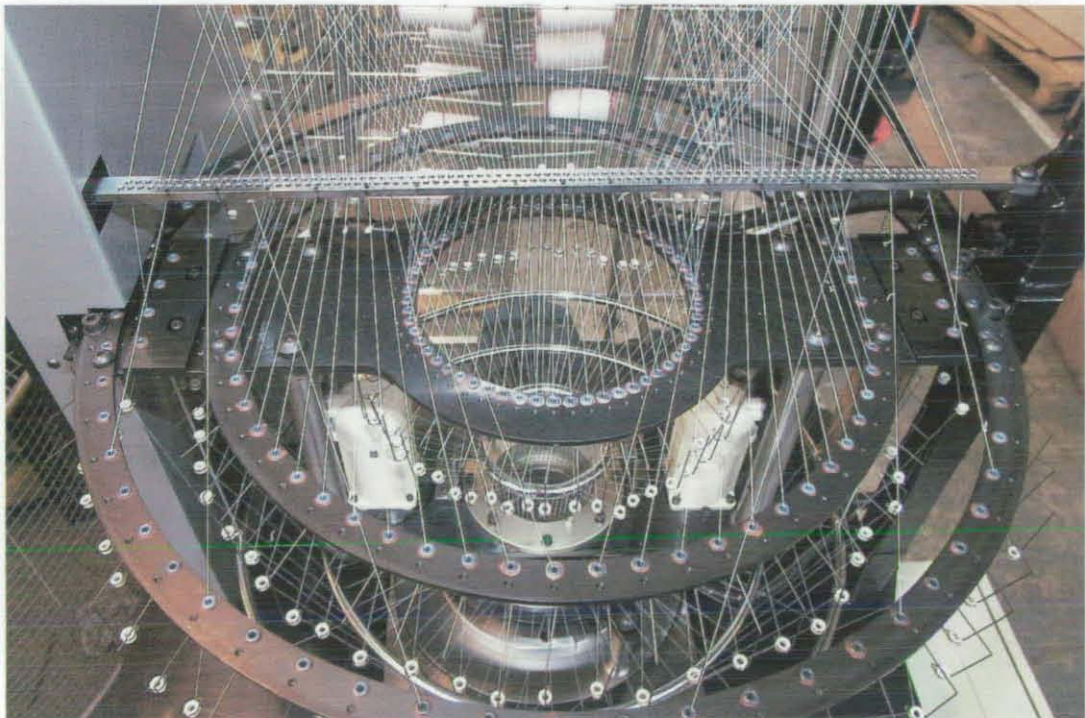


Figure 4-19. Let-off Yarn Supply Plan View

4.3.2.2 Takedown (or Take-up) Mechanism.

The main function of a takedown in a warp knitting machine is to maintain an adequate tension in the fabric being knitted. The takedown speed should be proportional to that of the let-off to maintain consistent fabric tension (unless special effects are sought by varying the tension of a given fabric during its production).

The most important requirements for the takedown mechanism of the circular warp knitting machine are;

- i. It should be positive in action, either continuous or intermittent as explained in Chapter 2.
- ii. It should be adjustable to ensure the versatility of the machine since every fabric produced can have a different setting; and is repeatable in order to reproduce production settings after changing the fabric structures.
- iii. Since the takedown mechanism will work in conjunction with the let-off to ensure consistent fabric quality, both mechanisms should be synchronised to the machine drive.

The takedown unit thought to be most suitable is based on one commonly used in weft knitting machines. An exploded view of the system as adapted for the warp knitting machine is shown in Figure 4-20.

The takedown is driven from the machine's main drive or from the let-off mechanism through timing belts and pulleys and a fixed right angle gearbox. A set of change gears then enable the user to adjust the speed ratio between the takedown and main drive or let-off. The fourth gear drives the central rubber covered roller. The other two are driven using spur gears and, as in the let-off, extra tension between the rollers is achieved by using compression springs. Three rollers are required to provide sufficient grip on the fabric to counteract the force imparted on the fabric by the needles when they rise to make a stitch.

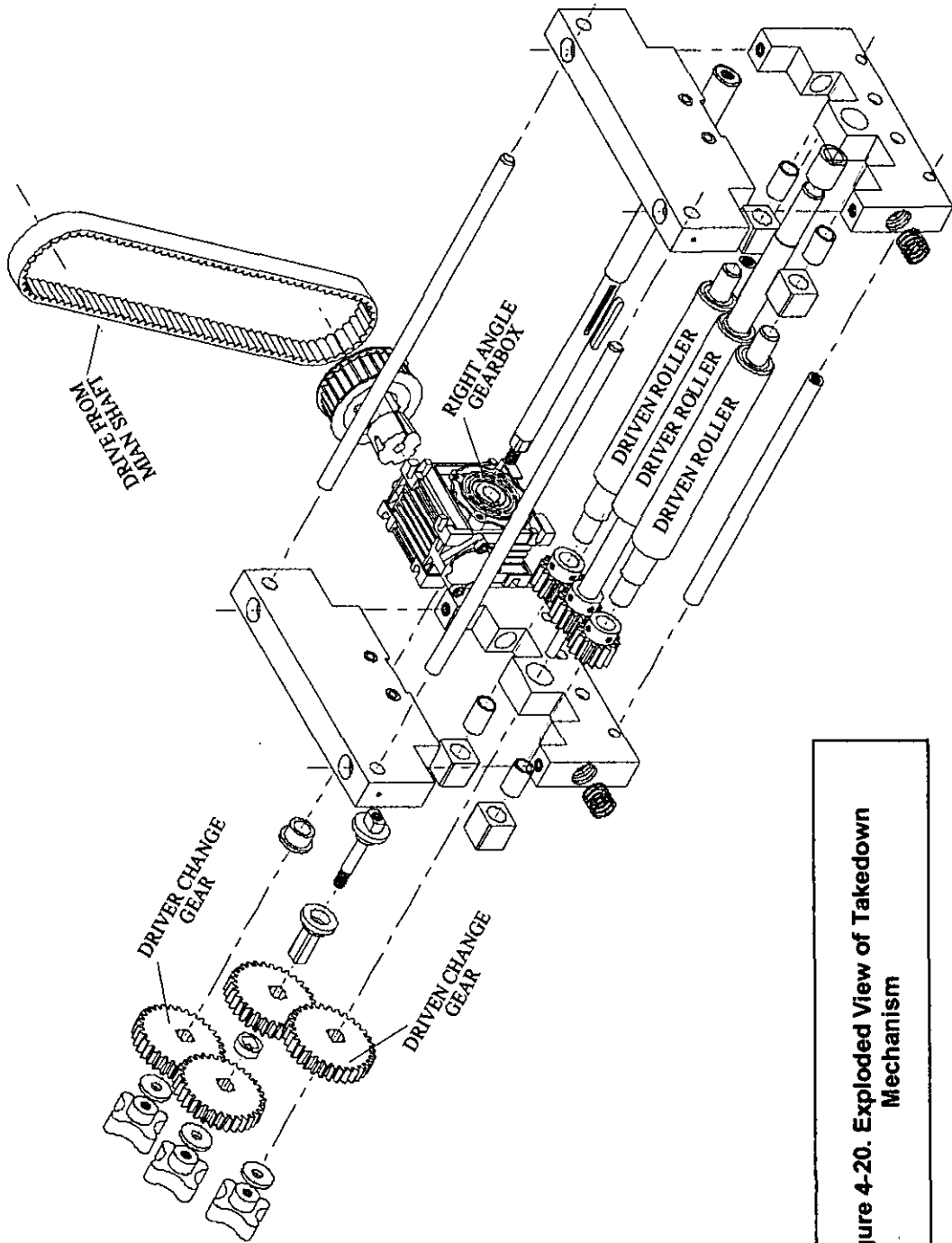


Figure 4-20. Exploded View of Takedown Mechanism

4.4 Conclusions

In this chapter, the methodology for developing a design specification was described. The main design decisions stemming from the PDS database provided a starting point for the generation of concepts for each of the functional assemblies of the machine.

The concepts generated were described and compared. In the case of the secondary mechanisms, the solutions implemented were also described. For the main mechanism, namely knitting and patterning, the preferred concepts were selected. The implementation of these solutions will be presented in the next four chapters; Chapters 5 and 6 deal with the design of the knitting mechanism, while Chapters 7 and 8 with that of the patterning mechanism.

Chapter 5. Knitting Mechanism.

5.1 Introduction

This chapter is the first of two dedicated to issues stemming from the knitting mechanism design and its main aim is to demonstrate which issues or parameters affect the performance of the mechanism and how the effect of each one can be characterised.

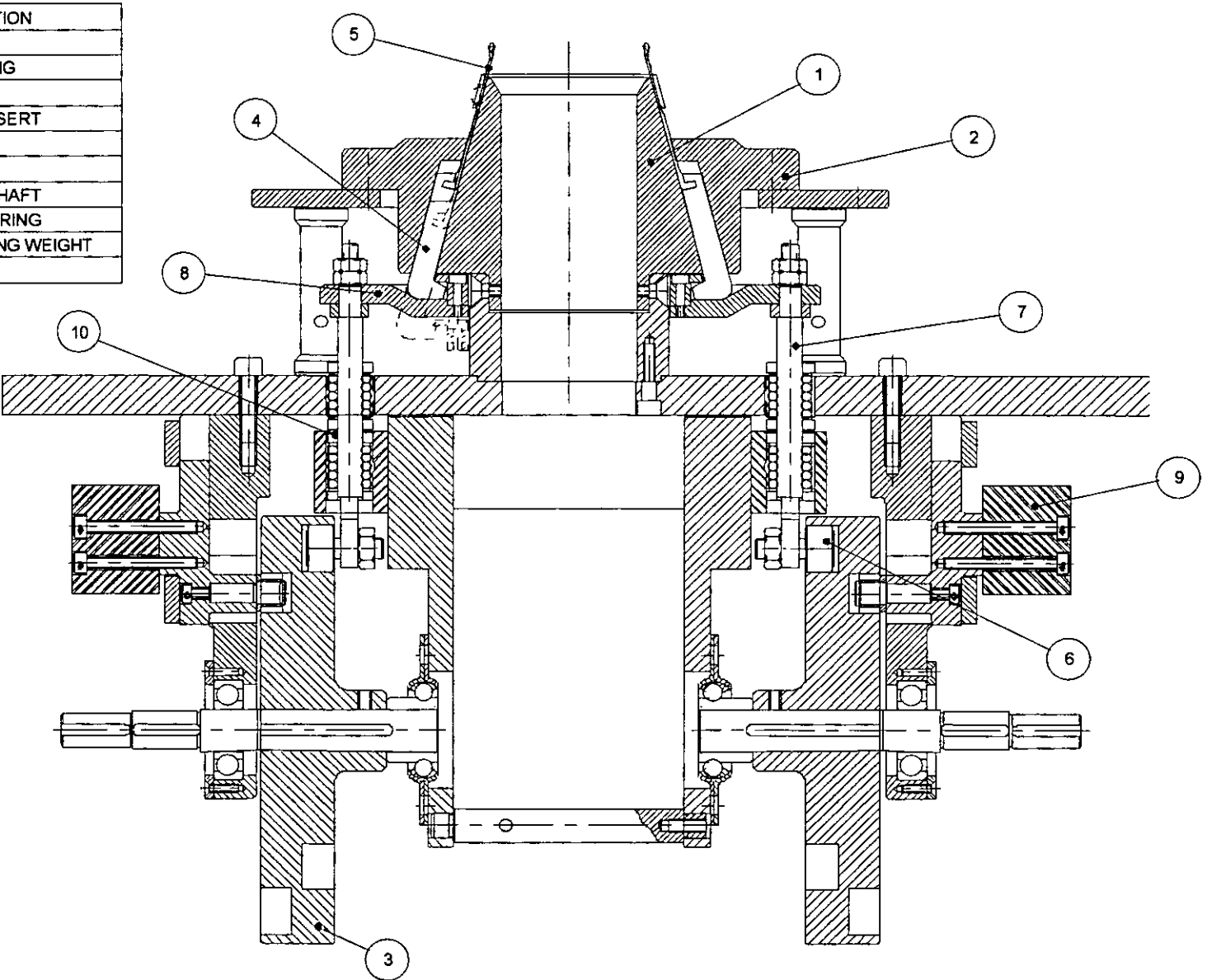
In order to achieve that aim; firstly, the design solution is described in section 5.2; then, the consequences of the design decisions are analysed theoretically in the form of a kinetic analysis of the mechanism in sections 5.3, 5.4 and 5.5 and; finally, the actual performance of the mechanism once designed and built is compared to the theoretical analysis in section.5.6.

5.2 Cam and Follower Design Solution

The cam and follower option was chosen for development with the circular warp knitting machine to be designed and manufactured, because of its convenience and simplicity in transforming rotating motion into a combination of vertical rises, dwells and falls.

Figure 5-1 shows a schematic assembly of the components of the knitting mechanism designed and built for the circular warp knitting machine..

The core of the knitting mechanism is the conical needle bed (see part 1 in Figure 5-1). It was designed and manufactured using techniques adapted from those used in the production of weft knitting cylinder. The needles slide inside tricks (narrow slots in the cylinder) and they are forced to remain parallel to the cone taper by a clamp ring (part 2 in Figure 5-1)



#	DESCRIPTION
1	TRICKED CONE
2	NEEDLE CLAMP RING
3	KNITTING CAM
4	STRNGTHENING INSERT
5	NEEDLE
6	CAM FOLLOWER
7	RECIPROCATING SHAFT
8	NEEDLE SUPPORT RING
9	COUNTERBALANCING WEIGHT
10	LINEAR BEARING

Figure 5-1. Schematic Assembly of Knitting Mechanism Components

At the top of each trick, a wider slot is manufactured to allow the loaded needle (with a loop around its hook), to slide below the verge level. The stitch lengths will be proportional to the length of travel below the verge level. Figure 5-2 shows the top part of the assembly with the threaded yarns, and the needles at their lowest position.

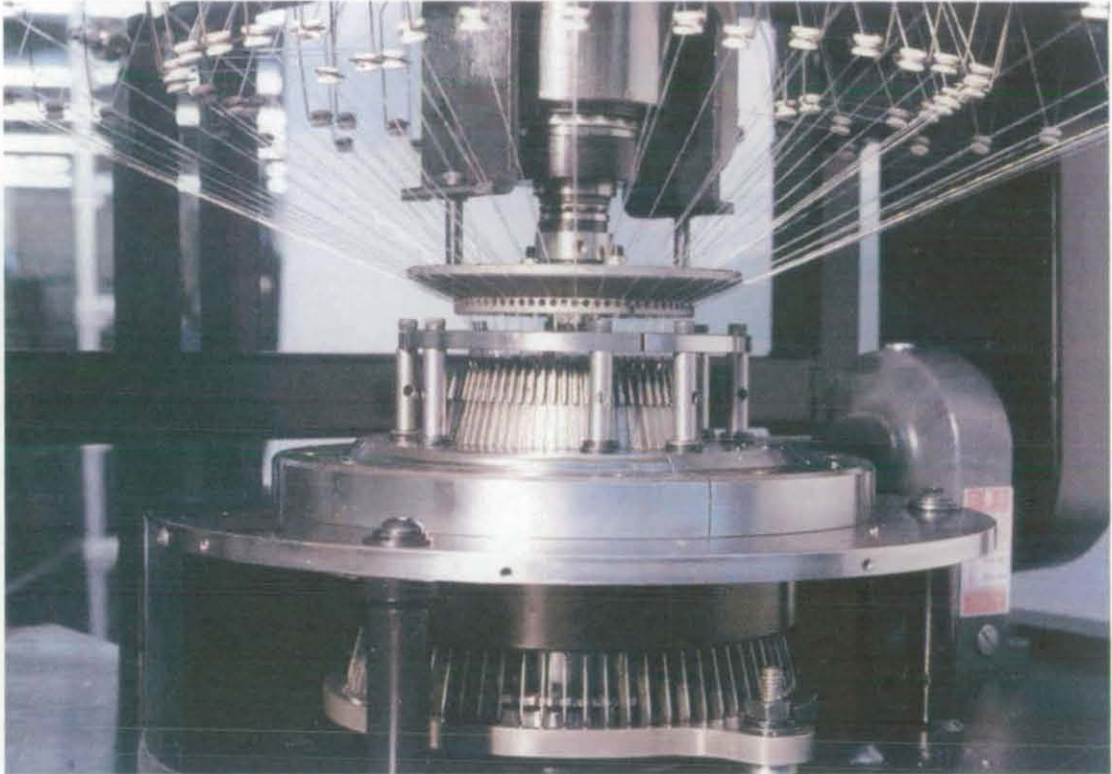


Figure 5-2. Conical Needle Bed with Needles (Down) and Yarns

The fabric is formed inside the cone and pulled downwards by the force from the rotating takedown rollers.

The length of the needle and stroke above the verge level, on the other hand, should be sufficient to ensure that the loop on the needle clears the latch spoon, when the needle is at its highest position. That is, when the needle is at its highest position the latch spoon is 3 or 4mm above the verge level (Figure 5-3).

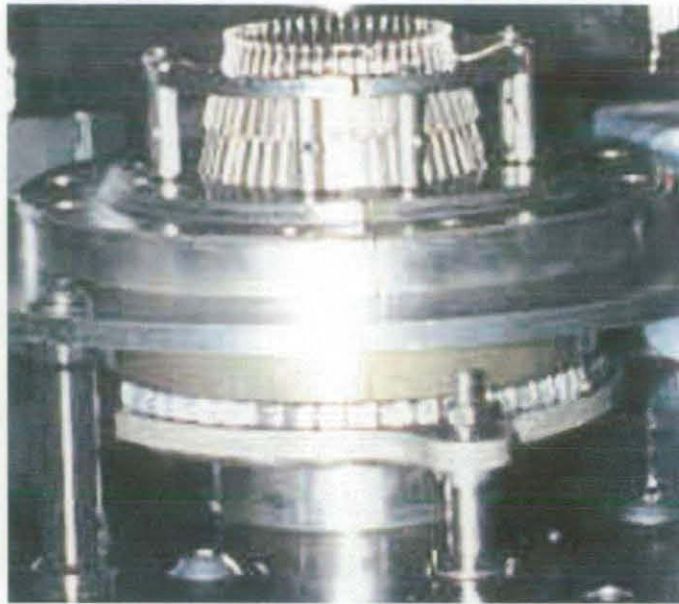


Figure 5-3. Needles at Their Highest Position

The needle selected (Groz Beekert HOFA 71.80.G01) would normally be clamped to the reciprocating parts using its butt. However, because the needles' motion is parallel to the conical needle bed, a means of transforming the vertical reciprocation motion imparted by the cam into the transverse motion of the needle was required. The solution was achieved by designing the strengthening inserts shown as part 4 in Figure 5-1. They have the same thickness (or gauge) as the needles (0.032 inches) and have a slot dimensioned and toleranced to fit a needle butt exactly, acting as an extension of the needle.

Their width, substantially larger than that of the needles, provides them with the strength required to withstand the bending moments that arise from the transformation from vertical to diagonal motion. The bending moments occur when the needle and insert pairs descend, for example, and the vertical downward pull tends to rotate the pair away from the needle bed but the bottom end of the trick and the needle clamp ring will force them to remain parallel to the cone taper.

The actual transformation of motion is created by the design of the lower section of the strengthening inserts and the way it is joined with the reciprocating parts. The interaction between the inserts and the needle support ring assembly can be described as follows:

When the needle and insert pairs are about to start their downward motion, the curved surface at the bottom of the insert is at the lower end of the tapered surface of the needle support ring (part 8 in Figure 5-1). This instant is captured in Figure 5-1.

As the needle support ring assembly moves downwards, the needle and insert pair move downward parallel to the cone taper sliding up the conical slope of the support ring. Therefore, at the needle and insert pair lowest point (see dotted insert in Figure 5-1), the curved surface of the insert is resting on the higher end of the needle support ring slope.

The needle support ring assembly includes a clamp ring, attached on top of the support ring itself. When the needles descend, they will actually be in contact with the clamp ring filleted surface, and when they rise the contact occurs between the support ring's tapered surface and the inserts.

The dimensioning and tolerancing of the support ring assembly is therefore important; firstly, the support ring taper must be parallel with the flat sliding planar surface of the inserts.

Also, the clearance left between the inserts and the two components of the support ring assembly should be minimal to avoid extra shock forces at the end of the rise or return motions of the cam.

The support ring taper angle affects the forces imparted onto the needle and insert pairs and can augment or reduce the bending forces. The free body diagrams later in the chapter will show this.

The support ring assembly is fixed rigidly to the two reciprocating shafts (part 7 in Figure 5-1). Each reciprocates vertically guided by two aligned linear bearings (part 10 in Figure 5-1), and is attached rigidly to a roller followers (part 6 in Figure 5-1) that moves inside the track milled on the face of a cam. Two identical cams are used in the mechanism (part 3 in Figure 5-1); their synchronicity is ensured by keyways added to the cam blanks to which the milling of the cam profile is referenced. The selection of the cam profile is discussed in detail later in this chapter and in Chapter 6.

The system is driven by a moment applied to the camshaft. The cam track transmits a force F to the follower in the direction of the pressure angle, that is, perpendicular to the instantaneous slope of the track. The vertical component of force F drives the needle support ring vertically.

A counterbalancing sub-assembly can also be added to the mechanism defined. Driving an equivalent mass to that of the needles, on a motion equally opposite, it was intended to reduce the shock forces of the original reciprocating mass. The effects of this assembly on the performance of the machine are discussed in more detail in section 5.6. The counter balancing weights (part 9 in Figure 5-1) are reciprocated vertically using a second cam track milled on the back face of the cam. The track's profile is a mirror image of the original with respect to the horizontal axis; in that way, when the needles rise, the counterbalancing weights descend (using the same displacement profile) and vice versa.

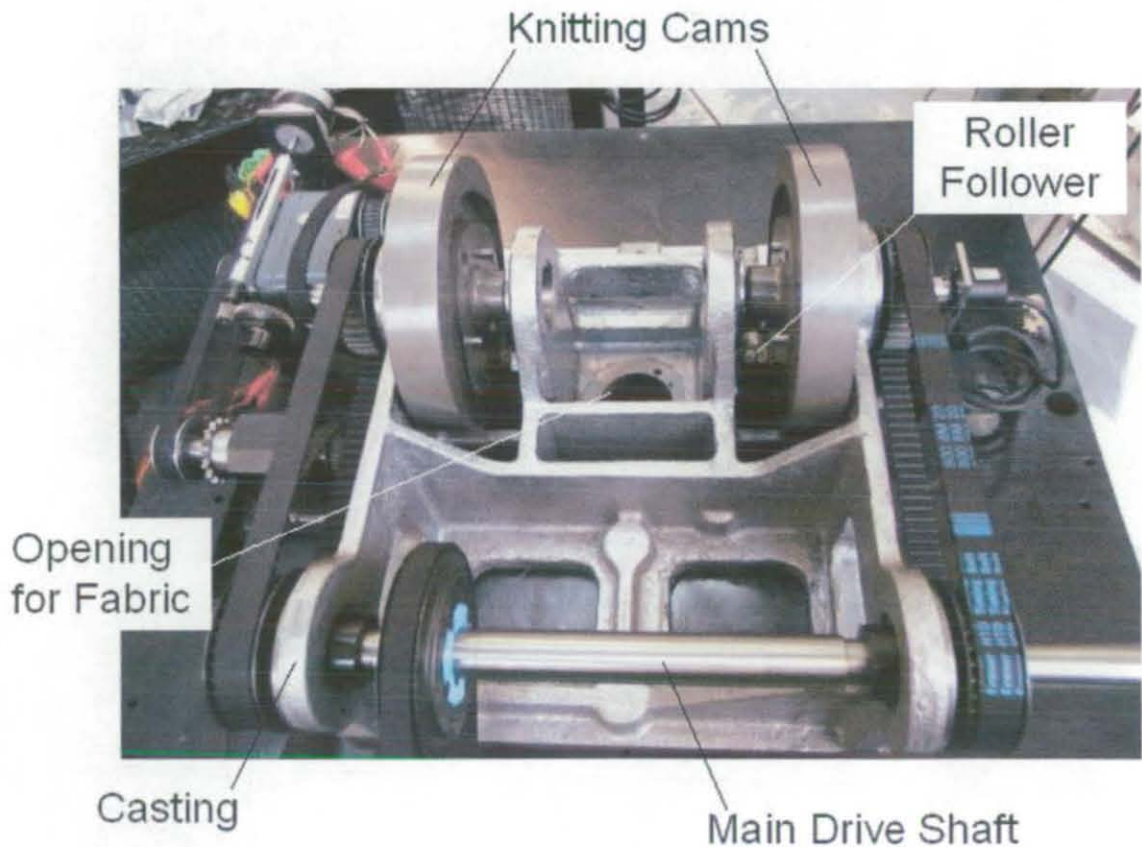


Figure 5-4. Picture of Casting for Knitting Mechanism

A casting was designed to include all the stationary and supporting parts below the conical needle bed, once the concept was proven in order to simplify the physical assembly of the mechanism. Figure 5-4 shows the assembly (viewed from the bottom). Figure 5-5 is a detail of the assembly showing the roller follower inside the cam track.



Figure 5-5. Detail of Roller Follower in Cam Track

There are two design issues that will greatly affect the performance of the system.

Firstly, it is necessary to design the most appropriate cam profile, since it defines the equation of the vertical driving force as a function of time; i.e. it provides an important part of the equation of motion for the system. It has been proposed in the concept evaluation, that this needle motion should include dwell periods during which the yarn movements take place. This

would be a main innovation to the general warp knitting cycle, but this will create the need for a completely different type of cam to those used at present in traditional flat warp knitting machines (mostly based around eccentric mechanisms).

Secondly, the optimum taper angle of the cone needs to be further investigated, as the success of this research and its uniqueness depends upon finding a more efficient interaction between the needle and yarn motions that create a tubular warp knitted fabric. By using a tricked cone to support the needles, two of the traditional movements performed by the needles can be merged into one movement. The optimum inclination of the cone depends upon other geometrical factors in the patterning mechanism design. The relationship between these factors is investigated further in Chapter 8.

Before considering these two design issues, the rise-dwell characteristic required by the warp knitting process must be briefly described, with some analysis of the prevailing forces and torques in the knitting mechanism, so as to obtain an equation of motion to describe the system that determines its dynamic behaviour. This equation depends on the cam profile selected. How the cam profile is selected and how it is optimised will be detailed later in this chapter and in the next.

The validity of the equation of motion derived, with the possibilities for its improvement, can then be analysed after manufacturing and testing the selected cam profile.

Rise-Dwell Characteristics: In order to analyse the forces exacted on the cam and the follower, it is important to know what the basic sections of the cam will look like, (without defining the exact rise and fall displacement profile of the cam at this stage).

The design of the rise-dwell characteristic of the cam (that is the illustration of the cam follower displacement curve as a function of the angles of rotation of the cam) is critical within the warp knitting machine application, as its design provides the synchronisation between the knitting and patterning

mechanisms. The maximum speed of the machine will depend on this synchronicity. It would therefore be most advantageous; to have a knitting mechanism design where the rise-dwell characteristic could be altered. Thus making it possible to compare the performance of the machine as the timing of the rises and dwells vary.

At the conceptual stage, a design aimed to allow as much time for underlapping as reasonably possible was intended to be used (as per schema in Figure 4-2.).

The dwells in this knitting cam profile represent the section times of the revolution of the cam where the underlaps and overlaps are carried out by the patterning mechanism. During each dwell section, the set of needles will remain stationary as the patterning rings wrap the threads around them.

The design in Figure 4-2 is symmetrical, that is:

- a) The angles of revolution used to rise and lower the needles are the same, meanwhile
- b) The angle of revolution given to perform the underlap is also equal to that given to perform the overlap.

This need not be the case. More generally, as the dwell representing the underlapping time (i.e. the dwell that occurs after lowering the needles) should be longer than that representing the overlapping time, because a knitting pattern can include longer underlaps, while the overlap always consists of wrapping the thread over a single needle only.

5.3 Kinetic Analysis

The forces acting on each of the knitting mechanism moving parts must be analysed to understand and predict their dynamic behaviour. For this purpose, the moving parts of the mechanism will be assumed to be rigid bodies. The mechanism will be modelled as a set of four moving parts: (i) the needles and strengthening inserts (Figure 5-6); (ii) the cam followers (Figure 5-8); (iii) the reciprocating shafts and needle support ring (Figure 5-7), and (iv) the cam (Figure 5-9).

5.3.1 Needles and Strengthening Inserts.

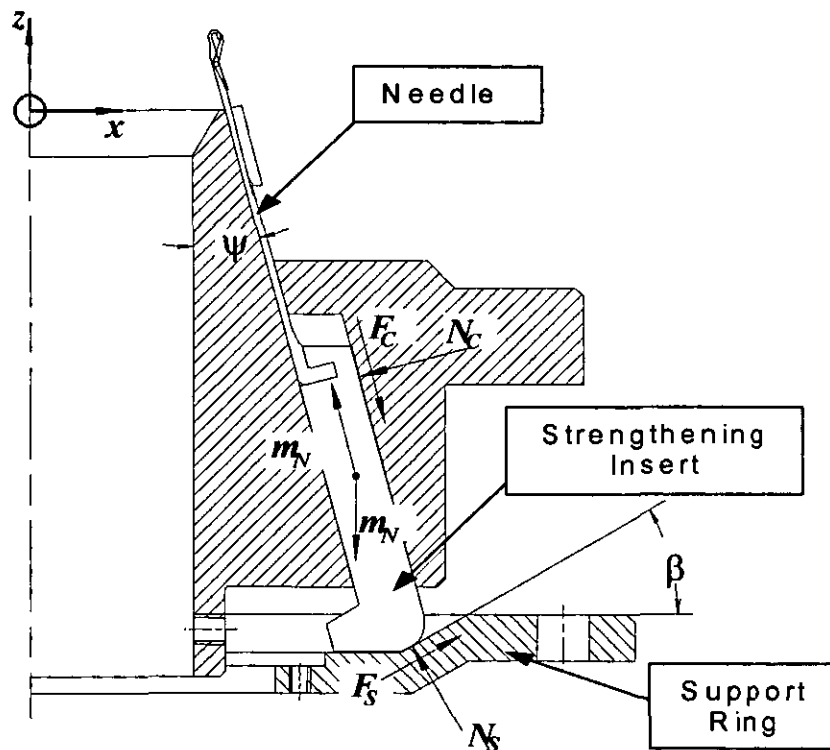


Figure 5-6. Forces on Needle and Strengthening Inserts.

Each pair of needles and strengthening insert will be treated for this analysis as a single body constrained to move in the direction of the cone taper. Refer to the free body diagram of Figure 5-6 during the analysis for the needle and insert pair.

By treating a needle and insert pair as a single rigid body, the force analysis provides the following relationships, assuming that the needles are moving up with relation to the cone;

The force on each pair in the y-direction is,

$$\sum F_{Ny} = m_N \cdot a_{Ny} = 0 \longrightarrow a_{Ny} = 0 \quad (5-1)$$

In the x-direction,

$$\sum F_{Nx} = m_N \cdot a_{Nx} \longrightarrow F_s \cdot \cos(\beta) - N_s \cdot \sin(\beta) + F_{CN} \cdot \sin(\psi) - N_{CN} \cdot \cos(\psi) = m_N \cdot a_{Nx} \quad (5-2)$$

In the z-direction,

$$\begin{aligned} \sum F_{Nz} &= m_N \cdot a_{Nz} \\ \longrightarrow F_s \cdot \sin(\beta) + N_s \cdot \cos(\beta) - F_{CN} \cdot \cos(\psi) - N_{CN} \cdot \sin(\psi) - m_N \cdot g &= m_N \cdot a_{Nz} \end{aligned} \quad (5-3)$$

where m_N is the mass of single pair of needle and insert,

a_N is the acceleration of the needle and insert pair in the direction of the cone taper,

a_{Nz} is the acceleration of the needle and insert pair in the direction of the z-axis,

n is the number of needles in the conical needle bed,

F_s is the magnitude of the friction force between the insert and the support plate,

N_s is the magnitude of the normal force exerted by the support plate on to an insert,

F_{CN} is the magnitude of the friction force between the insert and needle pair and the cone or clamp ring,

N_{CN} is the normal force exerted by the clamp ring or cone on to an insert and needle pair,

ψ is the cone taper angle, and

β is the taper angle of the support plate.

The first two equations change for each pair as it goes round the cone. But as can be readily seen, the x and y components of the forces on a needle and insert pair will be cancelled out by the forces on the pair directly opposite, making $a_{N_y} = 0$ and $a_{N_x} = 0$. Therefore, after all the needles and inserts are taken into account, the only remaining prevalent forces are those in the z or vertical axis. Equation (5-3) for the complete set of needles and inserts becomes;

$$\sum(\sum F_{Nz}) = \sum m_N \cdot a_{Nz} \longrightarrow$$

$$n \cdot [F_s \cdot \sin(\beta) + N_s \cdot \cos(\beta) - F_{CN} \cdot \cos(\psi) - N_{CN} \cdot \sin(\psi) - m_N \cdot g] = n \cdot m_N \cdot a_{Nz}$$

(5-4)

As the movement of the needles is constrained by the angle of the cone,

$$a_N = a_{Nz} \cdot \cos(\psi)$$

(5-5)

5.3.2 Reciprocating Shafts and Needle Support Plate.

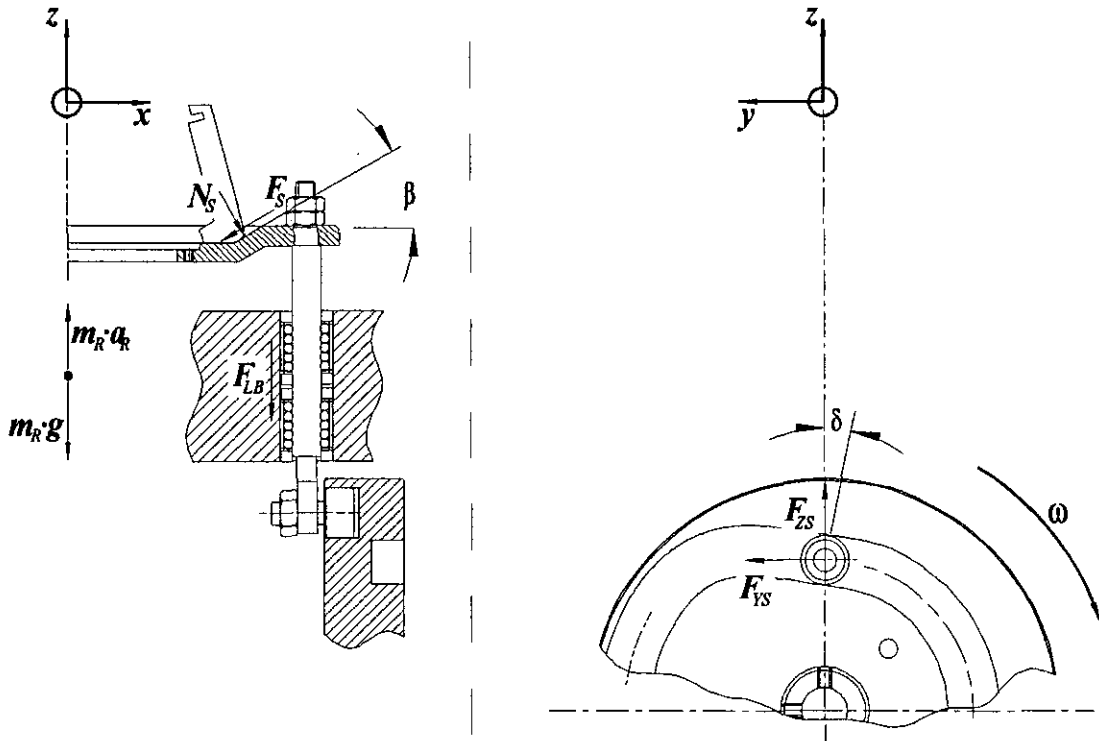


Figure 5-7. Forces on Reciprocating Shafts and the Needle Support Plate Ring

For this analysis, the reciprocating shafts and the needle support plate will be treated as a single rigid body. A free body diagram analysis for the group provides the following relationships assuming again that the needles are moving up with respect to the cone. The forces are shown on a cross-section of the group is shown in Figure 5-7.

$$\sum F_{Ry} = m_R \cdot a_{Ry} \longrightarrow -F_{YS} - N_{LB} = 0 \quad (5-6)$$

$$\sum F_{Rx} = m_R \cdot a_{Rx} \longrightarrow a_{Rx} = 0 \quad (5-7)$$

$$\begin{aligned} \sum F_{Rz} &= m_R \cdot a_{Rz} \\ \longrightarrow 2F_{ZS} - 2F_{LB} - nN_S \cdot \text{Cos}(\beta) - nF_S \cdot \text{Sin}(\beta) - m_R g &= m_R \cdot a_{Rz} \end{aligned} \quad (5-8)$$

where m_R is the mass of the reciprocating shafts, cam followers and support ring,

a_{Rx} is the acceleration of the same parts in the direction of the x-axis,

a_{Ry} is the acceleration of the same parts in the direction of the y-axis,

a_{Rz} is the acceleration of the same parts in the direction of the z-axis,

F_{LB} is the friction force between the linear bearing and the reciprocating shaft,

N_{LB} is the reaction force exerted by the linear bearing,

F_{yS} is the reaction force in the y direction at the rigid joint between the reciprocating shaft and the cam follower,

F_{zS} is the reaction force in the z direction.

Equations (5-6) and (5-7) both take into account that the x and y components of the friction with normal forces exerted to the support ring by the needles, are cancelled out. However, note that the force exerted by the cam onto the follower will have a component in the y direction when the needles are moving. This force must be compensated for by the y component of the friction between the cam and follower, with the reaction force at the linear bearings, which is the only stationary part of the mechanism, as the overall acceleration of the system in the y direction is zero.

5.3.3 Cam Followers

The third rigid body considered in the system comprises the two cam followers. The free body diagram for one of them is shown in Figure 5-8.

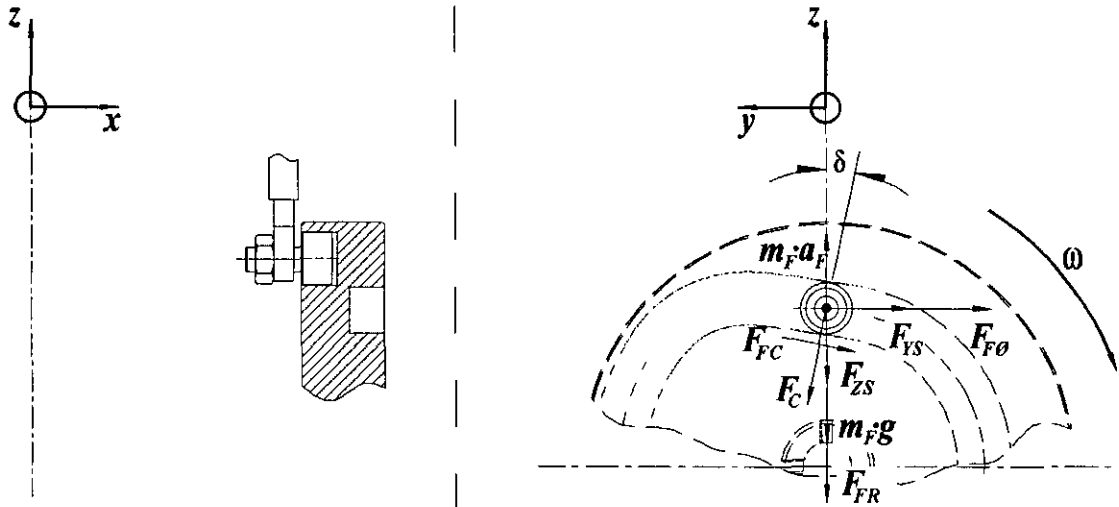


Figure 5-8. Forces on the Cam Follower

The force acting on the cam follower due to its rotation about the centre of the cam can be calculated from its radial and tangential components;

$$F_{FR} = m_F \cdot a_r = m_F (\ddot{L} - L\dot{\theta}^2) = m_F (\ddot{L} - \omega^2 L) \quad (5-9)$$

$$F_{F\theta} = m_F \cdot a_\theta = m_F (L\ddot{\theta} + 2\dot{L}\dot{\theta}) = 2m_F \omega \dot{L} \quad (\text{Cam rotating at constant speed}) \quad (5-10)$$

$$F_{FT} = \sqrt{F_{FR}^2 + F_{F\theta}^2} \quad (5-11)$$

where m_F is the mass of each of the cam followers,

a_r and a_θ are the radial and tangential accelerations of the cam followers, due to the cam's rotation.

L is the distance from the centre of rotation of the cam to the centre of the follower. It is a function of the cam's angular position.

\dot{L} and \ddot{L} are the cam follower velocity and acceleration in the radial direction respectively (the first and second derivatives of L with respect to time),

ω is the cam angular velocity, $\omega = \dot{\theta}$.

The pressure angle, δ , can also be expressed as a function of the angular position⁴⁹;

$$\delta = \arctan\left(\frac{L\left(\frac{dL}{d\theta}\right)}{m^2 + L^2 - m\left(\frac{dL}{d\theta}\right)}\right) - \arctan\left(\frac{m}{L}\right) \quad (5-12)$$

When the reciprocating shaft is in line with the centre of rotation of the cam, equation (5-12) can be simplified to;

$$\delta = \arctan\left(\frac{\left(\frac{dL}{d\theta}\right)}{L}\right) = \arctan\left(\frac{\dot{L}}{\omega L}\right) \quad (5-13)$$

The cam will exert on the cam follower a force normal to the instantaneous tangent in the profile. The vector representing this force will always pass through the contact point and the centre of the cam follower, although its direction will depend on the direction of orientation of the cam profile tangent. If the cam is turning clockwise and the cam profile tangent is negative as displayed in Figure 5-9, i.e. the needles are moving upwards, the bottom of the cam track will exert the force. When the needles are in their downward movement, the force is exerted by the upper cam track.

The bounce from one side of the cam track to the other side implies a sudden change in direction of the rotation of the cam follower about its centre.

Applying Newton law in the y and z directions,

$$\sum F_z = m_F \cdot a_{Fz}$$

$$\longrightarrow -F_{zs} - m_F(\ddot{L} - \omega^2 L) - m_F \cdot g + F_{FC} \cdot \sin \delta + F_C \cdot \cos \delta = m_F \cdot a_{Fz} \quad (5-14)$$

$$F_{Fy} = m_F \cdot a_{Fy} \longrightarrow -F_{ys} - m_F \omega \dot{L} + F_{FC} \cdot \cos \delta - F_C \cdot \sin \delta = 0 \quad (5-15)$$

where m_F is the mass of each of the cam followers,

a_{Fy} is the acceleration of the cam followers in the direction of the y-axis,

a_{Fz} is the acceleration of the cam followers in the direction of the z-axis,

F_{FC} is the friction force between cam and cam follower,

F_C is the magnitude of the force exerted by the cam,

5.3.4 Knitting Cams.

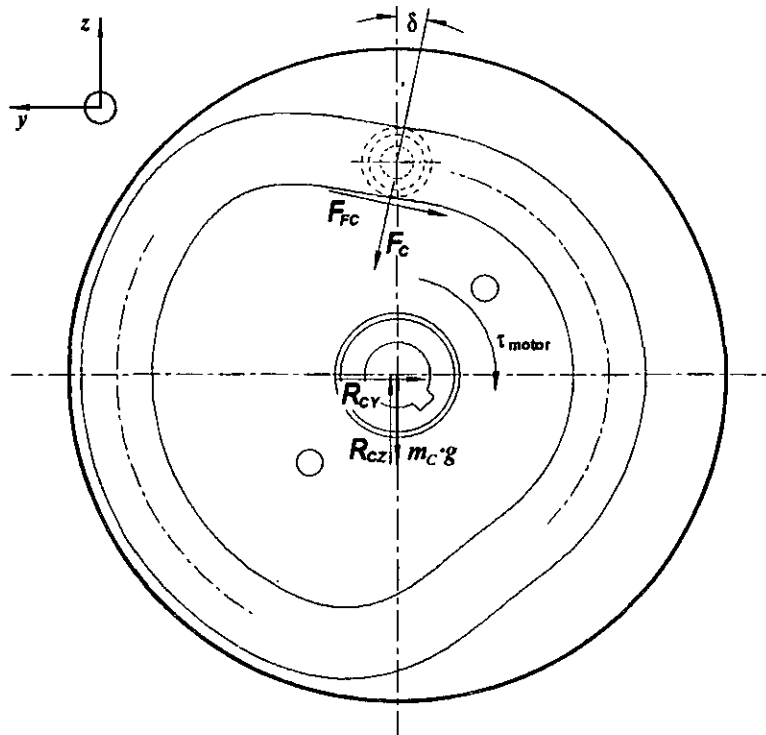


Figure 5-9. Forces on one of the knitting cam pair.

The fourth rigid body of the assembly is the pair of cams. There are no more external forces acting on the cams other than those equal and opposite to F_C and F_{FC} and the reaction force at the shaft. Assuming the cams are statically balanced, rotating at a constant rate and a torque τ_{motor} applied by the motor, the equations of motion become;

$$\sum F_{Rt} = m_R \cdot (a_{GR})_t = m_R \cdot \alpha \cdot r_G \longrightarrow F_C \cdot \sin(\delta) - F_{FC} \cdot \cos(\delta) + R_{CY} = 0 \quad (5-16)$$

$$\sum F_{Rn} = m_R \cdot (a_{GR})_n = m_R \cdot \omega^2 \cdot r_G \longrightarrow -F_C \cdot \cos(\delta) - F_{FC} \cdot \sin(\delta) + R_{CZ} - m_C \cdot g = 0 \quad (5-17)$$

$$\begin{aligned} \sum M_{GC} &= I_C \cdot \alpha \longrightarrow \\ & -\tau_{motor} + F_C \cdot \sin \delta \cdot (L - r_f \cos \delta - \bar{z}_C) - F_C \cdot \cos \delta \cdot (-\bar{y}_C - |m| - r_f \sin \delta) \\ & - F_{FC} \cdot \cos \delta \cdot (L - r_f \cos \delta - \bar{z}_C) - F_{FC} \cdot \sin \delta \cdot (-\bar{y}_C - |m| - r_f \sin \delta) + m_C \cdot g \cdot \bar{y}_C = 0 \end{aligned} \quad (5-18)$$

where I_C is the moment of inertia of the cam around its centre of rotation,

α is the angular acceleration of the cam, equal to zero because the cam is rotating at a constant angular velocity,

τ_{motor} is the torque produced by the motor.

r_f is the radius of the cam follower,

(\bar{y}_C, \bar{z}_C) are the co-ordinates of the cam's centre of gravity taking the centre of rotation as the origin,

m is the horizontal distance from the centre of rotation of the cam to the centre of the cam follower, that is, the distance the line of translation of the follower is offset from the cam centre, and,

m_C is the mass of the cam.

If the cam is statically balanced, i.e. the centre of rotation coincides with the centre of gravity, and the reciprocating shaft is in line with the centre of rotation, equation (5-18) becomes;

$$\sum M_{GC} = I_C \cdot \alpha \longrightarrow$$

$$-\tau_{motor} + F_C \cdot \text{Sin} \delta \cdot (L - r_f \text{Cos} \delta) + F_C \cdot \text{Cos} \delta \cdot (r_f \text{Sin} \delta) - F_{FC} \cdot \text{Cos} \delta \cdot (L - r_f \text{Cos} \delta) + F_{FC} \cdot \text{Sin} \delta \cdot (r_f \text{Sin} \delta) = 0$$

(5-19)

In both of the above equations, F, L and delta are functions of the angular position of the cam. Both functions are valid for the upward movement of the needles; on the downward portion, F_C will have a North Westerly orientation and the second term on the left hand side of both equations will become negative. Equation (5-19) can be rewritten for each of these two cases as;

$$-\tau_{motor} + F_C \cdot L \cdot \text{Sin} \delta = 0 \quad (\text{Upward movement})$$

(5-20)

$$-\tau_{motor} - F_C \cdot L \cdot \text{Sin} \delta + 2F_C r_f \cdot \text{Sin} \delta \cdot \text{Cos} \delta = 0 \quad (\text{Downward movement})$$

(5-21)

The instantaneous values of F, L and delta will depend on the cam profile selected, which will be characterised by an equation of movement in the form,

$$L = f(\theta) = f(\omega t)$$

At the interaction between parts where there is friction, the magnitude of the friction force can be expressed in terms of the normal force as $F_f = \mu_k \cdot N$, where μ_k is the kinematic friction coefficient between the two materials interacting. This provides four expressions relating friction and normal forces present in the equations above;

$$F_{FC} = \mu_C \cdot F_C$$

(5-22)

$$F_{CN} = \mu_{CN} \cdot N_{CN} \quad (5-23)$$

$$F_S = \mu_S \cdot N_S \quad (5-24)$$

$$F_{LB} = \mu_{LB} \cdot N_{LB} \quad (5-25)$$

On the other hand, the acceleration of the cam followers and the reciprocating shafts should be the same, since they are rigidly attached;

$$a_{FZ} = a_{RZ} \quad (5-26)$$

Similarly, the vertical acceleration of the needles and inserts should be equal to that of the reciprocating shafts;

$$a_{RZ} = a_{NZ} \quad (5-27)$$

Finally, these accelerations can also be equated to the acceleration of the cam profile, which is driving the system;

$$a_{NZ} = \ddot{L} \quad (5-28)$$

When the geometric variables (β, ψ, r_f, L) , the mass of the different components, the friction coefficients $(\mu_C, \mu_{CN}, \mu_{LB}, \mu_S)$ and the motor torque are known, a system of linear equations can be used to infer the forces and accelerations in the system. This can then provide expressions for the reactions at the cam shaft bearings and the linear bearings in terms of the known variables and of the cam rotation angle.

The linear system comprises 15 equations [(5-4), (5-6), (5-8), (5-14), (5-15), (5-16), (5-17), (5-19), (5-22), (5-23), (5-24), (5-25), (5-26), (5-27) and (5-28)] and 15 unknown forces and accelerations $(F_{YS}, F_{FC}, F_C, F_{ZS}, F_S, N_S, F_{CN}, N_{CN}, N_{LB}, F_{LB}, R_{CY}, R_{CZ}, a_{RZ}, a_{NZ}, a_{FZ})$.

The forces of interest are the reactions on the camshaft and linear bearings (N_{LB} , R_{CY} and R_{CZ}) as they will be the main contributors to the vibration of the machine.

$$R_{CY} = \frac{\tau_{mot} \cdot (\mu_c \cdot \text{Cos}\delta - \text{Sin}\delta)}{\text{Sin}\delta \cdot L - \mu_c \cdot \text{Cos}\delta \cdot L + \mu_c \cdot r_f} \quad (5-29)$$

$$R_{CZ} = \frac{(\tau_{mot} \cdot \text{Cos}\delta + \mu_c \cdot \tau_{mot} \cdot \text{Sin}\delta + m_c \cdot g \cdot \text{Sin}\delta \cdot L - m_c \cdot g \cdot \mu_c \cdot \text{Cos}\delta \cdot L + m_c \cdot g \cdot \mu_c \cdot r_f)}{\text{Sin}\delta \cdot L - \mu_c \cdot \text{Cos}\delta \cdot L + \mu_c \cdot r_f} \quad (5-30)$$

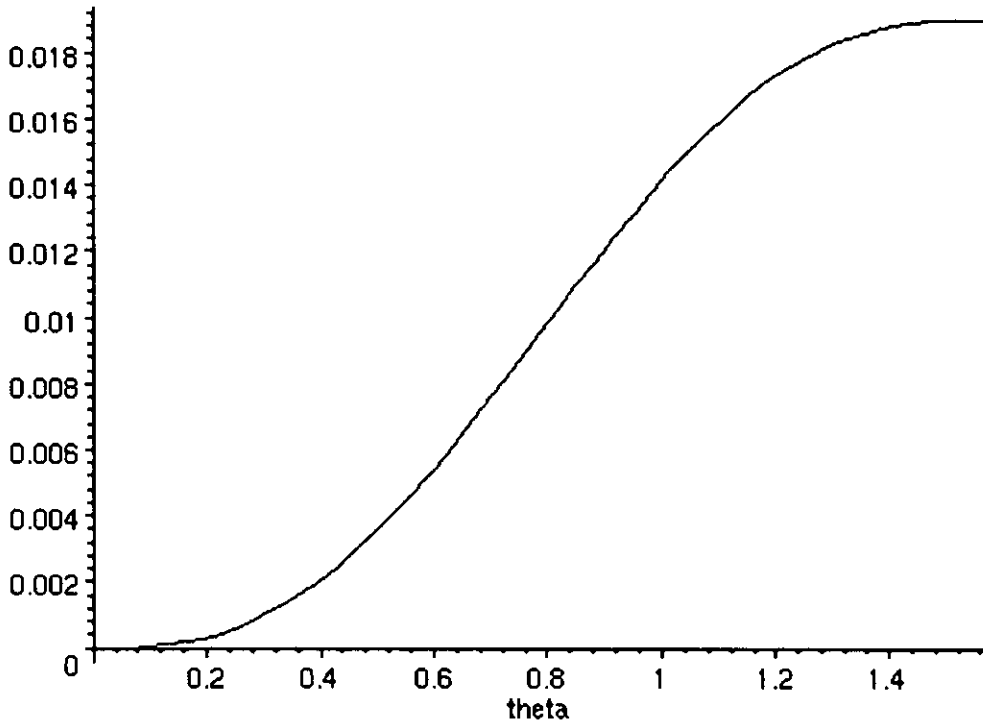
$$N_{LB} = \frac{m_f \cdot \omega \cdot \dot{L}(\text{Sin}\delta \cdot L - \mu_c \cdot \text{Cos}\delta \cdot L + \mu_c \cdot r_f) + \tau_{mot}(\text{Sin}\delta - \mu_c \cdot \text{Cos}\delta)}{\text{Sin}\delta \cdot L - \mu_c \cdot \text{Cos}\delta \cdot L + \mu_c \cdot r_f} \quad (5-31)$$

From equation (5-13), the relation between δ and L is known and the reaction forces can be expressed entirely in terms of L and its derivatives.

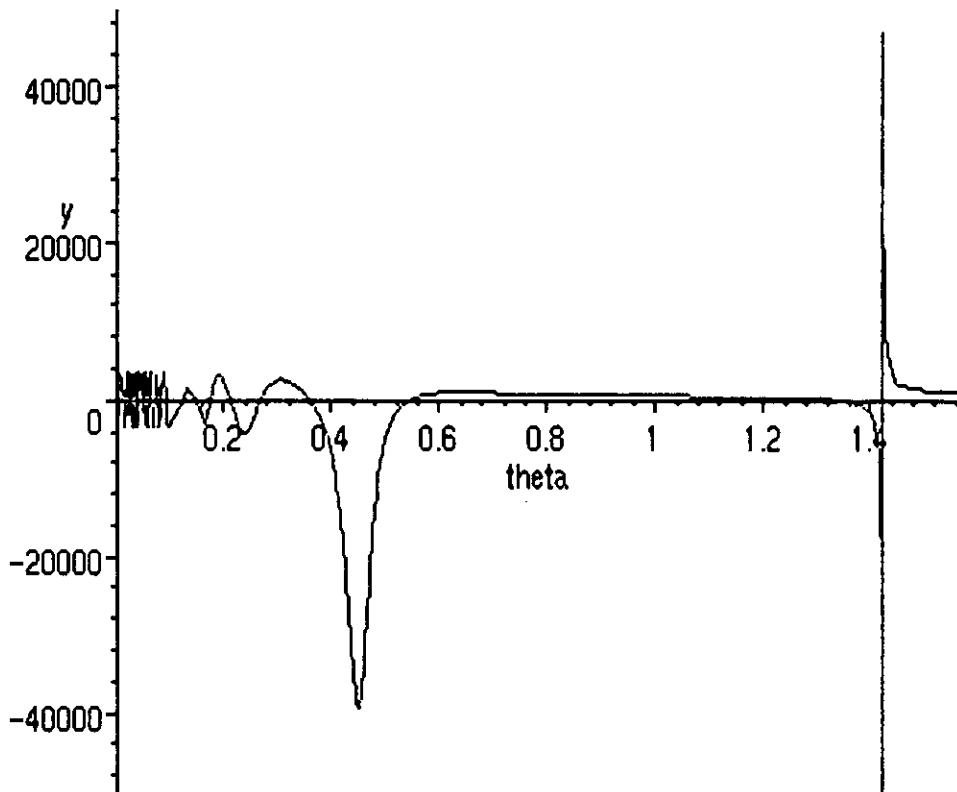
The resultant forces over the rising portion of a sample cycloidal profile are shown in Figure 5-10. The shape of these plots is very similar for other types of profiles such as 5-order polynomial and simple harmonic.

In section 5.5, different types of cam profiles are analysed and in Chapter 6 a new method for the design and optimisation of cam profiles is proposed. This will provide an explicit expression for L in terms of θ , the cam rotation angle, which can then be inserted in the equations for the reaction forces. In that way, the expressions found here for the reaction forces required in the camshaft bearings will provide a basis for the analysis of the modes of vibration of the machine.

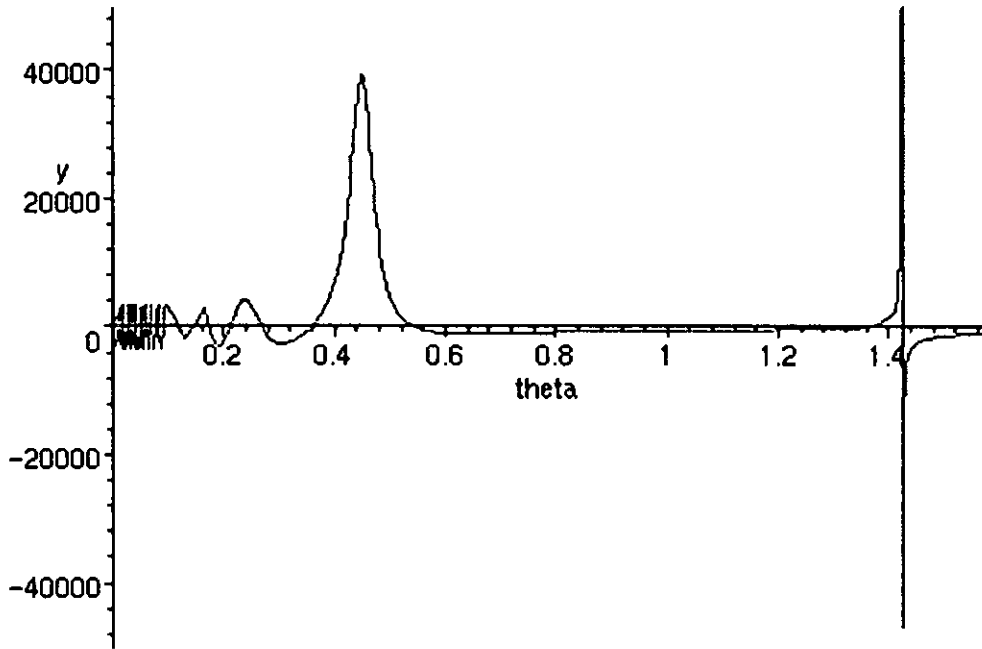
With the analysis presented above however, the form of the reaction forces in terms of the cam rotation has been established. Furthermore it can be noted that the cam system will be more prone to vibration at the beginning of the cycle where the three reaction force functions have a sinusoidal shape with a very high frequency.



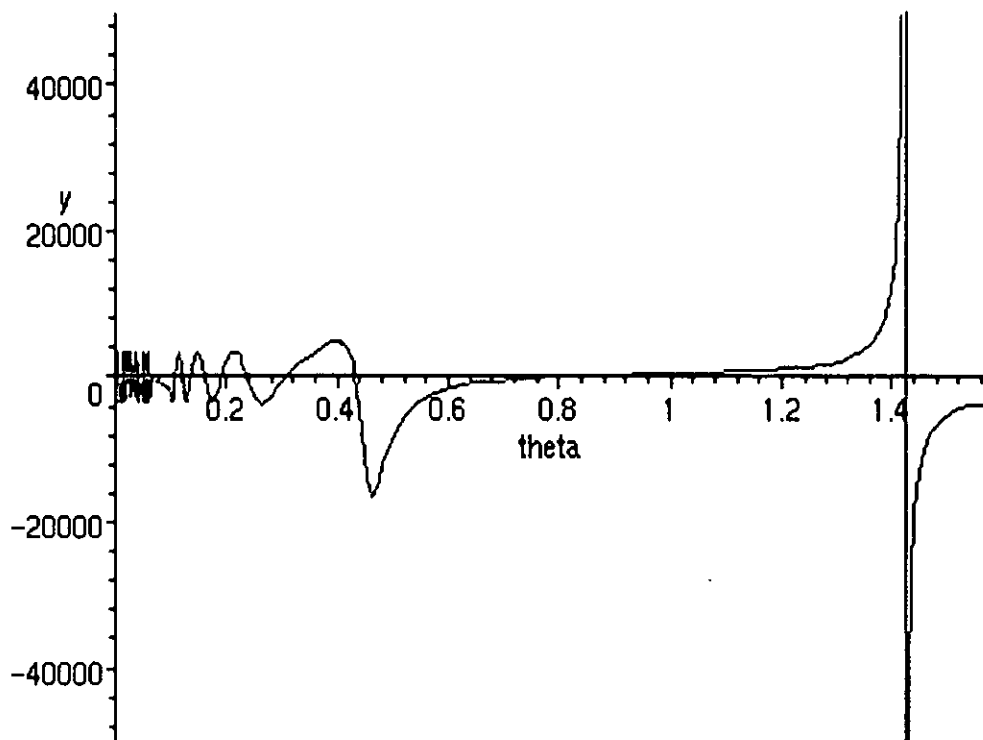
a) Follower Displacement, $L(\theta)$



b) Normal Force at the Linear Bearing, N_{LB}



c) y component of the Reaction Force at the Main Bearings, R_{Cy}



d) z component of the Reaction Force at the Main Bearings, R_{Cz}

Figure 5-10. Reactions for a Sample Cycloidal Profile

5.4 Effect of Elasticity

The previous analysis assumed that all the bodies in the knitting assembly were rigid. However this not the case, as the parts' elasticity will account for some distortion in the displacement of the reciprocating parts.

In order to simplify the analysis, the reciprocating assembly can be represented as a single mass, m_{RT} , with a resultant rigidity k and the system can be modelled as shown in Figure 5-11.

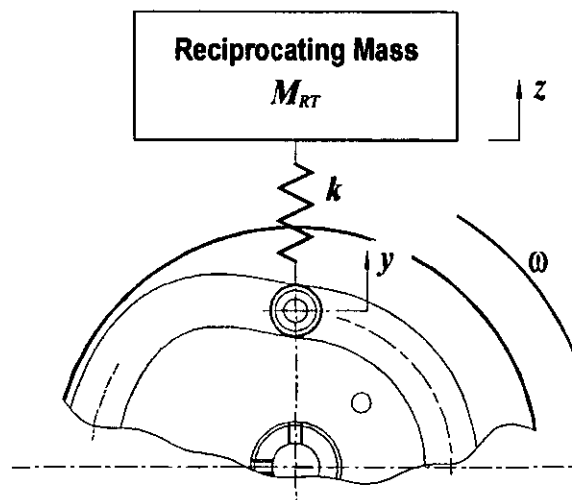


Figure 5-11. Elastic Model of the System

From a free body diagram of the reciprocating mass, the sum of forces acting in the vertical direction is,

$$\sum F_z \rightarrow k \cdot (y - z) - m_{RT} \cdot g - m_{RT} \cdot \ddot{z} = 0 \quad (5-32)$$

This provides the equation of motion of the reciprocating mass when rewritten as a differential equation on z ,

$$\ddot{z} + \frac{k}{m_{RT}} \cdot z = \frac{k \cdot y}{m_{RT}} \quad (5-33)$$

Let $\omega_n = \sqrt{\frac{k}{m_{RT}}}$, be the circular natural frequency of the system. The solution for (5-33) is of the form,

$$z = A \cdot \text{Cos}(\omega_n \cdot t) + B \cdot \text{Sin}(\omega_n \cdot t) + \frac{k \cdot y}{m_{RT} \cdot \omega_n^2} \quad (5-34)$$

Where y is the displacement function; $y = L(\theta) = L(\omega \cdot t)$ and the constants A and B depend on the boundary conditions. In the simplest case for analysis, when the cam profile is a straight line, the displacement function is

$$y = \frac{L_{\max} \cdot \theta}{\gamma} = \frac{L_{\max} \cdot \omega \cdot t}{\gamma} \quad (5-35)$$

Where L_{\max} is the full stroke of the follower rise and γ is the total angle in which the rise occurs. For this type of displacement, the constants A and B can be found by replacing $z = \dot{z} = 0$ at $t = 0$ in equation (5-34) and its derivative. It can be found that in this case $A = 0$ and $B = -\frac{k \cdot \dot{y}}{m_{RT} \cdot \omega_n^3}$.

Replacing A and B in (5-34), the latter becomes,

$$z = y - \dot{y} \cdot \text{Sin}(\omega_n \cdot t) \quad (5-36)$$

Equation (5-36) comprises a linear term and a negative sinusoidal one. The former represents the uniform rise given by equation (5-35).

Figure 5-12 shows the graph of this equation, together with that of the cam profile (and hence of the rigid follower). A dwell and the return portion of the cam profile are also shown. This effect should also contribute to the distortion of the follower displacement curves and to the vibration of the machine. As can be seen from Figure 5-12, the start and the end of the follower rise are again the sections with more propensity to have problems of vibration and distortion.

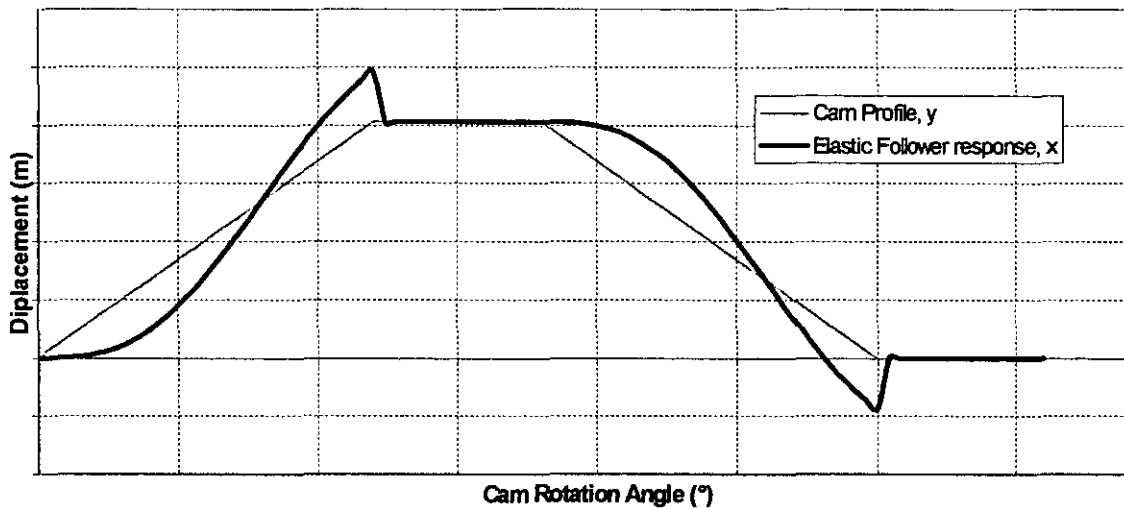


Figure 5-12. Effect of Bodies' Elasticity.

5.5 Cam and Profile Design

In order to initially select an appropriate cam profile for the knitting mechanism application, a comparative analysis of the three most common displacement curves was carried out. They are namely, parabolic, simple harmonic and cycloidal profiles. Subsequently, a polynomial expression for the cam profile was derived for the specific conditions that apply for the knitting mechanism. The analytical development of the standard and polynomial cam profiles is described in this section, which includes expanding on the reasons for the final selection. Then in Chapter 6 a method for optimising the profile selected is proposed.

The advantage of using one of the standard three profiles is that the calculations involved are easier. Also various computer programmes are available to calculate and display the displacement, velocity, acceleration and jerk curves for them, (given known values for: baseline radius; amplitude of the rise and dwells; and the sequence of events). The main criterion for selection is the avoidance of excessive vibration because the needles and support ring act as a reciprocating weight, and unless the design incorporates several knitting heads that balance each other, the machine will be prone to vibration.

The advantage of deriving a polynomial expression for the specific application, on the other hand, is that the shape of the various curves will be dictated by the end conditions as set by the designer; therefore the profile chosen will be the most appropriate for the application. However, large sets of equations need to be solved and graphs created from them, in order to view the displacement diagrams obtained from the polynomial expression.

Other issues affecting the design of cams discussed later in the chapter include: the effect of the value of baseline radius; the offset between the reciprocating axis and the centre of rotation; and the unbalance on the dynamic behaviour of the cam.

5.5.1 Cam Profiles

5.5.1.1 Parabolic, Simple Harmonic and Cycloidal profiles.

The equations that define the displacement of the follower and its derivatives in standard cam profiles will now be described. The analytical or graphical development of the equations will not be discussed in this document, as various textbooks already cover them. All of the profiles described below concentrate on a single rise movement; they are all symmetrical and so the return movement can be assumed to have the same characteristics.

The derivative curves shown in Figure 5-13, Figure 5-14, Figure 5-15 and Figure 5-16 intend to show the shape of the curves only and so the curves are not to scale. This is because, unlike the displacement curve, its derivatives amplitude will depend on the angular velocity (ω) with which the cam is rotating. Velocity is proportional to ω , acceleration to ω^2 and jerk to ω^3 .

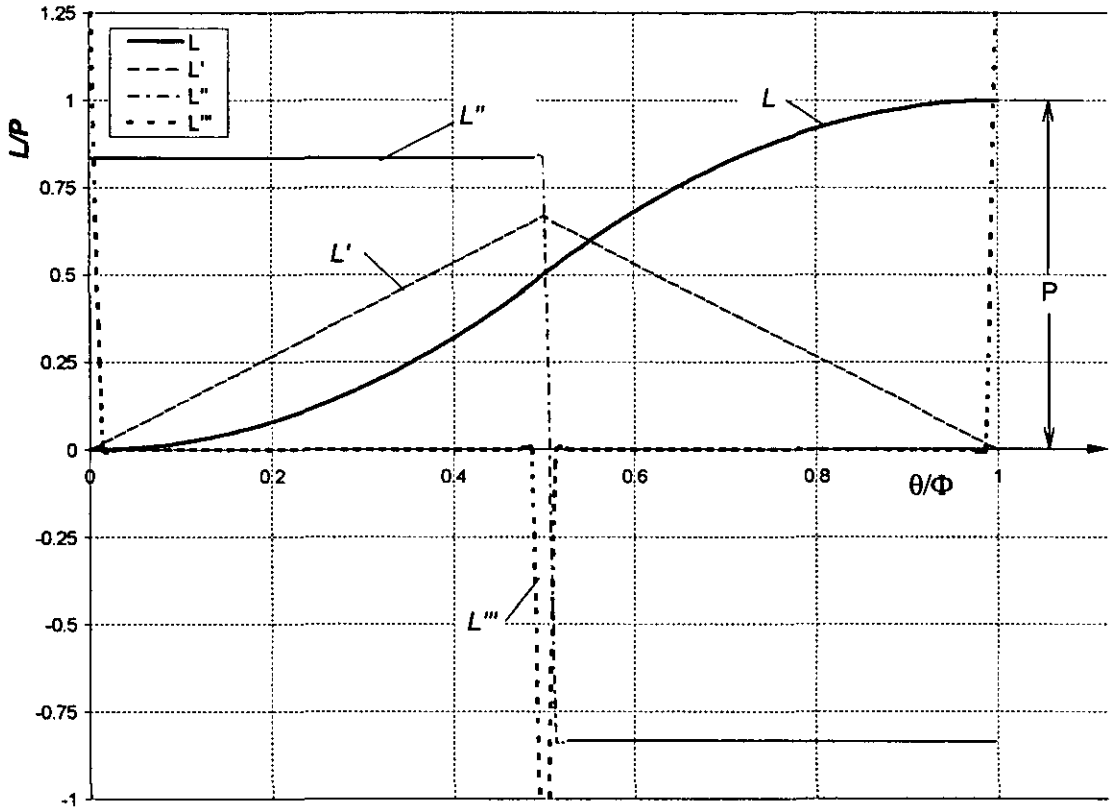


Figure 5-13. Displacement, Velocity, acceleration and jerk relations for parabolic motion

Parabolic Motion

The parabolic cam displacement profile (or constant acceleration profile) and its derivatives are shown in Figure 5-13, where P is the total rise stroke, Φ is the angle of cam rotation required to complete the rise, L is the displacement function and L' , L'' and L''' are the first three derivatives of displacement (i.e., velocity, acceleration and jerk).

The displacement curve is given by,

$$L = k(\theta)^2$$

(5-37)

where k is a constant, and,

θ is the angle of rotation.

The follower has a constant positive acceleration during the first half of the rise, and a negative constant acceleration for the second half. The jerk profile

has three undesirable infinite spikes due to the step changes in the acceleration level, making this design a poor choice where noise, vibration and wear are not tolerated.

This is because, in order to avoid vibration caused by the cam design, as many derivatives of displacement as possible should be continuous, or at least finite; the discontinuities in the acceleration curve displayed for this profile will result in sudden changes in the forces applied to the cam track and camshaft bearings, as acceleration is proportional to force, producing high levels of vibration.

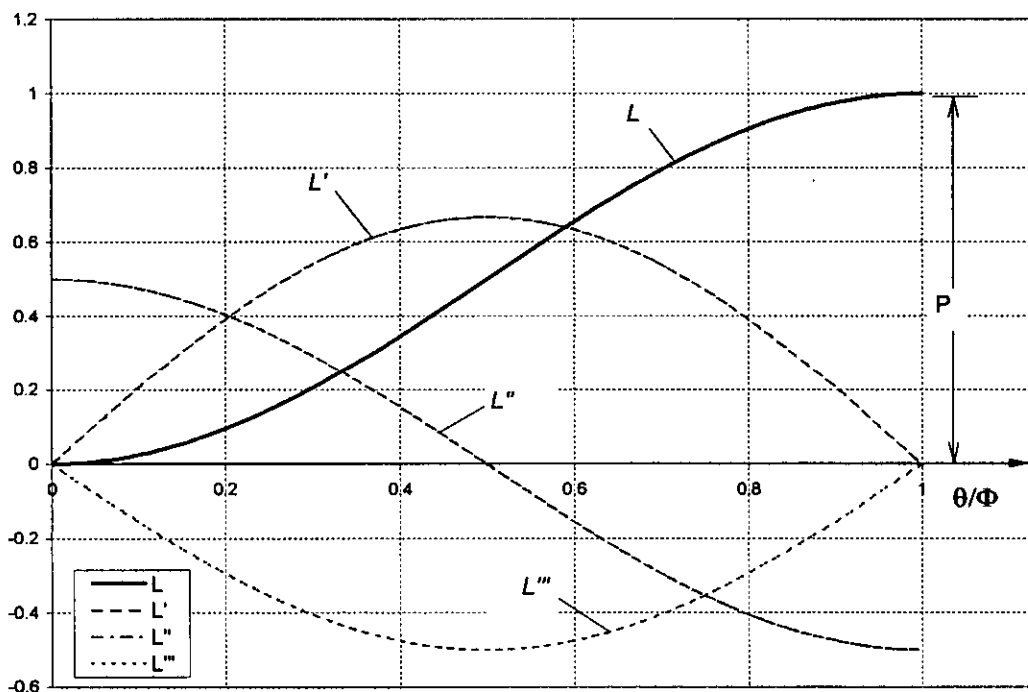


Figure 5-14. Displacement, velocity, acceleration and jerk relations for simple harmonic motion.

Simple Harmonic Motion

The displacement, velocity, acceleration and jerk curves for a simple harmonic displacement profile are shown in Figure 5-14 as a function of the angular position of the cam.

The displacement curve is given by,

$$L = \frac{P}{2} \left(1 - \cos \left(\frac{\pi\theta}{\Phi} \right) \right)$$

(5-38)

where P is the total rise stroke, and

Φ is the total angle of rotation in which the rise must be carried out.

All the curves of Figure 5-14 are sinusoidal in nature and therefore continuous in $(0, \Phi)$, not including the extremes. However, a dwell following the rise will force the acceleration to zero, with the step changes in the acceleration curve at the two extreme points again causing infinite spikes in the jerk curve, making it a poor choice if intending to reduce the vibration.

Cycloidal Motion

The cycloidal displacement profile and its derivatives (see Figure 5-15) is the only one of these standard profiles with three finite derivatives, and therefore is the most suitable for high-speed applications. It has, however, in comparison with the other profiles, higher values of maximum velocity and acceleration.

It is clearly deduced that the ideal profile requires continuous and finite acceleration curves throughout the cam profile, in order to ensure continuity in the jerk curve. This implies that all the higher derivatives (velocity and displacement) are also continuous and finite and that the value of the acceleration at the extremes of the range $(0, \Phi)$ is equal to zero.

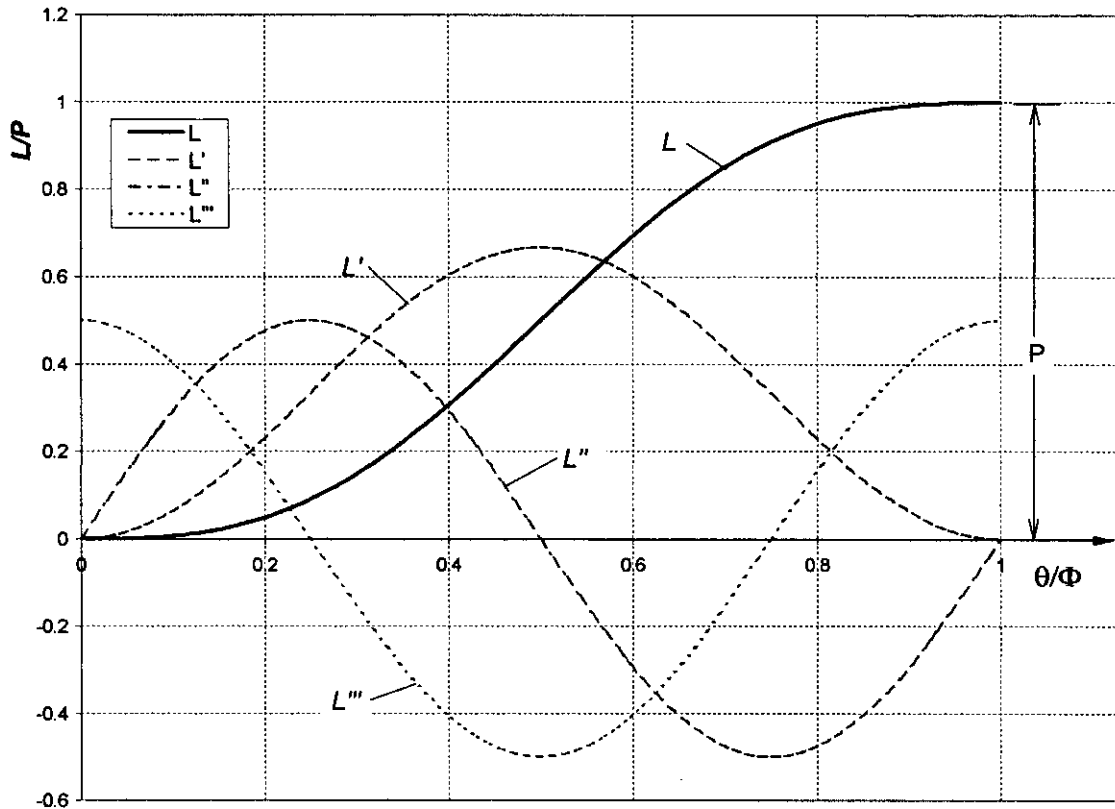


Figure 5-15. Displacement, velocity, acceleration and jerk relations for cycloidal motion.

The displacement curve in this case is given by,

$$L = \frac{\theta P}{\Phi} - \frac{P}{2\pi} \sin\left(\frac{2\pi\theta}{\Phi}\right)$$

(5-39)

Note that, although finite, the jerk curve will have step changes at the extremes, making it discontinuous.

Cam profiles can be designed using the same profile type for every rise or return or as a combination of different standard profiles within the 360° cycle. For example, a cam could be designed for the follower to rise 1" between 0° to 90° of rotation of the cam using a cycloidal profile, dwell until $\theta=180^\circ$, then returns to the baseline using a parabolic profile between 180° rotation and 360°.

The trend shown by the standard profiles show that the choice implies a compromise between either having higher values of maximum velocity and acceleration (and hence forces) with a continuous curve, or having punctual discontinuities (and hence infinite peaks) but with lower maximum values.

5.5.1.2 Polynomial Profile.

A polynomial profile is the means for designing the cam profile to the specific requirements of the application. In mathematical terms, a polynomial profile is only an extension of the standard ones described above, since any sinusoidal function can be expressed as a polynomial one. The difference is, that by using the method, which will be later described, in this section, every coefficient of the polynomial equation is calculated, in order to suit the actual application requirements, rather than to merely converge to a sine or cosine function.

In order to derive a polynomial profile for the cam motion, its displacement is defined by a standard n^{th} degree polynomial equation;

$$L \equiv c_n \theta^n + c_{n-1} \theta^{n-1} + \dots + c_2 \theta^2 + c_1 \theta + c_0$$

(5-40)

where L is the displacement, θ is the cam rotation angle and $c_0 \dots c_n$ are constants. The latter depend on the boundary conditions set by the application. For each boundary condition specified, a term is added to equation (5-40).

The conditions specified must ensure that the three derivatives of the displacement curve are continuous throughout their range, especially where the rise motion is joined with a dwell portion in the cam.

At the dwell portions, the displacement curve is defined by $L(x) = \text{Constant}$, therefore all its derivatives will be equal to zero. In order to achieve continuity in \dot{L} , \ddot{L} and $\ddot{\ddot{L}}$ throughout the 360 degrees of rotation, the rise and fall derivatives of the displacement function must also be zero where they join the dwells, (i.e. at the beginning and the end of the rise and return moves).

Then for the knitting mechanism application, at least a 7th degree polynomial will be required to satisfy the following boundary conditions:

$$\text{When } x = 0; \quad L = 0, \quad \dot{L} = 0, \quad \ddot{L} = 0, \quad \dddot{L} = 0.$$

$$\text{When } x = \Phi; \quad L = P, \quad \dot{L} = 0, \quad \ddot{L} = 0, \quad \dddot{L} = 0.$$

Where, x (in degrees) is the angle of rotation; Φ is the total angle in which the rise movement must be completed (75° for the initial design of the warp knitting machine); and where P is the total rise stroke (0.837 inches for the warp knitting machine).

None of the standard cam profiles studied earlier could comply with all of these conditions.)

The basic equation of motion (displacement) of the cam as an 8th degree polynomial becomes,

$$L = c_0 + \frac{c_1 X}{\Phi} + \frac{c_2 X^2}{\Phi^2} + \dots + \frac{c_8 X^8}{\Phi^8}, \quad \text{or} \quad L = \sum_{n=0}^8 \frac{c_n X^n}{\Phi^n} \quad (5-41)$$

where c_n are the polynomial coefficients.

The velocity acceleration and jerk equations will respectively be,

$$\dot{L} = \sum_{n=1}^8 \frac{n c_n X^{n-1}}{\Phi^n} \quad (5-42)$$

$$\ddot{L} = \sum_{n=2}^8 \frac{n(n-1) c_n X^{n-2}}{\Phi^n} \quad (5-43)$$

$$\dddot{L} = \sum_{n=3}^8 \frac{n(n-1)(n-2) c_n X^{n-3}}{\Phi^n} \quad (5-44)$$

The four equations above can now be evaluated on the boundary conditions specified to produce a set of eight equations. When solved, these will provide the appropriate coefficients to fully define the displacement curve. The set of equations is displayed in matrix form below,

$$\begin{pmatrix} 1 & 0 & 0 & 0 & 0 & 0 & 0 & 0 & 0 \\ 1 & 1 & 1 & 1 & 1 & 1 & 1 & 1 & 1 \\ 0 & 1/\Phi & 0 & 0 & 0 & 0 & 0 & 0 & 0 \\ 0 & 1/\Phi & 2/\Phi & 3/\Phi & 4/\Phi & 5/\Phi & 6/\Phi & 7/\Phi & 8/\Phi \\ 0 & 0 & 2/\Phi^2 & 0 & 0 & 0 & 0 & 0 & 0 \\ 0 & 0 & 2/\Phi^2 & 6/\Phi^2 & 12/\Phi^2 & 20/\Phi^2 & 30/\Phi^2 & 42/\Phi^2 & 56/\Phi^2 \\ 0 & 0 & 0 & 6/\Phi^3 & 0 & 0 & 0 & 0 & 0 \\ 0 & 0 & 0 & 6/\Phi^3 & 24/\Phi^3 & 60/\Phi^3 & 120/\Phi^3 & 210/\Phi^3 & 336/\Phi^3 \end{pmatrix} \begin{pmatrix} c_0 \\ c_1 \\ c_2 \\ c_3 \\ c_4 \\ c_5 \\ c_6 \\ c_7 \\ c_8 \end{pmatrix} = \begin{pmatrix} 0 \\ P \\ 0 \\ 0 \\ 0 \\ 0 \\ 0 \\ 0 \\ 0 \end{pmatrix} \quad (5-45)$$

Solving (5-45)simultaneously, the polynomial coefficients found are;

$$\begin{bmatrix} c_0 \\ c_1 \\ c_2 \\ c_3 \\ c_4 \\ c_5 \\ c_6 \\ c_7 \\ c_8 \end{bmatrix} = \begin{bmatrix} 0 \\ 0 \\ 0 \\ 0 \\ 35 \cdot P \\ -84 \cdot P \\ 70 \cdot P \\ -20 \cdot P \\ 0 \end{bmatrix}$$

(5-46)

The kinematic characteristics of this polynomial profile for a rise motion are plotted in Figure 5-16 after replacing the coefficients into (5-41), (5-42), (5-43) and (5-44).

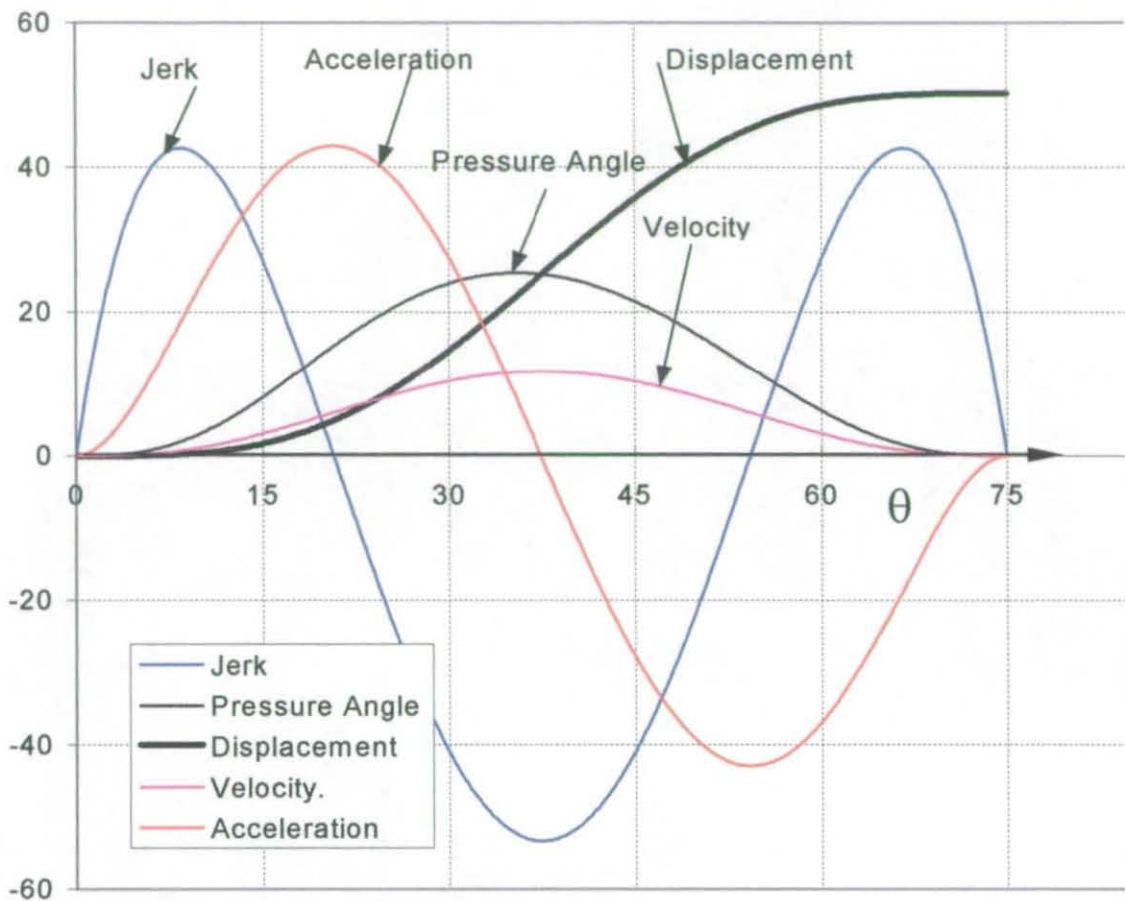


Figure 5-16. Motion Characteristics of Polynomial Profile.

As stipulated, the functions for displacement with its three derivatives are continuous in the range $[0, \Phi]$, including the end positions. Also, at the two extremes, the velocity, acceleration and jerk curves are zero, the same value that the dwell's respective curves will have.

The only disadvantage of this profile is that the maximum values of acceleration and velocity (and hence the pressure angle) are larger than those for the cycloidal profile.

A high pressure angle is not desirable, as it means that the point of contact on the follower is further away from the vertical (see δ in Figure 5-8), thereby increasing the tangential component of the forces between cam and follower. This creates two unwanted effects; firstly, it increases the horizontal reaction

forces creating vibration; secondly it reduces the vertical force available to reciprocate the needles.

According to the rise-dwell sequence described earlier in the chapter, a complete machine cycle displacement characteristic can now be described in four sections;

1. From $\theta = 0^\circ$ to $\theta = 60^\circ$; Rise from $L=0$ to $L= P$.
2. From $\theta = 60^\circ$ to $\theta = 180^\circ$; Dwell at $L = P$.
3. From $\theta = 180^\circ$ to $\theta = 240^\circ$; Fall from $L=P$ to $L=0$.
4. From $\theta = 240^\circ$ to $\theta = 360^\circ$; Dwell at $L=0$.

Having calculated the equations for the rise and fall displacement, as a function of the angular position of the cam for the different cam profiles, the equation of motion of the reciprocating system can be fully specified in sections, by substituting the chosen cam profile displacement curve in (5-30) and (5-31).

The analysis so far has shown, that the polynomial profile is the best design to suit the requirements of a given application; but in order to limit the values of maximum acceleration and velocity, some extra boundary conditions must be set (with a higher order polynomial to be used). For example, $\dot{L} = 0.3$ at $x = \frac{\Phi}{2}$. However, this is problematic, as it could have the effect of distorting the curves and adding other unwanted characteristics.

Ideally, it would be capable of optimising the curves to satisfy the boundary conditions while also minimising pressure angle. As there are no standard techniques of optimising the cam profile in this way, a new method has been proposed as part of this research as described in the next chapter.

5.5.2 Pressure Angle

There are three geometric parameters that must be selected regardless of the displacement profile chosen. They will affect the pressure angle; the baseline radius (R_o), the offset distance (m), and the follower radius (r_f).. From Figure 5-8, it is clear that only the component delivering the cam force

along the reciprocating shaft axis is useful for moving the needles & inserts set. In order to maximise this component, $\cos(\delta)$ should be maximised in order to make the pressure angle to become as small as possible.

Similarly, a small pressure angle will reduce friction between the reciprocating shaft and the linear bearing, as the horizontal reaction force will be smaller. (See Figure 5-7).

The pressure angle, (see Figure 5-8) defined by equation (5-12) or equation (5-13) on page 105, is directly proportional to the instantaneous velocity and inversely proportional to the value of the displacement. It is therefore easier to reduce the pressure angle by increasing the baseline radius. Once the cam profile is selected, the value of the baseline radius can be set according to the maximum pressure angle required. 30 to 35 degrees are quoted as being the largest pressure angles that can be used without causing dynamic problems.⁴⁸

Although the relationship is less straightforward, the value of m , the offset between the reciprocating axis and the centre of rotation, can also alter the pressure angle. If m is increased, the pressure angle will be reduced on the rising portion of the profile, while augmented on the falling motion.

5.5.3 Static and Dynamic Balance.

Another issue affecting the design of a cam, often overlooked by books covering this subject, is the importance of its static and dynamic balance. Static unbalance is created by having unevenly distributed mass on the rotating parts.

Calculating the centre of gravity of the cam track and drilling a hole in the cam at 180° from it can statically balance the cam. The size and position of the hole should transfer the centre of gravity of the cam to coincide with the centre of rotation;

$$\bar{x} = \frac{x' \cdot A_T - R_H \cdot \cos \phi \cdot \pi r^2}{A_T - \pi r^2} = 0$$

$$\bar{y} = \frac{y' \cdot A_T - R_H \cdot \sin \phi \cdot \pi r^2}{A_T - \pi r^2} = 0$$

(5-47)

where (x', y') are the co-ordinates for the centre of gravity of the cam with track; the centre of rotation is taken as the origin.

A_T is the area of the cam disk minus that of the track,

R_H is the radius at which the hole will be positioned from the centre of rotation,

ϕ is the angle from the horizontal at which the hole will be positioned.

r is the radius of the hole.

Generally, R_H will be determined by space constraints; for instance, it will need to be smaller than the baseline radius in the displacement curve. With R_H known, (5-47) can be solved simultaneously to find ϕ and r .

If the cam is not balanced statically, the centrifugal force created by the unbalanced mass will produce rotating reactions on the bearings supporting the cam shaft.

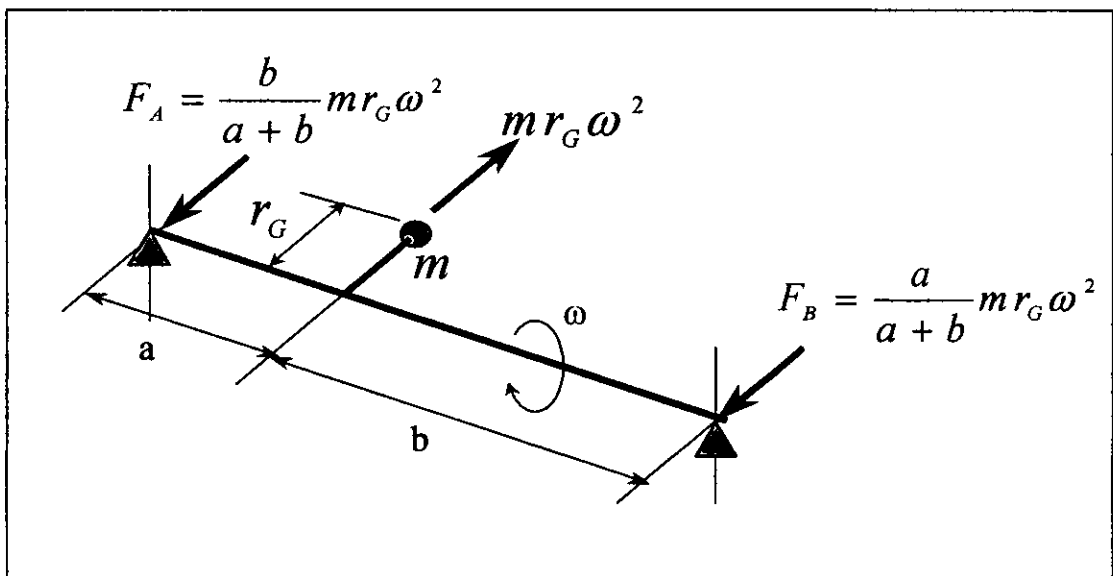


Figure 5-17. Static Unbalance

The vibratory effect of a static unbalance can be analysed by obtaining the equation of motion of the unbalanced elastic camshaft, which is derived from applying $\sum F = 0$ on any axis perpendicular to the shaft (see Figure 5-17);

$$\sum F_o = -kx - c\dot{x} - m\ddot{x} + m_U r_G \cos \omega t = 0 \quad (5-48)$$

where x is the displacement on the chosen axis,

k is the shaft stiffness,

c is the viscous damping coefficient,

m is the total mass of the system,

m_U is the unbalanced mass,

r_G is the distance from the centre of gravity of the unbalanced mass to the centre of rotation, and

ω is the angular velocity of the system, a constant.

The solution to the differential equation (5-48) is Error! Bookmark not defined.

$$x = \frac{m_U r_G \omega^2 \cos(\omega t - \Theta)}{\sqrt{(k - m\omega^2)^2 + c^2 \omega^2}} \quad (5-49)$$

where the phase angle Θ is defined as $\Theta \equiv \arctan\left(\frac{c\omega}{k - m\omega^2}\right)$.

The analysis of equation (5-49) is beyond the scope of this research. However, some relevant issues are raised to recognise vibration caused by unbalance, from the experimental tests carried out on the warp knitting machine. The description and analysis of these tests is detail later in this chapter.

The shaft will tend to vibrate with a frequency equal to the angular velocity of the shaft and amplitude given by

$$A = \frac{m_U r_G \omega^2}{\sqrt{(k - m\omega^2)^2 + c^2 \omega^2}}$$

(5-50)

Let $\omega_n \equiv \sqrt{\frac{k}{m}}$, the critical or natural frequency of the system, where the amplitude tends to infinity. When $\omega \ll \omega_n$ the vibration amplitude is very small (see Figure 5-18); however it increases very rapidly as it approaches $\omega = \omega_n$. Finally the vibration amplitude will tend to the value of $-r_G$ when $\omega \gg \omega_n$; where it will never return to zero.

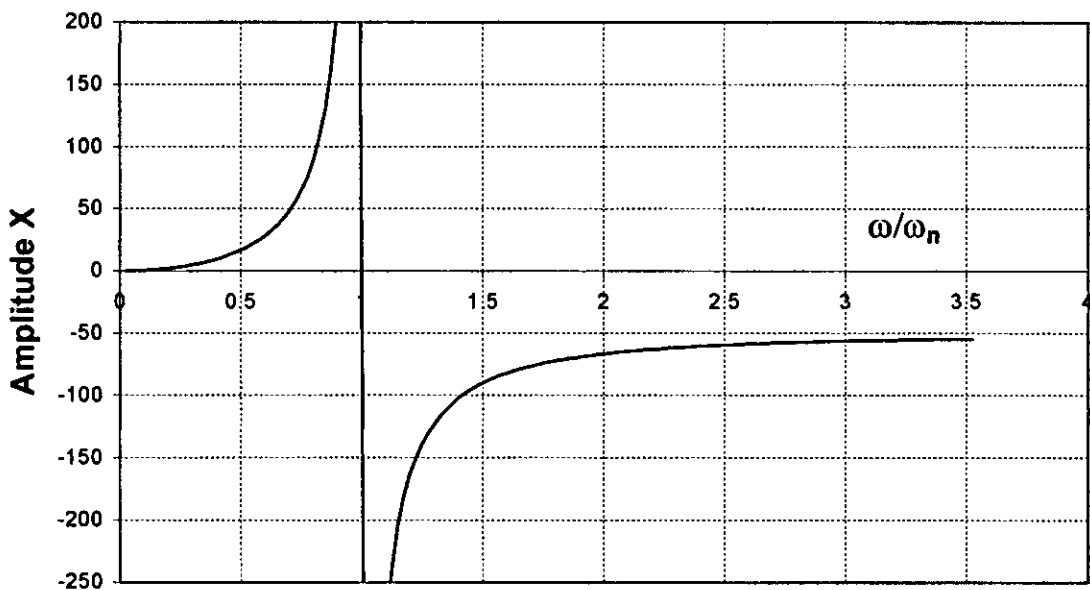


Figure 5-18. Simplified Vibration Amplitude.

It is clear from this analysis, that static unbalance will create unwanted and dangerous vibration modes to the system, causing rotating reaction forces on the cam shaft bearings, which are to be avoided whenever possible. In practical terms, there will always be some unbalance in the system, and hence there will be some vibration problems when $\omega = \omega_n$. The design should therefore ensure that the range of working angular velocities of the machine is as far from ω_n as is physically possible.

It is important to note that although this analysis provides an accurate description of static unbalance and its effects on a free cam, shaft and bearing system. It does not represent a complete model for the knitting mechanism, since it does not take into account the effect of the force exerted by the follower on to the cam.

In order to counteract some of the shock effects created by the reaction forces on the cam shaft bearings at the same time as balancing the cam statically; the solution proposed was to drive a weight equal in value to that of the reciprocating needles assembly, moving always in the opposite direction, by milling a second cam track on the other side of the cam.

The counterbalancing options are twofold:

(a) Balance cam statically but double horizontal forces. In order to balance the cam statically, the profile milled on the back plane will look like the original one rotated 180°. In this case, the counterbalancing weight is driven by a follower positioned at the upper part of the cam as shown in Figure 5-1. This therefore implies, that although the vertical components of the force almost cancel each other, the horizontal component is doubled.

(b) Balance horizontal forces but double static unbalance. Alternatively, in order to balance both of the horizontal and vertical components for the reaction forces with the counterbalancing weight, the cam followers driving the counterbalancing weight must be placed at the bottom of the cam. However, the profile will be exactly the same as the original one and the static unbalance will be doubled.

Either way, the vertical forces will not cancel each other out exactly. This is because the magnitude of the vertical component of the force, when the load on its upward movement is larger than that needed to drive the load on its downward movement, as was demonstrated by (5-20)and (5-21).

Option (a) was preferred due to space constraints in the circular warp knitting machine design. This solution balances the cam statically and reduces the shock forces due to the reciprocating mass, but it can also create more dynamic unbalance, as the second cam track involves milling out an equal

mass to that of the original cam track but in a different plane (see Figure 5-19). The two equal masses m_{U1} and m_{U2} will be subjected to centrifugal forces $m_{U1}r\omega^2$, which will create uneven reaction forces on the bearings at A and B. All of these forces will rotate with the shaft at velocity ω .

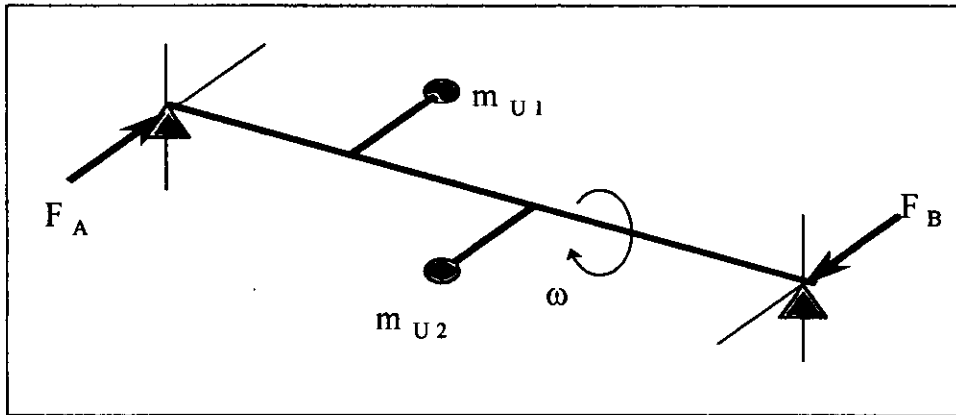


Figure 5-19. Dynamic Unbalance

In conclusion, the reciprocating mass composed of the needle support plate, the needles and strengthening inserts cannot be balanced dynamically by adding or removing a rotating weight. This will only achieve a reduction in the shock forces and unbalancing the revolving masses.

5.6 Experimental Measurement of Cam Follower

Displacement and Machine Vibration.

In this section, experimental measurements of vibration and follower displacement carried out by using two different sets of cams on the machine are described and analysed. The aims of the experiment are; firstly, to evaluate how accurately the cam follower describes the theoretical displacement curves.

Secondly, to establish what factors add to the alteration of the movement.

In addition, to understand the effect of: (i) varying the static unbalance of the cams and (ii) adding or removing the counterbalancing, weights on the displacement curves measured and the vibration of the machine.

Finally, to compare practically the two most suitable cams for high speed in order to ascertain whether the cam profile is a critical feature in the design of the knitting mechanism for the circular warp knitting machine.

5.6.1 Experiment Description

The set up used to measure the motion of the needles as imparted by the cams and the acceleration response of the machine consisted of systems for,

- 1) Recording the actual movement of the needles from an attached inductive displacement transducer (LVDT) to the reciprocating needle support plate. See Figure 5-20.
- 2) Fixing a piezoelectric accelerometer to different points on the machine structure to record the acceleration response.

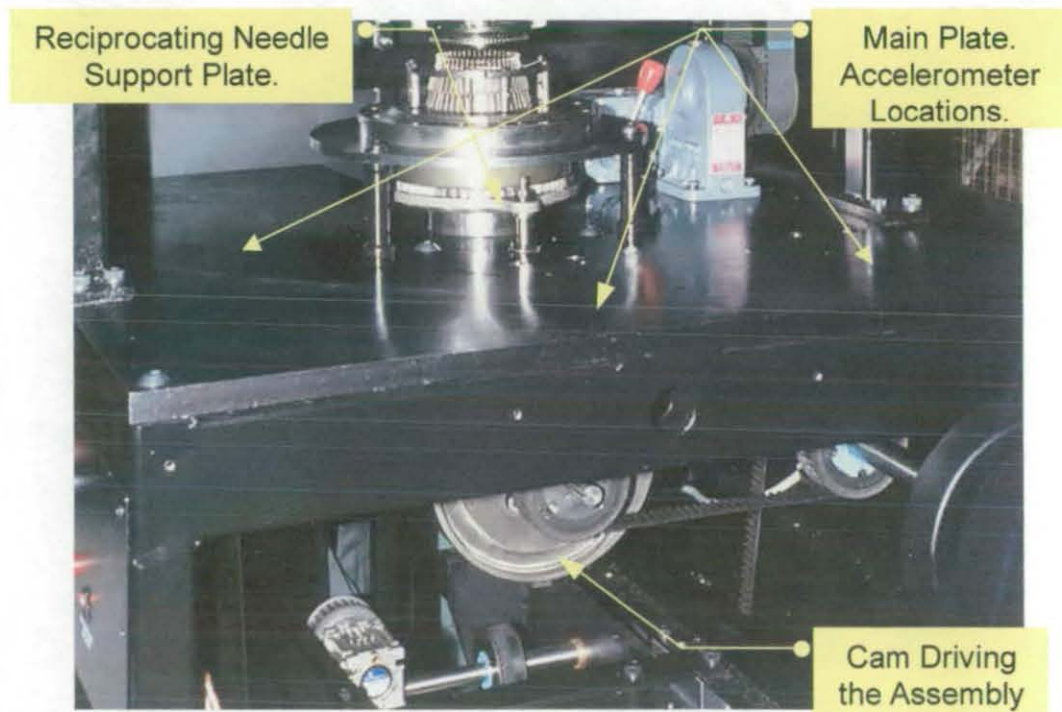


Figure 5-20. Knitting Mechanism

These two signals were synchronised to enable the analysis of the acceleration response in relation to the displacement function of the cam being used.

Two sets of cams were manufactured for the warp knitting machine prototype; one using a cycloidal profile and the other using a polynomial profile calculated in section 5.5. The former was chosen as it is the best suited for high velocities from the three standard profiles analysed, although the jerk curve has discontinuities at the point where the rise and fall movements meet the dwells. This drawback could be outweighed by the comparative ease of calculation.

The cycloidal cam pair was not balanced statically and had a smaller baseline radius, which created a larger maximum pressure angle. The cams with the polynomial profile, on the other hand, were balanced statically by introducing a second track on the other side of the cam and making a hole at 180° from the resultant centre of gravity. This track was used to drive a counterbalance weight equal in magnitude to the sum of the weights of all the reciprocating components.

The dwelling periods for each cam were also different. The cycloidal cam displacement profile was composed of a rise from 0° to 60° , followed by a 120° dwell, a return from 180° to 240° , followed by another 120° dwell (Figure 5-21).

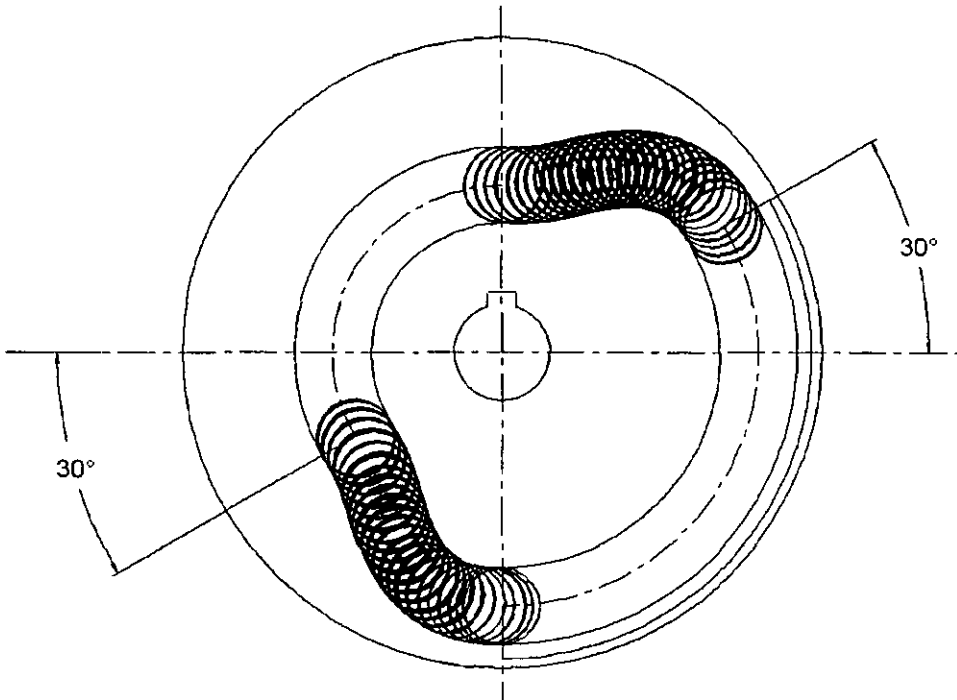


Figure 5-21. Cycloidal Cam.

The polynomial cam displacement profile, on the other hand, was composed of a rise from 0° to 75° , followed by a 90° dwell, a return from 165° to 240° , followed by a longer dwell of 120° (Figure 5-22). The longer dwell is intended for fabrics where longer underlaps are required.

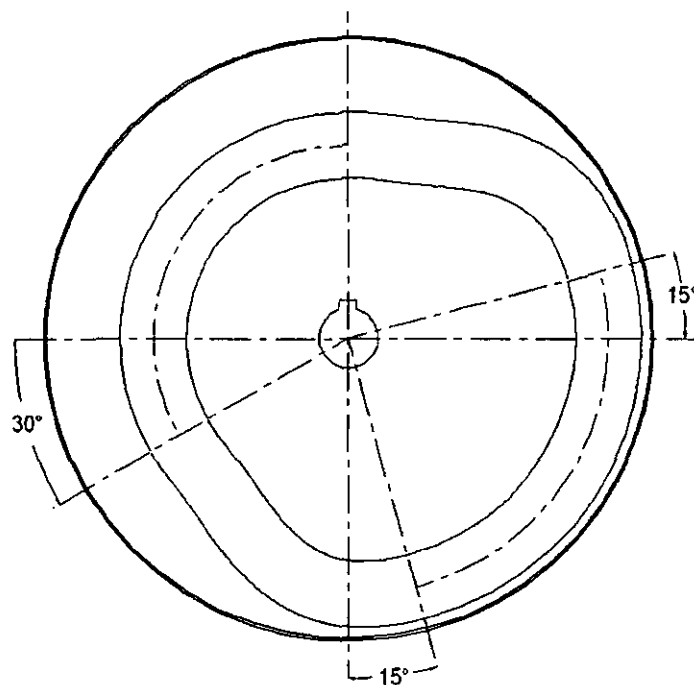


Figure 5-22. Polynomial Cam

Data was collected from the two different types of manufactured cams with the machine running at different speeds and with different amounts of load on the mechanism. In the polynomial cam's case, the tests also included adding weight to the cam to make it statically unbalanced and introducing the counterbalancing weights to help balance the vertical reciprocating forces.

Other changes, such as altering the reciprocating load by removing parts of the assembly, were made during the experiment to investigate their effects on the response.

Since three improvements were carried out to the polynomial cam mechanism design, a direct comparison between cam profiles cannot be made. These changes comprised; (i) statically balancing the cams, (ii) dynamically balancing the vertical forces created by the reciprocation of the needles and (iii) replacing the cycloidal displacement profile for the polynomial one.

Therefore, the analysis presented here is not a comparison of two cam pair results, but an explanation of the different vibration signatures and displacement curves to understand the effects that the different improvements can have on the dynamic response of the machine, using the theory developed in earlier chapters.

The inductive displacement transducer used in these experiments is an ACT model from RDP Electronics² with the following specification;

Input Requirements:	1V to 7V rms a.c. regulated at 5kHz
Linearity:	0.5% of full stroke guaranteed.
Output (full scale rms):	0.8 to 3.7 Volts per Volt (dependent on stroke)

The transducer is connected to an amplifier with an output of up to 18V and a linearity of 0.1% of full stroke.

² Grove Street, Heath Town, Wolverhampton, WV10 0PY, UK

The graph shown on Figure 5-23 is a typical response for the knitting mechanism of the circular warp knitting. The oscilloscope used throughout would export the signal data after averaging 256 cycles. As the signals are synchronised, the changes in the vibration levels throughout the cycle can be analysed.

The data is stored as a file of 1000 readings, representing the signals as they are seen in the oscilloscope monitor. The sampling frequency therefore depends on the scale set for the horizontal axis on the screen. Depending on the speed of the machine, it would sometimes be impractical to maintain the same sampling frequency for all the tests. Consequently, some of the tests were performed with two different sampling frequencies, in order to obtain a more accurate reading from a section of the cycle. See Figure 5-28.

5.6.2 Results and Analysis

5.6.2.1 Displacement Signal

The cam frequency for the response of Figure 5-23 was 5Hz ($\approx 125rpm$ of the machine drive shaft), using the cycloidal cam. In addition, the needles were taken off the reciprocating assembly. This should affect the response significantly as the friction of the needles inside their tricks amounts to a considerable load on the mechanism.

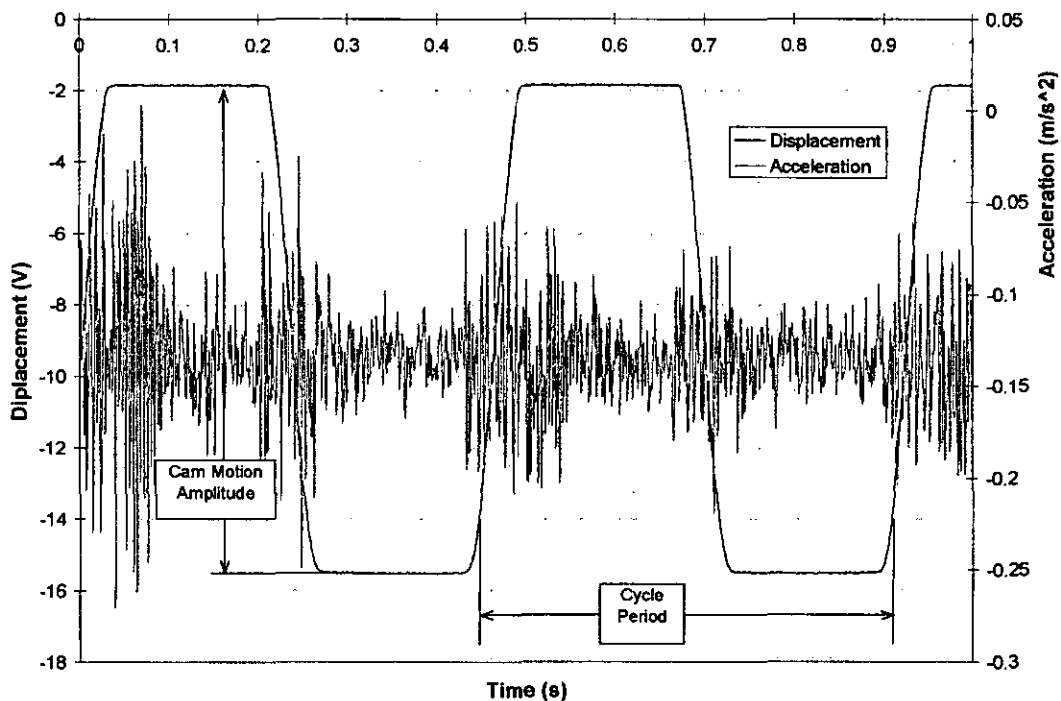


Figure 5-23. Machine Signature with Cycloidal Cam Running at 5Hz

Displacement Amplitude.

As shown in the figure above, the amplitude of the voltage signal from the displacement transducer should be equivalent to the full length of the cam's rise or return movements. The variation in the value of this amplitude for a given cam can be taken as a measure of the accuracy of the displacement transducer measurements, as the cam's stroke will not vary. In the case of the cycloidal cam the amplitude of the stroke is $0.706''=17.93\text{mm}$. The polynomial cam has a larger stroke of $0.837''=21.26\text{mm}$.

The signal's offset from the horizontal axis only means that the range of the displacement transducer that is being used is not near the extreme. The signal has been inverted to ensure that the upper dwell in the figure corresponds to the dwell after the needles have been raised to their highest position; the overlap dwell.

Displacement Cycle Time Period.

The machine's nominal angular velocity for each test was recorded from the machine's or the motor's rpm display. However, the measurement of the period from the displacement transducer's signal could also be used to calculate the frequency of the signal and thus the angular velocity of the cam. Since angular velocity is not a critical parameter, this double reading was only used as a verification tool.

Note that the angular velocity quoted in the tests either in rpm or Hz is that of the machine. The drive from the machine's motor to the cams is via timing pulleys and belts and there is a ratio from of 36/17 between the two.

Distortion in the Displacement Curve Due to Design Clearance

Even at this low speed, the displacement transducer signal is not linear and shows small peaks and valleys, especially noticeable at the dwell intervals. This seems to be the combination of several factors. The first of these is the clearance between the track and the follower (otherwise the follower would not be able to move in the track). This, however, only amounts to 0.05mm.

Figure 5-24 shows the response signature of the machine with the same cam and reciprocating assembly but running at 18.06Hz. The shape of the displacement signal changes considerably, especially at the beginning and end of the dwells. The amplitude of the displacement transducer signal is $13.637V=15.482V-1.845V$, where the top and bottom limits have been calculated from averages of the signal values through the dwells.

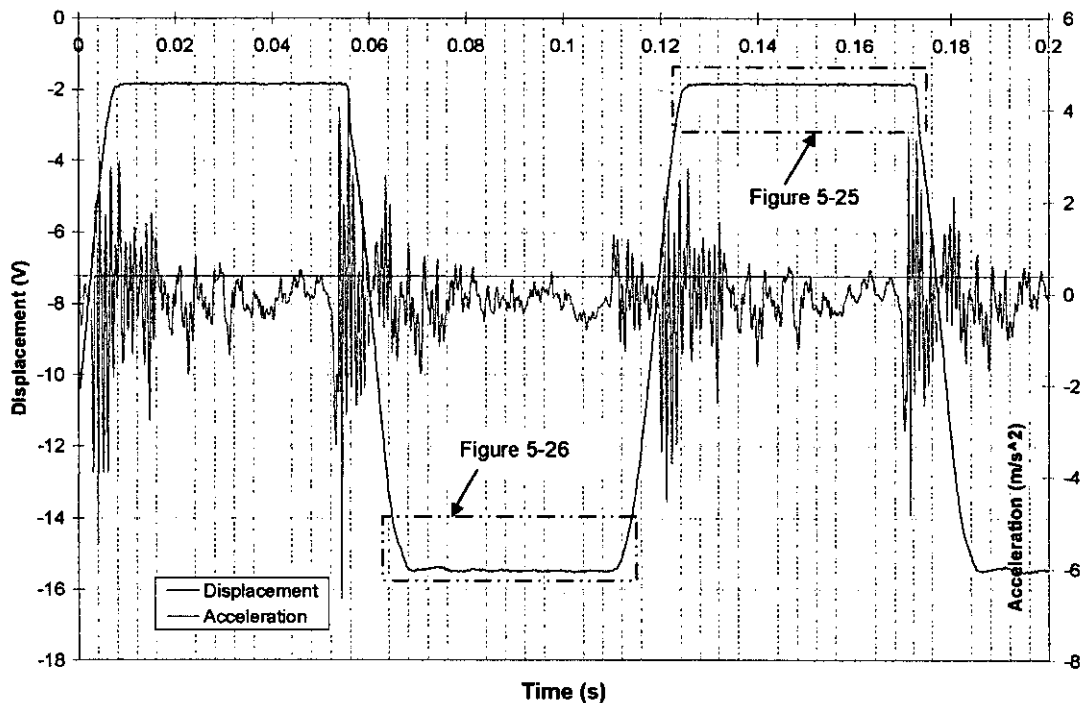


Figure 5-24. Cycloidal Cam Response at 18.06Hz

Knowing that the cam's stroke is 17.93mm, we can deduce that a volt in the displacement transducer signal equates to 1.315mm of displacement.

A closer look at one of these sections (see Figure 5-25), shows that at the overlap dwell, after the needles are raised, there is a variation in the transducer readings of $1.887 - 1.802 = 0.085\text{V}$, equivalent to 0.112mm. The other dwell has an even greater variation in the values; 1.163V, which is equivalent to 0.214mm (see Figure 5-26), which is much more than the original design clearance.

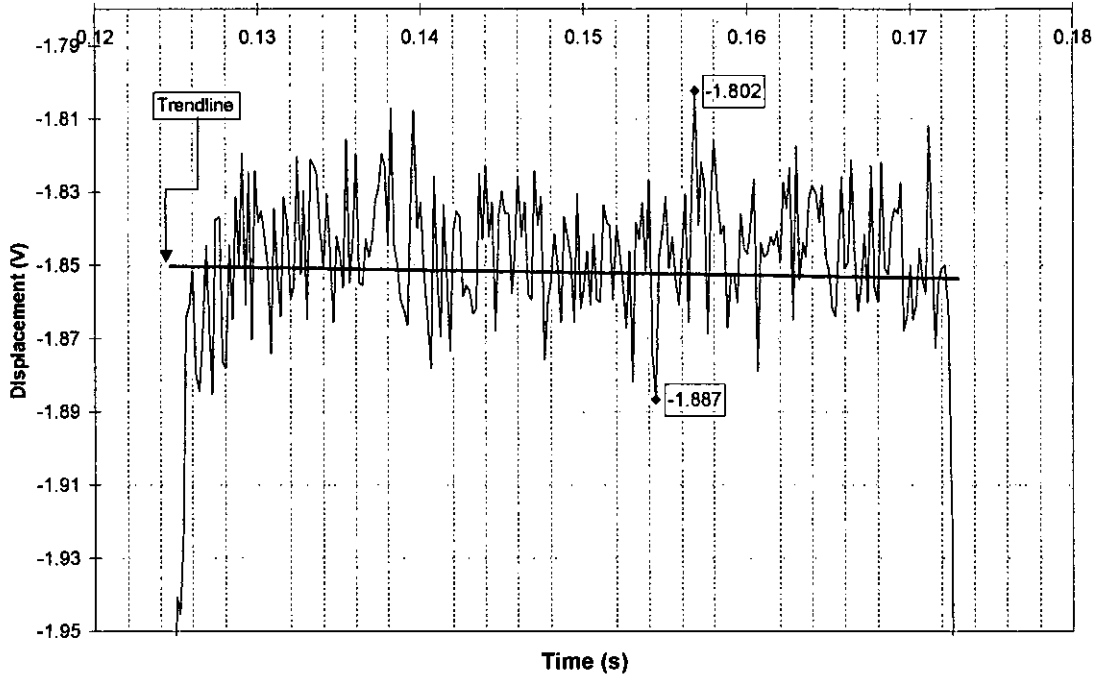


Figure 5-25. Detail of Displacement Signal for Underlap Dwell at 18.06Hz

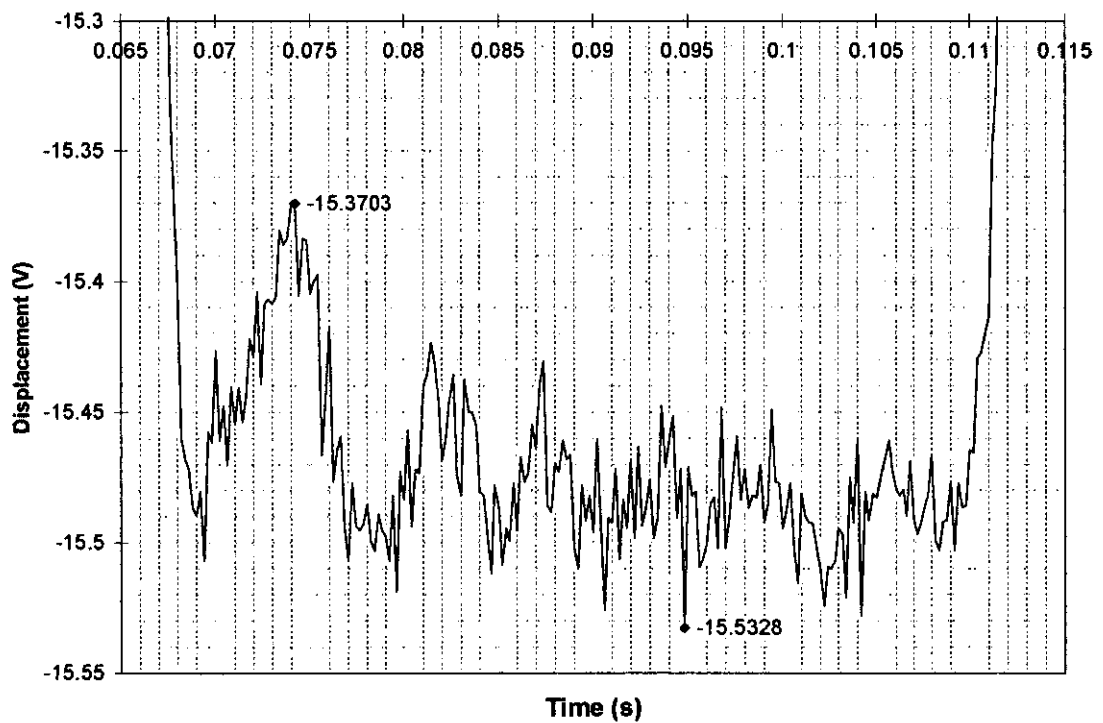


Figure 5-26. Detail of Displacement Signal for Cycloidal Underlap Dwell at 18.06Hz

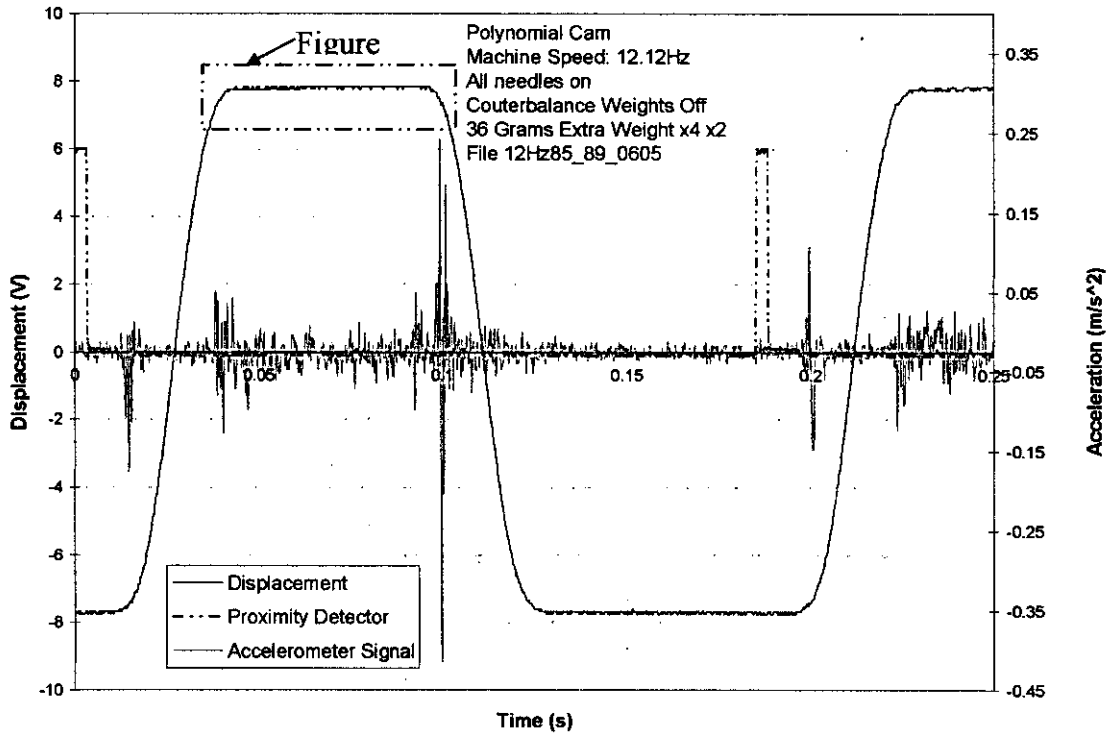


Figure 5-27. Polynomial Cam Response at 12.12Hz

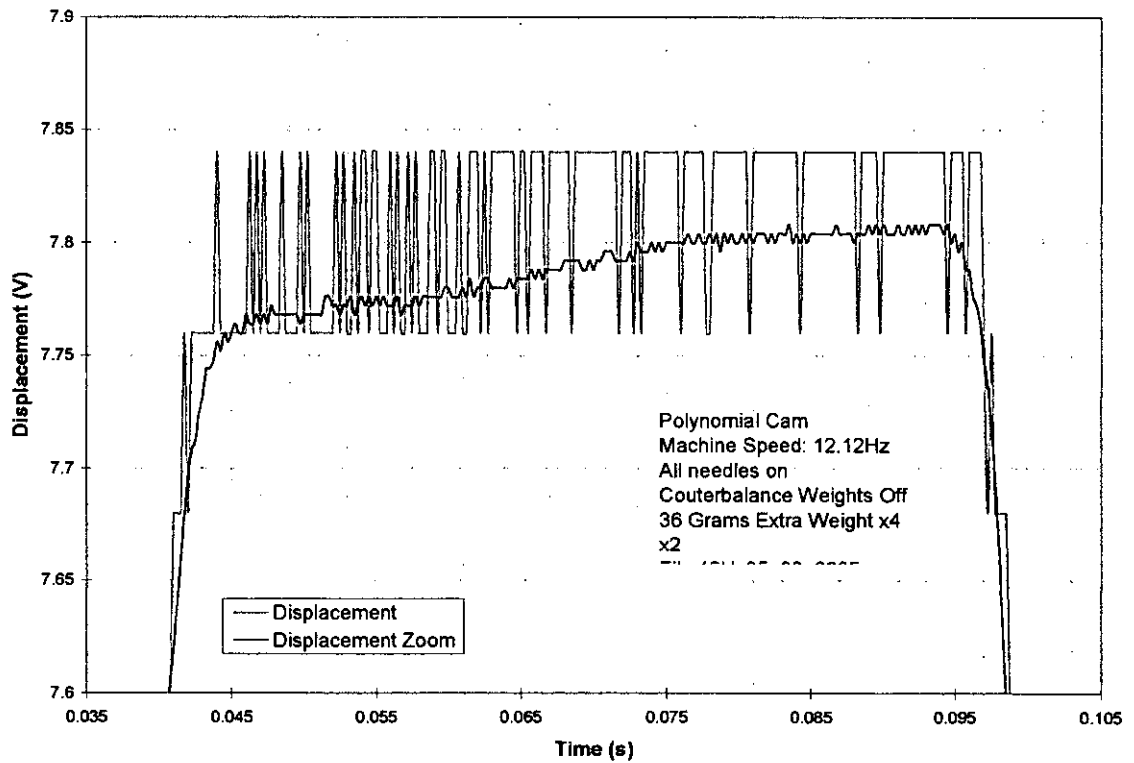


Figure 5-28. Detail of Displacement Signal for Polynomial Overlap Dwell at 12.12Hz

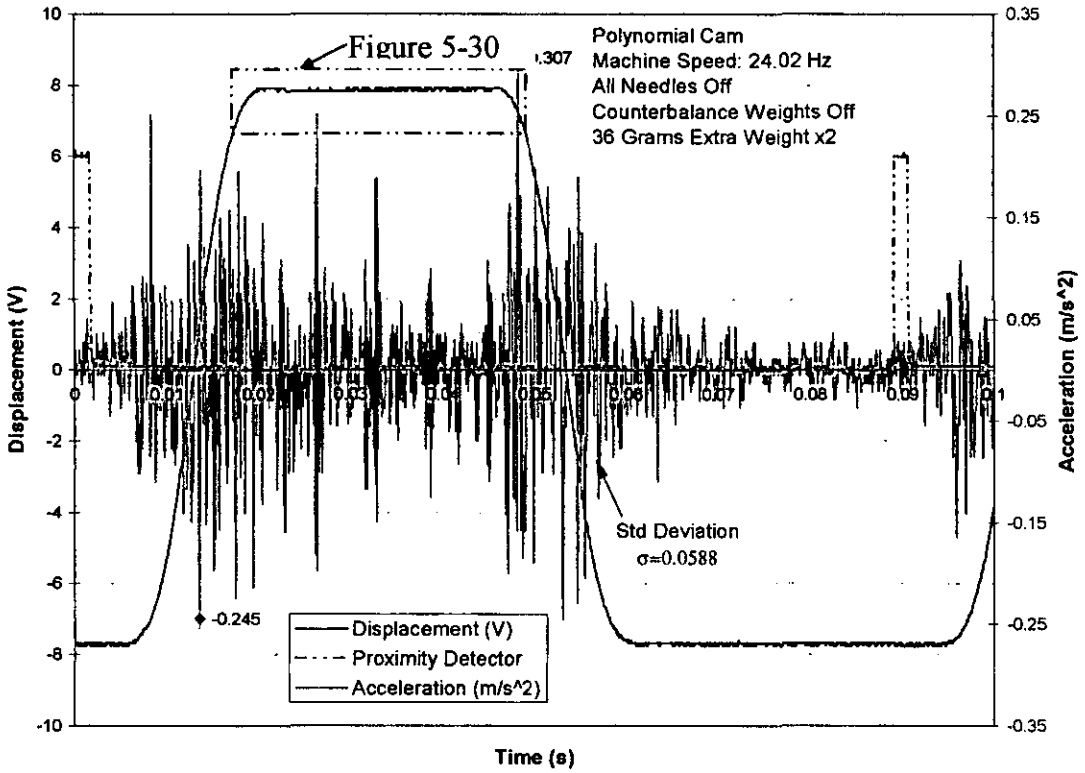


Figure 5-29. Polynomial Cam Response at 24.02Hz

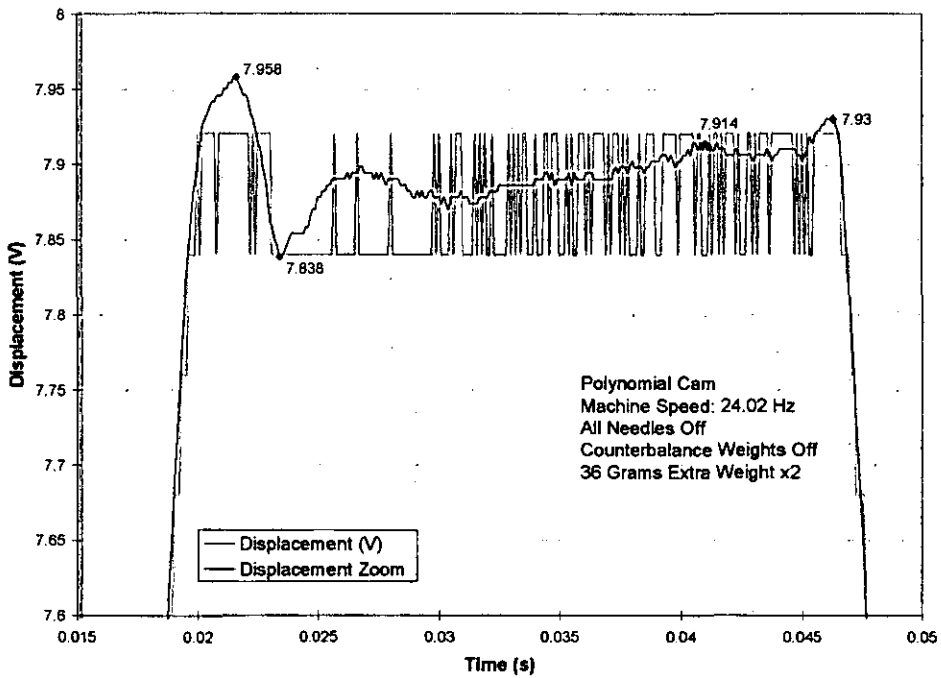


Figure 5-30. Detail of Displacement Signal for Polynomial Overlap Dwell at 24.02Hz

The polynomial cam's response is quite different. Figure 5-27 shows the response with the machine running at 12.12Hz, while Figure 5-29 shows that with the machine running at 24.02Hz. For both graphs, the displacement signal has been inverted; therefore, the overlap dwell (which is shorter) corresponds to the dwell in the upper part of the figure. In addition, an extra signal from a proximity detector has been recorded.

The proximity detector was fixed to one of the cams in order to synchronise the original measurements for displacement to the more accurate one labelled 'Displacement Zoom' in Figure 5-28 and Figure 5-30, to analyse the detail of the behaviour of the follower during the dwell periods.

From Figure 5-28 it is clear that in the polynomial cam's case at 12.12Hz, the follower does not bounce from side to side of the cam track, but displays a single gradual movement from the bottom to the top of the track. When the speed of the machine is increased to 24.02Hz and some unbalanced weight is added, the overshoot at both ends of the dwell are increased, but after a single bounce the movement returns to being a gradual one.

In Figure 5-28, the greatest variation of voltage throughout the dwell amounts to 0.04V, which is equivalent to a displacement of 0.055mm, just over the design clearance value. This is the ideal situation but the speed would probably be too low for an industrial application.

When the speed is raised to 24.02Hz, the amplitude of the first overshoot increases to 0.12V, equivalent to 0.164mm, which cannot be explained solely by the design clearance as the overshoot exceeds it.

Distortion in the Displacement Curve Due to Elasticity of the Bodies

A second reason for the variation from the theoretical displacement profile is the elasticity of the bodies, as discussed in section 5.4. The detail of the shape of the displacement curve for a single stroke of the cycloidal cam in Figure 5-31, overlaid with the theoretical displacement curve from equation (5-39) shows patently the features predicted in section 5.4 for the effects of bodies elasticity (see Figure 5-12). An overshoot at the end of the fall stroke that then settles down and an extended flat portion at the beginning of the

fall. Although it would be difficult to quantify the effect of elasticity, it is clear that it does play some part in the distortion of the displacement curve from the theoretical one.

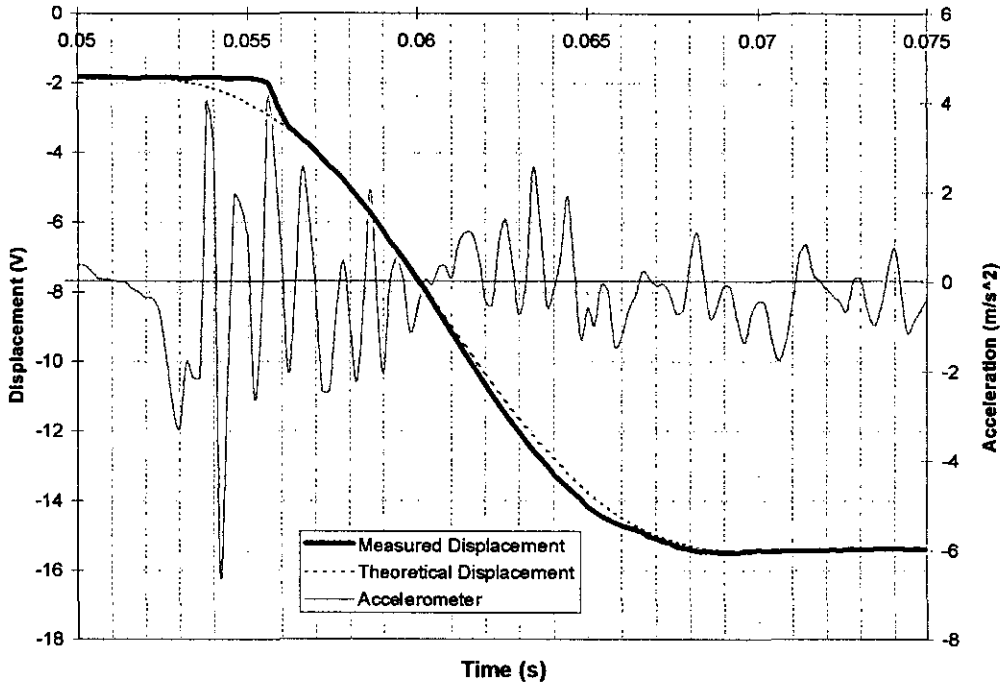


Figure 5-31. Theoretical vs. Measured Displacement Comparison

The vibration present in the machine will also affect the displacement transducer signal, but, as in the elasticity case, it would be very difficult to quantify this effect.

5.6.2.2 Accelerometer Signal

The accelerometer signal measures the level of vibration that the machine is undergoing at any given point in the cam cycle. This signal will inevitably include some noise.

The vibration amplitude, as would be expected, increases with the speed of the machine. When the machine was fitted with the cycloidal cam, the maximum operating speed was 18Hz; above this speed, the vibration of the machine was deemed unsafe. However, when using the polynomial cam, the maximum operating speed at which tests were carried out was 44Hz.

In both cases, the general pattern of the vibration signal had consistent features; firstly, there was a sudden magnification in the signal amplitude that seems to precede the start of the rise or return movements (see F1 in Figure 5-32). The acceleration signal is then reduced during the stroke (see F2) near the midpoint and increased again before the end of the stroke (see F3). Finally, it would settle to its minimum level during the dwell (see F4), the acceleration at the dwell after the needles rise always showing a larger amplitude than at the dwell after the needles return to their low position.

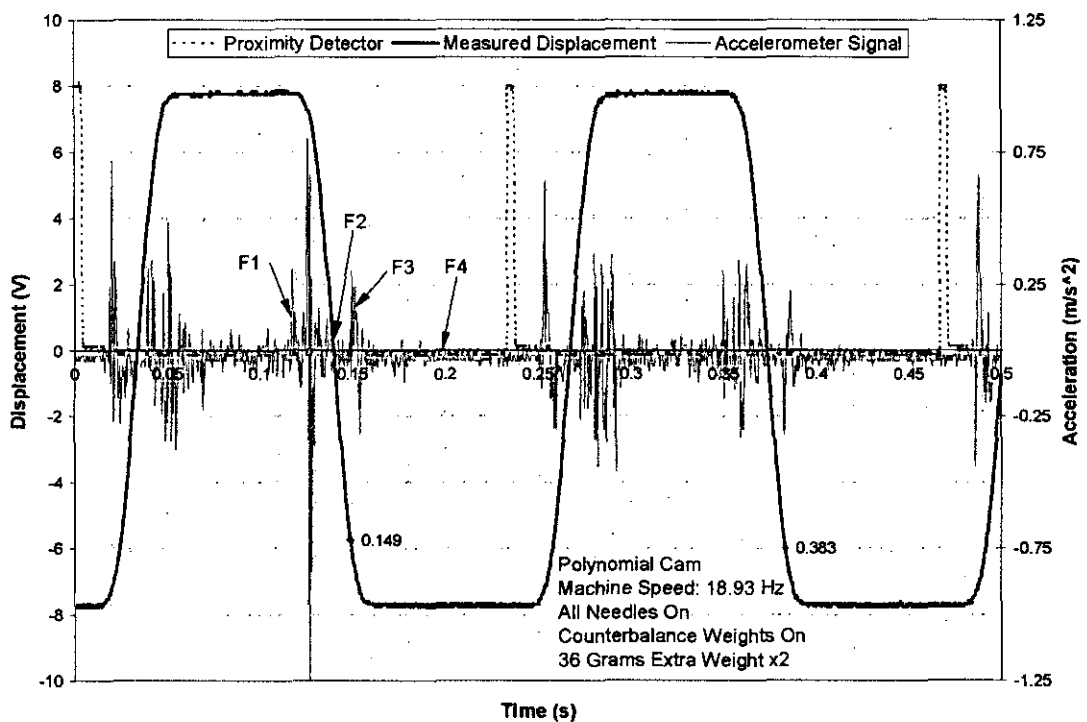


Figure 5-32, Polynomial Cam Response at 18.93Hz

As the speed of the machine increases the amplitude of the signal increases and the settled periods during the dwells are reduced (see Figure 5-29).

These features can only be explained as a combination of several factors; namely, the bodies' elasticity, the cam profile used, the static unbalance and the effect of the counterbalancing assembly. Each one will be discussed separately in the following paragraphs.

The fact that the initial increase in acceleration amplitude starts before the follower's movement is partly due to the effect of the elasticity of the bodies explained in the previous section.

Effect of the Cam Profile

The effect of the cam profile in the vibration signature of the machine becomes evident when the second derivative of the displacement profile (that is, the theoretical acceleration of the follower) is superimposed on the vibration response. See Figure 5-33.

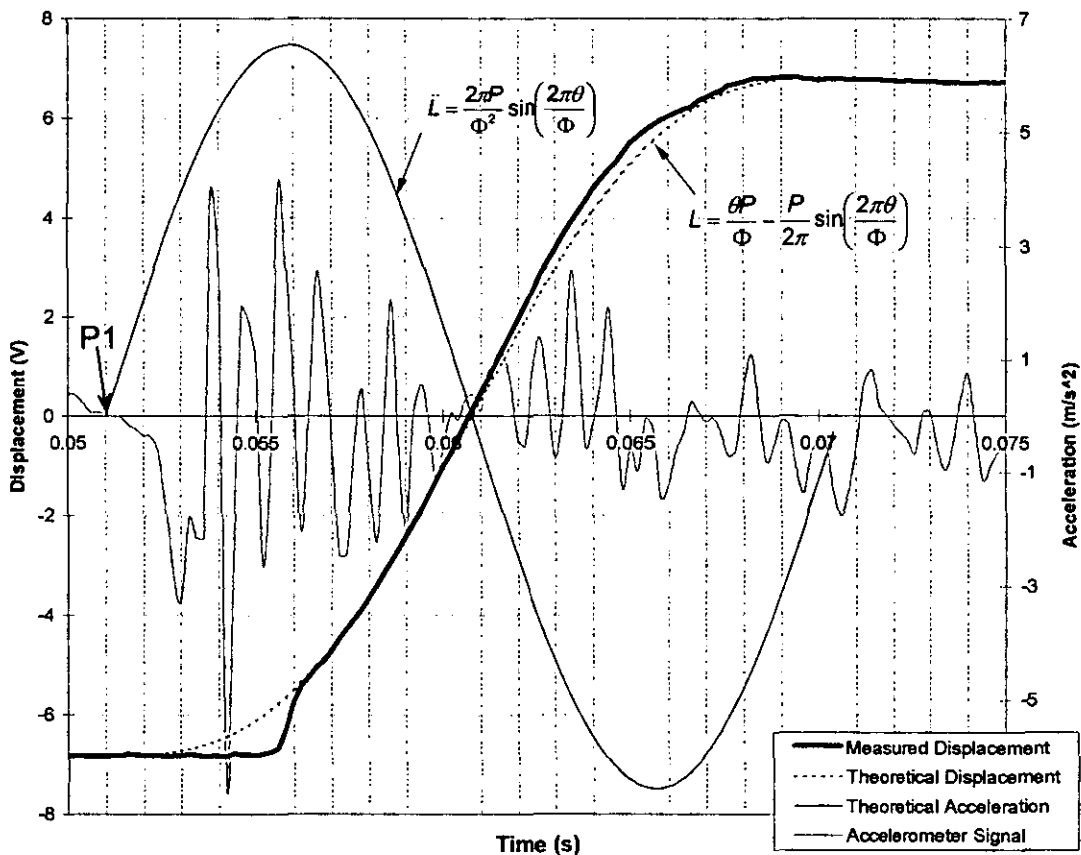


Figure 5-33. Theoretical Acceleration Superimposed to the Rise Portion of the Cycloidal Cam's Response at 18.06 Hz

During the first quarter of the rise, where the magnitude of the theoretical acceleration is increasing, so too is the amplitude of the measured acceleration signal. That amplitude then decreases when the theoretical acceleration curve is also decreasing, coinciding at the midpoint of the rise

where the theoretical acceleration is zero and the measured vibration is at its lowest level. Throughout this first half of the rise, the velocity of the follower is increasing and reaches its maximum at the rise midpoint, where the acceleration is zero.

After the inflection point in the middle of the rise, the velocity starts decreasing; hence, the negative sign of the acceleration curve. There is a second surge in the vibration amplitude in the third quarter of the rise, when the acceleration magnitude is increasing (although negative), and again a reduction when the acceleration magnitude decreases in the last quarter. However, the vibration amplitude in the first half is consistently greater than for the rest of the stroke, on both the cycloidal and polynomial cams.

The reading of acceleration taken on the structure of the machine represents the addition of the effects of all the sources of vibration. In this portion of the cycle, it seems to include the effect of the increasing acceleration of the cam in the first quarter and the forces on the cam shaft bearings calculated in section 5.3. As shown by Figure 5-10 and the kinetic analysis on which the figure is founded, the forces on the camshaft bearings would peak at a third ($\frac{1}{3}$) of the rise and settle until the end of the stroke where another greater peak appears. The early peak would account for the larger vibration amplitude in the first half.

This not only proves the importance of the selection of the cam displacement profile in the dynamic response of the machine, but it also corroborates the analysis carried out in section 5.3.

The second derivative of the cycloidal displacement function changes from being horizontal throughout the preceding dwell to a steep angle at the beginning of the rise (see p1 in Figure 5-33). It is here that it seems the response can be improved, as this sudden change of tangent in the acceleration curve (and hence a discontinuous jerk curve see, Figure 5-15) is creating the increase in vibration amplitude. The polynomial cam is intended to improve the situation, having forced it to have a zero jerk at the beginning and end of the stroke with boundary conditions and therefore softening the

change in acceleration at the start of the stroke. See Figure 5-34, where the theoretical displacement and acceleration curves have been overlaid to the response obtained for a single stroke of the polynomial cam at a similar speed.

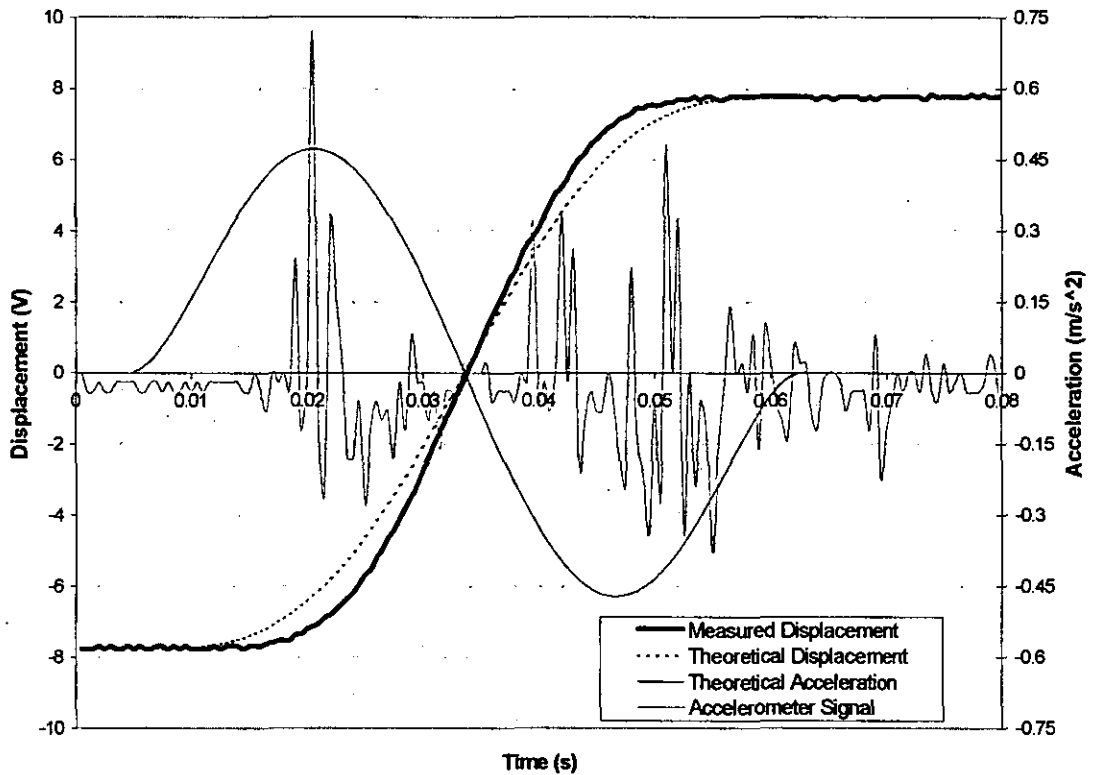


Figure 5-34. Theoretical Acceleration Superimposed to the Rise Portion of the Polynomial Cam's Response at 18.93 Hz

The figure shows how the sudden burst of vibration at the start of the rise has been eliminated. The peak in vibration still coincides with the maximum acceleration point and the vibration remains for the second quarter of the rise, this is possibly due to the peak in the bearing reactions.

The vibration of the third quarter has not been eliminated. This might be because the boundary conditions did not include forcing the jerk to be zero at the rise midpoint. On the contrary, the jerk curve has one of its maximum magnitudes at this point (see Figure 5-16). Note that the vibration amplitude

has been reduced by an order of magnitude compared to that of the cycloidal cam response at a similar speed (Figure 5-33).

With regards to ease of manufacture, the two profiles are at equal levels. The main advantage of the polynomial profile is given by the continuity of its velocity, acceleration and jerk curves. This implies however, larger maximum acceleration and velocity.

Effect of the Static Unbalance

The effect of static unbalance could be isolated only for the polynomial cam pair. Since these cams were balanced at the manufacturing stages, weights (in the form of magnetic parts) were attached to the cams to create static unbalance. The response was measured with the cam running at similar speeds with and without the unbalanced weight.

The magnets amounted to up to 150gms of unbalanced weight. Since this weight is relatively small compared to the weight of the cam itself and the loads to which it is subjected when the needles are sliding in their slots, the effect of the unbalance is best appreciated when the needles have been removed. The response shown in Figure 5-29 was recorded in similar conditions as that shown in Figure 5-35, except that the former included unbalanced weights and the latter does not.

When the two vibration signatures are compared, it can be seen that the effect of the unbalanced mass is an overall increase in the amplitude of the vibration, both during the rise and return movements and during the dwell. The overall standard deviation of the acceleration data for the unbalanced test is higher than that of the balanced one even though the latter was taken at a higher speed; from equation (5-50), the amplitude of the vibration is proportional to the unbalanced mass, the distance from the centre at which the mass is rotating and the angular speed of rotation.

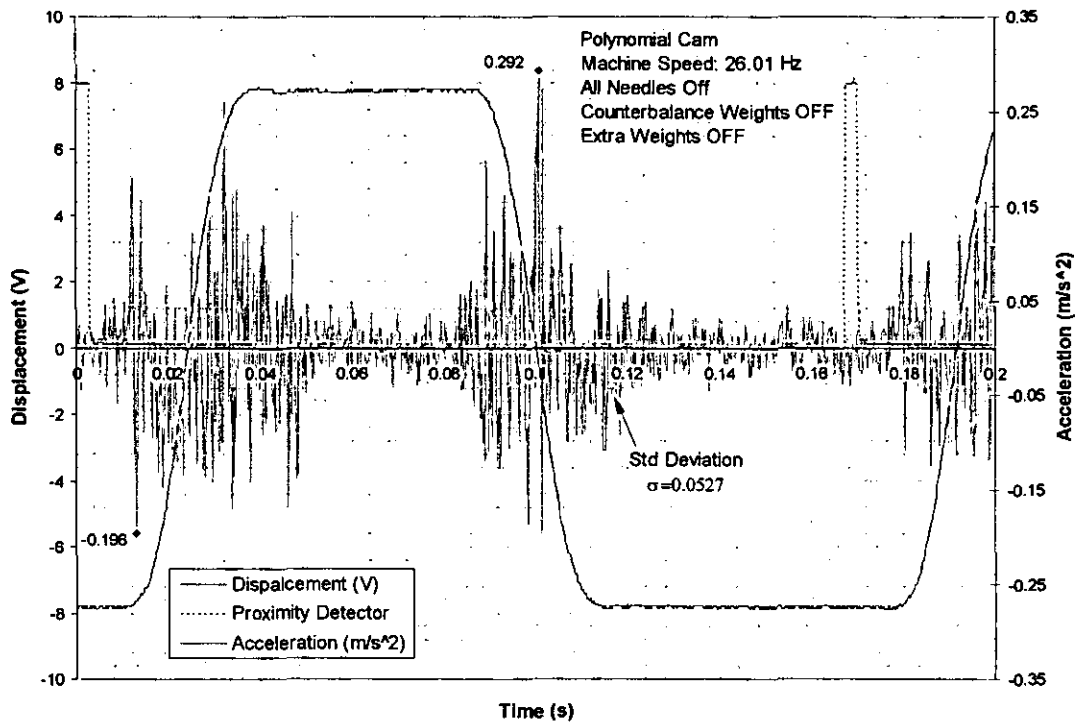


Figure 5-35. Polynomial Cam Response at 26.01Hz

Effect of the Counterbalancing Assembly

The effect of the counterbalancing assembly can be analysed by comparing the response with and without attaching it at similar conditions.

Figure 5-36 shows the response of the mechanism without the counterbalancing weights. It can be seen that the worse vibration occurs at the beginning of the rise and return movements and at the start of the dwells. Although the maximum amplitude consistently takes place in the first quarter of the downward movement, it settles down before the end of the stroke and the vibration during the underlap dwell is low. On the other hand, the amplitude increases at the last portion of the upward movement, and this together with the shock forces at the end of the travel, make the vibration amplitude higher in the overlap dwell than in the underlap dwell.

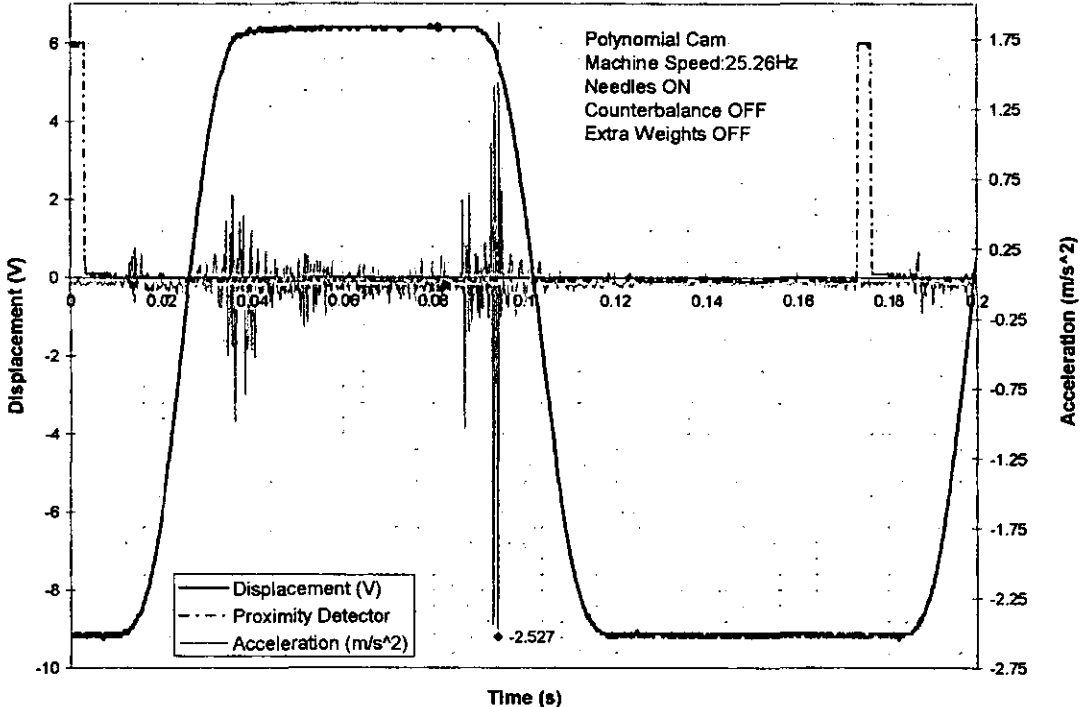


Figure 5-36. Polynomial Cam Response without Counterbalancing Weights

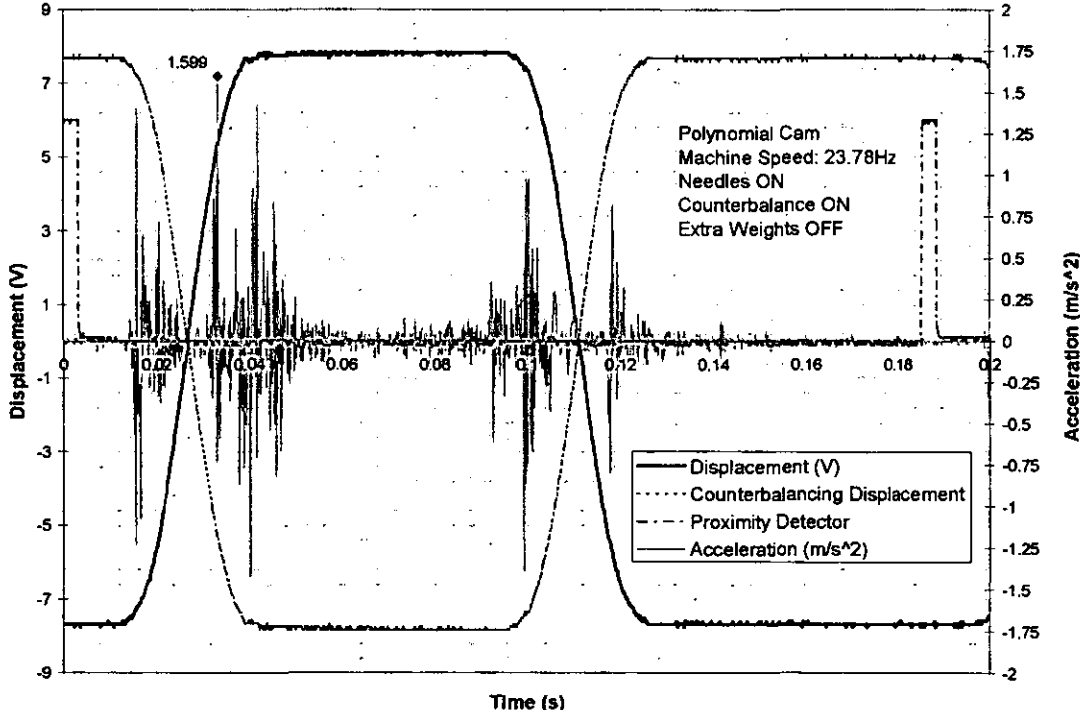


Figure 5-37. Polynomial Cam Response with Counterbalancing Weights

Figure 5-37 shows the response obtained when the counterbalancing assembly is attached. Although not recorded, the displacement of the counterbalancing weight has been added to the graph by inverting the original displacement signal as it helps to illustrate the behaviour of the mechanism. The overall maximum amplitude is reduced substantially (from 2.527 m/s^2 to 1.599 m/s^2), but the negatives consequences also elicited can outweigh this positive effect;

Firstly, the vibration present at the beginning of the needle's downward movement (now reduced in amplitude) is reproduced at the beginning of their upward movement, due to the fact it is also the downward movement of the counterbalancing weights.

In addition, a new burst of vibration appears at the end of the needle's downward movement, again created by the counterbalancing weights' upward movement.

5.6.3 Experimental Measurements Conclusions

The optimisation of the cam's performance and the reduction of vibration levels is a critical part of this project, since the use of a cam incorporating dwelling time for the overlaps and underlaps is an important design decision in the design of the new circular warp knitting machine. The need for a reciprocating action in the knitting mechanism is inevitably going to make it prone to vibration.

Several factors have been proven to affect the level of vibration present in the machine; namely, the cam profile, elasticity of the parts, and static and dynamic balance. Wherever possible these factors have been isolated in order to analyse their effect. It is not possible, however, to quantify the level to which each one contributes to the overall vibration signature and therefore only a qualitative analysis has been carried out, supported by existing theory describing their effects.

The effect of the elasticity of the bodies can only be reduced by increasing their rigidity; that is, using different materials. This however, will increase the cost and make it more difficult to be produced commercially.

The effects of the static unbalance can never be completely eradicated. The solution proposed here of milling the reverse side of the cam is ideal for statically balancing the cam; it represents a better solution than merely drilling a hole equivalent to the unbalanced mass because every radial slice ($\delta\theta$) of cam track will be balanced by an equal slice in the reverse cam track.

Using the reverse cam track to drive counterbalancing weights does not yield a satisfactory result, because, although the amplitude of the overall vibration response is reduced, the forces created by the counterbalancing weight generate other unwanted vibration. The reciprocating mass cannot be balanced by another rotating mass. The best means of eliminating the inertia forces produced by the reciprocating mass would be to use multiple needle heads phased at the correct angles so as to cancel the effects of the rotating forces⁵⁰. This set up was not practicable within this research due to its cost.

The continuity of the displacement derivatives achieved by the design of the polynomial cam proved to be an important factor in the vibration response of the mechanism. However, the result of a continuous jerk curve is twofold; the gradual change of acceleration at the extremities of the stroke show a positive change in the response but the higher maximum acceleration value yields a higher vibration at 25% and 75% of the movement. The next chapter proposes a method to minimise the jerk, and hence the maximum acceleration value, but keep the gradual change in acceleration at the ends of the movement.

5.7 Conclusions

The chapter has described in more detail the design of the cam-follower concept option when using a conical needle bed; the concept selected after the evaluation described in Chapter 4. It also theoretically analysed the kinetic consequences of that design decision. Finally it demonstrated the actual performance of the mechanism through the experimental measurement of its vibration and cam displacement.

It may be concluded from Section 5.3, that the selection of a conical needle bed (rather than a circular one) creates unwanted horizontal components in the forces which increase with the taper angle. It is therefore important to demonstrate its usefulness in increasing the patterning capabilities. Since in kinetic terms, the optimum taper angle would be 0 degrees. It is left to the patterning model in Chapter 8 to evaluate an optimum taper angle, for a given set of patterning requirements.

From the experimental work: in Section 5.6 it is clear that static unbalance, dynamic unbalance and elasticity of the body and the cam profile; are all major contributors to the performance of the machine. While static unbalance can be corrected, it can sometimes create more dynamic unbalance.

Regarding balancing the reciprocating mass, the counterbalancing assembly used to prove the positive effects of reducing the vertical shock forces, led to other unwanted effects. An optimum solution for this problem has been outlined; using a series of phased knitting heads to balance the rotating

forces created by the dynamic imbalance, but the manufacturing of this solution was beyond the scope of this project.

In relation to the cam profile, the polynomial cam was demonstrated to have better results due to the continuity for three of the displacement derivatives. However, there is no accepted method of reducing the high maximum acceleration and velocity resulting from ensuring the continuity of the derivative curves. The next chapter describes and demonstrates a method for optimising the jerk curve devised and proposed as part of this research.

Chapter 6. Optimised Cam Motion Based on Piecewise Polynomials

6.1 Introduction

Cam motion synthesis has been studied extensively as the use of cams has been widespread in many industries. Textbooks give formulaic methods of synthesis for a number of 'standard' profiles^{49,51}. Authors of these books, however, are less able to give recommendations as to how to optimise a cam profile for a certain application. Polynomial profiles, which are defined with a number of breakpoints in the profile for which the designer can define boundary conditions, are the most suitable for optimisation because the displacement, velocity, acceleration and jerk can be controlled for any critical point in the cam profile.

Farouki⁵² et al describe an approach to cam design focusing on the transferability of the cam profile into CNC machines or CAD systems.

Yu and Lee⁵³ use a standard non-linear optimisation technique to investigate the effect of the features of a motion curve, such as the velocity, the acceleration and the boundary continuity on the minimum size of the cam.

Textbooks^{49,51} describe the method for synthesising a polynomial profile for a single cam motion. However, using Piecewise Polynomials (PP), the complete cam profile can be designed as a combined linear system. PP are the best suited for implementation of a computer aided design and manufacturing program as it can be generalised and is not case dependant. However, in order to use PP to design a cam profile, values for the displacement and its derivatives at the profile breakpoints must be known. This can sometimes make the procedure impractical.

Wang and Yang⁵⁴ (1996) used a quadratic programming (QP) algorithm to optimise the shape of the motion profile created using PP such that the jerk

level is reduced to a minimum. The optimisation is carried out using any unspecified breakpoint boundary conditions as variables. That is, by assuming that unspecified breakpoint boundary conditions can take any value. However, this method can only handle some combinations of boundary conditions and the authors did not explain the advantages and limitations of the method.

This chapter re-defines the method illustrating its restrictions, without which it cannot be used reliably. In addition, improvements carried out to the implementation are also demonstrated by application examples using Maple Mathematics Software.

6.2 Piecewise Polynomials

The PP method is based on describing the displacement of a cam follower with a series of polynomial expressions; one for each segment of the profile. The method will be explained conducting Case Study No. 1 in parallel to illustrate the theory.

The displacement imparted by a cam profile comprising n steps can be described using a polynomial function for each one of the non-dwelling segments in the form,

$$y_i(\theta) = \sum_{j=1}^k b_{ij} (\theta - \beta_i)^{j-1} \quad , \quad \forall \theta \in \{\beta_i \leq \theta \leq \beta_{i+1}\} \quad , \quad i = 1, \dots, n-1 \quad (6-1)$$

where θ : Cam angle

b_{ij} : Displacement coefficients, given by boundary conditions.

k : Polynomial order

β_i : The i^{th} breakpoint in the profile in radians.

n : Number of breakpoints in the profile.

Velocity, acceleration, jerk and any subsequent derivatives of the displacement functions can be expressed similarly as:

$$v_i(\theta) = \dot{y}_i(\theta) = \sum_{j=2}^k b_{ij} \cdot (j-1) \cdot (\theta - \beta_i)^{j-2},$$

$$\forall \theta \in \{\beta_i \leq \theta \leq \beta_{i+1}\}, \quad i = 1, \dots, n-1$$

(6-2)

$$a_i(\theta) = \ddot{y}_i(\theta) = \sum_{j=3}^k b_{ij} \cdot (j-1) \cdot (j-2) \cdot (\theta - \beta_i)^{j-3},$$

$$\forall \theta \in \{\beta_i \leq \theta \leq \beta_{i+1}\}, \quad i = 1, \dots, n-1$$

(6-3)

$$j_i(\theta) = \dddot{y}_i(\theta) = \sum_{j=4}^k b_{ij} \cdot (j-1) \cdot (j-2) \cdot (j-3) \cdot (\theta - \beta_i)^{j-4},$$

$$\forall \theta \in \{\beta_i \leq \theta \leq \beta_{i+1}\}, \quad i = 1, \dots, n-1$$

(6-4)

$$s_i(\theta) = y_i^{(4)}(\theta) = \sum_{j=4}^k b_{ij} \cdot (j-1) \cdot (j-2) \cdot (j-3) \cdot (j-4) \cdot (\theta - \beta_i)^{j-5},$$

$$\forall \theta \in \{\beta_i \leq \theta \leq \beta_{i+1}\}, \quad i = 1, \dots, n-1$$

(6-5)

Where, $v_i(\theta)$: Polynomial function describing velocity for the i^{th} segment.

$a_i(\theta)$: Polynomial function describing acceleration for the i^{th} segment.

$j_i(\theta)$: Polynomial function describing jerk for the i^{th} segment.

$s_i(\theta)$: Polynomial function describing jerk's derivative for the i^{th} segment.

All the above functions are determined by differentiating the displacement with respect to θ ; constant angular velocity (ω) is assumed.

$$v(t) = \frac{\partial y}{\partial t} = \frac{\partial y}{\partial \theta} \cdot \frac{\partial \theta}{\partial t} = v(\theta) \cdot \omega$$

(6-6)

Yao⁵⁵ has carried out research on optimising cam profiles using variable angular velocity. However, it is not always economically sound to implement 'Active Control' of a cam mechanism, as it requires the use of a servo drive and a motion control system in place of a standard drive.

Case Study 1: For a cam profile comprising three breakpoints and polynomial order 8, equations (6-1) to (6-5) become;

Segment 1:

Displacement;

$$y_1(\theta) = b_{1,1} + b_{1,2}(\theta - \beta_1) + b_{1,3}(\theta - \beta_1)^2 + b_{1,4}(\theta - \beta_1)^3 + b_{1,5}(\theta - \beta_1)^4 + b_{1,6}(\theta - \beta_1)^5 + b_{1,7}(\theta - \beta_1)^6 + b_{1,8}(\theta - \beta_1)^7$$

Velocity;

$$v_1(\theta) = b_{1,2} + 2 \cdot b_{1,3}(\theta - \beta_1) + 3 \cdot b_{1,4}(\theta - \beta_1)^2 + 4 \cdot b_{1,5}(\theta - \beta_1)^3 + 5 \cdot b_{1,6}(\theta - \beta_1)^4 + 6 \cdot b_{1,7}(\theta - \beta_1)^5 + 7 \cdot b_{1,8}(\theta - \beta_1)^6$$

Acceleration;

$$a_1(\theta) = 2 \cdot b_{1,3} + 6 \cdot b_{1,4}(\theta - \beta_1) + 12 \cdot b_{1,5}(\theta - \beta_1)^2 + 20 \cdot b_{1,6}(\theta - \beta_1)^3 + 30 \cdot b_{1,7}(\theta - \beta_1)^4 + 42 \cdot b_{1,8}(\theta - \beta_1)^5$$

Jerk;

$$j_1(\theta) = 6 \cdot b_{1,4} + 24 \cdot b_{1,5}(\theta - \beta_1) + 60 \cdot b_{1,6}(\theta - \beta_1)^2 + 120 \cdot b_{1,7}(\theta - \beta_1)^3 + 210 \cdot b_{1,8}(\theta - \beta_1)^4$$

S;

$$s_1(\theta) = 24 \cdot b_{1,5} + 120 \cdot b_{1,6}(\theta - \beta_1) + 360 \cdot b_{1,7}(\theta - \beta_1)^2 + 840 \cdot b_{1,8}(\theta - \beta_1)^3$$

Segment 2:

Displacement;

$$y_1(\theta) = b_{2,1} + b_{2,2}(\theta - \beta_1) + b_{2,3}(\theta - \beta_1)^2 + b_{2,4}(\theta - \beta_1)^3 + b_{2,5}(\theta - \beta_1)^4 + b_{2,6}(\theta - \beta_1)^5 + b_{2,7}(\theta - \beta_1)^6 + b_{2,8}(\theta - \beta_1)^7$$

Velocity;

$$v_1(\theta) = b_{2,2} + 2 \cdot b_{2,3}(\theta - \beta_1) + 3 \cdot b_{2,4}(\theta - \beta_1)^2 + 4 \cdot b_{2,5}(\theta - \beta_1)^3 + 5 \cdot b_{2,6}(\theta - \beta_1)^4 + 6 \cdot b_{2,7}(\theta - \beta_1)^5 + 7 \cdot b_{2,8}(\theta - \beta_1)^6$$

Acceleration;

$$a_1(\theta) = 2 \cdot b_{2,3} + 6 \cdot b_{2,4}(\theta - \beta_1) + 12 \cdot b_{2,5}(\theta - \beta_1)^2 + 20 \cdot b_{2,6}(\theta - \beta_1)^3 + 30 \cdot b_{2,7}(\theta - \beta_1)^4 + 42 \cdot b_{2,8}(\theta - \beta_1)^5$$

Jerk;

$$j_1(\theta) = 6 \cdot b_{2,4} + 24 \cdot b_{2,5}(\theta - \beta_1) + 60 \cdot b_{2,6}(\theta - \beta_1)^2 + 120 \cdot b_{2,7}(\theta - \beta_1)^3 + 210 \cdot b_{2,8}(\theta - \beta_1)^4$$

S;

$$s_1(\theta) = 24 \cdot b_{2,5} + 120 \cdot b_{2,6}(\theta - \beta_1) + 360 \cdot b_{2,7}(\theta - \beta_1)^2 + 840 \cdot b_{2,8}(\theta - \beta_1)^3$$

6.2.1 Boundary Conditions

A designer will generally be able to define the desired displacement values at each breakpoint. A follower rise and dwell cycle of 50mm amplitude for example, would be treated as a profile with three breakpoints; $\beta_1 = 0^\circ, \beta_2 = 180^\circ, \beta_3 = 360^\circ$ with the displacement boundary conditions $y(\beta_1) = 0, y(\beta_2) = 50\text{mm}, y(\beta_3) = 0$. Other design requirements will determine the velocity, acceleration, jerk or s function at the boundaries between segments.

In general, these Boundary conditions can be expressed as the following sets of $n-1$ equations;

$$y_i(\beta_i) = \text{Disp}_i, \quad i = 1, \dots, n-1; \quad (6-7)$$

$$\begin{aligned} v_i(\beta_i) &= \text{Vel}_i, \quad i = 1, \dots, n-1; \\ a_i(\beta_i) &= \text{Accel}_i, \quad i = 1, \dots, n-1; \\ j_i(\beta_i) &= \text{Jerk}_i, \quad i = 1, \dots, n-1; \\ s_i(\beta_i) &= S_i, \quad i = 1, \dots, n-1; \end{aligned} \quad (6-8)$$

Where $\text{Disp}_i, \text{Vel}_i, \text{Accel}_i, \text{Jerk}_i$ and S_i are constants. Note that in equations (6-8), each segment function is used to define only one of the boundaries of the segment, although polynomial functions are defined over two boundaries (i.e. segment 1 is defined over β_1 and β_2).

For Case Study 1, the boundary conditions on displacement (equations (6-7)) would provide $n-1$ explicit equations;

$$b_{1,1} = \text{Disp}_1, b_{2,1} = \text{Disp}_2. \quad (6-9)$$

Similarly the explicit equations derived from boundary conditions on the different displacement derivatives in the case of a 3-breakpoint cam profile are found from substituting boundary conditions on the expression for $v(\theta)$, equation (6-2):

$$b_{1,2} = \text{Vel}_1, b_{2,2} = \text{Vel}_2, \quad (6-10)$$

on the expression for $a(\theta)$, equation (6-3):

$$b_{1,3} = \frac{\text{Accel}_1}{2}, b_{2,3} = \frac{\text{Accel}_2}{2}, \quad (6-11)$$

on the expression for $j(\theta)$, equation (6-4):

$$b_{1,4} = \text{Jerk}_1 / 6, b_{2,4} = \text{Jerk}_2 / 6, \quad (6-12)$$

and on the expression for $s(\theta)$, equation (6-5):

$$b_{1,5} = s_1 / 24, b_{2,5} = s_2 / 24. \quad (6-13)$$

6.2.2 Continuity Conditions

Further equations are derived from ensuring continuity on the displacement function and its derivatives. The condition of continuity throughout the cam profile can be expressed as a set of equations evaluating the polynomial motion functions at the boundary points. In the case of continuous displacement of the follower (which is necessary for the manufacture of the cam), continuity will be given by the following $(n-1)$ equations;

$$\begin{cases} y_i(\beta_{i+1}) = y_{i+1}(\beta_{i+1}), i = 1, \dots, n-2 \\ y_{n-1}(\beta_1) = y_1(\beta_1) \end{cases} \quad (6-14)$$

The latter ensures continuity at the end of the profile. Similar sets of equations can be deduced for each of the displacement derivatives;

$$\begin{cases} v_i(\beta_{i+1}) = v_{i+1}(\beta_{i+1}), i = 1, \dots, n-2 \\ v_{n-1}(\beta_1) = v_1(\beta_1) \end{cases} \quad (6-15)$$

⋮

$$\begin{cases} s_i(\beta_{i+1}) = s_{i+1}(\beta_{i+1}), i = 1, \dots, n-2 \\ s_{n-1}(\beta_1) = s_1(\beta_1) \end{cases}$$

The continuity equations derived for Case Study 1's cam profile with 3 breakpoints and polynomial order of 8 are;

Continuity in displacement:

$$\begin{aligned}
 & b_{1,1} + b_{1,2}(\beta_2 - \beta_1) + b_{1,3}(\beta_2 - \beta_1)^2 + b_{1,4}(\beta_2 - \beta_1)^3 + b_{1,5}(\beta_2 - \beta_1)^4 + b_{1,6}(\beta_2 - \beta_1)^5 \\
 & \quad + b_{1,7}(\beta_2 - \beta_1)^6 + b_{1,8}(\beta_2 - \beta_1)^7 = b_{2,1} \\
 & b_{2,1} + b_{2,2}(\beta_3 - \beta_2) + b_{2,3}(\beta_3 - \beta_2)^2 + b_{2,4}(\beta_3 - \beta_2)^3 + b_{2,5}(\beta_3 - \beta_2)^4 + b_{2,6}(\beta_3 - \beta_2)^5 \\
 & \quad + b_{2,7}(\beta_3 - \beta_2)^6 + b_{2,8}(\beta_3 - \beta_2)^7 = b_{1,1}
 \end{aligned}
 \tag{6-16}$$

Continuity in velocity:

$$\begin{aligned}
 & b_{1,2} + 2 \cdot b_{1,3}(\beta_2 - \beta_1) + 3 \cdot b_{1,4}(\beta_2 - \beta_1)^2 + 4 \cdot b_{1,5}(\beta_2 - \beta_1)^3 + 5 \cdot b_{1,6}(\beta_2 - \beta_1)^4 \\
 & \quad + 6 \cdot b_{1,7}(\beta_2 - \beta_1)^5 + 7 \cdot b_{1,8}(\beta_2 - \beta_1)^6 = b_{2,2} \\
 & b_{2,2} + 2 \cdot b_{2,3}(\beta_3 - \beta_2) + 3 \cdot b_{2,4}(\beta_3 - \beta_2)^2 + 4 \cdot b_{2,5}(\beta_3 - \beta_2)^3 + 5 \cdot b_{2,6}(\beta_3 - \beta_2)^4 \\
 & \quad + 6 \cdot b_{2,7}(\beta_3 - \beta_2)^5 + 7 \cdot b_{2,8}(\beta_3 - \beta_2)^6 = b_{1,2}
 \end{aligned}
 \tag{6-17}$$

⋮

Continuity in jerk:

$$\begin{aligned}
 & 6 \cdot b_{1,4} + 24 \cdot b_{1,5}(\beta_2 - \beta_1) + 60 \cdot b_{1,6}(\beta_2 - \beta_1)^2 + 120 \cdot b_{1,7}(\beta_2 - \beta_1)^3 \\
 & \quad + 210 \cdot b_{1,8}(\beta_2 - \beta_1)^4 = 6 \cdot b_{2,4} \\
 & 6 \cdot b_{2,4} + 24 \cdot b_{2,5}(\beta_3 - \beta_2) + 60 \cdot b_{2,6}(\beta_3 - \beta_2)^2 + 120 \cdot b_{2,7}(\beta_3 - \beta_2)^3 \\
 & \quad + 210 \cdot b_{2,8}(\beta_3 - \beta_2)^4 = 6 \cdot b_{1,4}
 \end{aligned}
 \tag{6-18}$$

The expressions in (6-16)through to (6-18) provide a set of equations that, expressed as a linear system of equations, can be used to determine the polynomial coefficients b_{ij} of the cam displacement profile.

6.2.3 Polynomial Order

The designer must calculate the polynomial order(k) that will not under or over constrain the system depending on the specific design requirements.

The system will need to solve $k \cdot (n - 1)$ coefficients defined in equation (6-1); therefore, the same number of equations will be required to solve them. The boundary conditions described in (6-7) and (6-8) provide $n - 1$ equations for each of the displacement derivatives. Similarly, the continuity conditions in (6-14) and (6-15) provide $n - 1$ equations for each of the displacement derivatives.

On the other hand, the polynomial function describing each segment (6-1) has k unknown coefficients, making the total number of unknowns in the profile $k \cdot (n - 1)$. In order to solve them as a linear system, the same number of equations is required.

The procedure to calculate the appropriate polynomial order is easily illustrated using an example. For Case Study 1, the designer of a cam profile with 3 breakpoints has specific requirements for the cam's displacement;

$$y(\beta_1) = 0, y(\beta_2) = 50mm \quad (6-19)$$

In addition, he requires that the velocity and acceleration at all breakpoints be equal to zero:

$$\begin{aligned} v_i(\beta_i) &= 0, \quad i = 1, \dots, n-1; \\ a_i(\beta_i) &= 0, \quad i = 1, \dots, n-1; \end{aligned} \quad (6-20)$$

Finally, it is an implicit requirement for any cam profile that the displacement function is continuous throughout, as it would not be possible to manufacture the cam otherwise.

The polynomial order can be derived as follows. The designer would have $n - 1$ equations relating to the displacement boundary conditions (6-19),

$n - 1$ equations ensuring continuity of the follower's displacement (6-14) and a final $2 \cdot (n - 1)$ given by equations (6-20). Therefore the system will not be over or under-constrained when;

Number of Coefficients to solve = Number of Equations

(6-21)

$$k \cdot (n - 1) = 4 \cdot (n - 1) \Rightarrow k = 4$$

Wang erroneously states that an eighth-order polynomial is necessary to ensure that the motion gives continuous displacement, velocity and acceleration profiles and to allow the user to specify a dwell period between any two cam rotation breakpoints. For each set of design requirements, the number of equations available must be calculated and the required polynomial order derived from (6-21).

Only when the designer provides breakpoint boundary conditions for four derivatives of the displacement profile (displacement, velocity, acceleration, jerk or s) and has set the continuity conditions on all of them, will an eighth order polynomial be suitable for defining each segment of the profile.

Thus, the first improvement that can be made to the method is to allow the designer more flexibility in deciding the polynomial order according to the boundary conditions available. The displacement derivatives used need not be consecutive. Depending on the requirements of the application any combination can be used. Similarly continuity can be imposed on any of the displacement derivatives.

This correction will become even more important later in the optimisation process, when -as it will be shown later in the chapter- not any derivative can be used to calculate the polynomial coefficient, the choice is dependent on the function being optimised.

6.2.4 Solving for the Polynomial Coefficients

Once the polynomial order has been defined, the explicit form of the motion profile can be expressed as the polynomial function (6-1). The objective of imposing the different boundary and continuity conditions is to create a linear system of equations that will enable the designer to solve for the polynomial coefficients defined in the displacement function.

Case Study 2 is a worked example of the process using Maple and is described below. It is based on the design of a single dwell cam for which the boundary conditions applied are summarised in Table 6-1. The Maple program is enclosed as Appendix D

Table 6-1 . Boundary Conditions for Piecewise Polynomials Case Study No. 2.

Breakpoint No.	Cam Angle β	Displacement	Velocity	Acceleration	S
1	0°	0	0	0	0
2	90°	100mm	0	0	0
3	180°	100mm	0	0	0
4	360°	0	0	0	0

1. Establish the number of breakpoints required:

$$n = 4;$$

Note that although the number of breakpoints specified includes one at 360°, the boundary conditions given for it must be the same as those given for breakpoint 1 at 0°.

2. Ascertain the boundary conditions to be used.

$y, \dot{y}, \ddot{y}, y^4$ plus continuity in all of them; a total of 8 conditions.

3. Define the polynomial order according to the boundary conditions specified above.

$$k = 8;$$

4. Derive the equations from the boundary and continuity conditions for all segments, in terms of the polynomial coefficients.

Boundary;

$$\begin{aligned} b_{1,1} &= Disp_1; & b_{2,1} &= Disp_2; & b_{3,1} &= Disp_3; \\ b_{1,2} &= Vel_1; & b_{2,2} &= Vel_2; & b_{3,2} &= Vel_3; \\ 2b_{1,3} &= Accel_1; & 2b_{2,3} &= Accel_2; & 2b_{3,3} &= Accel_3; \\ 24b_{1,5} &= s_1; & 24b_{2,5} &= s_2; & 24b_{3,5} &= s_3; \end{aligned}$$

(6-22)

Continuity.

Continuity in displacement can be expressed as

$$\begin{aligned} b_{1,1} + 1.571b_{1,2} + 2.467b_{1,3} + 3.876b_{1,4} + 6.088b_{1,5} + 9.563 b_{1,6} + \\ 15.022b_{1,7} + 23.596 b_{1,8} &= b_{2,1} \\ b_{2,1} + 1.571b_{2,2} + 2.467b_{2,3} + 3.876b_{2,4} + 6.088b_{2,5} + 9.563 b_{2,6} + \\ 15.022b_{2,7} + 23.596 b_{2,8} &= b_{3,1} \\ b_{3,1} + 3.142b_{3,2} + 9.870b_{3,3} + 31.006b_{3,4} + 97.409b_{3,5} + 306.020 \\ b_{3,6} + 961.389b_{3,7} + 3020.293b_{3,8} &= b_{1,1} \end{aligned}$$

(6-23)

Similar sets of equations are derived for continuity in velocity, acceleration and S. The full set of equations is included in Appendix D

5. Write these equations in matrix form, constructing a linear system in terms of the polynomial coefficients.

$$[\bar{M}] \cdot [\bar{b}_{i,j}] = 0$$

(6-24)

where each row in $[\bar{M}]$ represents one of the equations in (6-22) & (6-23).

Solving the system, each coefficient is expressed as a function of the breakpoints $\beta_1 \dots \beta_{n-1}$ and the values for the boundary conditions $Disp_1 \dots Disp_{n-1}, Vel_1 \dots Vel_{n-1}, \dots, s_1 \dots s_{n-1}$:

$$\begin{pmatrix} b_{1,1} \\ b_{1,2} \\ b_{1,3} \\ \\ b_{1,4} \\ \\ b_{1,5} \\ \\ \\ b_{1,6} \\ \\ \vdots \\ \\ b_{3,8} \end{pmatrix} = \begin{pmatrix} Disp_1 \\ Vel_1 \\ \frac{1}{2} Accel_1 \\ \\ \frac{1}{360} (4 s_1 \beta_1^4 + \beta_1^4 s_2 - 4 \beta_2 \beta_1^3 s_2 - 16 s_1 \beta_2 \beta_1^3 + 24 s_1 \beta_2^2 \beta_1^2 \\ + 6 \beta_2^2 \beta_1^2 s_2 + 420 Accel_1 \beta_1^2 - 120 \beta_1^2 Accel_2 - 16 s_1 \beta_2^3 \beta_1 \\ - 4 \beta_2^3 \beta_1 s_2 - 1560 Vel_1 \beta_1 - 840 Accel_1 \beta_2 \beta_1 + 240 \beta_2 \beta_1 Accel_2 \\ - 960 \beta_1 Vel_2 + 4 s_1 \beta_2^4 + s_2 \beta_2^4 + 420 Accel_1 \beta_2^2 - 120 Accel_2 \beta_2^2 \\ + 960 Vel_2 \beta_2 - 2520 Disp_2 + 2520 Disp_1 + 1560 Vel_1 \beta_2) / (\\ \beta_1^3 - 3 \beta_2 \beta_1^2 + 3 \beta_2^2 \beta_1 - \beta_2^3) \\ \\ \frac{1}{24} s_1 \\ \\ \frac{1}{120} (7 s_1 \beta_1^4 - 2 \beta_1^4 s_2 - 28 s_1 \beta_2 \beta_1^3 + 8 \beta_2 \beta_1^3 s_2 + 42 s_1 \beta_2^2 \beta_1^2 \\ - 12 \beta_2^2 \beta_1^2 s_2 - 240 Accel_1 \beta_1^2 + 180 \beta_1^2 Accel_2 - 28 s_1 \beta_2^3 \beta_1 \\ + 8 \beta_2^3 \beta_1 s_2 - 360 \beta_2 \beta_1 Accel_2 + 1200 \beta_1 Vel_2 + 480 Accel_1 \beta_2 \beta_1 \\ + 1320 Vel_1 \beta_1 + 7 s_1 \beta_2^4 - 2 s_2 \beta_2^4 - 240 Accel_1 \beta_2^2 + 180 Accel_2 \beta_2^2 \\ - 2520 Disp_1 - 1320 Vel_1 \beta_2 + 2520 Disp_2 - 1200 Vel_2 \beta_2) / (\\ -\beta_2^5 + \beta_1^5 + 5 \beta_2^4 \beta_1 - 10 \beta_2^3 \beta_1^2 + 10 \beta_2^2 \beta_1^3 - 5 \beta_2 \beta_1^4) \\ \\ \vdots \\ \\ -\frac{1}{120} (4 s_3 \beta_4 \beta_3^3 - 120 Accel_3 \beta_4 \beta_3 - 6 s_3 \beta_4^2 \beta_3^2 + 4 s_3 \beta_4^3 \beta_3 \\ - s_3 \beta_4^4 - s_3 \beta_3^4 - 720 Disp_1 + 720 Disp_3 + 60 Accel_3 \beta_3^2 \\ + 60 Accel_3 \beta_4^2 - 60 \beta_3^2 Accel_1 - 60 \beta_4^2 Accel_1 + \beta_4^4 s_1 + \beta_3^4 s_1 \\ + 6 \beta_4^2 \beta_3^2 s_1 - 4 \beta_4 \beta_3^3 s_1 - 4 \beta_4^3 \beta_3 s_1 + 360 \beta_4 Vel_1 - 360 \beta_3 Vel_1 \\ + 360 Vel_3 \beta_4 - 360 Vel_3 \beta_3 + 120 \beta_4 \beta_3 Accel_1) / (-35 \beta_4^3 \beta_3^4 \\ + 21 \beta_4^2 \beta_3^5 - 7 \beta_4 \beta_3^6 + 35 \beta_4^4 \beta_3^3 - \beta_4^7 + \beta_3^7 - 21 \beta_4^5 \beta_3^2 \\ + 7 \beta_4^6 \beta_3) \end{pmatrix}$$

(6-25)

6. Replacing the boundary conditions of Table 6-1 into (6-25), the polynomial coefficients can be calculated explicitly. In this case :

$$\begin{aligned}
 & \begin{bmatrix} b_{1,1} & b_{1,2} & b_{1,3} & b_{1,4} & b_{1,5} & b_{1,6} & b_{1,7} & b_{1,8} \\ b_{2,1} & b_{2,2} & b_{2,3} & b_{2,4} & b_{2,5} & b_{2,6} & b_{2,7} & b_{2,8} \\ b_{3,1} & b_{3,2} & b_{3,3} & b_{3,4} & b_{3,5} & b_{3,6} & b_{3,7} & b_{3,8} \end{bmatrix} \\
 = & \begin{bmatrix} 0 & 0 & 0 & 180.609 & 0 & -219.594 & 139.798 & -25.428 \\ 100 & 0 & 0 & 0 & 0 & 0 & 0 & 0 \\ 100 & 0 & 0 & -22.576 & 0 & 6.862 & -2.184 & 0.199 \end{bmatrix}
 \end{aligned}
 \tag{ 6-26 }$$

7. Replacing the values above into (6-1), the polynomial function describing the displacement of the follower is completely defined in terms of the boundary values given by the designer.

$$\left\{ \begin{array}{l}
 y_1 = 180.609\theta^3 - 219.594\theta^5 + 139.798\theta^6 - 25.428\theta^7 \quad \forall \theta \in \{\beta_1 \leq \theta \leq \beta_2\} \\
 \hline
 y_2 = 100 \quad \forall \theta \in \{\beta_2 \leq \theta \leq \beta_3\} \\
 \hline
 y_3 = 100 - 22.576(\theta - \pi)^3 + 6.862(\theta - \pi)^5 - 2.184(\theta - \pi)^6 + 0.199(\theta - \pi)^7 \quad \forall \theta \in \{\beta_3 \leq \theta \leq \beta_4\}
 \end{array} \right.
 \tag{ 6-27 }$$

Figure 6-1 shows the displacement function and its derivatives. All the boundary and continuity conditions are met.

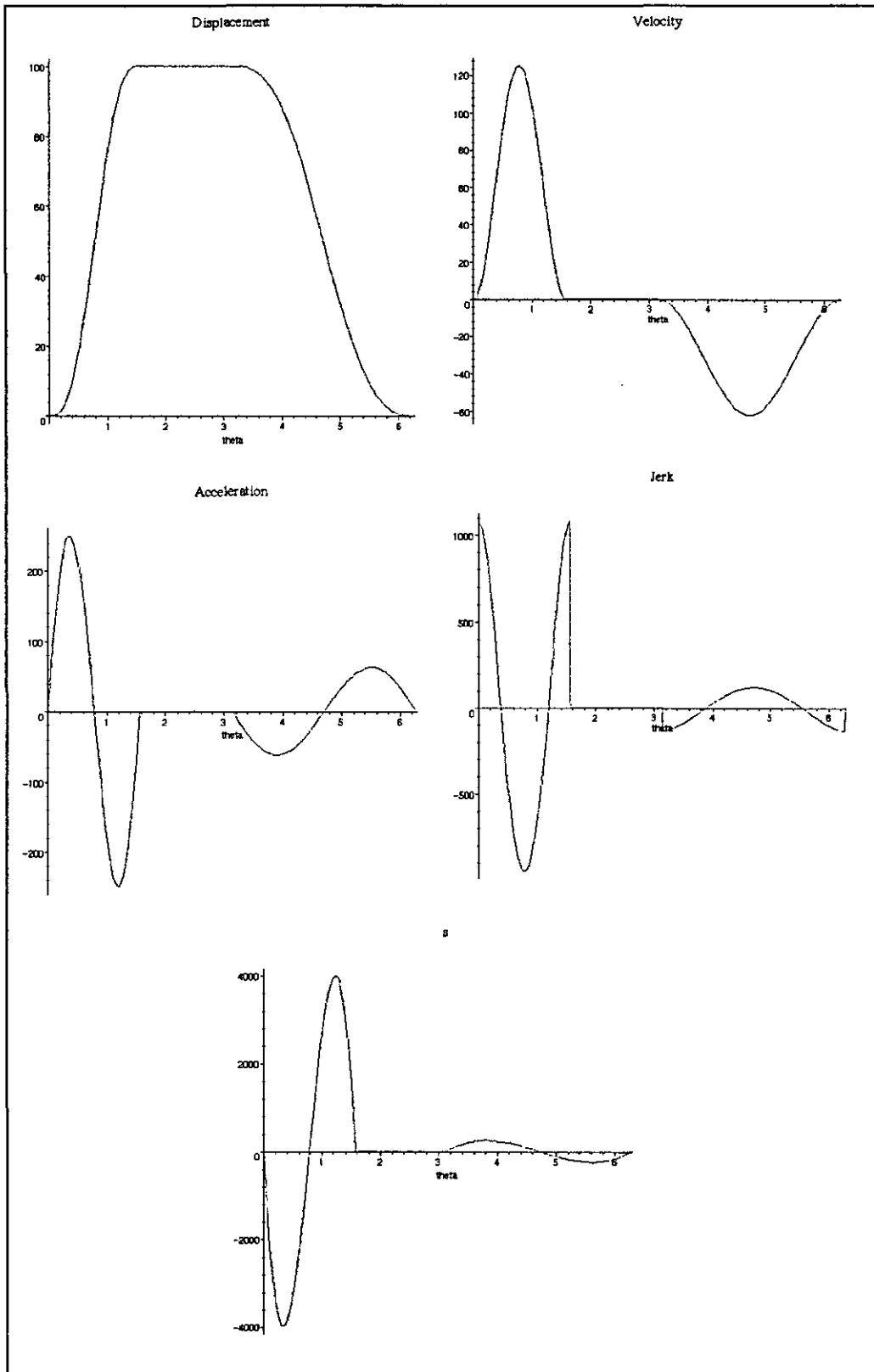


Figure 6-1. Displacement Derivatives Of Cam Profile Using Piecewise Polynomials.

6.2.5 Dwells

The use of Piecewise Polynomials is ideal for computer aided cam design, as the polynomial function is calculated by a mathematical package leaving the designer the only task of specifying the boundary values. However, a drawback is that it cannot be utilised when the cam profile includes dwells. When a dwell is defined between two breakpoints, the displacement function is reduced to $y_i = Disp_i$, and its derivatives $\dot{y}_i = 0$, $\ddot{y}_i = 0$, $\dddot{y}_i = 0, \dots$. In this case, if treated as the eighth order polynomial of equation (6-1), $b_{i1} = Disp_i$; $b_{ix} = 0 \quad x = 2, \dots, n-1$. Wang's optimising method, as it will be explained later in this paper, fails to recognise this as a special case, leaving all coefficients undefined. The result is that while the method acknowledges the endpoint boundary condition and the continuity conditions, it allows the profile inside the endpoints to vary. That is, $b_{ix} \neq 0$ for $x = 2, \dots, n-1$. Instead of a dwell, the method could result in a bell like profile maintaining the start and endpoints at the value required for the dwell.

Table 6-2. Boundary Conditions for Modified Case Study 2. Incorrect Dwell Conditions.

Breakpoint No.	Cam Angle β (Degrees)	Displacement (mm)	Velocity (mm/rad)	Acceleration (mm/rad ²)	S (mm/rad ⁴)
1	0°	0	0	25	0
2	90°	100	20	0	10
3	180°	100	0	50	30
4	360°	0	0	25	0

In order to avoid this, all boundary conditions referring to the adjoining breakpoints of a dwell must be specified as zero, as shown in the worked

example above. The consequences of not doing so are easier to illustrate at this stage, by changing the boundary conditions of the previous case study. Let the boundary conditions of another application be specified as in Table 6-2

Following the same method as before, the displacement function is, again, expressed as a set of Piecewise Polynomials. This function and its derivatives are plotted in Figure 6-2. It can easily be seen that the dwell portion no longer exists between the 2nd and 3rd breakpoints.

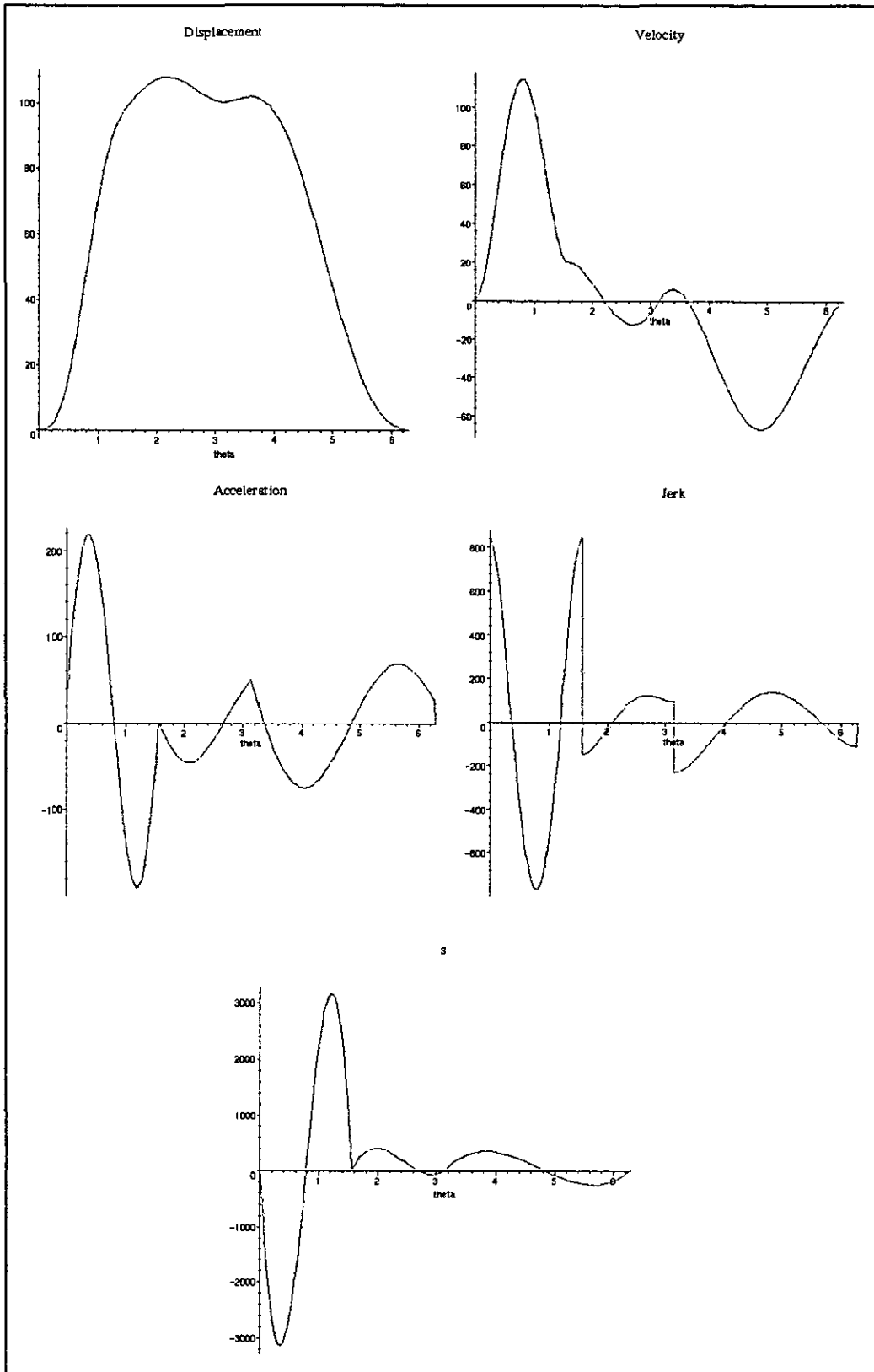


Figure 6-2. Displacement Derivatives of Profile with Incorrect Dwell Boundary Conditions

6.3 Optimisation

Piecewise Polynomials are very useful especially when the designer knows the boundary values required for each breakpoint and each of the derivatives used. This is not necessarily the case in all applications. Many practical problems only have specific requirements for the follower displacement values, while others might have a requirement for velocity at the midpoint of a given segment of the profile, but not a displacement requirement at the same point. In his shape optimisation method, Wang proposes a procedure by which the jerk is 'optimised' (i.e. minimised) to avoid noise, vibration and possible structural damage using the unspecified boundary conditions as variables.

6.3.1 Procedure

The method is based on the assumption that the designer does not specify a value for all the boundary conditions, $Disp_1 \dots Disp_{n-1}, Vel_1 \dots Vel_{n-1}, \dots, s_1 \dots s_{n-1}$, and that jerk continuity has not been used as one of the boundary and continuity conditions to solve the polynomial coefficients. Wang does not state the latter assumption; however it is important if the method is to be applied to any other type of optimisation. In general, it should be stated that the function to be optimised cannot be used to generate any of the equations that are used to form linear system (6-24), described in the previous section.

This is because the equation used in the optimisation will be added later to the set of equations of the linear system. Therefore, if it is already present, the system will become under constrained and it would be impossible to solve.

Table 6-3. Case Study 3. Optimised Cam Application Requirements.

Breakpoint No.	Cam Angle β	Displacement	Velocity	Acceleration	S
1	0°	0	0	-	-
2	180°	100mm	0	-	-
3	360°	0	0	-	-

Case Study 3 will be developed in parallel with the optimisation method explanation. The corresponding Maple program is enclosed in Appendix E. The simplest cam profile will be used: a single rise-and-return profile with no dwells and amplitude of 100mm. In order to apply the optimisation method, only some of the boundary conditions must be specified. Table 6-3 summarises the application's requirements.

Steps 1 through to 6 of the Piecewise Polynomial method explained above are carried out for the new profile. In this case $n = 3$; and four displacement derivatives and continuity conditions will be used, making $k = 8$. After step 6, all the polynomial coefficients can be expressed in terms of the boundary conditions.

Let \bar{X}_S be defined as a vector containing all the boundary values used to define the linear system (6-24) for which the designer has specified a value, and \bar{X}_D be defined as a vector containing the boundary conditions not specified by the designer; that is, the design variables that will enable the profiles to be modified to optimise a function. In this case study: $\bar{X}_S = [Disp_1, Vel_1, Disp_2, Vel_2] = [0, 0, 100, 0]$ and $\bar{X}_D = [Accel_1, s_1, Accel_2, s_2]$ (values not defined in Table 6-3). Note that the boundary conditions for the

last breakpoint are not used, as they are always the same as those of the first one.

Let \bar{X} be the vector produced when concatenating the previous two:
 $\bar{X} = [\bar{X}_S | \bar{X}_D]^T$. \bar{X} should contain all the boundary values used in linear system (6-24) $Disp_1 \dots Disp_{n-1}, Vel_1 \dots Vel_{n-1}, \dots, s_1 \dots s_{n-1}$ to solve the polynomial coefficients. (Note that these do not include $Jerk_1 \dots Jerk_{n-1}$ because jerk could not be included in the initial linear system)

Finally, let $cjvec$ be the number of elements in \bar{X} and m be the number of elements in \bar{X}_S . The number of elements in \bar{X}_D is $(cjvec - m)$. In the example, $cjvec = 8, m = 4$.

On the other hand, by imposing jerk continuity onto the polynomial function, $n - 1$ new equations are derived;

$$Contddy := \begin{cases} 6b_{1,4} + 75.398b_{1,5} + 592.176b_{1,6} + 3720.753b_{1,7} + 20455.909b_{1,8} = 6b_{2,4} \\ 6b_{2,4} + 75.398b_{2,5} + 592.176b_{2,6} + 3720.753b_{2,7} + 20455.909b_{2,8} = 6b_{1,4} \end{cases} \quad (6-28)$$

Substituting the equations for the polynomial coefficients found earlier (6-25), two equations in terms of the boundary conditions are derived. Equations (6-28) can then be re-written as another linear system;

$$[\bar{A}] \cdot \bar{X} = 0 \quad (6-29)$$

where $[\bar{A}]$ is a fully defined $(n - 1) \times cjvec$ matrix. In the example $[\bar{A}]$ becomes the following 2x8 matrix;

$$[\bar{A}] = \begin{bmatrix} -2.709 & 2.709 & -0.36 \times 10^{-7} & 0.210 \times 10^{-8} & -1.273 & 4.456 & 0.105 & 0.419 \\ 2.709 & -2.709 & 0.38 \times 10^{-7} & -0.76 \times 10^{-7} & 4.456 & -1.274 & 0.419 & 0.105 \end{bmatrix} \quad (6-30)$$

Equation (6-29) can also be written as;

$$[\bar{A}_s | \bar{A}_D] \cdot \begin{bmatrix} \bar{X}_s \\ \bar{X}_D \end{bmatrix} = 0 \Rightarrow [\bar{A}_D] \cdot [\bar{X}_D] = [\bar{B}]$$

(6-31)

where $[\bar{A}_D]$ is a $(n-1) \times (c\text{vec} - m)$ submatrix,

$$[\bar{B}] \equiv -[\bar{A}_s] \cdot [\bar{X}_s], \text{ and}$$

$[\bar{A}_s]$ is a $(n-2) \times m$ sub-matrix.

The right hand side of (6-31) represents a new linear system where \bar{X}_D are the unknowns, since \bar{X}_s , $[\bar{A}_s]$ and $[\bar{A}_D]$ are specified. However, the system cannot be solved immediately, as $[\bar{A}_D]$ is not a square matrix. The system should be under-constrained, that is, $(n-1) < (c\text{vec} - m)$. The additional constraints will be given by equations derived from the function being optimised.

$[\bar{A}_D]$ can be further partitioned after applying the pivoting Gaussian elimination to the linear system in (6-31) in rows. The linear system can be re-written as:

$$[\bar{A}_{DU} | \bar{A}_{DV}] \cdot \begin{bmatrix} \bar{X}_{DU} \\ \bar{X}_{DV} \end{bmatrix} = [\tilde{B}]$$

(6-32)

where $[\bar{A}_{DU}]$ is an $(n-2) \times (n-2)$ upper triangular matrix.

\bar{X}_{DU} are the dependent design variables,

\bar{X}_{DV} are the independent design variables.

$$[\tilde{B}] \equiv [\bar{P}] \cdot (-[\bar{A}_s] \cdot [\bar{X}_s]).$$

$[\bar{P}]$ is a matrix containing the row interchange information from the Gaussian elimination.

After partitioning and Gaussian elimination, the example's $[\bar{A}_{DU}]$, $[\bar{A}_{DV}]$ and $[\tilde{B}]$ are calculated:

$$[\bar{A}_{DU}] = \begin{bmatrix} 4.456 & -1.273 \\ 0 & 4.093 \end{bmatrix}$$

$$[\bar{A}_{DV}] = \begin{bmatrix} 0.419 & 0.105 \\ 0.224 & 0.449 \end{bmatrix}$$

$$[\tilde{B}] = \begin{bmatrix} 270.913 \\ -193.509 \end{bmatrix}$$

(6-33)

Rearranging (6-32), \bar{X}_{DU} can be expressed as;

$$\bar{X}_{DU} = [\bar{G}] \cdot \bar{X}_{DV} + [\bar{B}_U]$$

(6-34)

where $[\bar{G}] \equiv -[\bar{A}_{DU}]^{-1}[\bar{A}_{DV}]$,

$$[\bar{B}_U] \equiv [\bar{A}_{DU}]^{-1} \cdot [\tilde{B}].$$

which can also be expressed in terms of \bar{X}_D , if the Gaussian elimination is done with row interchanges only;

$$\bar{X}_D^T = \begin{bmatrix} [\bar{G}] \\ [I] \end{bmatrix} \cdot \bar{X}_{DV}^T + \begin{bmatrix} [\bar{B}_U] \\ [0] \end{bmatrix}$$

(6-35)

These manipulations are followed in the case study to produce $[\bar{G}]$ and $[\bar{B}_U]$:

$$[\bar{G}] = \begin{bmatrix} -0.110 & -0.055 \\ -0.055 & -0.110 \end{bmatrix}$$

$$[\bar{B}_U] = \begin{bmatrix} 47.283 \\ -47.283 \end{bmatrix}$$

(6-36)

The design variables contained in \bar{X}_{DU} and \bar{X}_{DV} have been called dependent and independent design variables respectively because, at this stage, those in \bar{X}_{DV} can be assigned arbitrarily while those in \bar{X}_{DU} have to satisfy (6-34).

The additional constraints will be given by equations derived from the function being optimised. Wang used the Jerk as his optimising function and expressed the total jerk throughout the cam profile in the form of the following equation:

$$J_{TOTAL} = \sum_{i=1}^{n-1} \int_{\beta_i}^{\beta_{i+1}} [\ddot{y}_i(\theta)]^2 d\theta^3, \quad (6-37)$$

which is minimised when

$$\frac{\partial J_{TOTAL}}{\partial \bar{X}} = 0 \quad (6-38)$$

This is only true, however when $1 \leq \ddot{y}_i(\theta) \leq -1$. The most accurate way to express the total jerk is

$$J_{TOTAL} = \sum_{i=1}^{n-1} \int_{\beta_i}^{\beta_{i+1}} |\ddot{y}_i(\theta)| d\theta \quad (6-39)$$

However, Wang does not use (6-39) because it does not suit the Quadratic Programming method used later in the paper. This is because absolute value cannot be transformed into a linear system or expressed as a matrix, while the square value of a function can be.

³ Wang uses an approximation of equation (6-37) in which the integral is replaced by a sum over l segments: $J_{TOTAL} = \sum_{i=1}^{n-1} \sum_{j=1}^l [\ddot{y}_i(\theta)]^2$. This is not necessary when using Maple Mathematics.

\ddot{y}_i can be expressed in vector form as $\ddot{y}_i = \bar{e}_i \cdot \bar{X}^T$, where \bar{e}_i will have non-zero elements only when they relate to the i^{th} and the $(i+1)^{\text{th}}$ boundary conditions in \bar{X} . \ddot{y}_i^2 can be expanded using a positive definite symmetric matrix as follows;

$$\ddot{y}_i^2 = (\bar{e}_i \cdot \bar{X}^T)^2 = \bar{X} \cdot [\bar{q}_i] \cdot \bar{X}^T \quad (6-40)$$

where, $[\bar{q}_i] = \int_{\beta_i}^{\beta_{i+1}} e_i \cdot e_i^T d\theta$. Replacing (6-40) into (6-37), the total jerk becomes;

$$J_{TOTAL} = \sum_{i=1}^{n-1} \bar{X} \cdot [\bar{q}^i] \cdot \bar{X}^T = \bar{X} \cdot \left(\sum_{i=1}^{n-1} [\bar{q}^i] \right) \cdot \bar{X}^T = \bar{X} \cdot [\bar{Q}] \cdot \bar{X}^T \quad (6-41)$$

Where $[\bar{Q}] = \sum_{i=1}^{n-1} [\bar{q}^i]$, is a fully specified block diagonal matrix. For Case Study 3, $[\bar{Q}]$ is:

$$[\bar{Q}] = \begin{bmatrix} 4.941 & -4.941 & 0.002 & 0.007 & 4.060 & -4.060 & -0.032 & 0.032 \\ -4.941 & 4.941 & -0.002 & -0.007 & -4.060 & 4.060 & 0.032 & -0.032 \\ 0.002 & -0.002 & 12.969 & 11.404 & 0.003 & -0.004 & -0.001 & -0.001 \\ 0.007 & -0.007 & 11.404 & 12.978 & -0.003 & 0.006 & -0.002 & -0.000 \\ 4.060 & -4.060 & 0.003 & -0.003 & 5.913 & -2.045 & -0.045 & 0.008 \\ -4.060 & 4.060 & -0.004 & 0.006 & -2.045 & 5.909 & 0.008 & -0.044 \\ -0.032 & 0.032 & -0.001 & -0.002 & -0.045 & 0.008 & 0.020 & 0.011 \\ 0.032 & -0.032 & -0.001 & -0.000 & 0.008 & -0.044 & 0.011 & 0.020 \end{bmatrix} \quad (6-42)$$

The expression for J_{TOTAL} can be transformed into a partition form to discriminate between the specified and the unspecified portions of \bar{X} :

$$J_{TOTAL} = [\bar{X}_S | \bar{X}_D] \cdot \begin{bmatrix} [\bar{Q}_{11}] & [\bar{Q}_{12}] \\ [\bar{Q}_{21}] & [\bar{Q}_{22}] \end{bmatrix} \cdot \begin{bmatrix} \bar{X}_S^T \\ \bar{X}_D^T \end{bmatrix} \quad (6-43)$$

Expanding (6-43);

$$J_{TOTAL} = \bar{X}_S \cdot [\bar{Q}_{11}] \cdot \bar{X}_S^T + 2 \cdot \bar{X}_D \cdot [\bar{Q}_{21}] \cdot \bar{X}_S^T + \bar{X}_D \cdot [\bar{Q}_{22}] \cdot \bar{X}_D^T \quad (6-44)$$

Note that \bar{X}_S is known and \bar{Q} can be computed. The only unknown variable in (6-44) is \bar{X}_D . Let $\eta \equiv \bar{X}_S \cdot [\bar{Q}_{11}] \cdot \bar{X}_S^T$ and $\zeta \equiv [\bar{Q}_{21}] \cdot \bar{X}_S^T$, which can be treated as constants. Equation (6-44) can be re-written as

$$J_{TOTAL} = \eta + 2 \cdot \bar{X}_D \cdot \zeta + \bar{X}_D \cdot [\bar{Q}_{22}] \cdot \bar{X}_D^T \quad (6-45)$$

Substituting (6-35) into (6-45),

$$J_{TOTAL} = \eta + 2 \cdot \left(\begin{bmatrix} \bar{G} \\ \bar{I} \end{bmatrix} \cdot \bar{X}_{DV}^T + \begin{bmatrix} \bar{B}_U \\ 0 \end{bmatrix} \right)^T \cdot \zeta + \bar{X}_D \cdot [\bar{Q}_{22}] \cdot \left(\begin{bmatrix} \bar{G} \\ \bar{I} \end{bmatrix} \cdot \bar{X}_{DV}^T + \begin{bmatrix} \bar{B}_U \\ 0 \end{bmatrix} \right) \quad (6-46)$$

This can be expanded and then simplified and rearranged in terms of \bar{X}_{DV} ,

$$J_{TOTAL} = \eta_v + 2 \cdot \left(\begin{bmatrix} \bar{G} \\ \bar{I} \end{bmatrix} \cdot \bar{X}_{DV}^T \right)^T \cdot \zeta + \left(\begin{bmatrix} \bar{G} \\ \bar{I} \end{bmatrix} \cdot \bar{X}_{DV}^T + \begin{bmatrix} \bar{B}_U \\ 0 \end{bmatrix} \right)^T \cdot [\bar{Q}_{22}] \cdot \left(\begin{bmatrix} \bar{G} \\ \bar{I} \end{bmatrix} \cdot \bar{X}_{DV}^T + \begin{bmatrix} \bar{B}_U \\ 0 \end{bmatrix} \right) \quad (6-47)$$

Where $\eta_v \equiv \eta + 2 \cdot \begin{bmatrix} \bar{B}_U \\ 0 \end{bmatrix}^T \cdot \zeta$,

$$J_{TOTAL} = \eta_v + 2 \cdot \left(\begin{bmatrix} \bar{G} \\ \bar{I} \end{bmatrix} \cdot \bar{X}_{DV}^T \right)^T \cdot \zeta + \left(\left(\begin{bmatrix} \bar{G} \\ \bar{I} \end{bmatrix} \cdot \bar{X}_{DV}^T \right)^T + \begin{bmatrix} \bar{B}_U \\ 0 \end{bmatrix}^T \right) \cdot \left([\bar{Q}_{22}] \cdot \begin{bmatrix} \bar{G} \\ \bar{I} \end{bmatrix} \cdot \bar{X}_{DV}^T + [\bar{Q}_{22}] \cdot \begin{bmatrix} \bar{B}_U \\ 0 \end{bmatrix} \right)$$

$$\begin{aligned}
 J_{TOTAL} = \eta_v + 2 \cdot \left(\begin{bmatrix} \bar{G} \\ I \end{bmatrix} \cdot \bar{X}_{DV}^T \right)^T \cdot \zeta + \left(\left(\begin{bmatrix} \bar{G} \\ I \end{bmatrix} \cdot \bar{X}_{DV}^T \right)^T \cdot [\bar{Q}_{22}] \cdot \begin{bmatrix} \bar{G} \\ I \end{bmatrix} \cdot \bar{X}_{DV}^T \right) + \left(\begin{bmatrix} \bar{B}_U \\ 0 \end{bmatrix} \right)^T \cdot [\bar{Q}_{22}] \cdot \begin{bmatrix} \bar{B}_U \\ 0 \end{bmatrix} \\
 + \left(\begin{bmatrix} \bar{B}_U \\ 0 \end{bmatrix} \right)^T \cdot [\bar{Q}_{22}] \cdot \begin{bmatrix} \bar{G} \\ I \end{bmatrix} \cdot \bar{X}_{DV}^T + \left(\left(\begin{bmatrix} \bar{G} \\ I \end{bmatrix} \cdot \bar{X}_{DV}^T \right)^T \cdot [\bar{Q}_{22}] \cdot \begin{bmatrix} \bar{B}_U \\ 0 \end{bmatrix} \right)
 \end{aligned}
 \tag{6-48}$$

Applying the theorem that the transpose of a product of matrices is the product of the matrices in reverse order⁵⁶,

$$\begin{aligned}
 J_{TOTAL} = \eta_v + 2 \cdot \bar{X}_{DV} \cdot \begin{bmatrix} \bar{G} \\ I \end{bmatrix}^T \cdot \zeta + \bar{X}_{DV} \cdot [\bar{Q}_V] \cdot \bar{X}_{DV}^T + \bar{B}_{UV} \\
 + \left(\begin{bmatrix} \bar{B}_U \\ 0 \end{bmatrix} \right)^T \cdot [\bar{Q}_{22}] \cdot \begin{bmatrix} \bar{G} \\ I \end{bmatrix} \cdot \bar{X}_{DV}^T + \left(\bar{X}_{DV} \cdot \begin{bmatrix} \bar{G} \\ I \end{bmatrix}^T \cdot [\bar{Q}_{22}] \cdot \begin{bmatrix} \bar{B}_U \\ 0 \end{bmatrix} \right)
 \end{aligned}
 \tag{6-49}$$

Where, $[\bar{Q}_V] \equiv \begin{bmatrix} \bar{G} \\ I \end{bmatrix}^T \cdot [\bar{Q}_{22}] \cdot \begin{bmatrix} \bar{G} \\ I \end{bmatrix}$, and

$$\bar{B}_{UV} \equiv \begin{bmatrix} \bar{B}_U \\ 0 \end{bmatrix}^T \cdot [\bar{Q}_{22}] \cdot \begin{bmatrix} \bar{B}_U \\ 0 \end{bmatrix}.$$

Factorising \bar{X}_{DV} ,

$$J_{TOTAL} = \eta_v + \bar{B}_{UV} + 2 \cdot \bar{X}_{DV} \cdot \zeta_V + \bar{X}_{DV} \cdot [\bar{Q}_V] \cdot \bar{X}_{DV}^T
 \tag{6-50}$$

Where $\zeta_V \equiv \begin{bmatrix} \bar{G} \\ I \end{bmatrix}^T \cdot \left([\bar{Q}_{22}] \cdot \begin{bmatrix} \bar{B}_U \\ 0 \end{bmatrix} + \zeta \right)$.

The total jerk is minimised its derivative is equal to zero. See (6-38).

$$\frac{\partial J_{TOTAL}}{\partial \bar{X}_{DV}} = 2\zeta_V + 2[\bar{Q}_V] \cdot \bar{X}_{DV}^T = 0$$

(6-51)

Therefore, the jerk is minimised when:

$$\bar{X}_{DV}^T = -[\bar{Q}_V]^{-1} \cdot \zeta_V = \begin{bmatrix} -60.917 \\ 61.944 \end{bmatrix} \quad (6-52)$$

Replacing the values found for \bar{X}_{DV} into (6-34), \bar{X}_{DU} can also be calculated;

$$\bar{X}_{DU} = [\bar{G}] \cdot \bar{X}_{DV} + [\bar{B}_U] = \begin{bmatrix} 50.567 \\ 50.736 \end{bmatrix} \quad (6-53)$$

That is, the unspecified boundary conditions should be set to

$$\begin{bmatrix} X_{D1} \\ X_{D2} \\ X_{D3} \\ X_{D4} \end{bmatrix} = \begin{bmatrix} Accel_1 \\ Accel_2 \\ s_1 \\ s_2 \end{bmatrix} = \begin{bmatrix} 50.567 \\ -50.735 \\ -60.917 \\ 61.944 \end{bmatrix} \quad (6-54)$$

in order to obtain the minimum Jerk requirement.

Having calculated all the design variables, the cam's displacement PP functions and hence, the total jerk throughout the profile are fully defined. The total jerk can now be calculated from (6-37).

$$J_{TOTAL} = \sum_{i=1}^{n-1} \int_{\beta_i}^{\beta_{i+1}} [\ddot{y}_i(\theta)]^2 d\theta = 7,842.71 \quad (6-55)$$

Figure 6-3 show the displacement function and its derivatives for the case study. Notably, all the boundary conditions (design ones as well as the specified ones) are met and there is continuity of all the derivatives.

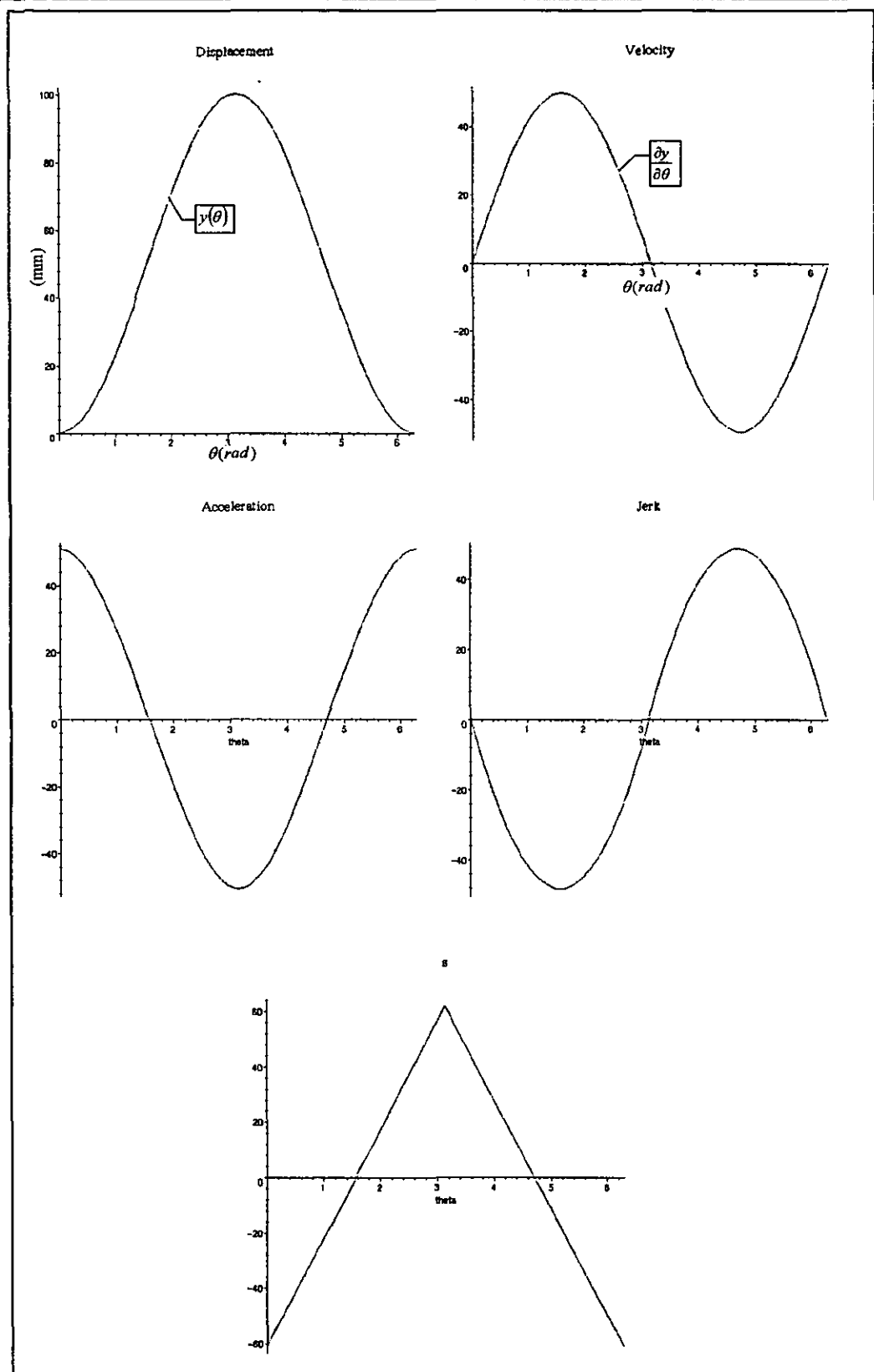


Figure 6-3. Displacement Derivatives for Optimised Case Study

6.3.2 Proof of Minimum

Initially, a simplified proof of the minimum jerk was carried in the example by altering the values of the dependent design variables (or boundary conditions) in \bar{X}_D by a very small amount. It caused the Total Jerk value to increase from 7,842.71 to 7,858.56 and the Jerk graph is no longer continuous. Refer to Figure 6-4 and Appendix E Section Proof of Minimum. A more reliable proof of the minimum is obtained by plotting the total jerk function versus each of the design variables, while maintaining the others constant at the minimum values obtained for them.

In the case study discussed in the previous section, for instance, there were four design variables; $Accel_1, Accel_2, s_1, s_2$, and it was found that the condition of minimum jerk would be satisfied when;

$$\begin{bmatrix} X_{D1} \\ X_{D2} \\ X_{D3} \\ X_{D4} \end{bmatrix} = \begin{bmatrix} Accel_1 \\ Accel_2 \\ s_1 \\ s_2 \end{bmatrix} = \begin{bmatrix} 50.567 \\ -50.735 \\ -60.917 \\ 61.944 \end{bmatrix}$$

(6-54)

Since it would be impossible to visualise the jerk as a function of four variables, a graph of the jerk function in terms of each of the design variables is constructed. The other variables are set to the values in (6-54). It is clearly seen in Figure 6-5 that the jerk minimum occurs at the values predicted.

The value of the minimum jerk calculated will vary if the specified boundary conditions change. This optimisation method will provide the minimum total jerk given the specified conditions. Should the designer of the previous example decide to specify different set of boundary conditions, the displacement functions and their derivatives will change accordingly and the value of the minimum jerk will be a different one.

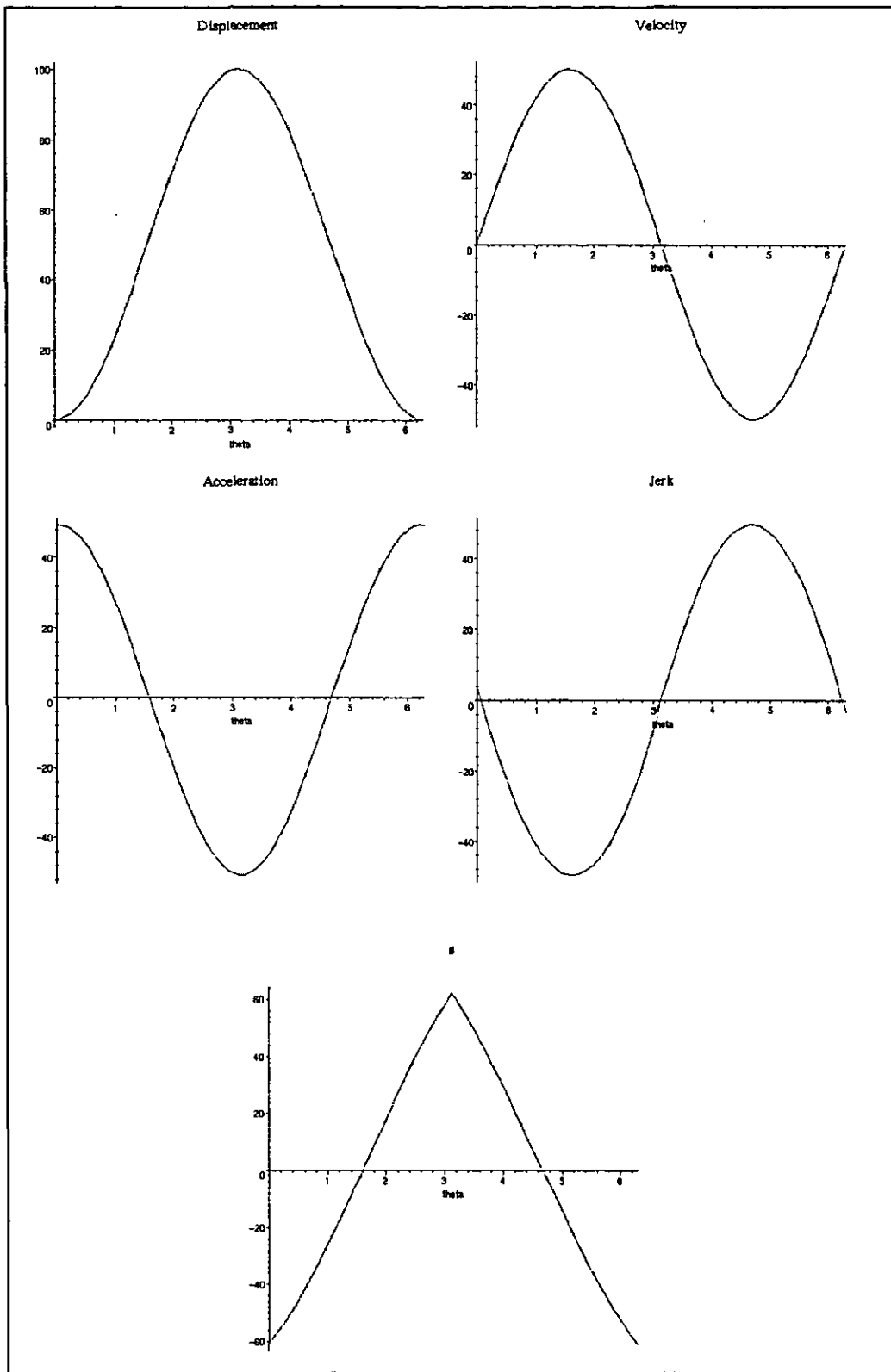


Figure 6-4. Displacement Derivatives using Replacement Values for Design Variables

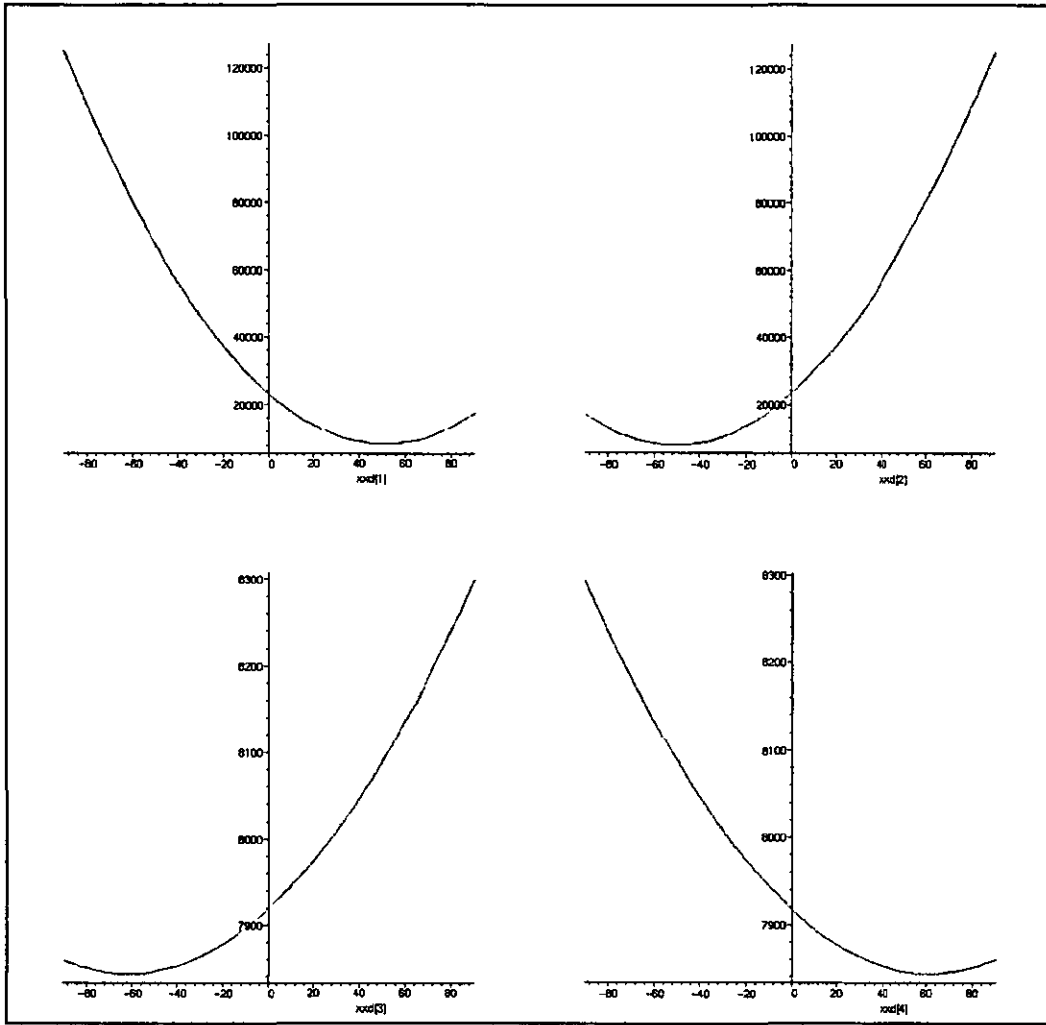


Figure 6-5. Proof of Minimum. Jerk in terms of each of the design variables.

Table 6-4. Modified Application Requirements

Breakpoint No.	Cam Angle β	Displacement	Velocity	Acceleration	S
1	0°	0	-	-	0
2	180°	100mm	-	-	0
4	360°	0	-	-	0

For example, given the new boundary conditions shown in Table 6-4, the displacement and its derivatives calculated for minimum jerk are shown in Figure 6-6. Note that the displacement boundary conditions have remained unchanged.

Using the procedure outlined in the previous example, it is easily proven that the profile calculated will, in fact, still produce the minimum jerk for these conditions.

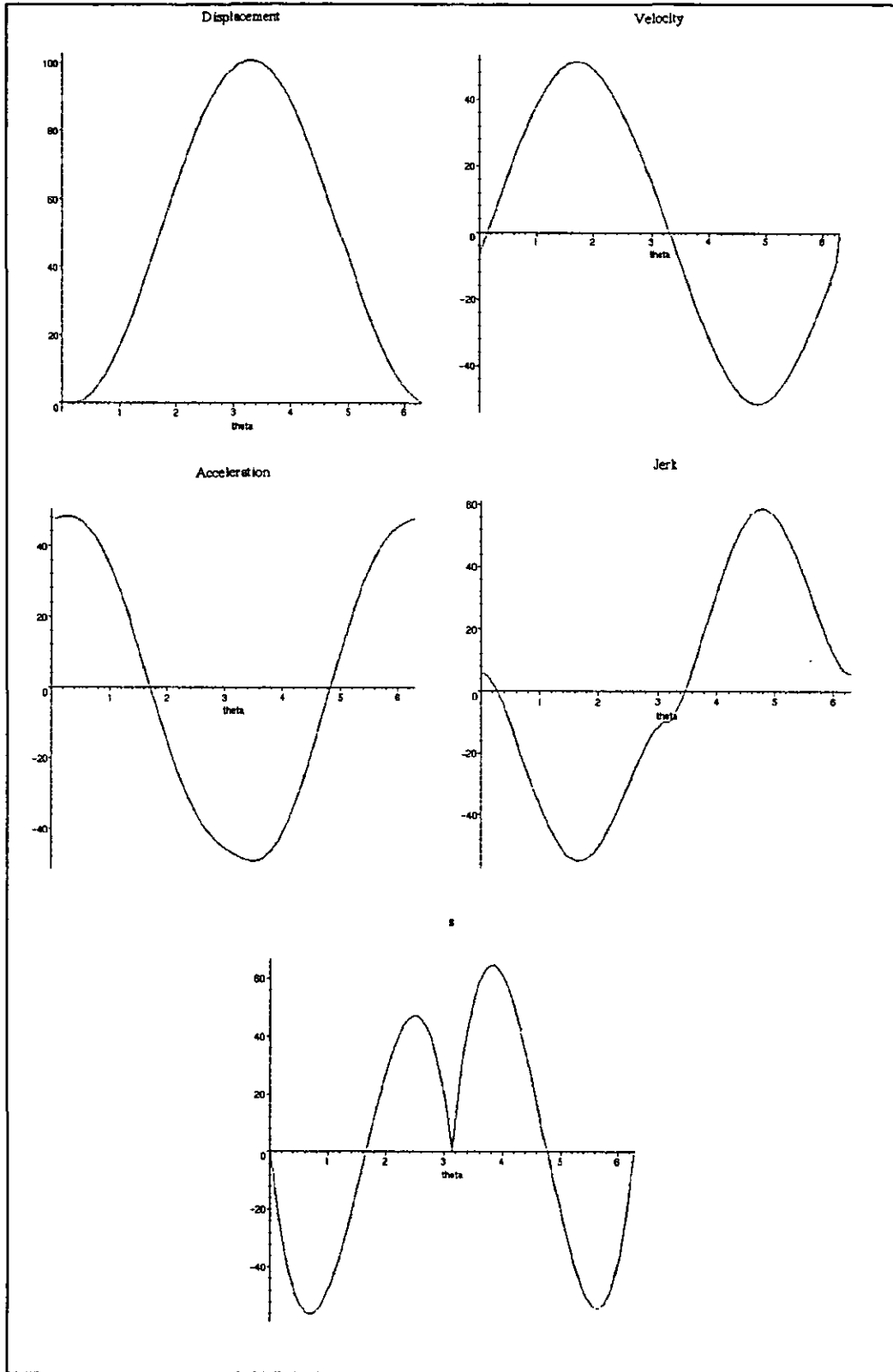


Figure 6-6. Displacement Derivatives for Modified Boundary Conditions

6.3.3 Case Study 4. Incorrect Boundary Conditions Specified.

Table 6-5 shows a new set of boundary conditions. The displacement values remain unchanged, and in this case, the designer wishes to specify the acceleration values at the breakpoints. Figure 6-7 shows the displacement function for the cam profile and its derivatives after following the same optimisation method described earlier. The displacement profile is clearly unpractical, although it has not violated the boundary conditions stipulated by the designer. The polynomial found for the displacement is such that the cam would go below $y(\theta)=0$ (the boundary condition for displacement at $\beta_3 = 360^\circ$) before reaching β_3 , making the total amplitude of the movement larger than what the designer wanted.

This is a similar problem to the one encountered with giving the incorrect boundary conditions for dwells. The optimising method cannot guarantee anything about the profile where the cam angle (θ) is not a boundary condition because it is based on piecewise polynomials.

Table 6-5. Case Study 4. Design Requirements Including Acceleration

Breakpoint No.	Cam Angle β	Displacement	Velocity	Acceleration	S
1	0°	0	.	0	.
2	180°	100mm	.	0	.
3	360°	0	.	0	.

Furthermore, after following the same optimising procedure, the values obtained for the design variables are

$$\begin{bmatrix} Vel_1 \\ Vel_2 \\ S_1 \\ S_2 \end{bmatrix} = \begin{bmatrix} 27.0 \\ 0.8 \\ 862.3 \\ -862.3 \end{bmatrix}$$

(6-56)

Figure 6-8 shows that the values calculated for the design variables in order to minimise the jerk do not correspond to the function's minimum.

In this case, the technique has not worked because the designer has set the values of the boundary conditions for acceleration. The function being optimised is the integral of jerk ;

$$\begin{aligned} J_{TOTAL} &= \sum_{i=1}^{n-1} \int_{\beta_i}^{\beta_{i+1}} \ddot{y}_i(\theta) \cdot d\theta = \sum_{i=1}^{n-1} [\dot{y}_i(\theta)]_{\beta_i}^{\beta_{i+1}} \\ &= \sum_{i=1}^{n-1} \dot{y}_i(\beta_{i+1}) - \dot{y}_i(\beta_i) = \sum_{i=1}^{n-1} Accel_{i+1} - Accel_i \end{aligned}$$

(6-57)

Therefore, acceleration boundary conditions cannot be specified. More generally, however, this case study demonstrates that the graphical proof of minimum will point out on any boundary conditions specified erroneously.

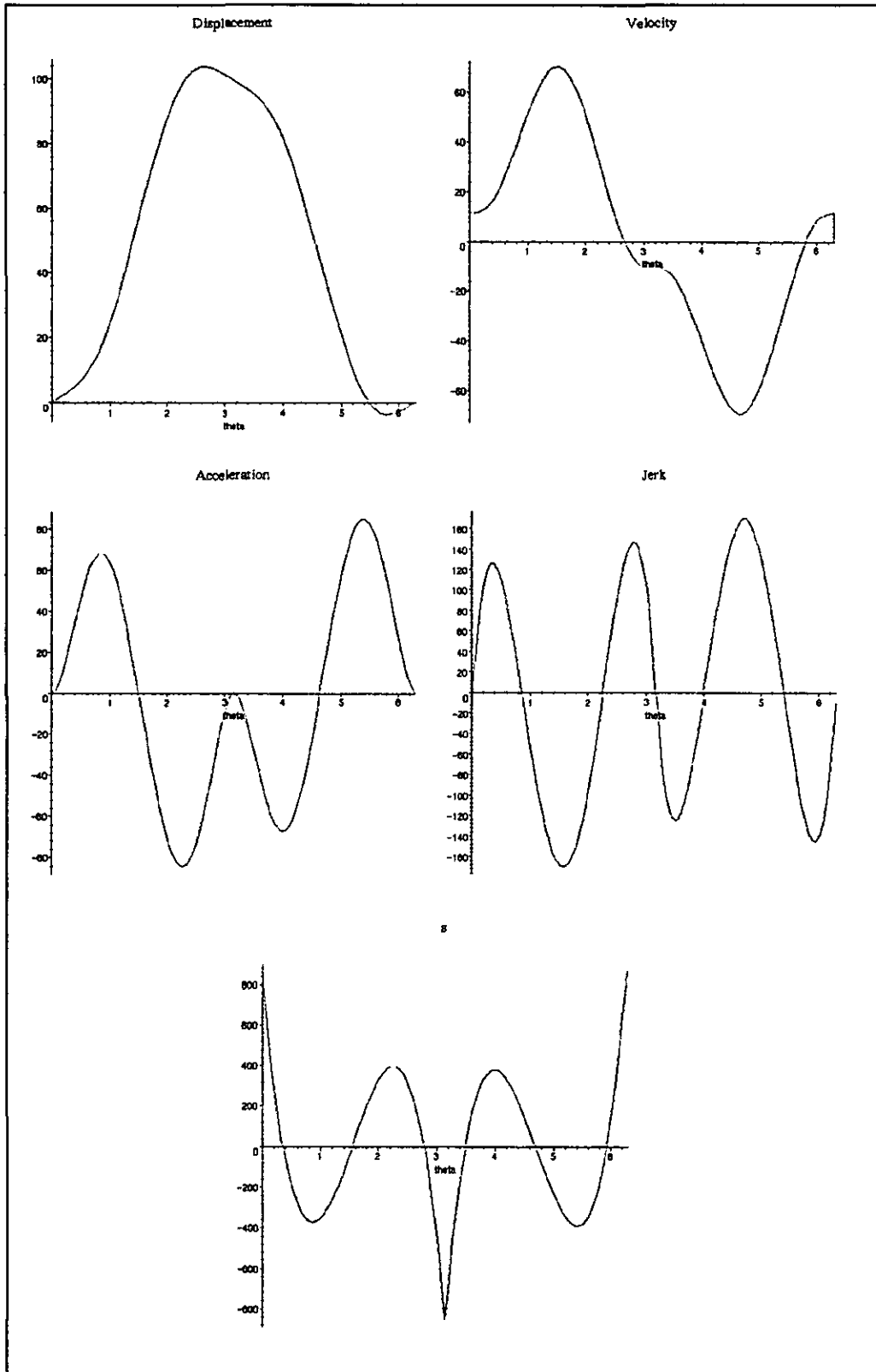


Figure 6-7. Case Study 4. Displacement Derivatives

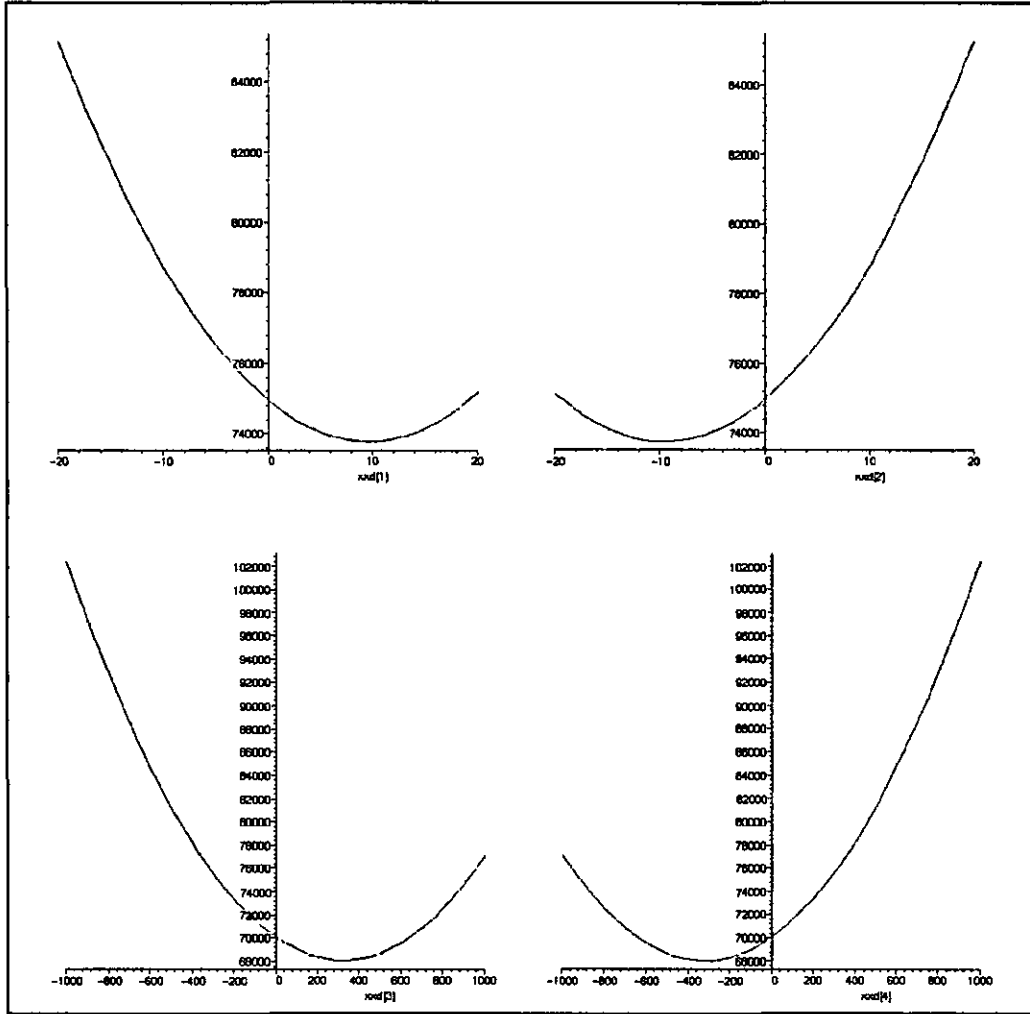


Figure 6-8. Case Study 4. Jerk In terms of the Design Variables

6.4 Optimisation method applied to the warp knitting cam

The displacement requirements of the warp knitting cam are summarised in Table 6-6's displacement column. A smooth profile is required for the rise and the return segments, $1 \rightarrow 2$ and $3 \rightarrow 4$ respectively. However, dwells are required between the two main motions. As found earlier, when dwells occur, all boundary conditions for the two breakpoints of a dwell must be set to zero. Therefore, all the boundary conditions of the table are specified. Under these conditions, only the piecewise polynomials (without optimisation) method can be applied to find suitable polynomial expressions for the cam displacement.

Applying the method described in page 166, the polynomial expressions for the displacement of the warp knitting cam are found. See (6-58). The displacement PP and its derivatives are illustrated in Figure 6-9 .

Table 6-6. Warp Knitting Machines Design Requirements

Breakpoint No.	Cam Angle β	Displacement	Velocity	Acceleration	S
1	0°	0	0	0	0
2	90°	0.837"	0	0	0
3	180°	0.837"	0	0	0
4	270°	0	0	0	0
5	360°	0	0	0	0

$$\left. \begin{array}{l}
 y_1 = 11.028\theta^5 - 23.402\theta^6 + 19.155\theta^7 \\
 \quad - 7.113\theta^8 + 1.006\theta^9 \quad \forall \theta \in \{0 \leq \theta \leq \frac{\pi}{2}\} \\
 \hline
 y_2 = 0.837 \quad \forall \theta \in \{\frac{\pi}{2} \leq \theta \leq \pi\} \\
 \hline
 y_3 = 0.837 - 11.028(\theta - \pi)^5 + 23.402(\theta - \pi)^6 \\
 \quad - 19.155(\theta - \pi)^7 + 7.113(\theta - \pi)^8 - 1.006(\theta - \pi)^9 \quad \forall \theta \in \{\pi \leq \theta \leq \frac{3\pi}{2}\} \\
 \hline
 y_4 = 0 \quad \forall \theta \in \{\frac{3\pi}{2} \leq \theta \leq 2\pi\}
 \end{array} \right\}$$

(6-58)

The values of the polynomial coefficients found can be used as inputs in a customised spreadsheet application to produce an appropriate NC code for

the manufacture of the cam. However, if the designer wants to optimise a specific function, extra breakpoints can be created between existing ones to produce unspecified boundary conditions. Table 6-7 is an expanded version of Table 6-6, where four extra breakpoints have been created in order to produce 14 unspecified boundary conditions. The values of these can be determined using the optimisation method described from page 174. The displacement values for the new breakpoints (4 and 7) were specified as half the value of the total rise to ensure a symmetric polynomial function.

The creation of new breakpoints illustrates the versatility of Piecewise Polynomials in the design of cams. Since the linear system used is applied only at the breakpoints, any number of breakpoints can be added between existing ones without compromising the original boundary conditions.

Table 6-7. Warp Knitting Machines Expanded Design Requirements

Breakpoint No.	Cam Angle β	Displacement	Velocity	Acceleration	S
1	0°	0	0	0	0
2	45	0.4185"	-	-	-
3	60°	-	-	-	-
4	90°	0.837"	0	0	0
5	180°	0.837"	0	0	0
6	210°	-	-	-	-
7	225	0.4185"	-	-	-
8	270°	0	0	0	0
9	360°	0	0	0	0

On the other hand, in order to apply the optimisation method a minimum of unspecified boundary conditions are necessary. This requirement stems from the linear system created when applying a continuity condition on jerk, which provides the linear system to be solved in the optimisation procedure in terms of the design variables (equation (6-31));

$$[\bar{A}_D] \cdot [\bar{X}_D] = [\bar{B}]$$

$[\bar{A}_D]$ is a $(n-1) \times (cjvec - m)$ matrix. $(cjvec - m)$ is the number of design variables; that is, the number of unspecified boundary conditions. The optimisation procedure can only be applied when $(cjvec - m) > (n - 1)$. An appropriate number of breakpoints can always be chosen in order to satisfy the latter inequality as $cjvec$ will generally depend on the number of breakpoints, n .

In the warp knitting case, for instance, $cjvec = 4 \cdot (n - 1)$. Therefore, $4 \cdot (n - 1) - m > (n - 1) \Rightarrow n > 7$. The optimisation technique can be applied to the system if there are at least eight breakpoints in the profile.

The polynomial displacement function (after optimising for minimum jerk) and its derivatives are shown in Figure 6-10. The displacement function found after minimising the jerk is expressed as a set of Piecewise Polynomials in (6-59), and it can be proven that the minimum Jerk condition has been met. The complete Maple program is enclosed in Appendix F. In this case, there were $n = 9$ breakpoints and $cjvec = 32$ boundary conditions in total; $m = 18$ of which were specified. $[\bar{A}_D]$ was an 8×14 matrix. The first 8 of the 14 unspecified design variables will be dependent ones, while the remaining 6 will be independent. See equation (6-32). The order in which \bar{X} , and \bar{X}_D in particular will affect the results. The most critical boundary conditions, such as displacement ones, should be defined at the end on the vector, to ensure they are independent design variables.

$$y_1 = .16 \times 10^{-27} \theta^5 + 9.531 \theta^5 - 15.882 \theta^6 + 7.040 \theta^7 \quad \forall \theta \in \{0 \leq \theta \leq \frac{\pi}{4}\}$$

$$y_2 = 0.419 + 1.223(\theta - \frac{\pi}{4}) - 0.290(\theta - \frac{\pi}{4})^2 \\ - 1.341(\theta - \frac{\pi}{4})^3 + 9.846(\theta - \frac{\pi}{4})^4 \\ - 85.648(\theta - \frac{\pi}{4})^5 + 268.088(\theta - \frac{\pi}{4})^6 \\ - 285.144(\theta - \frac{\pi}{4})^7 \quad \forall \theta \in \{\frac{\pi}{4} \leq \theta \leq \frac{\pi}{3}\}$$

$$y_3 = .697 + .825(\theta - \frac{\pi}{3}) - 1.136(\theta - \frac{\pi}{3})^2 \\ - .406(\theta - \frac{\pi}{3})^3 - 5.726(\theta - \frac{\pi}{3})^4 + 30.260(\theta - \frac{\pi}{3})^5 \\ - 44.695(\theta - \frac{\pi}{3})^6 + 21.955(\theta - \frac{\pi}{3})^7 \quad \forall \theta \in \{\frac{\pi}{3} \leq \theta \leq \frac{\pi}{2}\}$$

$$y_4 = 0.837 \quad \forall \theta \in \{\frac{\pi}{2} \leq \theta \leq \pi\}$$

$$y_5 = .837 + .2 \times 10^{-27} (\theta - \pi)^3 - 16.248(\theta - \pi)^5 \\ + 35.775(\theta - \pi)^6 - 21.955(\theta - \pi)^7 \quad \forall \theta \in \{\pi \leq \theta \leq \frac{4\pi}{3}\}$$

$$y_6 = 0.697 - 0.825(\theta - \frac{4\pi}{3}) - 1.136(\theta - \frac{4\pi}{3})^2 \\ - 0.406(\theta - \frac{4\pi}{3})^3 - 5.726(\theta - \frac{4\pi}{3})^4 \\ + 74.949(\theta - \frac{4\pi}{3})^5 - 254.466(\theta - \frac{4\pi}{3})^6 \\ + 285.144(\theta - \frac{4\pi}{3})^7 \quad \forall \theta \in \{\frac{4\pi}{3} \leq \theta \leq \frac{5\pi}{4}\}$$

$$y_7 = 0.419 - 1.223(\theta - \frac{5\pi}{4}) - 0.290(\theta - \frac{5\pi}{4})^2 \\ + 1.341(\theta - \frac{5\pi}{4})^3 + 9.846(\theta - \frac{5\pi}{4})^4 \\ - 25.880(\theta - \frac{5\pi}{4})^5 + 22.820(\theta - \frac{5\pi}{4})^6 \\ - 7.040(\theta - \frac{5\pi}{4})^7 \quad \forall \theta \in \{\frac{5\pi}{4} \leq \theta \leq \frac{3\pi}{2}\}$$

$$y_8 = 0 \quad \forall \theta \in \{\frac{3\pi}{2} \leq \theta \leq 2\pi\}$$

(6-59)

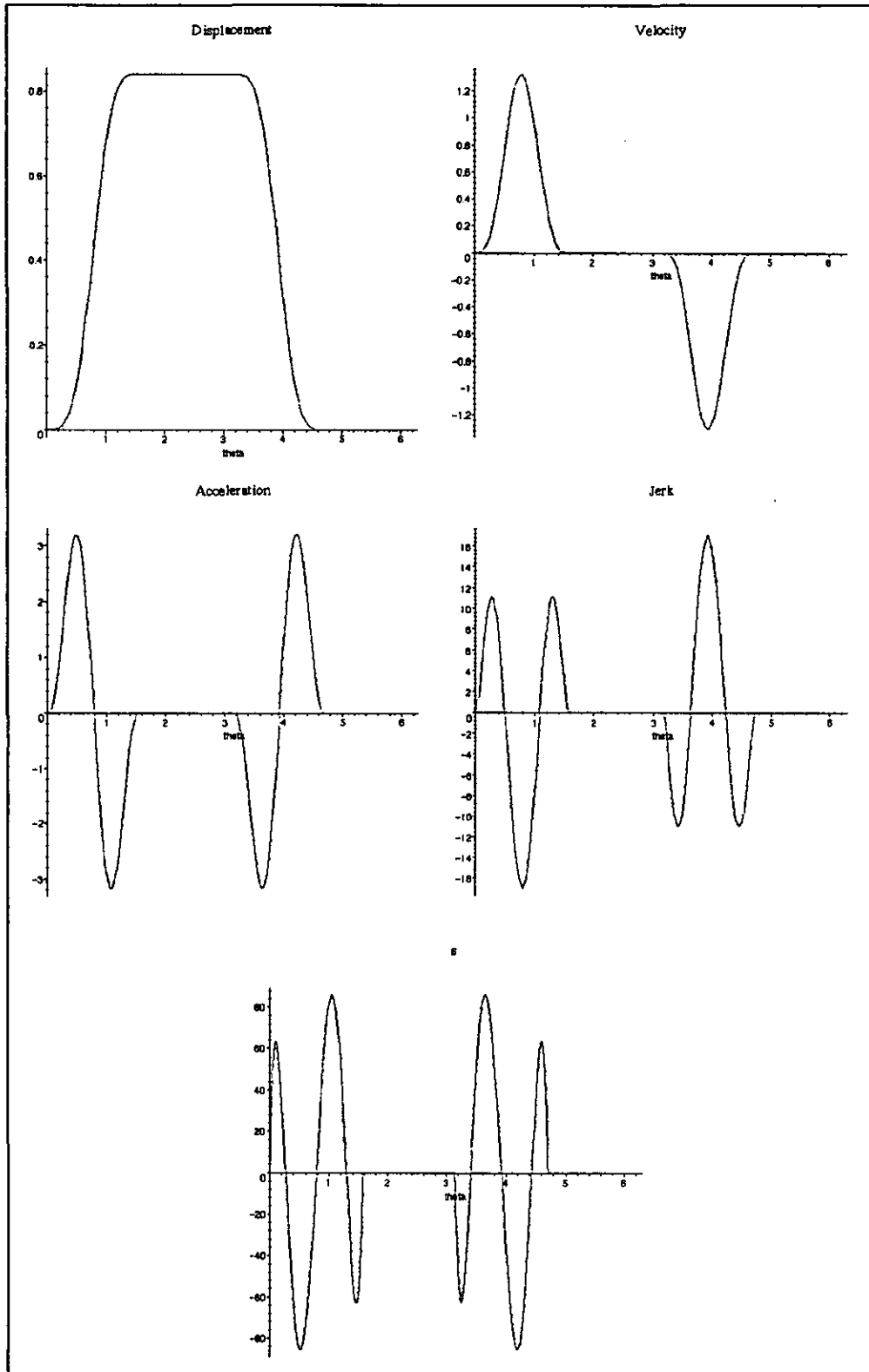


Figure 6-9. Warp Knitting Displacement Derivatives without Optimising

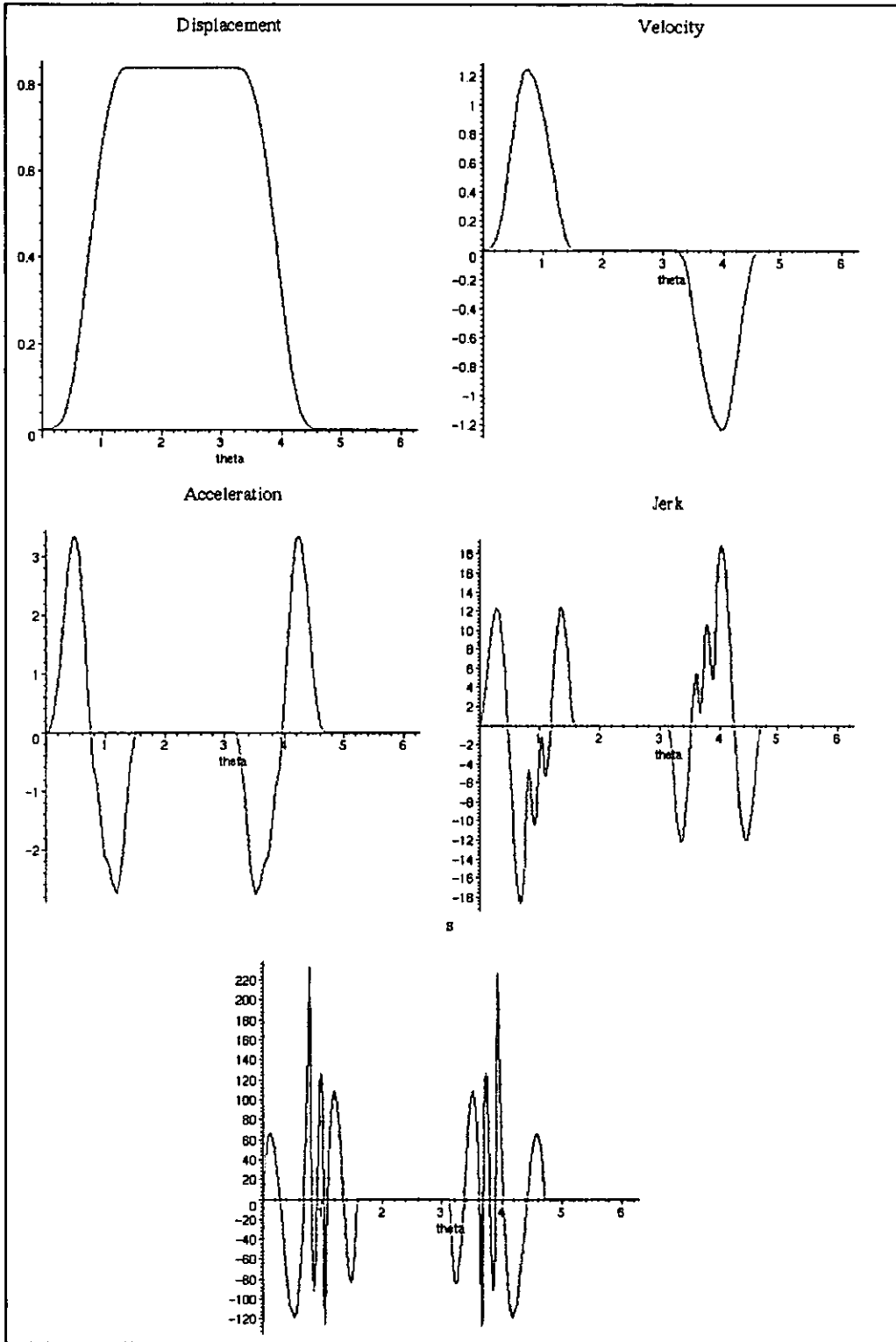


Figure 6-10. Warp Knitting Displacement Derivatives after Optimising

6.5 Conclusions

A method of synthesising a cam profile based on the use of piecewise polynomials together with an optimisation technique has been presented. Special cases and limitations have been discussed and illustrated, making the procedure complete and systematic for any design requirements. The implementation of the method requires a mathematics software application, as the calculations involved are lengthy. The examples shown were implemented using Maple Mathematics, but other mathematics programs could be used.

Polynomial profiles, which are defined with a number of breakpoints in the profile for which the designer can define boundary conditions, are the most suitable for optimisation because the displacement, velocity, acceleration and jerk can be controlled for any critical point in the cam profile. Textbooks^{49,51} describe the method for synthesising a polynomial profile for a single cam motion. However, using piecewise polynomials, the complete cam profile can be designed as a combined linear system.

The optimisations technique described here goes even further, manipulating the variables in the linear system to select the ideal combination in order to optimise a given expression.

Certain requirements for the method to work have been illustrated. Firstly, a procedure to choose the appropriate polynomial order has been illustrated. Secondly, it has been proven that dwells must be treated as special cases; all boundary conditions at the two breakpoints adjoining the dwell segment must be specified as zero.

Thirdly, the linear system from which the coefficients are derived (Equation (6-24)) cannot contain the optimising function's boundary conditions. That is, if optimising acceleration of a given profile, the linear system cannot contain $Accel_1, \dots, Accel_n$.

In addition, a means to prove the results are valid has been explained. This proof should be carried out on any cam design to ensure that the designer

has not, unaware, specified boundary conditions that will invalidate the result.

The method has then successfully been applied to the design of the circular warp knitting machine cam.

Chapter 7. Patterning Mechanism

7.1 Introduction: Patterning Mechanism Overview

The patterning mechanism's main function is to provide the needles with yarns at the appropriate points in the knitting cycle following a specified sequence, to produce a given knitted pattern. The mechanism is based on patterning rings through which the yarns are threaded. These rings need to be then rotated in order to provide each needle with a yarn, which it collects on its downward movement

As was explained earlier, the use of a cone to enhance the interaction between the needle and yarn movements, is one of the main innovations of this warp knitting machine design. By using a tricked cone to support the needles, two of the movements traditionally performed by the needles and the guide bars are now merged into a single motion of needles.

The patented patterning mechanisms for circular warp knitting machines have three common factors (Borenstein, 1986⁵⁷ and Ragosa, 1990⁵⁸), they are mechanically controlled; use two patterning rings controlled by open face cams; use a maximum pattern length of twelve machine cycles (a larger number of machine cycles in a pattern would require a larger cam, but the space in which the cam fits is limited).

Patterning mechanisms in traditional flat warp knitting machines, employ three main mechanisms to produce stitches: (i) a knitting mechanism that reciprocates the needles vertically; (ii) a swinging mechanism to move the yarns from the front to the back of the needles and vice versa; (iii) a shogging mechanism to produce the overlaps and underlaps parallel to the plane on which the needles are laid.

A pattern consists of a chain of different length underlaps, so the flexibility of the machine patterning depends on the ease of modifying the movements performed by its shogging mechanism and the length of its pattern chain.

The warp knitting needle cycle for a flat knitting machine can be described as comprising six stages as detailed in Chapter 2, Figure 2-1.

For a circular machine, the yarns are threaded through radially perforated rings. The shogging movement becomes a rotation of these rings. The pattern chain is comprised of a number of rotational ring movements synchronised with the main mechanism already reciprocating the needles.

Patterns using a circular machine cycle can be divided into four stages, unlike the flat machine's six stages: (i) the needles rise to their uppermost position inside the cylinder tricks, (the rings are preferably stationary while this occurs); (ii) the needles will then dwell in their high position, while the patterning rings rotate the necessary angle to wrap each yarn in front of a needle hook, called the overlap; (iii) the needles are lowered inside the cylinder tricks, bringing down with them the yarn inside their hooks, (the rings will preferably stationary while this occurs). (iv) the needles reach the lowest position and stop, the rings will then rotate to place the yarns behind the needles stem (underlap), (the extent of which depends upon the pattern desired).

In brief, the rings perform two rotations and two dwells during a machine cycle. The direction and amplitude of these rotations will depend upon the fabric structure being created. The overlap will always be created and will be carried out over one needle only, however the underlap can be under several needles, which could therefore necessitate a larger rotation of the ring.

The larger the number of rings the greater the patterning possibilities. However, the amount of space to place them and the complexity of the yarn paths restricts the number of patterning rings present in a machine.

7.2 System requirements

The products created by a circular warp knitting machine were found to be packaging fabrics, ladies stockings, bandage materials and other technical textiles or processes (e.g. prosthetic limb manufacturing). The system requirements were summarised in the product design specification, itself produced after carrying out market research on customer needs for a circular knitting machine to make these products.

With regard to the patterning mechanism, it was found that most applications do not require more than a 4-needle underlap, also the minimum gauge in the relevant applications is 4 needles per inch. The verge diameter is not critical for the netting applications; it varies in the range of 75 - 100 mm for the stockings application and for medical applications it varies more widely between 10mm and 150mm.

Based on this research, it was decided to design the patterning mechanism for a 75 mm diameter verge cone. This small size is the most complex in the stockings range, yet falls well within the range of sizes for the bandages production. Therefore it is ideal for proving new concepts.

It was estimated that that the patterning ring rotation required for the underlap was equivalent to twice the angle between the number of needle spaces. That is, a 2 needle underlap requires a rotation of the patterning ring over 4 needles. (This assumption was to be investigated further later with the patterning geometric model)

With 36 needles in the cylinder (the coarsest gauge needed), each needle is positioned at 10° from its neighbours. A 4 needle underlap will require a rotation equivalent to 8 needle spaces, which is equivalent to 80° .

Therefore the overall system requirement was fixed to be able to perform a maximum rotation of up to 80° in a single underlap.

The fabric designer can alter the portion of the knitting cam cycle allocated to this patterning ring movement, as described in the rise dwell characteristic section in Chapter 5. In the initial design of the circular warp-knitting

machine, the cam profile provided 75° each for the rise and return movements; 90° for the overlap and 120° for the underlap.

If the 80° rotation of the patterning ring must be performed during the time it takes up the knitting cam to rotate 120° . Assuming that the maximum speed of the machine is 1000rpm, a single knitting cycle takes place in 60ms, leaving 20ms to perform the underlap and 15ms for the overlap rotation.

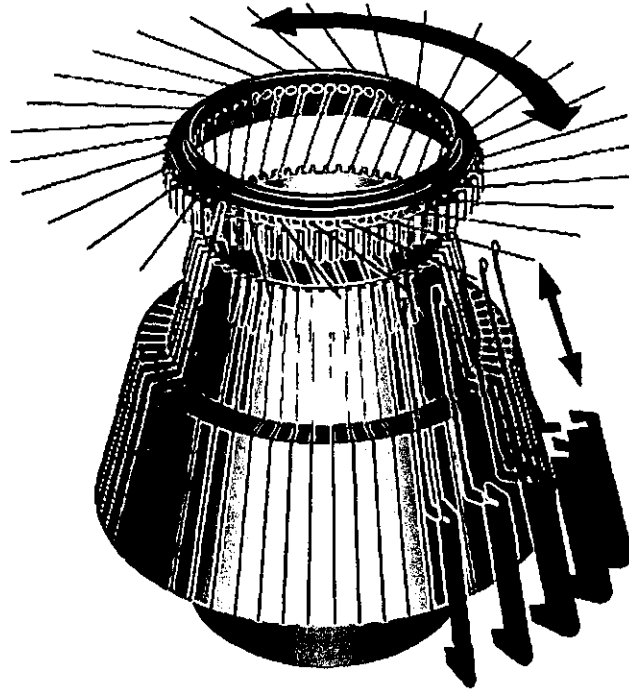


Figure 7-1. A patterning ring and needles on a circular warp knitting machine

For the length of patterns, it is clear that any increase above the existing maximum (12 courses per pattern) will represent not only a competitive advantage commercially, but also broaden the functional uses of the machine for other product creations exclusive to the circular warp knitting machine production process.

Similarly, an increase in the number of rings available is a positive functional asset for the machine design, especially in the stockings and medical textile industries, where more intricate fabric designs are sought.

The most important requirements driving the patterning mechanism design, are therefore: (a) the number of rings, (b) the maximum underlap rotation, (c) the maximum number of courses per pattern, and (d) the time allowed to perform an underlap (especially in the electronically controlled version of the design).

7.3 Mechanical Solution

The mechanical system of the circular warp knitting machine (Figure 7-2) converts a translation motion created by the patterning cam, into a rotation of the patterning ring, by means of a number of pivots and mechanical linkages (See Figure 7-5). Where the configuration and length of the linkage components is always constrained by the available space for the machine size. (E.g. to create a longer pattern with a circular motion of the ring, while maintaining appropriate pressure angles in the cam, the baseline radius of the cam must increase, (which is impossible without enlarging the machine)).

The patterning cam is driven directly from the main shaft via timing belts and pulleys, to ensure its synchronicity with the knitting mechanism. A cam has a cam track milled on either side, each track providing the movements to drive one patterning ring. Each cam track is made up of a sequence of underlap-stroke-dwell and overlap-stroke-dwell cycles; each cycle representing a knitted course, the angle provided for each cycle within the cam depending upon the number of courses in the pattern.

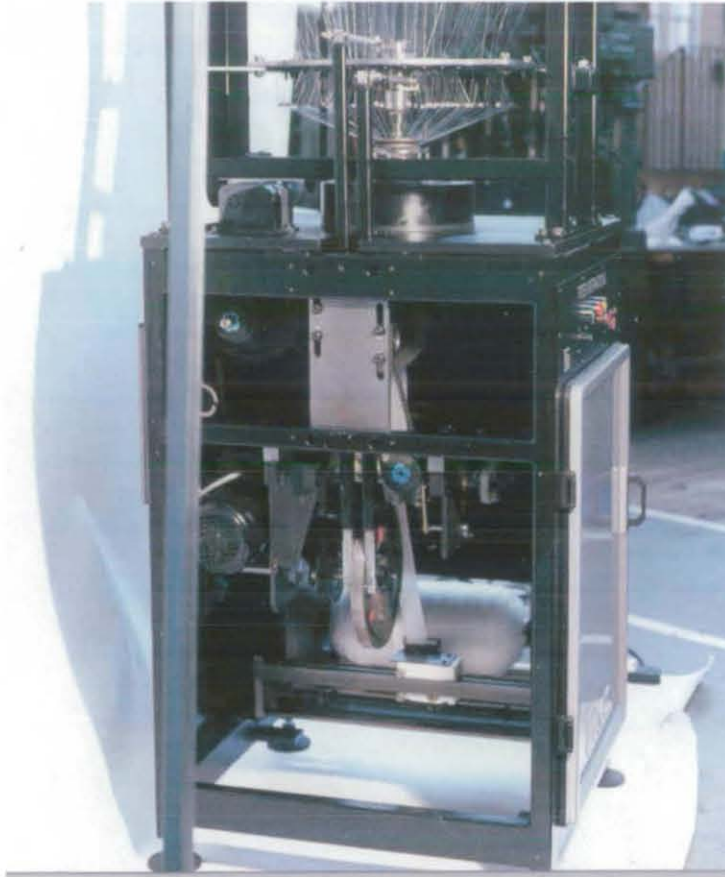


Figure 7-2. Mechanical Patterning Mechanism.

Figure 7-3 shows two cams made for different 8 course patterns. In this case each cycle takes place in $360^\circ/8 = 45^\circ$, and it will be composed of a 15° underlap stroke, followed by 9.375° dwell, then by a 11.25° overlap stroke and finally by another 9.375° dwell. This is to coincide with the knitting cam's $120^\circ \rightarrow 75^\circ \rightarrow 90^\circ \rightarrow 75^\circ$ cycle, ensuring that the patterning rings move when the needles are stationary and vice versa. Each of the cycles in the 6-course patterns Figure 7-4 shown in will be similarly distributed over $360^\circ/6 = 60^\circ$.



Figure 7-3. Cams for 8-course Patterns.



Figure 7-4. Cams for 6-course Patterns

The synchronisation of the cam being fitted into the machine at the right position to coincide with the knitting cycle, is simply ensured by a key slot machined into the cam blank. The means to adjust the number of knitting cycles in one rotation of the patterning cam is also incorporated into the design; where the user can change a timing pulley and a jockey pulley whenever the length of the pattern changes. This ensures that, the ratio of

turns of the knitting cam per single turn of the patterning cam, both coincide with the number of courses per pattern.

The length of each shogging stroke depends on the amplitude of rotation of the patterning ring required. The maximum shogging stroke required determines the baseline radius for the cam as a very large shogging movement in a short portion of the patterning cam will yield unworkable pressure angles, which can produce excessive vibration. A cam rise or return movement will cause a lever to rotate around its pivot (see Figure 7-5). The other end of the lever will in turn, pull or push a connecting rod, which will cause the appropriate patterning ring to rotate anticlockwise or clockwise (respectively). Both of the connecting rods are designed to steer the rings through a pivot located at the same radial distance, in order to minimise the difference in the movements required to produce the same pattern. However, because of the position of the yarns on each ring with respect to the needles, there is always some difference in the amplitude of the stroke required to generate an equal underlap with each of the rings, therefore the profiles milled on either side of a cam for the same underlap will also differ.

The means for small amplifications of the cam movement is also incorporated in the design, by allowing the each levers' pivot to slide vertically in a slot. See Figure 7-6. However, substantial amplification is not deemed suitable (although it would reduce the length of strokes required to come from the cam), the vibration generated would also be magnified and therefore make the patterning inaccurate. With the pivot in the midpoint of the lever, the movement required by the connecting rods to achieve the desired shog, must be reproduced (in the opposite direction) by the cam tracks underlap and overlap strokes.

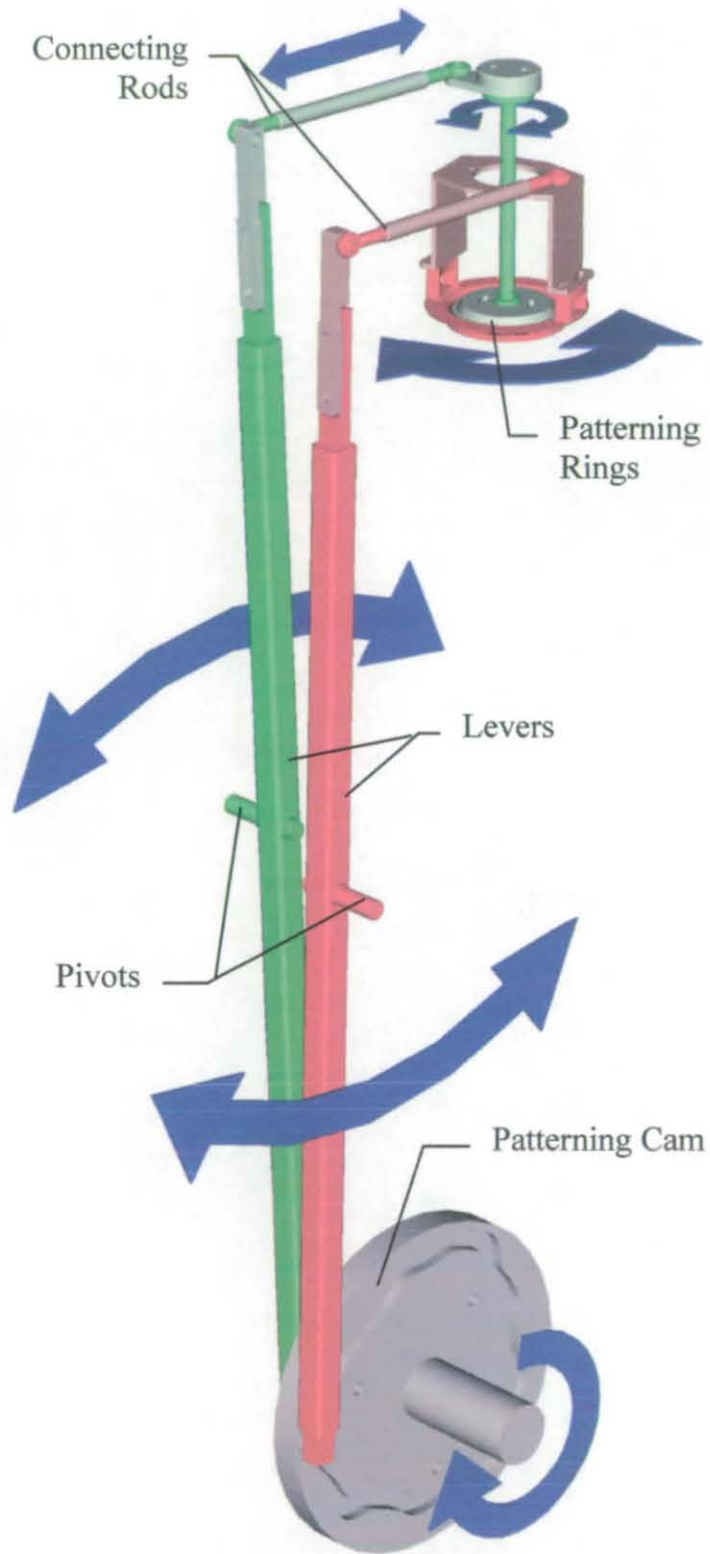


Figure 7-5. Mechanical Design Patterning mechanism

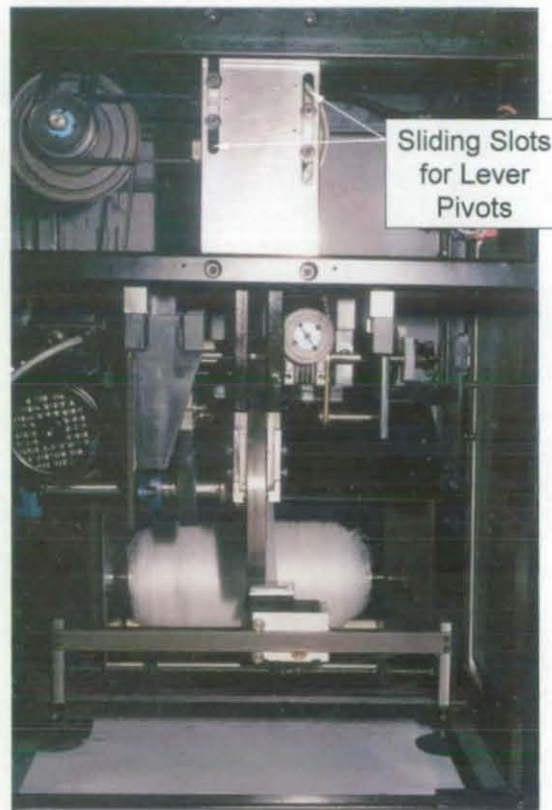


Figure 7-6. Lever Pivots Slide in Slots to Provide Amplification of the Cam Movements.

The strokes were initially calculated by graphically analysing where the yarns would need to be placed, in order to perform a given underlap or overlap. With all the geometric conditions that parameterise the fixed patterning mechanism (i.e. known cone taper, verge diameter, radii of the rings, etc.) this is an effective way of calculating the movements required to produce a given pattern. The next chapter proposes a mathematical model, which can predict shog stroke amplitudes for different values of the geometrical parameters. Once the concept of combining a tapered cone with shogging patterning rings was proven in the first design, the mathematical model was created to optimise the performance of the patterning mechanism, and to investigate the effect of varying the different geometric parameters.

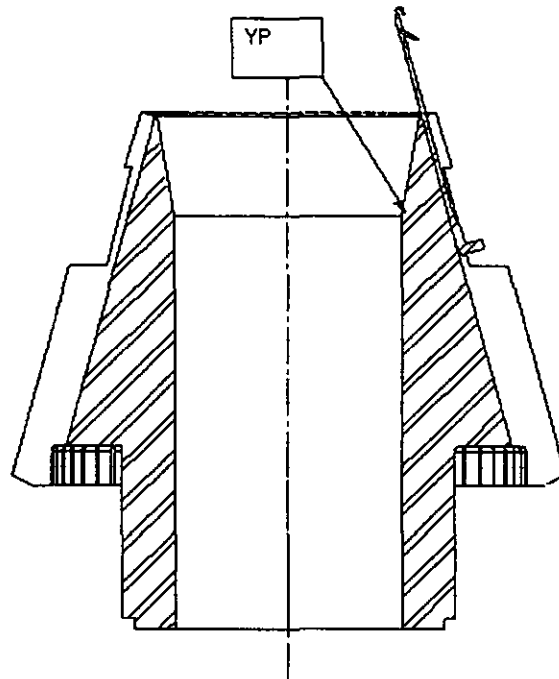


Figure 7-7. Position of Yarn After a Course

Figure 7-8 illustrates the graphical method of calculating the cam strokes. It is based on a simplified plan view of the needles at their lowest and highest positions. For this graphical model, each yarn is assumed to rest after a course directly underneath the needle where it constructed the last stitch, i.e. at the bottom of the verge taper. (See YP in Figure 7-7). A shogging yarn is therefore represented by a line extending from that point to the position of the hole in the ring through which is threaded. The diameter of each of the rings is shown in the figure, the indexing diameter (i.e. the diameter at which the connecting rods pivots are attached to the rings).

The progression of amplitudes for the shogging movements is built, by following the chain notation sequence (that defines the specific pattern) and measuring the appropriate vertical distance for each shog in the chain sequence.

**6 COURSE HEXAGON
48 NEEDLE CYLINDER**

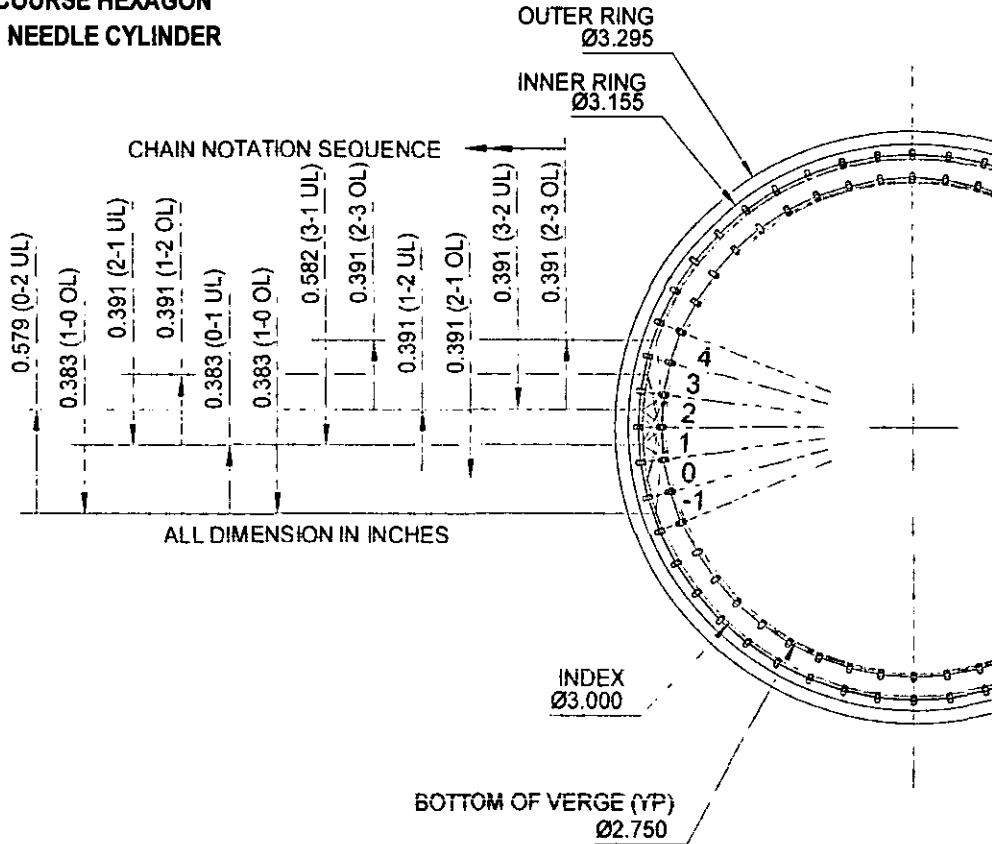


Figure 7-8. Example of Stroke Calculation Using Graphical Method

This appropriate distance for an underlap is measured from the last yarn position (YP in Figure 7-7), to a position where the line representing the yarn falls behind the target needle and in front of the next needle using the representation of the needles at their lowest position (outer ring of needles). In the case of an overlap, the vertical distance is measured from YP to a position where the line representing the yarn falls in front of the target needle and sufficiently near the needle to ensure that the hook will collect the yarn on its way down, using the representation of the needles at their highest position (inner ring of needles).

Although the line representing the yarn is constructed to the ring's diameter, the distance of interest for indexing is that where the yarn-line intersects the index diameter.

In practice, it was found that the tension of the fabric below combined with the elasticity of the yarns, would make the yarns move slightly to either side of the needle where they last made a stitch. For this reason, in order for the graphical method to work, the yarn-lines must be drawn just short of the needle next to the target (and not at the midpoint between the two).

A tailor made computer application was developed to create the cam profile program. This is then downloaded into a Numerical Control (NC) milling machine. A spreadsheet is filled with the sequence of underlap and overlap strokes required to produce a specific pattern (after being calculated using the graphical method described earlier or by any other means). The spreadsheet also requires the end-user to input:

- i. The rise angles for each stroke,
- ii. The start angle (i.e. the angle at which the pattern starts with relation to the keyhole in the cam blank),
- iii. The direction in which the profile is to be milled (clockwise or anticlockwise),
- iv. The baseline radius of the cam,
- v. The cam follower radius, and
- vi. The cutter radius..

A macro contained in the spreadsheet uses this information to produce: (a) the text document containing the NC program ready to be read by the milling machine to make the cams, as well (b) a file in a graphical exchange format (EXF) that can be read by a CAD program with the complete cam track profile.

The EXF file produced for a 6-course hexagon net fabric is shown in Figure 7-10. The chain notation sequence for this fabric structure is,

$$2-3 \cdot | 2-1 \cdot | 2-3 \cdot | 1-0 \cdot | 1-2 \cdot | 1-0 \cdot |$$

Note that the chain notation sequence lists overlaps only, while the sequence shown in the EXF drawing includes underlaps.

The type of structure produce with this cam is shown in

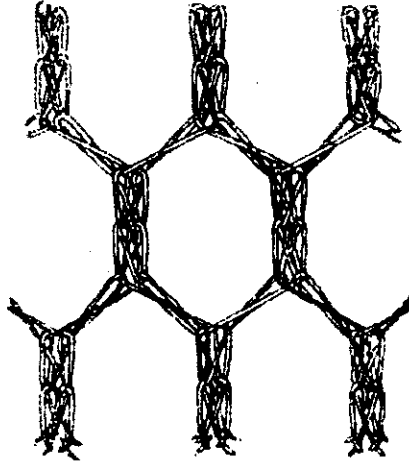
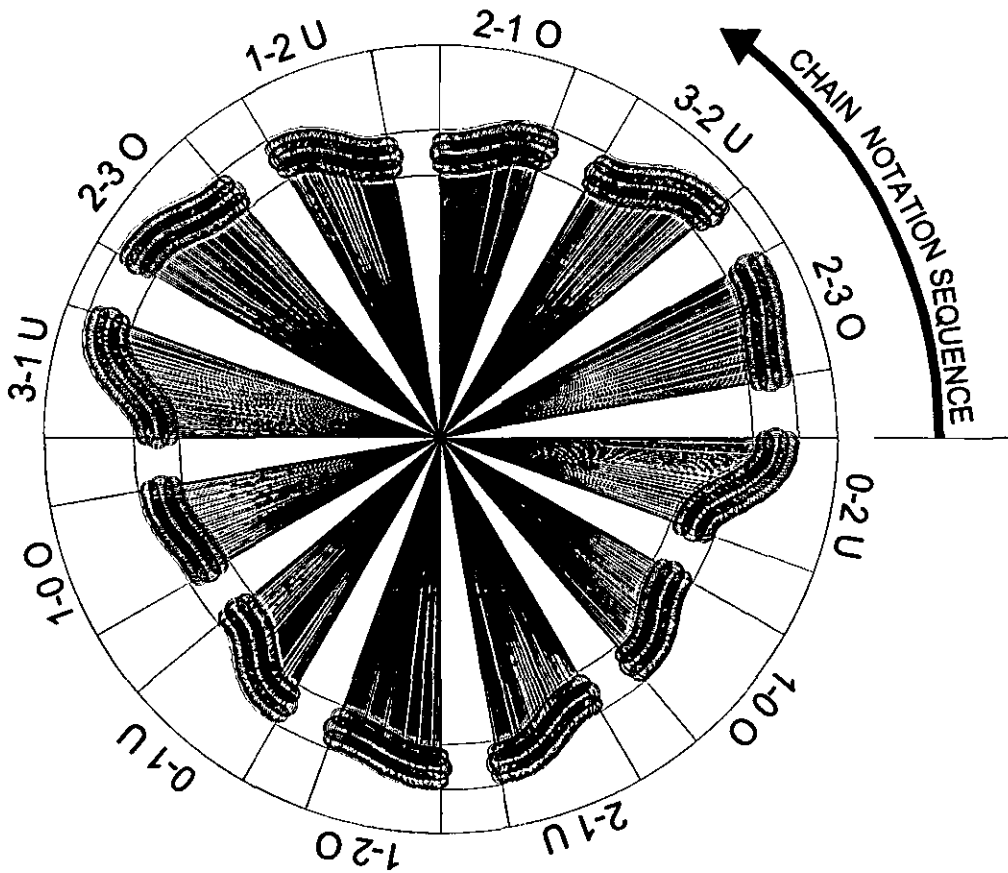


Figure 7-9. 6-course Hexagon Fabric Structure.



6 COURSE HEXAGON
48 NEEDLE CYLINDER
OUTER RING

Figure 7-10. EXF File Example for a 6-course Pattern

Once on the knitting machine, the cam in motion was filmed using a high-speed video recorder (200 frames per second). This revealed that there was no excessive vibration of the follower in the cam-track; even when viewed frame by frame the follower was not seen to leave the side of the track on which it was rolling.

Although the cam-follower mechanism ran smoothly, the high-speed video showed excessive vibration of the patterning rings. The contrast between the smooth running of the cam follower and irregular motion of the rings suggests that the latter is created by the elasticity of the mechanical linkages. The speed of the machine would therefore always be constrained by the mechanical properties and the dimensions of the linkages.

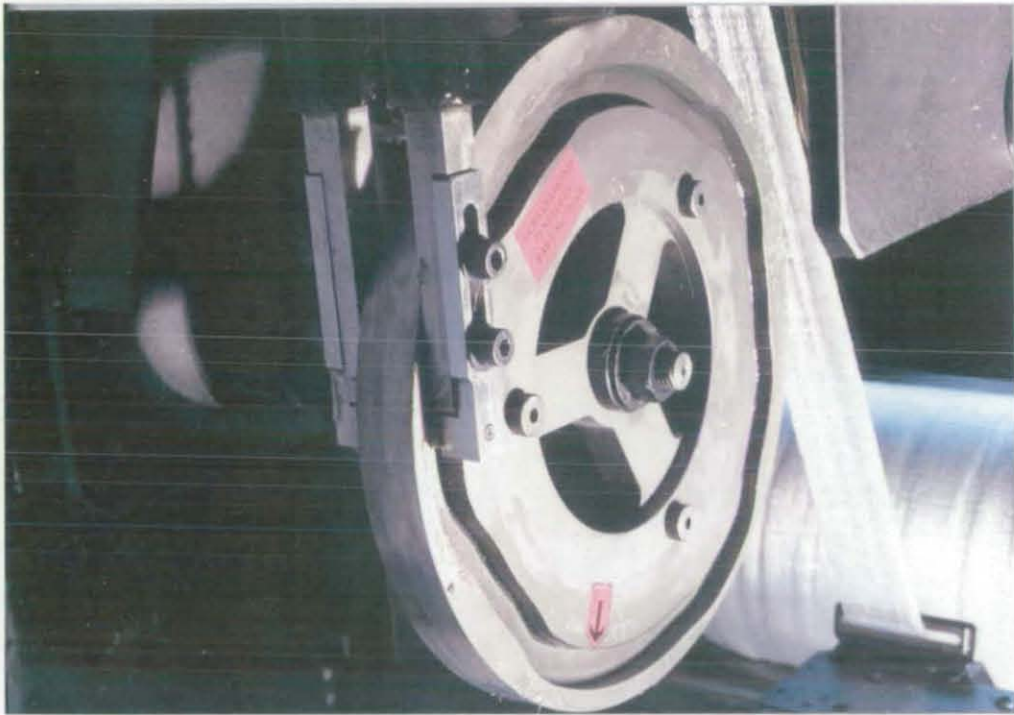


Figure 7-11. Cam Follower Running on a Patterning Cam with no excessive vibration or wear

The main innovations achieved with the mechanical patterning mechanism solution built as part of this research were; 1) the use of enclosed cam followers in the patterning cams reduces shock and vibration effects created when using open face cams; 2) improvements in the manufacturing process of the patterning cams by a tailor-made software tool to create the milling programs of the patterning cam; and 3) enhancement of the cam performance by using cycloidal profiles for each segment.

This mechanical design proved that the circular warp knitting mechanism concept is feasible. However, a design that allowed for more patterning flexibility, with ultimately higher operational speeds, was required in order to manufacture more complex fabric designs used in the medical and stocking industries.

7.4 Servo-controlled Solution

An entirely new approach to the patterning mechanism problem was to control the rings using servomotors. Although a more costly solution, it has the potential of creating pattern chains that are only restricted by the size of the memory of the hardware used (ie hundreds of machines cycles rather than 12) and reducing the time and parts required to change from one pattern to another.

In addition, a servomotor would produce a rotational motion, when coupled via timing belts and pulleys; it could drive the patterning rings directly. There is no need for the mechanical transformation of translational motion to rotational motion, which would have been required if other electronically controlled linearly actuated mechanical devices were used, such as linear pneumatic actuators.

Servomotors were selected over stepper motors because of the speed of reaction and position control requirements given by the knitting application. Any electronic solution of the patterning mechanism problem requires an external means of synchronising it with the knitting mechanism, as the mechanical links are lost.

The main knitting mechanism, that is, the one responsible for the needle motion could also be servo-controlled to give further control over the synchronisation between needles and yarns. Yao et al (2000)⁶¹ proposed such a method, to improve the motion characteristics of a cam follower by controlling the cam speed using servodrives. However, this was not considered relevant to proving new concepts pertaining to a circular warp knitting machine, so this section of the chapter relates to the servo control of the patterning mechanism only.

The main constraint in the design of the patterning rings assembly is space for, although consideration must be given to the complex web of yarns coming into the assembly (see Figure 7-13, Figure 7-12 and Figure 7-14), the radial movements required to perform the same underlap from a ring further away from the needles is substantially larger than that required by a ring near the needles. The rings are therefore placed as near as possible to each other.

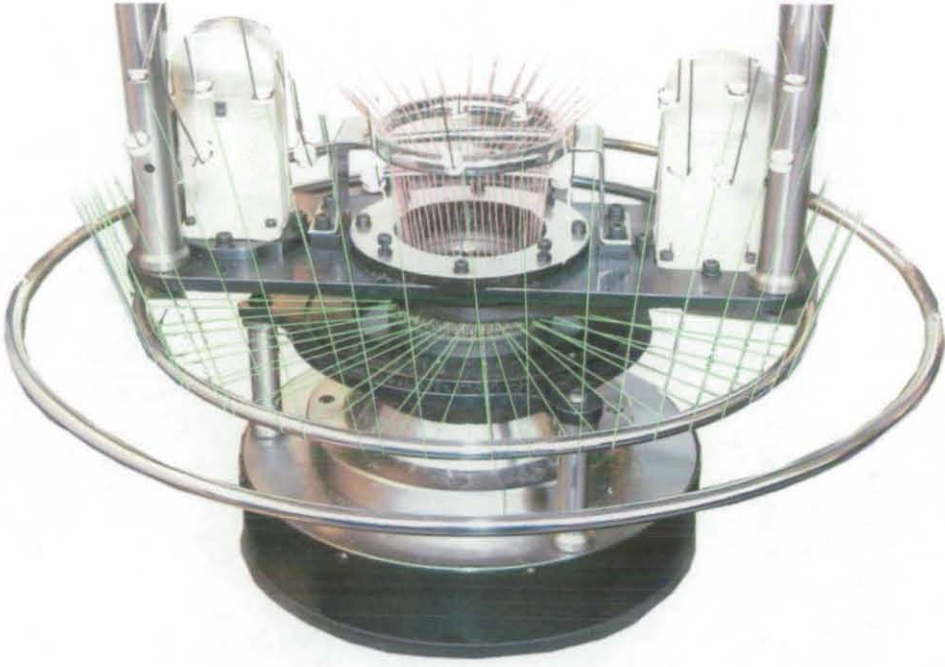


Figure 7-12. View of Patterning Mechanism With Two Rings Threaded

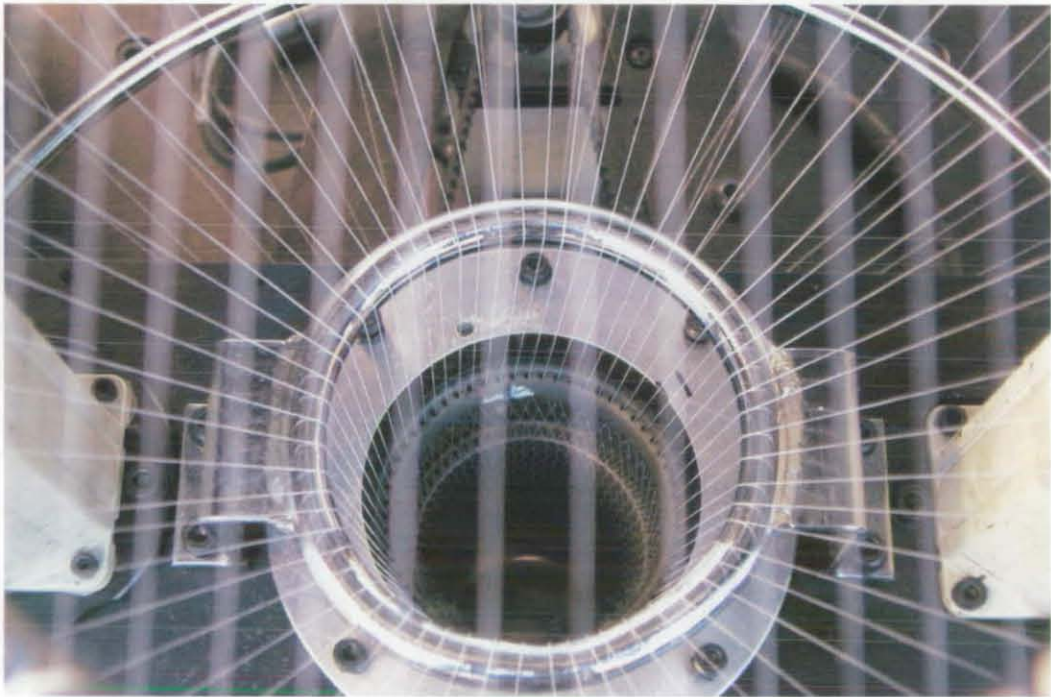


Figure 7-13. View of the Yarns Threaded in the Top Patterning Ring



Figure 7-14. Yarn Paths from Let-off Units to Three Rings

For this reason of proximity, each of the rings is drilled with holes for eyelets through which the yarns are threaded and rotates around a thin bearing that separates it from the next ring. See Figure 7-15.

A material with the properties to withstand the high abrasion that the yarns will inflict on the holes, and yet to act as a bearing rotating intermittently in 20ms bursts of high speed is difficult to find.

The solution was to use an aluminium alloy containing elements such as silicon, which make it suitable as a bearing, and apply a hard ceramic coating, which gives it the hardness required against abrasion.



Figure 7-15. Exploded Patterning Rings Assembly



Figure 7-16. Servomotor Controlled Patterning Mechanism.

The rings are connected to the servomotor shafts by timing pulleys as shown in Figure 7-16. The servomotors are powered by drives contained in a side cabinet of the machine (see Figure 7-17). The patterns are programmed by downloading a program prepared by the user on a Personal Computer (PC) interface. The PC is connected via a serial port to a motion controller. When the machine is running, the motion controller will send the required sequence of signals to the drives and the PC need no longer be available.



Figure 7-17. Patterning Mechanism Control and Drives

Alternatively, The PC can be used to send single commands directly to each of the rings, via the motion controller and the drive. This gives the user a useful means of creating new patterns directly on the machine.

7.5 Motor Selection

In order to select the most cost-efficient servomotor capable of meeting the patterning mechanism requirements, a new method of selecting servomotors is proposed in this section of the chapter.

Advances in high-speed applications are out-pacing advances in the control performance of servo drives. To close this gap, improved control is being developed such that the designer now has more choice in motors drives and motion controllers. Iwasaky et al (1996)⁶², for example, presented a high-accuracy trajectory-control method and its auto-tuning.

In the area of servo-drives used in high-speed machinery to replace traditional mechanical linkages (such as gears or belts), Beaven et al (1995)⁶³ show that a reduction of cycle time is made possible by the application of set-point gain scheduling to high-speed independent drives. This involves the transition from one controller to another at a set point in the cycle by changing the gain values within the motion.

Research devoted to the optimisation of the control loop used by the servomotor, however, is beyond the scope of this research. Instead, the emphasis here is given to the process of selection of existing motors and drives and how to optimise it.

7.5.1 Selection Optimisation

The main parameters involved in the selection of a servomotor are the torque required by the system (including the torque required by the servomotor itself) and the speed at which the motor will run. Different angular velocity profiles can be used to perform a given rotational movement within a set time.

When using a triangular speed profile (see Figure 7-18), the shaft angular velocity can be expressed as;

$$\theta = \frac{\omega_{\max} \cdot t}{2} \quad (7-1)$$

$$\alpha = \frac{\Delta\omega}{\Delta t} = \frac{\omega_{\max}}{t/2} = \frac{4\theta}{t^2}$$

(7-2)

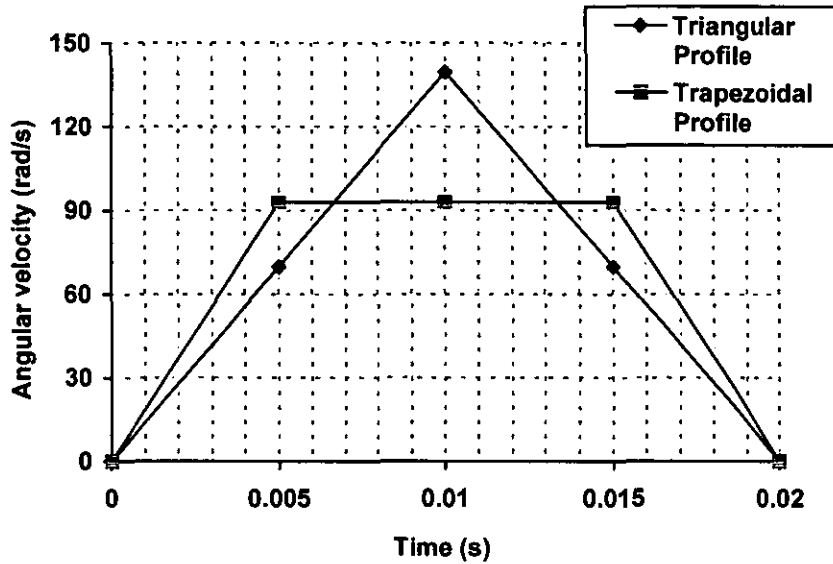


Figure 7-18. Motor Requirements

The minimum angular acceleration the system would require (that is, in the case of the triangular profile) is

$$\alpha = \frac{4\theta}{t^2} = \frac{4 \cdot (1.396 \text{ rad})}{(0.02 \text{ s})^2} = 13963 \text{ rad/s}^2$$

Which will reach in 10ms an angular velocity of

$$\omega_{\max} = \frac{2\theta}{t} = \frac{2 \cdot (1.139 \text{ rad})}{0.02 \text{ s}} = 113.9 \text{ rad/s} = 1333 \text{ rpm}$$

If the time allowed for accelerating and decelerating is reduced, the speed curve will turn into the trapezoidal shape shown (see Figure 7-18), while the acceleration needed would increase together with the torque and power requirements. The maximum angular velocity, however, would decrease. The area below both curves is the same as it represents the angular position achieved after the displacement. The angular position can therefore be expressed as;

$$\theta = \omega \cdot t_{acc} + \omega \cdot (t_{total} - 2 \cdot t_{acc}) \quad (7-5)$$

Rearranging this equation to find an expression for the maximum angular velocity,

$$\therefore \omega = \frac{\theta}{(t_{total} - t_{acc})} \quad (7-6)$$

The maximum angular velocity as a function of the time required to accelerate the load to achieve it (t_{acc}) is plotted in Figure 7-19 .

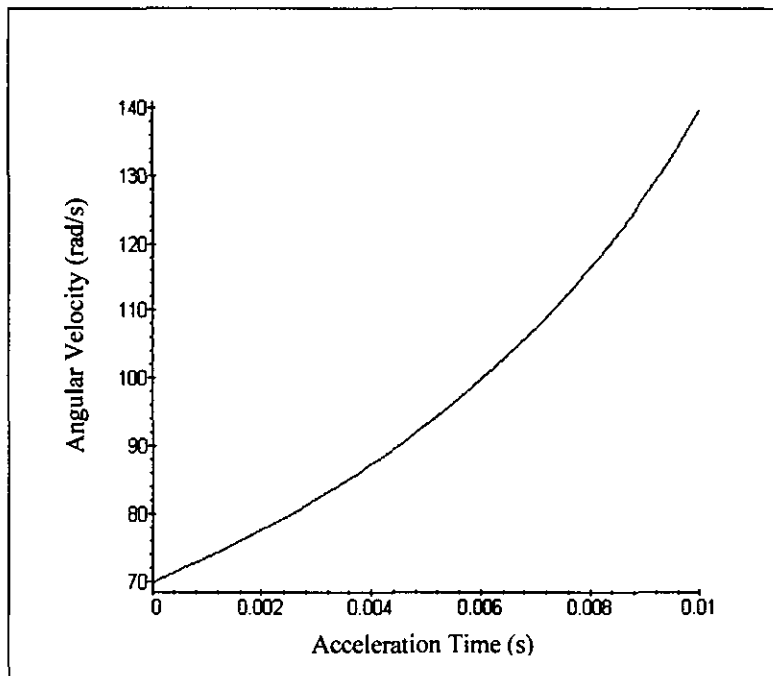


Figure 7-19. Time Required To Reach The Maximum Angular Velocity

The acceleration required to reach the maximum angular velocity in t_{acc} , for a given trapezoidal profile, is equal to $\alpha = \frac{\omega}{t_{acc}}$. The torque requirements of the servomotor are directly proportional to the acceleration and the total

inertia of the system, and therefore inversely proportional to the acceleration time (see equation (7-8) and Figure 7-20):

$$T = I_{TOTAL} \alpha = (I_{motor} + I_{load}) \cdot \alpha = (I_{motor} + I_{load}) \cdot \frac{\omega}{t_{acc}} \quad (7-8)$$

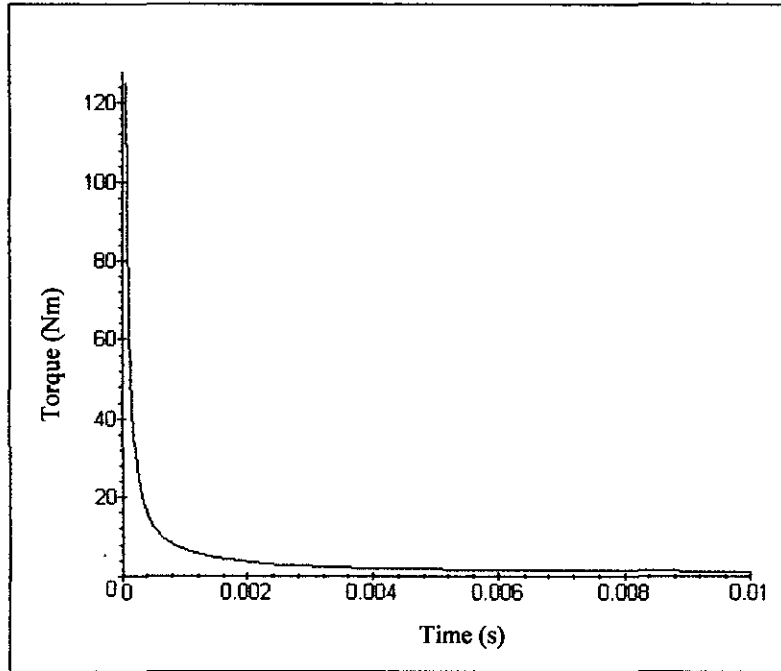


Figure 7-20. Torque required to reach the maximum angular velocity

We can also obtain an expression for Torque in terms of angular velocity, which represents the relationship between the two variables traditionally used for selecting the appropriate servomotor;

$$T = \frac{I_{TOTAL} \cdot \omega^2}{(\omega \cdot t - \theta)} \quad (7-10)$$

A better criterion for selecting the servomotor is its size, which is proportional to its power and therefore its cost. In order to obtain the smallest motor capable of fulfilling the system requirements, the power used to perform the move must be minimised. The power requirement can be expressed as;

$$P = T \cdot \omega = \frac{I_{TOTAL} \cdot \omega^3}{(\omega t - \theta)}$$

(7-12)

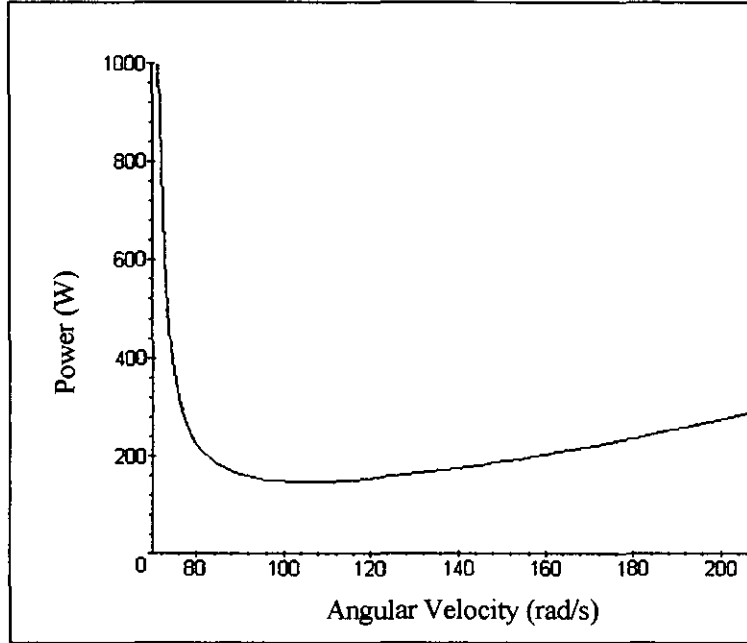


Figure 7-21. Power vs. maximum angular velocity

Equation (7-12) is plotted in Figure 7-21. The minimum power requirement will be given by solving

$$\frac{\partial P}{\partial \omega} = \frac{I_{TOTAL} \cdot \omega^2 [3(\omega t - \theta) - t]}{(\omega t - \theta)^2} = 0$$

(7-14)

The root of this expression occurs at $\omega = 104.71 \text{ rad/s}$ for the warp knitting patterning system (see Figure 7-22). This makes the minimum power required $P = 61 \text{ W}$. Selecting this value of the angular velocity, ω , will in turn establish the optimum values of torque (T) for the system, acceleration time (t_{acc}), and the value of the acceleration (α).

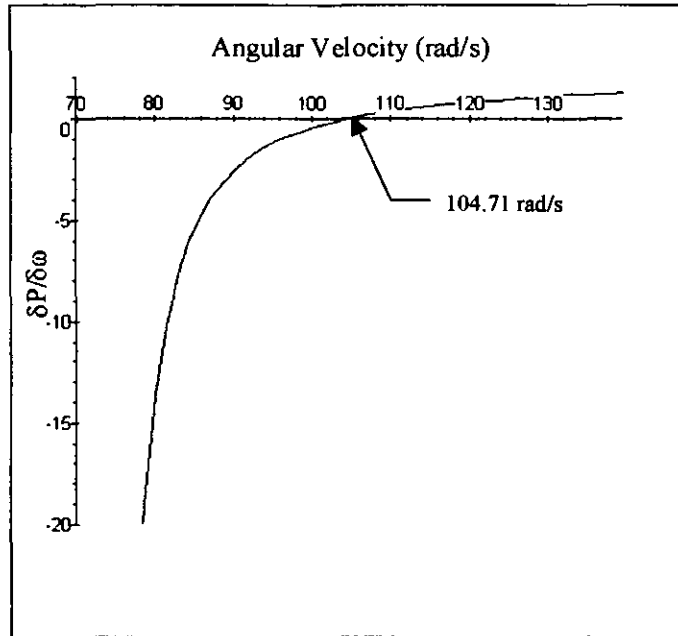


Figure 7-22. Minimum power requirement.

By selecting a servomotor using these values, it will ensure that the motions can be performed maximising the servomotor potential.

7.5.2 Measurement of Motor and Drive Response

The patterning mechanism requirements included one relating to the motor's response; being able to perform an 80° rotation within 20ms.

Although the selection process presented above ensures that the motor has sufficient power to accelerate the load in the calculated t_{acc} , the drive response might not be fast enough to achieve the motion required within the specified time.

The only variable given by the manufacturers related to fast response is the mechanical time constant, defined as the time required for a motor to reach 63.2% of its rated speed or as;

$$\tau_m = \frac{J \cdot R}{K_E \cdot K_T}$$

(7-16)

where, J = Motor moment of inertia,

R = Armature resistance,

K_E = Voltage constant,

K_T = Torque constant.

Even when the figures seem to confirm that a motor is capable of meeting the requirements, manufactures do not like to assure users of the drive's response capabilities before running tests.

As part of the research tests were carried out on two servo drives to ensure that they were capable of reacting as fast as was necessary. Two servomotor and drive sets were tested. For the purpose of this research they will be referred to as motor A and motor B. The specification given by their respective manufacturers is summarised in Table 7-1.

Both motors and recommended motion drives were tested with and without load and their results differ greatly.

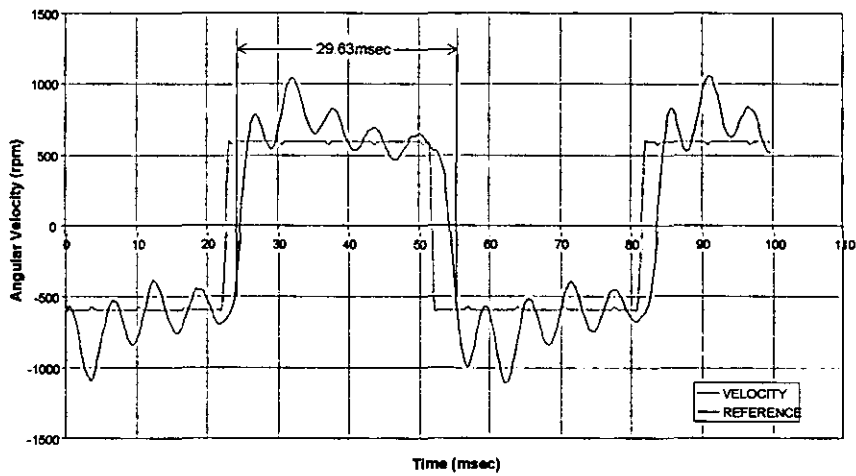
There control loops are also different; while motor A responds to a step velocity input, with time to maximum velocity set to zero, Motor B follows a different control loop where the velocity is corrected every millisecond. Therefore, the only valid comparison that can be made from the graphs is the minimum time each motor requires to perform a given rotation. . Figure 7-23 shows the best response of the respective motors without any load. Motor B could perform the motion in a minimum of 13.15ms, that is, accelerating in 6.5ms. Motor A, on the other hand, performed the motion in a minimum of 21ms. The latter therefore fails to meet the circular warp knitting patterning requirement, even without the load.

The mechanical time constant is lower for motor B (Table 7-1). However, according to the constant for that motor, 1740rpm should be reached in 0.43ms rather than the 6ms it actually needed during the test. We can only conclude, therefore, that a low mechanical time constant is desirable in a fast response system, but that it does not relate exactly to the practical results.

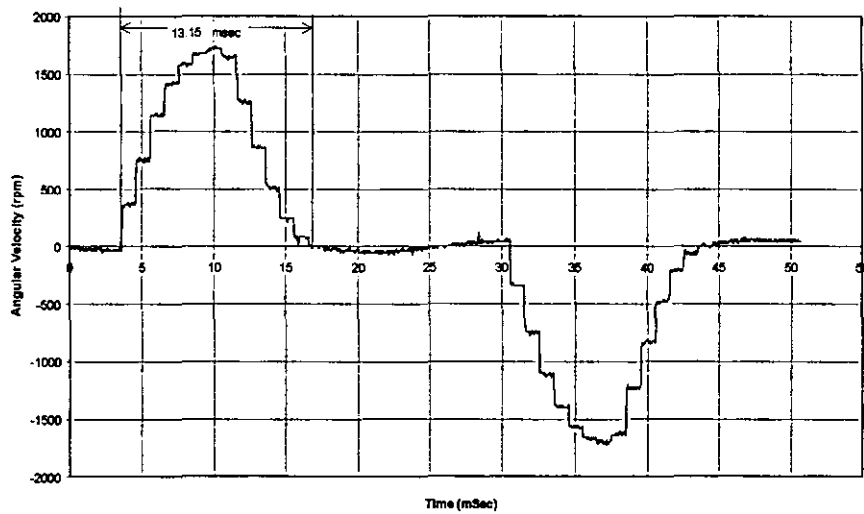
Table 7-1. Specifications of Two Servomotors Considered

	Motor A	Motor B
Rated Output Power (W)	-	400
Rated Torque (N-m)	1.47	1.30
Rated Speed (rpm)	-	3000
Maximum Speed (rpm)	7000	5000
Rated rms Current (A)	2.1	2.5
Peak Current (A)	8.0	10.5
Rotor Inertia (Kg-m ²)	4.7×10^{-5}	3.7×10^{-5}
Mechanical Time Constant (ms)	1.00	0.47
Electrical Time Constant (ms)	1.4	3.9
Torque Constant (Nm/A)	0.73	0.36
Voltage Constant (V _{rms} /krpm)	44.6	-
Resistance (Ω)	11.6	1.1
Inductance (mH)	24.8	4.3

The difference in the performance is probably related to the difference in the mechanical construction of the two motors as well as the control algorithms used. In the case of Motor A system, proportional, velocity and acceleration feed forward gains were needed to obtain the best response shown in Figure 7-23 (a), while Motor B showed its best performance when only the proportional gain was set to 60%.



(a) Motor A



(b) Motor B

Figure 7-23. Best response for an 80° motion - without load

Motor B, which gave a better response without load, was then tested with a disc manufactured to simulate the same reflected inertia as the real system would have. This simplified test method ensures that the motor can respond within the required time in frictionless system. It does not take into account

the load created by the varying tension of the yarns as the motor is moving to position them near the required needle.

The patterning mechanism for the knitting machine was then designed, built and tested. It consists of three rings each controlled by servomotors. See Figure 7-16. The motors are only linked to the load by pulleys and belts, ensuring an appropriate gear ratio. The mechanism is no longer restricted by mechanical properties of the linkages, nor does it convert translational motion into rotational motion of a ring.

The mechanism was tested without yarns and the maximum rotation (80°) was achieved repeatably, alternating direction, in the specified time of 20ms. Each 80° motion is equivalent accelerating from zero to 139rpm in 10ms and decelerating to zero again in the remaining 10ms, which illustrates the very fast response of the system.

In addition, changing the knitting pattern can easily be done by entering a new set of values into the motion controller memory and involves no changes of mechanical parts.

The development of a new knitting pattern is reduced to stepping the motor until it reaches the desired position for each motion and recording those values. It no longer requires milling a new cam and it can involve as much iteration as necessary.

Moreover, the number of steps in a pattern is only restricted by memory capabilities of the motion controller. A pattern can reach hundreds of steps while the mechanical design has only used cams with up to 12-step patterns.

7.6 Conclusion

This section of the chapter presents two solutions to the problem of designing a patterning mechanism for a circular warp knitting machine. The mechanical solution proposed (using an enclosed cam-track) represents significant improvements on the few existing mechanical design concepts.

The servo-controlled mechatronic design, however, is an entirely new concept. It requires very fast responses and uses AC brushless servomotors

to control three patterning rings via a belt and pulley arrangement. Not only does it make the pattern capabilities significantly better than any mechanical system, it also meets the response requirements that will allow the machine to be run at 1000 rpm.

Both mechanisms have been manufactured and tested on separate machines, and are now commercially available.

In addition, Section 7.5 puts forward a new method for the selection of servomotors. Based on minimising the power required to perform the fastest motion required by the application, it ensures the selection of the smallest servomotor suitable for the application. This is very significant as it minimises the cost of the system: servomotor power capabilities determine its frame size, which in turn governs its cost.

Chapter 8. Modelling the pattern creation process

8.1 Introduction

In a circular warp knitting machine, geometric parameters such as the taper angle of the needle bed, the diameter of the patterning rings and the distance between the patterning rings and the needles can either enhance or hinder the patterning capabilities of the machine. This chapter describes an approach to modelling the yarn and needle paths in a circular warp knitting machine that uses a conical needle bed in order to optimise its performance.

Such a model would also allow the designer to select the dimensions and geometric constraints of the patterning mechanism according to the fabric patterns required.

Mathematical models of this kind have only been created for weft knitting machines²⁷, where they have been aimed at inferring fabric characteristics.

In a warp knitting machine, the patterning mechanism's main function is to provide the needles with yarns at the appropriate points in the knitting cycle following a specified sequence, to produce a given knitted pattern. The interaction between the patterning and knitting mechanism of a warp knitting machine is paramount to maximise the machine production.

The knitting cycle of a latch needle machine is shown schematically in Figure 2-1 and explained in section 2-2. The movements performed by needles and guide bars in a flat warp knitting machine are mainly rectilinear and therefore, the calculation of the amplitude of the shogging movements is straightforward.

On a circular warp knitting machine, the interaction of the patterning mechanism and the needles' movement should produce the same actions as those of a flat-bed machine. The patterning mechanism of the circular machine investigated in this chapter is based on patterning rings through which the yarns are threaded, where the rings need to be rotated in order to provide a given needle with yarn, which it collects on its downward movement. For this model, a conical needle bed has been used to enhance the interaction between the needle and yarn movements. By using a tricked cone to support the needles, the swinging motion performed by the yarns is no longer required, therefore simplifying the patterning mechanism, which itself improves the overall efficiency of the design. An exploded assembly of the design is shown in Figure 8-1, where the bearings and supports have been greyed out to emphasise the conical needles bed and patterning rings.

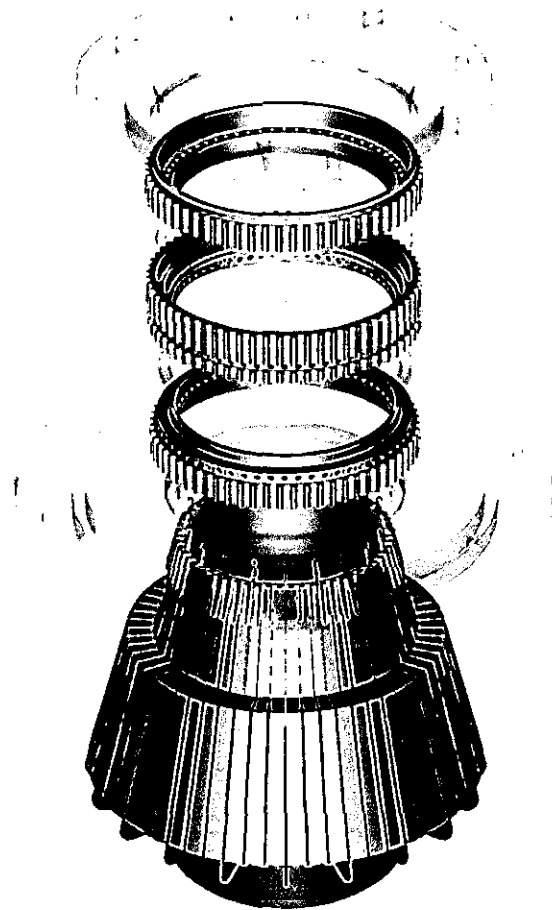


Figure 8-1. Exploded Assembly of Tricked Cone and Patterning Rings.

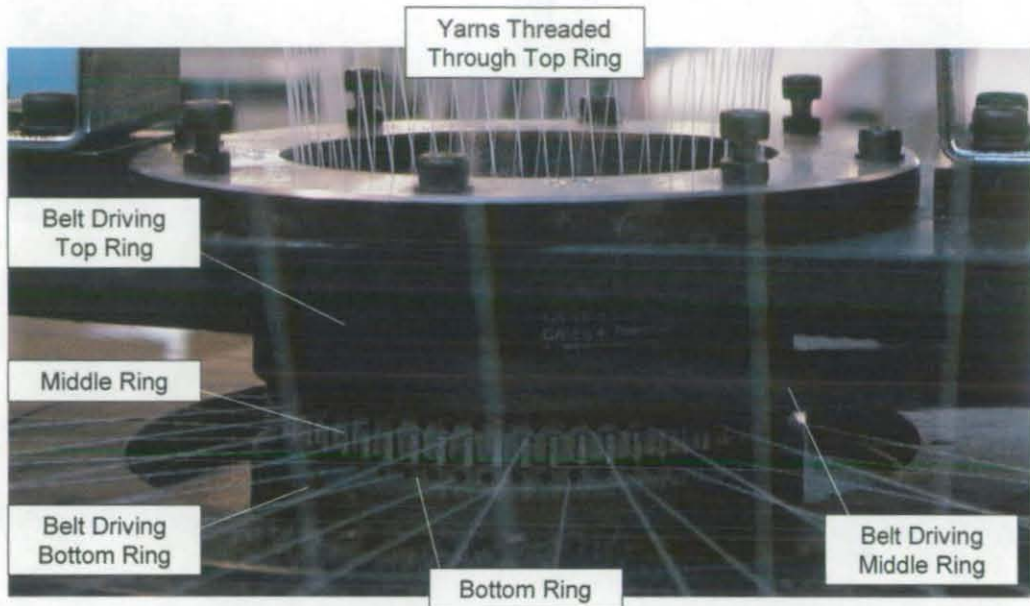


Figure 8-2. Assembled Patterning Rings and Yarns

Figure 8-2 shows the patterning rings assembly in working conditions, with yarns threaded through them. The lower bearing obstructs the needles from view.

Several geometrical factors in the design of the patterning mechanism are all interrelated. They include; the inclination of the cone, the distance from the patterning rings to the needle hooks and the diameter of the rings. This chapter analyses the equations that govern the relationship between the different geometric parameters in order to create a mathematical model that describes the shogging motions which successfully create a stitch on a circular warp knitting machine.

8.2 Description of the Mathematical Model

The critical point in the knitting action is the amplitude of the yarns' underlap and overlap shogs in order to ensure that the yarn will wrap the required needle at the overlap. A two-needle underlap, for instance, should position the yarn adequately to ensure that, after the needles rise (Figure 8-3), the yarn will wrap the appropriate needle as it performs the overlap.

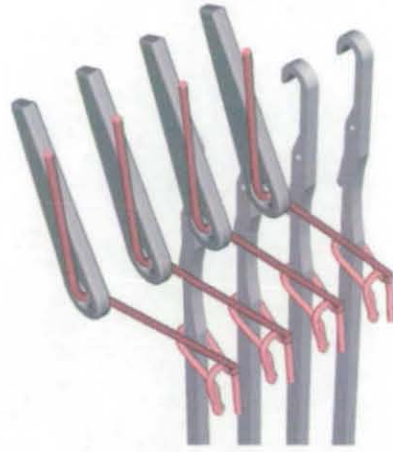


Figure 8-3. Needle Rise After a Two-Needle Underlap

A successful underlap-overlap combination must also ensure that the yarn will be placed at a position where it will wrap above the spoon of the open latch and under the needle hook. This will guarantee that the overlap will neither wrap the yarn under the needle latch nor slide the yarn above the hook.

By using a mathematical model, the designer can predict whether a successful underlap-overlap combination can be achieved with a given set of geometric constraints.

The objective of carrying out a geometric analysis of the patterning mechanism is to allow the designer to select the dimensions and geometric constraints of a patterning mechanism in accordance to the fabric patterns required by the user. This therefore creates a direct relationship between the design of the mechanism and the user requirements. No such tool exists at present and mechanisms of this kind are designed based on past experience rather than on true fabric-led requirements.

The model is based on creating a set of equations used to predict the intersection of a yarn after the underlap-overlap shogs with the plane in which the target needle moves (that is, the needle on which the next stitch is to be produced). This will enable the designer to investigate the advantages of different values for parameters such as cone taper, cone verge diameter,

height of patterning rings and shog amplitude for the creation of a specific fabric pattern. The patterning mechanism design for a machine that will produce a fabric pattern, which requires only a single needle underlap, can have, for example, larger patterning rings than one for producing a fabric that requires two needles underlaps.

Geometric Parameters

The geometric parameters found to affect the design of the patterning mechanism are defined below (Refer to Figure 8-4);

- R_R (m): Radius at which the yarn eyelets are situated on the patterning ring.
- R_V (m): Radius of the bottom of the verge ring,
- R_N (m): Radius of the top of the verge ring,
- NN : Number of needles in the cone.
- U : Number of needles the underlap will cover.
- α_n (rad): Needles Angular Pitch. $\alpha_n = 2\pi / NN$,
- PL (m) : Displacement of the needles (parallel to the cone),
- s (m): Vertical distance between the top and bottom of the verge ring,
- H (m): Vertical distance between the top of the verge ring and the patterning ring,
- β (deg): Half cone angle; that is, the angle between the needles the z-axis (vertical).

For each machine design, only some of these parameters will be controllable, others might be restricted by the method of manufacture of a part or the accessibility of the mechanism to an operator.

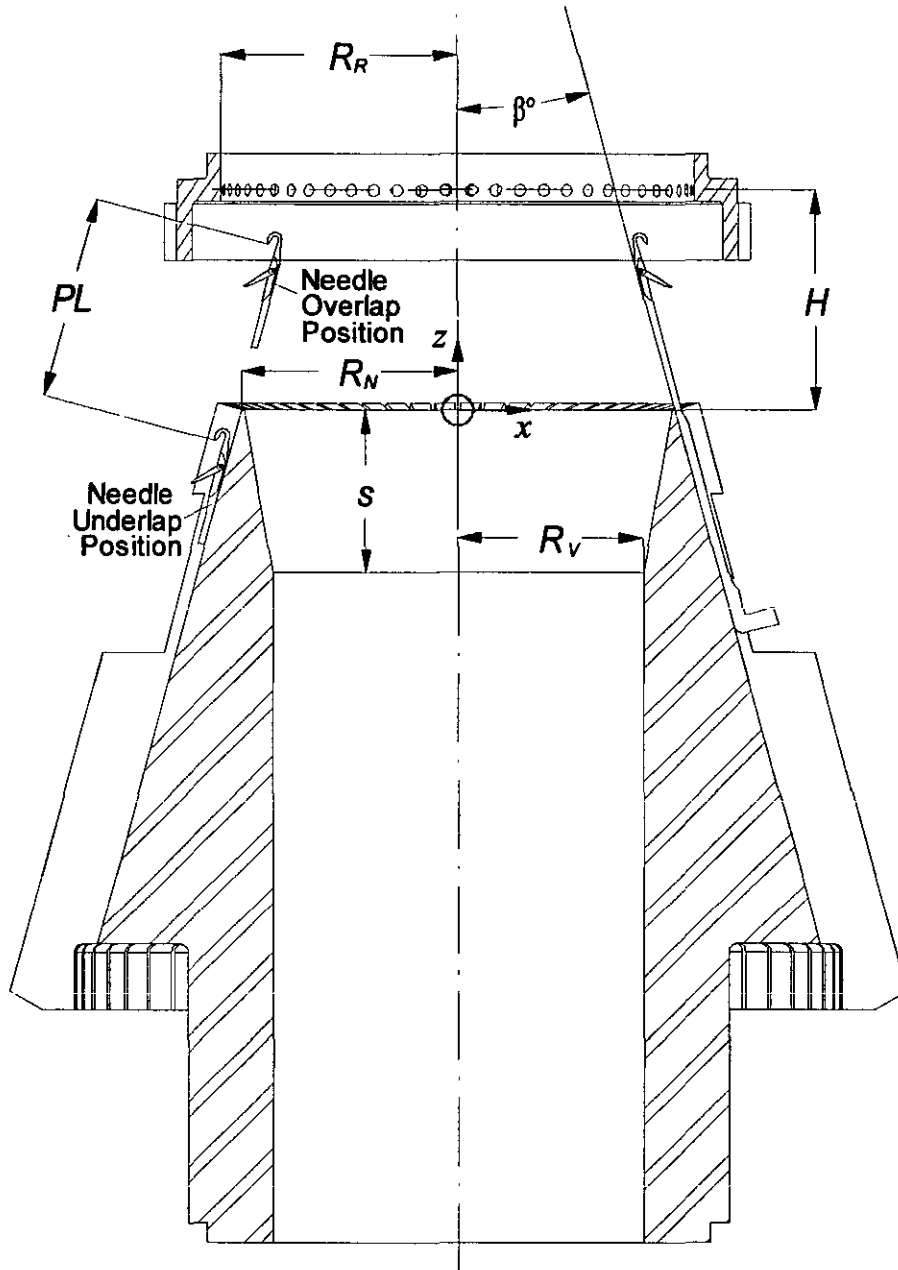


Figure 8-4. Cone section using plane through target needle

The model developed considers two instants of the stitch formation process; namely, the end of the overlap and the end of the underlap. The figures reproduced from Figure 2-2 as Figure 8-5 (c) and (e) respectively illustrate the two instants. The model can be used to calculate the minimum rotation of the patterning rings that will enable a given underlap-overlap combination, or whether that combination is not possible for the mechanism dimensions used.

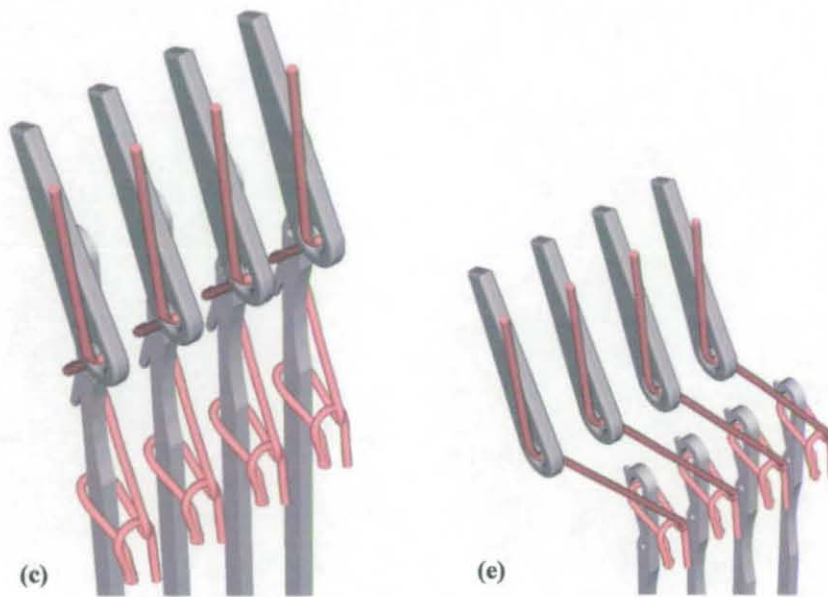


Figure 8-5. Overlap and Underlap

The requirements for a valid underlap-overlap combination differ greatly depending on whether both shog motions are carried out in the same or in opposite directions. For that reason, the analysis is divided into two main sections;

1. Underlap and Overlap in the same direction.
2. Underlap and Overlap in opposite directions.

8.3 Underlap and Overlap in opposite directions.

The analysis was carried out for an underlap motion going past the target needle, in the first instance. That is, the succeeding overlap will rotate the patterning ring in the opposite direction to the underlap.

When the overlap is performed in the opposite direction to the preceding underlap, the thread can be divided for analysis purposes, into two distinctive parts; one from the last stitch to a point on the back of the target needle (which in this case is the same as the underlap target needle); and the second from that point at the back of the needle to the respective eyelet in

the patterning ring. In this case the yarn is effectively wrapped around the needle, like the one shown in Figure 8-5 (c).

During the underlap the needles are in their low position. Each thread should travel from where the last stitch has been cast behind the needles. Its end position should allow the target needle to rise in front of the thread. It should also be at an appropriate height, to enable the thread to pass under the needle hook and over the latch spoon when the overlap is performed.

In order to investigate if the thread will comply with these requirements, the intersection between the vector representing the thread and the plane on which the target needle moves (Figure 8-6) needs to be expressed in terms of the geometric design parameters listed above. This point will be defined as the 'underlap intersection'.

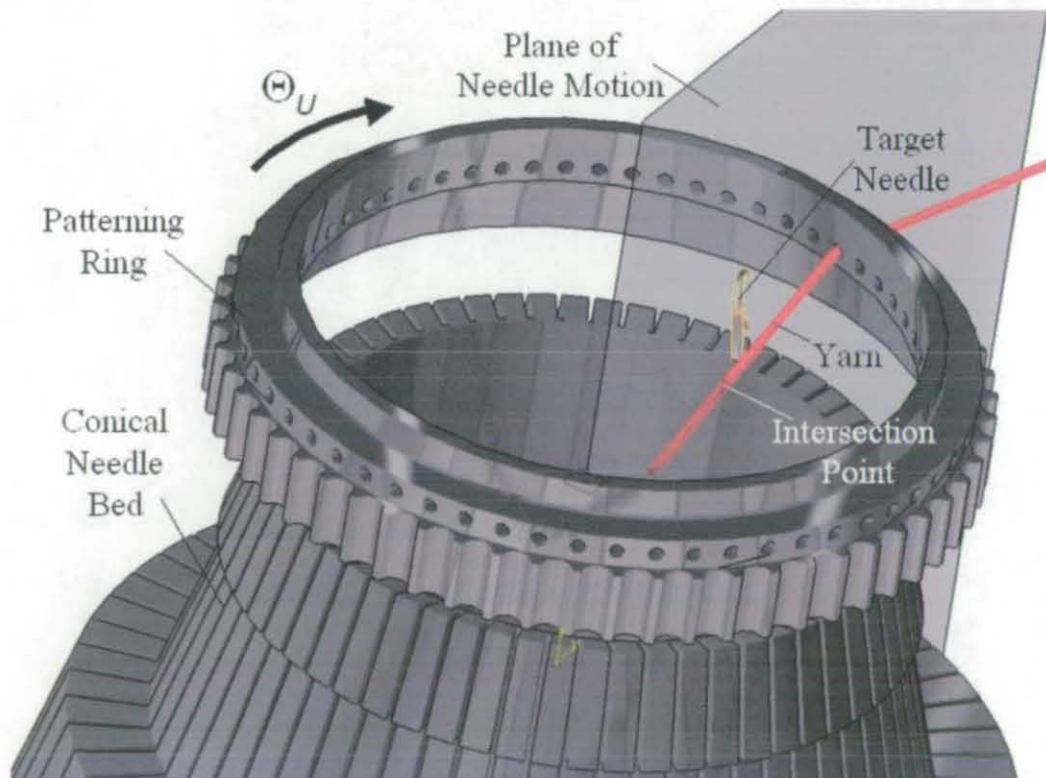


Figure 8-6. Underlapping Yarn.

The importance of the underlap intersection point satisfying the knitting requirements lies in that the position of the thread at the end of the underlap determines if the overlap will be performed correctly.

8.3.1 Underlap

The conditions for a successful underlap are based on where the underlap intersection point lies in relation to the target needle. Figure 8-7 illustrates this claim.

First, the Underlap Intersection point must lie behind the underlap needle. Graphically this is reflected in Figure 8-7 as being to the right of the line representing the back of the needle. That is a line at β° from the vertical axis and intersecting the x-axis at R_N .

The underlap intersection point must also enable the thread to pass under the needle hook when the overlap is performed. Expressed graphically, this condition implies that the projection of the second part of the yarn onto the target needle plane should not be above the line labelled 'underlap limit line' in Figure 8-7. The line, shown from the centre of the patterning ring eyelet and through the needle hook point, represents the overlapping yarn in the extreme case when the yarn just actually touches the hook point. Should the overlapping yarn be any higher, it would not be collected by the needle on its descent. The underlap intersection point should therefore lie below (to the left in the figure) of the underlap limit line to ensure a successful underlap-overlap combination.

These two conditions provide a permissible area for the underlap intersection point, which can be expressed in terms of the geometrical parameters defined earlier. In the following sections the equations and inequalities to describe the underlap intersection point and to judge its suitability are detailed further.

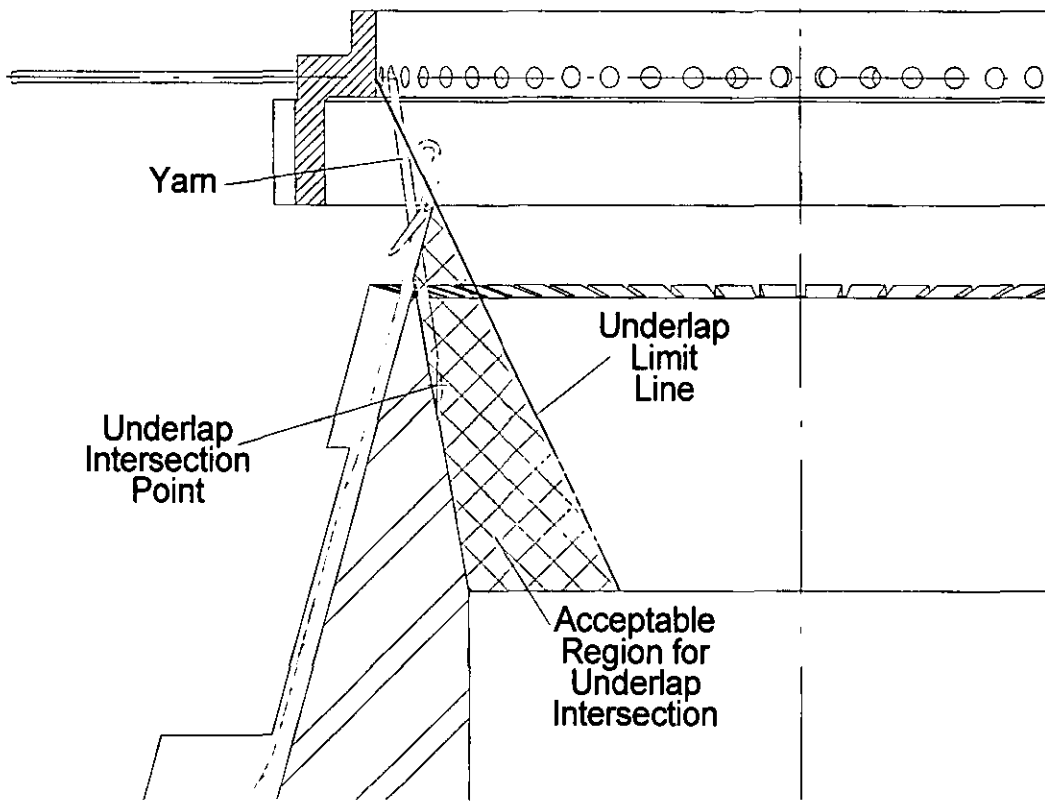


Figure 8-7. Illustration of Acceptable Region for intersection point.

8.3.1.1 Thread Vector

The underlapping thread can be represented (Figure 8-8) by a vector (\vec{T}_U) from the bottom of the verge ring underneath the last needle on which the thread produced to the eyelet on the patterning ring at the position where it has finished the underlap. The deflection of this vector depends on the amplitude of the shog motion.

The following definitions are necessary for the geometrical analysis:

Θ_U is defined as the anticlockwise angle on the x-y plane between a vector from the origin to the start point of vector \vec{T}_U and one from the origin to the end of \vec{T}_U , for a given shog amplitude (a negative Θ_U will represent a clockwise angle).

For this analysis; the origin was arbitrarily set at the centre-top of the verge ring; n is defined as the last needle on which a stitch was cast; and N is the underlap target needle.

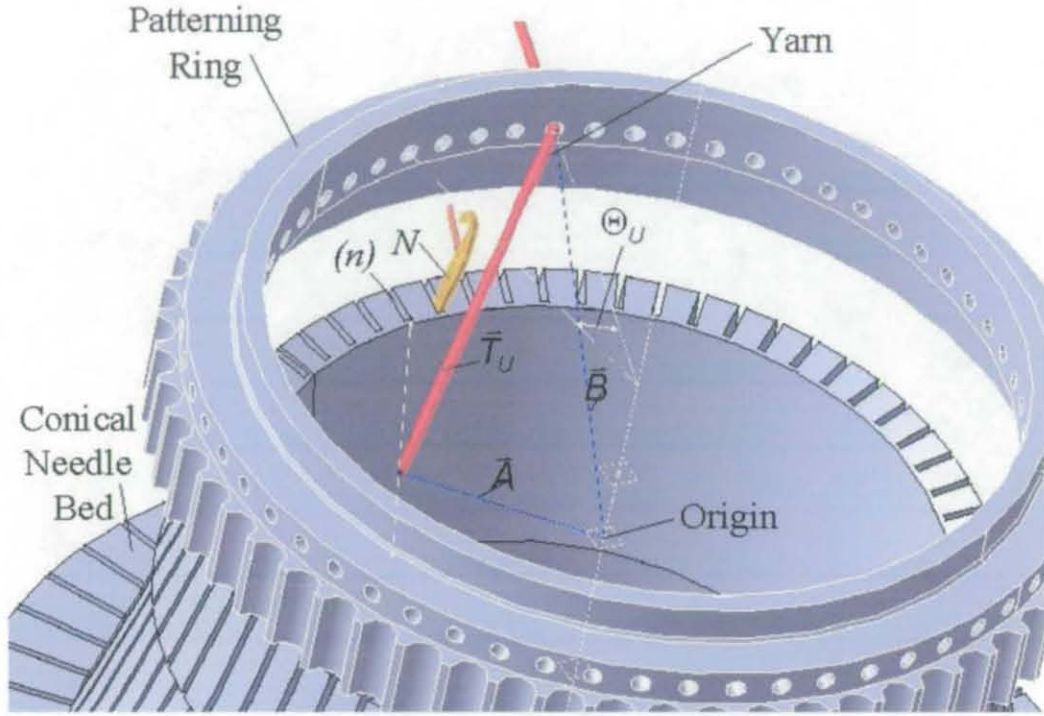


Figure 8-8. Yarn Vector Construction

Graphically, the thread vector \bar{T}_U can be described in terms of two vectors; \bar{A} from the origin the last stitch, and \bar{B} from the origin of the eyelet in the patterning ring (Figure 8-8);

$$\bar{T}_{U(N)} = (-\bar{A}) + \bar{B} \quad (8-1)$$

The thread vector will have components in x , y and z as Figure 8-9 illustrates. (The needle bed has been omitted for simplicity).

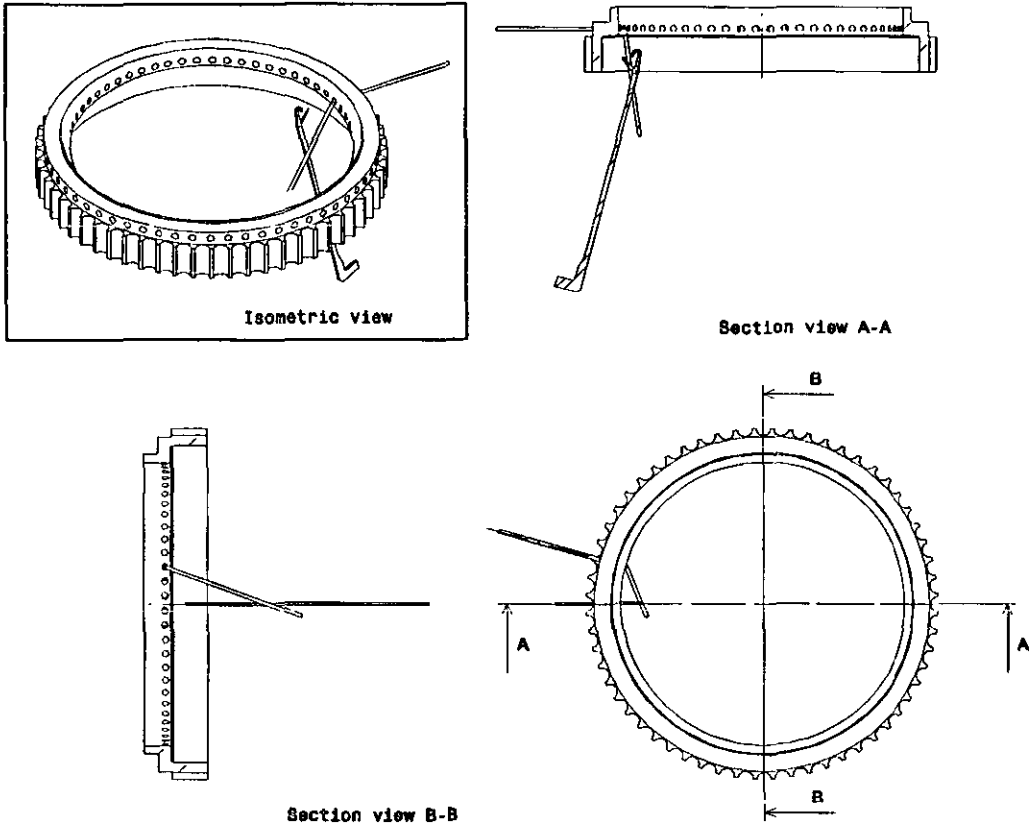


Figure 8-9. Thread Vector Projections.

Let n be the needle on which the last stitch was performed, and therefore $n = (N - U)$. The vectors \vec{A} and \vec{B} can be expressed as:

$$\vec{A} = R_V \hat{r} + \alpha_n n \hat{\theta} - s \hat{k}, \text{ or}$$

$$\vec{A} = (R_V \cdot \cos(\alpha_n n)) \hat{j} + R_V \sin(\alpha_n n) \hat{j} - s \hat{k}$$

(8-2)

$$\vec{B} = R_R \hat{r} + (\alpha_n n + \Theta_U) \hat{\theta} + H \hat{k}, \text{ or}$$

$$\vec{B} = R_R \cdot \cos(\alpha_n n + \Theta_U) \hat{j} + R_R \cdot \sin(\alpha_n n + \Theta_U) \hat{j} + H \hat{k}$$

(8-3)

\bar{T}_U becomes,

$$\begin{aligned}\bar{T}_U &= [R_R - R_V]\hat{j} + [\Theta_U]\hat{\theta} + [H + s]\hat{k}, \text{ or} \\ \bar{T}_U &= [R_R \cdot \cos(\alpha_n n + \Theta_U) - R_V \cos(\alpha_n n)]\hat{j} \\ &\quad + [R_R \cdot \sin(\alpha_n n + \Theta_U) - R_V \sin(\alpha_n n)]\hat{j} + [H + s]\hat{k}\end{aligned}\tag{8-4}$$

$$\bar{T}_U = [(R_R - R_V)\cos(\Theta_U)]\hat{j} + [(R_R - R_V)\sin(\Theta_U)]\hat{j} + [H + s]\hat{k}\tag{8-5}$$

The thread vector equation can be rewritten in parametric form, according to the following theorem;

A line in 3-dimensional space that passes through the point $P_0 (x_0, y_0, z_0)$ and is parallel to the non-zero vector $\bar{V} = \langle a, b, c \rangle = a\hat{i} + b\hat{j} + c\hat{k}$ has a parametric equation.

$$\begin{cases} x = x_0 + at, \\ y = y_0 + bt, \\ z = z_0 + ct \end{cases}\tag{8-6}$$

Using $(x_0, y_0, z_0) = (R_R \cos(\alpha_n n + \Theta_U), R_R \sin(\alpha_n n + \Theta_U), H)$ and (8-4) or (8-3) as \bar{V} ;

$$\begin{cases} x = R_R \cos(\alpha_n n + \Theta_U) + [R_R \cos(\alpha_n n + \Theta_U) - R_V \cos(\alpha_n n)] \cdot t, \\ y = R_R \sin(\alpha_n n + \Theta_U) + [R_R \sin(\alpha_n n + \Theta_U) - R_V \sin(\alpha_n n)] \cdot t, \\ z = H + [H + s] \cdot t \end{cases}\tag{8-7}$$

8.3.1.2 Target Needle Plane Equation

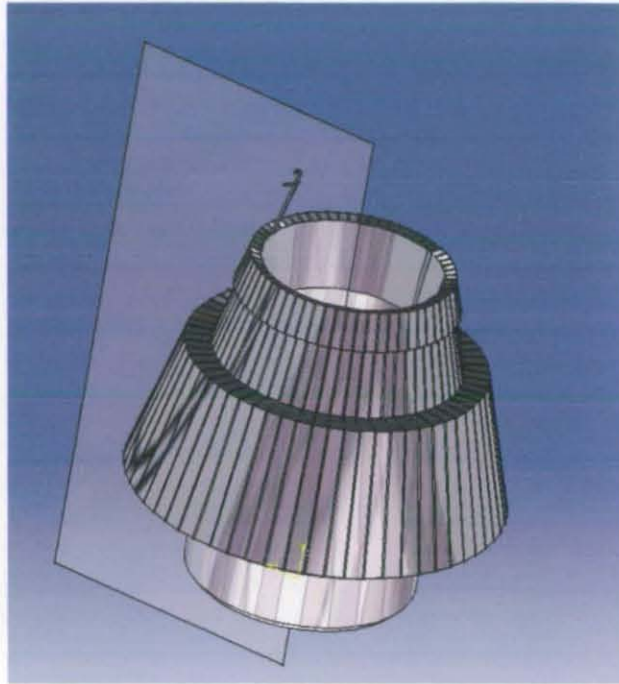


Figure 8-10. Needle Plane for Geometrical Analysis

Three non co-linear points are used to find the equation of the normal to the plane on which the target needle is moving (Figure 8-10), since,

- If P_1 , P_2 and P_3 , are non co-linear, but on the same plane.

$$\overline{P_1P_2} \times \overline{P_1P_3} \Rightarrow \text{Normal to the plane.}$$

- A plane in 3-dimensional space is uniquely determined by specifying a point in the plane and a vector perpendicular to the plane ('Normal Vector').

The plane of the target needle passes through the origin, and therefore $P_1 = (0,0,0)$. The two other points can be defined at the top of the verge ring the bottom of the verge ring or any point on the surface of the cone, on the path (trick) of the target needle. For convenience, the top and bottom of the verge where selected as P_2 and P_3 ;

$$P_2 = [R_v, (\alpha_n N), -s] \text{ in polar co-ordinates, or}$$

$$P_2 = [(R_V \cos(\alpha_n N), (R_V \sin(\alpha_n N)), -s] \text{ in Cartesian co-ordinates.} \quad (8-8)$$

$$P_3 = [R_N, (\alpha_n N), 0] \text{ in polar co-ordinates, or}$$

$$P_3 = [(R_N \cos(\alpha_n N), (R_N \sin(\alpha_n N)), 0] \text{ in Cartesian co-ordinates.} \quad (8-9)$$

The equation of a vector normal to the plane can be obtained by calculating $\overline{P_1 P_2} \times \overline{P_1 P_3}$;

$$\overline{P_1 P_2} \times \overline{P_1 P_3} = \begin{vmatrix} \hat{i} & \hat{j} & \hat{k} \\ R_V \cos(\alpha_n N) & R_V \sin(\alpha_n N) & -s \\ R_N \cos(\alpha_n N) & R_N \sin(\alpha_n N) & 0 \end{vmatrix} \quad (8-10)$$

$$\begin{aligned} \overline{P_1 P_2} \times \overline{P_1 P_3} &= (s \cdot R_N \sin(\alpha_n N))\hat{j} - (s \cdot R_N \cos(\alpha_n N))\hat{k} \\ &+ (R_N R_V \sin(\alpha_n N) \cos(\alpha_n N) - R_N R_V \sin(\alpha_n N) \cos(\alpha_n N))\hat{k} \end{aligned} \quad (8-11)$$

$$\overline{P_1 P_2} \times \overline{P_1 P_3} = (s \cdot R_N \sin(\alpha_n N))\hat{j} - (s \cdot R_N \cos(\alpha_n N))\hat{k} \quad (8-12)$$

The equation of the plane can be rewritten as

$$A_p(x-x_0) + B_p(y-y_0) + C_p(z-z_0) = 0 \quad (8-13)$$

Taking $P_0(x_0, y_0, z_0) = (0, 0, 0)$;

$$A_p \cdot x + B_p \cdot y + C_p \cdot z = 0 \quad (8-14)$$

$$sR_N \sin(\alpha_n N) \cdot x - sR_N \cos(\alpha_n N) \cdot y = 0 \quad (8-15)$$

8.3.1.3 Intersection Point

The intersection point between the needle plane and the thread vector can be defined as;

$$P_i \equiv (x_i, y_i, z_i) = \left. \begin{array}{l} x_i = x_0 + at_i \\ y_i = y_0 + bt_i \\ z_i = z_0 + ct_i \end{array} \right\} \quad (8-16)$$

where t_i can be found by substituting (x_i, y_i, z_i) equations onto the equation of the plane: equation (8-15).

Using the same notation for the coefficients in equations (8-13) and (8-6), and noting that the intersection point must comply with the equation of the plane;

$$\begin{aligned} A_p \cdot x_i + B_p \cdot y_i + C_p \cdot z_i &= 0 \\ \therefore A_p \cdot (x_0 + at_i) + B_p \cdot (y_0 + bt_i) + C_p \cdot (z_0 + ct_i) &= 0 \\ \therefore t_i &= \frac{-(A_p x_0 + B_p y_0 + C_p z_0)}{(A_p a + B_p b + C_p c)} \end{aligned} \quad (8-17)$$

We can now substitute the expression for t_i into equation (8-16)to find the co-ordinates of the intersection point;

$$P_i \equiv (x_i, y_i, z_i) = \left. \begin{array}{l} x_i = x_0 + a \left[\frac{-(A_p x_0 + B_p y_0 + C_p z_0)}{(A_p a + B_p b + C_p c)} \right] \\ y_i = y_0 + b \left[\frac{-(A_p x_0 + B_p y_0 + C_p z_0)}{(A_p a + B_p b + C_p c)} \right] \\ z_i = z_0 + c \left[\frac{-(A_p x_0 + B_p y_0 + C_p z_0)}{(A_p a + B_p b + C_p c)} \right] \end{array} \right\} \quad (8-18)$$

where;

$$\begin{aligned}
x_0 &= R_R \cos(\alpha_n n + \Theta_U), \\
y_0 &= R_R \sin(\alpha_n n + \Theta_U), \\
z_0 &= H, \\
a &= [R_R \cos(\alpha_n n + \Theta_U) - R_V \cos(\alpha_n n)], \\
b &= [R_R \sin(\alpha_n n + \Theta_U) - R_V \sin(\alpha_n n)], \\
c &= [H + s], \\
A_p &= sR_N \sin(\alpha_n N), \\
B_p &= -sR_N \cos(\alpha_n N); \text{ and,} \\
C_p &= 0.
\end{aligned}$$

Having found the equations defining the co-ordinates of the underlap intersection point, its suitability can only be determined if the equations of the lines representing the back of the needle and the 'Underlap Limit' are known.

The underlap-overlap combination is successful if $P_i \equiv (x_i, y_i, z_i)$ satisfies two inequalities indicating being under the underlap limit line and the line of the back of the needle.

8.3.2 Overlap

In the case of the underlap and overlap in opposite directions, the overlap movement is the less critical one, as the underlap has already ensured that the motion can be performed. When the overlap movement starts, the needles are at their highest position. As the ring starts to rotate in the opposite direction, the side of each needle will hold the thread.

In this case the overlap angle should only be sufficient to ensure that the thread has swung to the opposite side of the target needle.

8.4 Underlap and Overlap in the Same Direction

In the case where the underlap and overlap making a stitch are performed in the same direction, both shog motions can be treated as a single rotation of the ring by adding their amplitudes.

The intersection of the yarn vector after the compound shog with the plane on which the target needle moves (in this case not the same as the underlapping one) will define whether the complete motion is possible.

The conditions for a successful overlap are illustrated in Figure 8-11, where the needle is shown at its highest position just after the overlap has been performed.

Firstly, the yarn has to be collected as the needles are lowered, the overlap intersection must lie within the hook catchment area. This area extends from the needle stem to a line parallel to the needle and passing through the needle hook, as shown in Figure 8-11.

In addition, the yarn shog should place the yarn under the needle hook (and not brush the needle over the hook). A line perpendicular to the needle passing through the needle hook point represents this condition. The overlap intersection must lie under this line.

Finally, the latch must trap the yarn as the needle descends. Therefore the intersection point must occur within the area swept by the latch swing.

The permissible area for the overlap intersection is the intersection of the areas representing each of the three conditions described above to ensure a successful stitch.

As an approximation, the permissible area is defined in the model as a rectangular region on the target needle plane. The top of the rectangle is given by the z-coordinate of the needle hook point and the bottom by that of the latch spoon. See Figure 8-11.

The area between the top and bottom of the rectangle is defined as the height range while the area between the two sides of the rectangle is defined as the distance range.

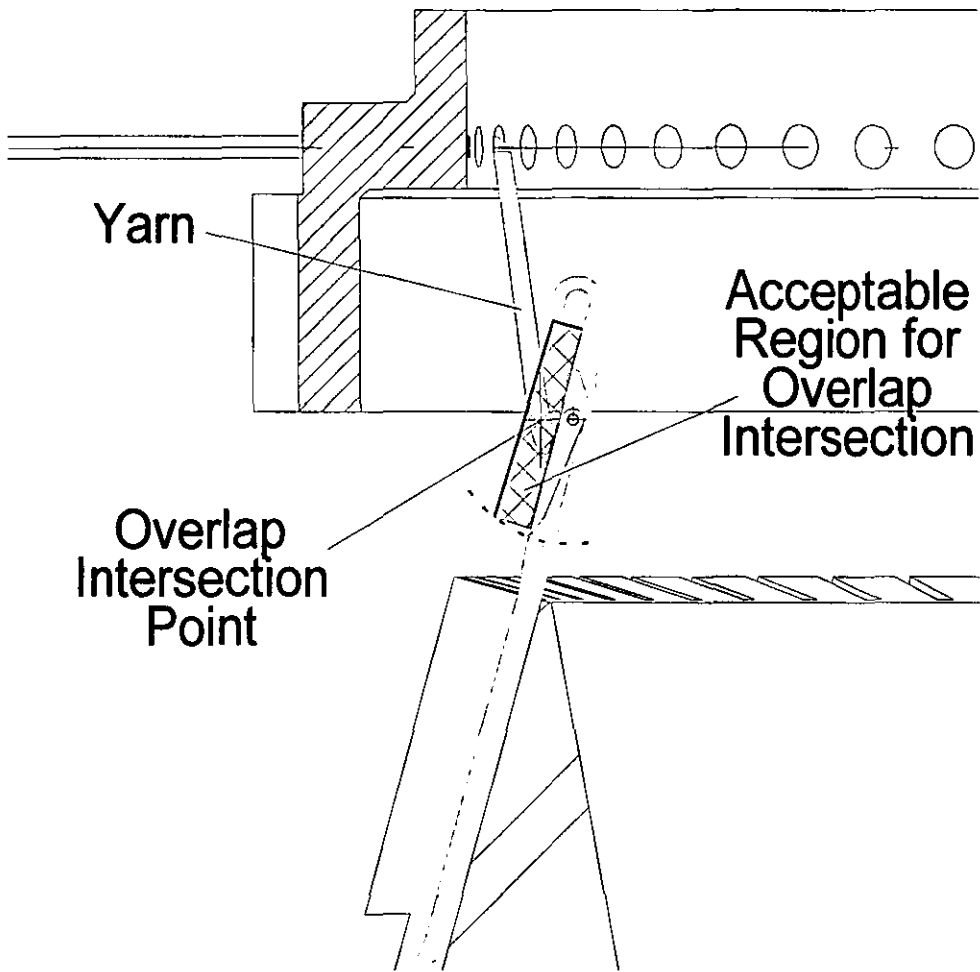


Figure 8-11. Acceptable Area Overlap Intersection

8.4.1 Overlap

The overlap motion begins after the needle has risen to its highest position and each thread is at either side of the overlap target needle (which is not the same target needle as that for the preceding underlap).

In this case the yarn will not wrap around the needle when the overlap is performed but it will merely be positioned under the overlap target needle hook.

For this reason, it can be modelled simply as a longer underlap; that is, the thread vector will be represented by equations (8-7), replacing Θ_U for an

extended angle ($\Theta_U + \Theta_{OL}$), where Θ_{OL} is the overlap portion of the angle rotated by the patterning ring. The plane with which the intersection is found is that of the overlap target needle which is $N \pm 1$ (depending on the direction of both underlap and overlap).

8.4.2 Underlap

Once the minimum valid overlap angle is found, the underlap angle will be the largest angle for which the underlap target needle (that is, the one adjacent to the overlap needle) can rise in front of the yarn. That is, the underlap intersection point is behind the vector representing the needle stem.

8.5 Shog Angle Calculation Algorithm

The algorithm developed to calculate shogging angles is the means of attaining the objective of forecasting the patterning capability of the patterning mechanism before committing to a specific design. The goal of the algorithm is to predict whether an underlap-overlap combination is possible for a mechanism with a given set of geometric parameters.

The process carried for each of the two main cases is described in the flowcharts of Figure 8-12 and Figure 8-13. As it can be seen from the flowchart, either branch of the flowchart will yield results for minimum overlap and underlap rotations or a message stating that the stitch cannot be completed using the parameters defined for the mechanism. The processes outlined in the flowchart are detailed in later sections of this paper.

This is an invaluable tool for the designer of patterning mechanisms, as they will know in advance whether the combination of underlap and overlap required could be performed by the mechanism designed. However, the goal of the model is not only to predict whether given combinations are possible once the design has been carried out, but also to provide the designer with the best values for the geometric parameters. A design can then be manufactured based on the suggested parameter values, in the knowledge that all the underlap-overlap combinations required will be attainable.

8.5.1 Underlap and Overlap in the Same Direction

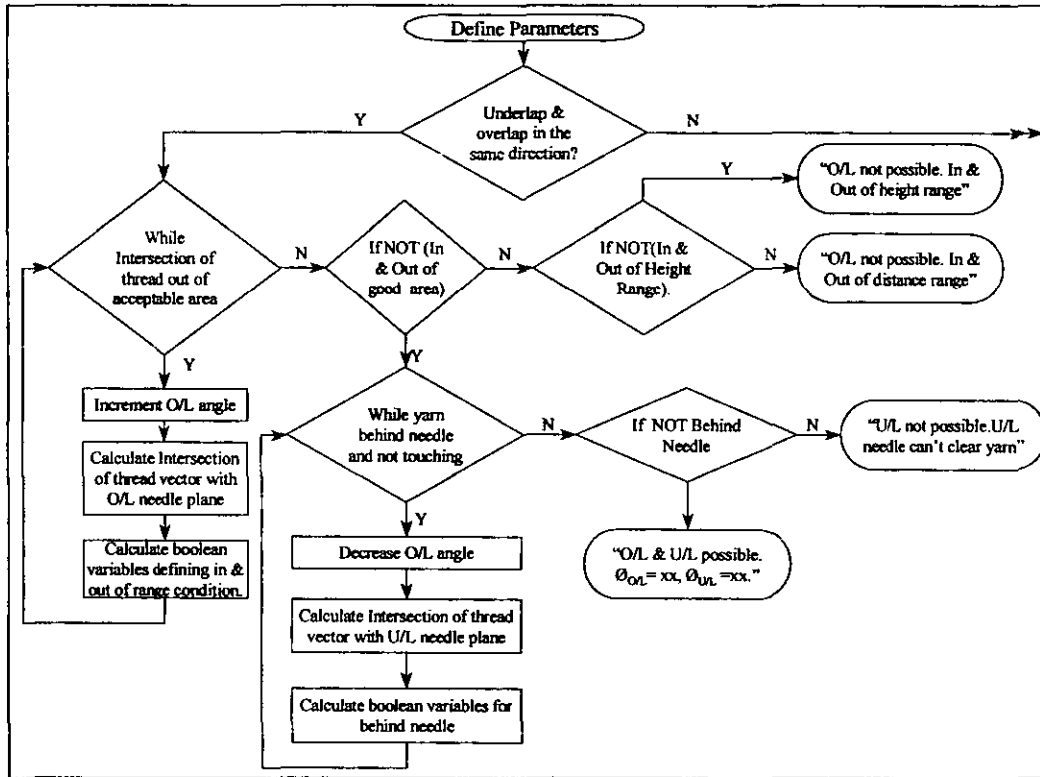


Figure 8-12. Flowchart for Overlap and Underlap in the same Direction

The algorithm flowchart to find the overlap and underlap angles is shown in Figure 8-12. After the designer has entered the geometric parameters, the overlap target needle plane, the equations of the lines surrounding the acceptable area are calculated as these will not change. The overlap angle is initialised as zero and will be incremented on each loop (in the overlapping direction) while the overlap intersection is not within the acceptable area shown in Figure 8-11. This ensures that the overlap angle found is the minimum angle that will provide with an acceptable underlap-overlap combination.

Every time the angle is incremented a thread vector is defined for the new angle, and with this, an intersection point will be calculated. At the beginning of the next iteration, this point is evaluated on the set of inequalities that

define the acceptable area, in order to decide whether or not to enter a new loop.

The conditions of the iterative loop ensure that the intersection point does not enter and exit either the height or the distance range (as defined in section 8.4), as that would imply that the overlap is not possible.

To illustrate this point, let the overlap intersection point found for Θ_1 be within the distance range but outside and above the height range. The next iteration, when the ring has rotated $\Theta_1 + \delta$ gives a new intersection point, nearer the needle stem but still above the height range. If, after i iterations, the intersection point occurs outside of both ranges (i.e. it has entered and exited the distance range), the overlap will not be possible because the yarn will not re-enter the distance range.

Should this happen, the algorithm ends by recording that the overlap is not possible and the cause of the failure to find one.

If a satisfactory overlap intersection point is found on the other hand, the overlap angle is recorded and an associated underlap angle is found by another iterative process.

In order to consider the underlap part of the movement, a new target needle plane is calculated using the underlap needle (that is, the one adjacent to the overlap target needle).

The underlap angle is initialised as $\Theta_U = \Theta_O$, the successful overlap found, and decreased on each iteration. In this case there is only one condition for a satisfactory underlap intersection, namely that it lies behind the needle stem.

If the underlap angle reaches the underlap target needle angle (i.e. $\Theta_U = \alpha_N \cdot N$) and the intersection point is not behind the needle, then the underlap cannot be performed. This can occur especially in small gauge machines, where the spacing of the needles does not allow a yarn to be laid behind a needle and in front of the adjacent one.

8.5.2 Underlap and Overlap in Opposite Directions

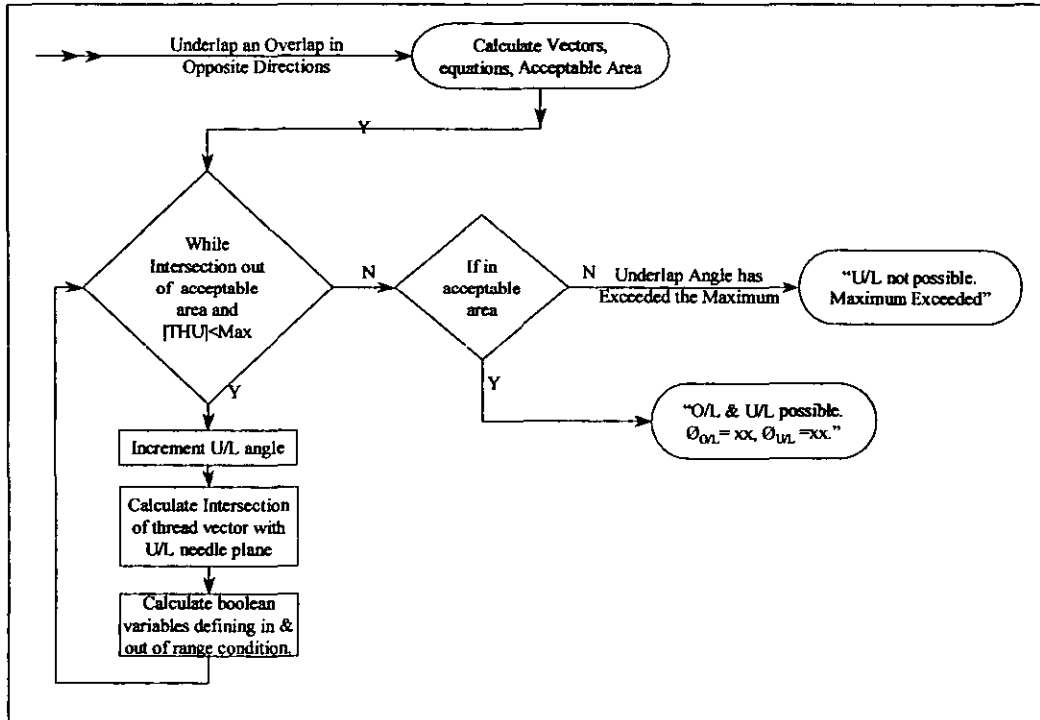


Figure 8-13. Flowchart for Overlap and Underlap in opposite Directions

The algorithm flowchart to find the overlap and underlap angles for this case is shown in Figure 8-13. After the designer has entered the geometric parameters, the underlap target needle plane, and the equations of the lines surrounding the acceptable area are calculated, as these will not change. The overlap angle is initialised as the angle required to place the yarn exactly above the target needle ($\Theta_U = \alpha_N \cdot N$), and will be incremented on each loop (in the underlapping direction) while the underlap intersection is not within the acceptable area shown in Figure 8-7. This ensures that the underlap angle found is the minimum angle that will provide an acceptable underlap-overlap combination.

As in the previous case, every time the angle is incremented a thread vector is defined for the new angle and with it an intersection point will be calculated. At the beginning of the next iteration, this point is evaluated on

the set of inequalities that define the acceptable area, in order to decide whether or not to enter a new loop.

Again, only if a suitable underlapping angle is found, its value is recorded. The associated overlap angle is not calculated because, as explained in section 8.3, in this case the existence of a suitable underlapping angle is sufficient to ensure that the underlap-overlap combination is possible.

Algorithm Execution

A program was written using the Maple Mathematics software package to reflect the algorithm explained above. The Program code is enclosed in Appendix G. After inputting all of the geometric parameters. Its output will be a set of overlap and underlap angles, or a message explaining which motion is not possible to perform and a reason why.

It is clear that the number of variables involved, make it impossible for us to analyse each and every one. Therefore, some variables must be selected by experience or decided upon constraints and availability of parts (e.g. the dimensions of the needle). However, variables such as the cone taper and the position and diameter of the patterning rings, can make a substantial difference on the maximum shogging angle, which is ultimately what needs to be optimised in the mechanism.

The design process of the knitting head of a circular warp knitting machine should mainly depend on the fabrics intended to be manufactured on it. The size and material of the yarns to be used largely define the needle types and gauges that can be used. On the other hand, the size and tightness of the fabric approximately define the cone diameter (except in the case of nets) and the machine gauge respectively.

The fabric specification determines the maximum number of needles to underlap in a single motion. The model explained in the sections above provides with a means of deciding on selected geometric parameters involved.

The machine designer can predict if the fabrics specified could be manufactured and change the knitting head design accordingly. Potentially, the model and the program can reduce the cost of re-work substantially, as the lack of a geometric model can result in a incorrect design and consequently, loss of time and money.

8.6 Circular Warp Knitting Case

The algorithm was used to analyse the effect of varying the cone taper angle on the range of fabrics that could be produced with the machine. The bending force applied to the strengthening inserts will increase as the cone taper angle increases. Therefore, the optimum design would be the one that allows the underlap-overlap combinations required for the fabrics intended to be produced, using smallest cone taper angle.

The design of a 3" (76.2mm) diameter circular warp knitting machine head with 60 needles was used for the study. The needle specification was defined by the types of yarns to be used; Groz Beckert Hofa 71.80.G01.

The geometric parameters used can be summarised as follows;

- $R_R = 1.595$ inches (40.51mm).
- $R_V = 1.347$ inches (34.21mm).
- $R_N = 1.492$ inches (37.90mm).
- $\alpha_n = 6^\circ$.
- $PL = 0.866$ inches (22.01mm).
- $s = 0.565$ inches (14.35mm).
- $H = 0.813$ inches (20.65mm).

The objective of the case study is to analyse the effect of varying the cone taper angle on the possible underlap-overlap (U-O) combinations. Table 8-1 illustrates the results for U-O combinations in the same direction, which is generally more difficult to achieve than the equivalent U-O in opposite directions.

Table 8-1. Effect of Cone Taper on Possible U-O Combinations

Cone Taper (°) $= 2 \cdot \beta$	Underlap-Overlap Set			
	Underlap (No. of Needles)	Set Possible	Overlap Angle (°) /Reason	Underlap Angle (°) /Reason
0	1	✓	12.6	10.8
	2	×	U/L needle can't clear yarn.	
5	1	✓	14.3	13.2
	2	×	U/L needle can't clear yarn.	
15	1	✓	17.2	16.0
	2	✓	24.6	23.5
	3	×	U/L needle can't clear yarn.	
25	1	✓	18.9	17.8
	2	✓	27.5	25.8
	3	✓	35.0	33.2
	4	✓	41.8	40.7
	5	×	U/L needle can't clear yarn.	
30	1	✓	19.5	18.3
	2	✓	28.1	26.9
	3	✓	36.1	35.0
	4	✓	43.5	41.8
	5	×	U/L needle can't clear yarn.	
45	1	✓	Entered and Exited Distance Range	
	2	✓		
	3	✓	39.0	37.8
	4	✓	47.0	45.8
	5	✓	54.4	52.7
	6	×	U/L needle can't clear yarn.	
60	1	×	Entered and Exited Distance	

	2	x	Range	
	3	x		
	4	x		
	5	✓	58.4	56.7
	6	x	U/L needle can't clear yarn	
	75	1	x	Entered and Exited Distance Range
2		x		
3		x		
4		x		
5		x		
6		x		

It is seen from Table 8-1 that the effect of the cone taper angle is not straightforward. Although for smaller taper angles, an increase in the taper leads to longer underlaps being possible, once the taper reaches 45 degrees, it is the smaller underlaps that become impossible to perform. Moreover, once the taper angle reaches 75 degrees, no underlap is possible.

From these results, the designer can safely conclude that the taper used for the cone should be less than 45 degrees. It would be very difficult to predict this outcome without a geometric model.

On the other hand, the overlap and underlap angles required for a single-needle underlap increase as the cone taper increases. An increase in the underlap angle implies a reduction of speed in the patterning mechanism (as the ring will have to travel further). Therefore, the designer of a circular warp knitting machine to be used for manufacturing fabrics requiring up to two-needle underlaps will probably choose to design the cone with a 15 degree taper. Smaller cone taper angles are desirable from the kinetics considerations of the needle support plate drive and its effects on the forces exerted on the strengthening inserts.

Similar analyses can be applied to other design variables. For instance, for a machine equipped with several patterning rings, each ring will be positioned

at a different height; it is therefore useful to know the effect of varying the height and diameter of the different rings on the underlapping possibilities before being committed to a given design.

8.7 Conclusions

The geometrical relationships between the patterning and knitting mechanisms in a circular warp knitting machine are not easy to visualise. The geometrical model described here is an invaluable aid for the designer to maximise the machine's performance.

The circular warp knitting machine case study shows how the model described here can be used to alter design parameters according to the fabric intended to be produced.

The case study has also demonstrated that it is advantageous to use a tricked cone rather than a tricked cylinder as the needle bed in circular warp knitting machines, because the patterning capabilities are increased for these particular geometric parameters up to a cone taper angle of about 30°. It has also shown how the effect of increasing the cone taper angle on the patterning capabilities of the machine becomes detrimental for angles larger than 45°. This proves that there is an optimum value for a given set of geometric parameters and that the optimum value can be found using the algorithm proposed.

Chapter 9. Conclusions and Suggestions for Future Work

9.1 Achievements

This research has been successful in its main aim of developing an innovative warp knitting machine with commercial potential to produce tubular fabrics, by using modern approaches to design methodology and mechanisms analysis and synthesis.

Once the concepts were proven, the mechanical version of the circular warp knitting machine was manufactured (Figure 9-1) and sold to a packaging net producer, and the electronically controlled version was also manufactured and exhibited at the 1999 ITMA (International Textile Manufacturing Association) exhibition in Paris (Figure 9-2).

The main aspects of the design discussed in this thesis are those relating to the knitting and patterning mechanisms, as they are clearly the systems critical to the efficient performance of the machine. The main innovation in relation to the knitting mechanism is the implementation of a solution using a conical needle bed, which avoids the need for the swinging action of traditional flat-bed warp knitting machines. This concept was designed, implemented and tested during the course of this research. The theory and analysis supporting the design decisions have been developed.

Initially, the main design concepts were selected and the direction of the research was identified. The methodology used to conceive an initial Product Design Specification (PDS) has been guided by the design requirements. It is clear from the research and the PDS database that the two critical mechanisms in a circular warp knitting machine are the knitting and patterning ones. This has clearly defined the direction of the rest of the research.

The cam-follower concept to reciprocate the needles when using a conical needle-bed has been designed, tested and analysed in detail. The kinetic consequences of this design have been theoretically analysed. Finally the actual performance of the mechanism through the experimental measurement of its vibration and cam displacement has also been demonstrated. The experimental work has clearly demonstrated that static unbalance, dynamic unbalance and elasticity of the body and the cam profile are all major factors affecting the performance of the machine. In relation to the cam profile, the polynomial cam has been demonstrated to produce better results due to the continuity for three of the displacement derivatives.

Two solutions to the problem of designing a patterning mechanism for a circular warp knitting machine have been implemented. The all mechanical solution using an enclosed cam-track has represented significant improvements on the known existing mechanical design concepts. However, the patterning capability is limited by physical cam size.

The servo-controlled mechatronic patterning mechanism design, on the other hand, is an entirely new concept. The novelty of this design lies in its simplicity and compactness based on the appropriate selection of servomotors able to drive the patterning rings directly. This space-efficient design avoids the traditional transformation of translation to rotation motion. It requires very fast responses and uses AC brushless servomotors to control three patterning rings via a belt and pulley arrangement. Moreover, the electronic control allows for greater flexibility in the pattern design; the length of the patterns is only constrained by the memory capacity of the motion controller connected to the servomotors.

A mathematical model of the pattern creation process has been presented to allow the designer to set selected geometric constraints of the patterning mechanism according to the fabric patterns required. The circular warp knitting machine case study has clearly illustrated the advantages of the use of a tricked cone rather than a tricked cylinder as the needle bed, since the patterning capabilities are increased. The model of the pattern creation process has proved both the effectiveness of the conical needle bed and

provided a means to ensure that the design of the two mechanisms is according to the fabrics required by the user.

In addition to the achievements related to novel design concepts, the research has also successfully contributed to areas of engineering not confined to warp knitting machine design; firstly, a novel cam optimisation procedure has been proposed and secondly, a new method for the selection of servomotors has been suggested.

A method of synthesising a cam profile based on the use of Piecewise Polynomials together with an optimisation technique has been developed. Special cases and limitations have been discussed and illustrated, making the procedure complete and systematic for any design requirements. The method has also been successfully applied to the design of the circular warp knitting machine cam.

A new servomotor selection procedure, based on minimising the power required to perform the fastest motion required by the application, ensures the selection of the smallest servomotor suitable for the application. This is very significant as it minimises the cost of the system: servomotor power capabilities determine its frame size, which in turn governs its cost.

In summary, the major achievements of the research and technological developments reported in this thesis are:

- A novel tricked-cone needle-bed concept to eliminate the need for the swinging motion of the guide bars.
- Servomotor driven patterning mechanism with almost infinite patterning capability.
- Mathematical modelling of pattern creation for circular warp knitting machine with circular yarn guide rings.
- Cam profile design optimisation using piecewise polynomials.
- A methodology to select most suitable and economic servomotor for a given application.
- Implementation of both, a mechanical and a mechatronic prototype machines.

9.2 Suggestions for Future Work

9.2.1 Fabric Development

The natural continuation of this research would be to investigate further the possibilities that the new design has for fabric development; this was beyond the scope of this research.

Warp knitting (for both circular and flat-bed machines) would benefit from more research in the loop formation process. The modelling of the loops will be the starting point for a pattern recognition system, essential for the advancement of new fabric design and fabric analysis. Research in this area has only been carried out for weft knitting fabrics, whose structure tends to be more consistent because the loops' shape does not change significantly for different fabric structures and is therefore easier to recognise digitally.

Warp knitting loops distort according to the fabric structure, the number of threads in the warp, the relative elasticity of the different yarns used, etc. Modelling of the loops of a warp knitting fabric will require a thorough understanding of the behaviour of the different yarns under tension and when twisted, to predict the relative positions they will take when the fabric is relaxed. However, while this tool does not exist, fabric design will continue to depend on manual trials.

9.2.2 Electronic Control of Patterning

The mathematical model presented in Chapter 8 was used to show the effect of varying some geometrical constraints on the patterning capabilities. It can also be used to predict the angles required to produce a given fabric structure. Although this has been achieved to some extent, manual fine-tuning has been necessary (due to the elasticity and mobility of the yarns) to ensure the fabric will be produced without faults. This function can be improved with a more thorough understanding of the yarns behaviour, ideally to the point when a fabric designer only needs to provide the machine with the yarn characteristics and the chain stitch notation of the fabric structure, and the machine calculates the movements of the patterning rings.

9.2.3 Cam Design

The development of an optimisation technique for the design of a cam profile described in Chapter 6 stopped short of the manufacture of the cam with the profile proposed for the knitting case. The manufacture of a cam optimised by the method put forward would be an important step in the practical confirmation of the theory presented.

In order to further the research started here in the field of cam profile design, profiles manufactured before and after the optimisation could be tested in term of the vibration they create in a given mechanism.

9.2.4 Warp Knitting Machine Design

In relation to the design concepts, this research can be seen as the starting point of a new category of warp knitting machines which can evolve in different directions;

Firstly, as said in earlier chapters, the design of the knitting mechanism would benefit from the addition of phased knitting heads. One of the main causes of vibration in the machines manufactured is the unbalanced reciprocating load. Several measures, explained in Chapter 5, were taken to reduce the vibration. However, it was clear that it is impossible to balance all the dynamic forces acting on a knitting mechanism with a single knitting head. An appropriate continuation of this research would be to analyse and test the dynamic behaviour of circular warp knitting machines with multiple knitting heads, whose reciprocation is not simultaneous, but phased at a given cam rotation angle. In this way, one head can eliminate some of the rotating forces created when balancing the reciprocating load of another.

Secondly, depending on the requirements of the fabrics, combinations of mechanical and electronic patterning rings could be investigated as a means to reduce the cost but not the patterning capabilities. The mechanical rings could be used to knit common ground structures, while the electronic rings would overlay elaborate designs.

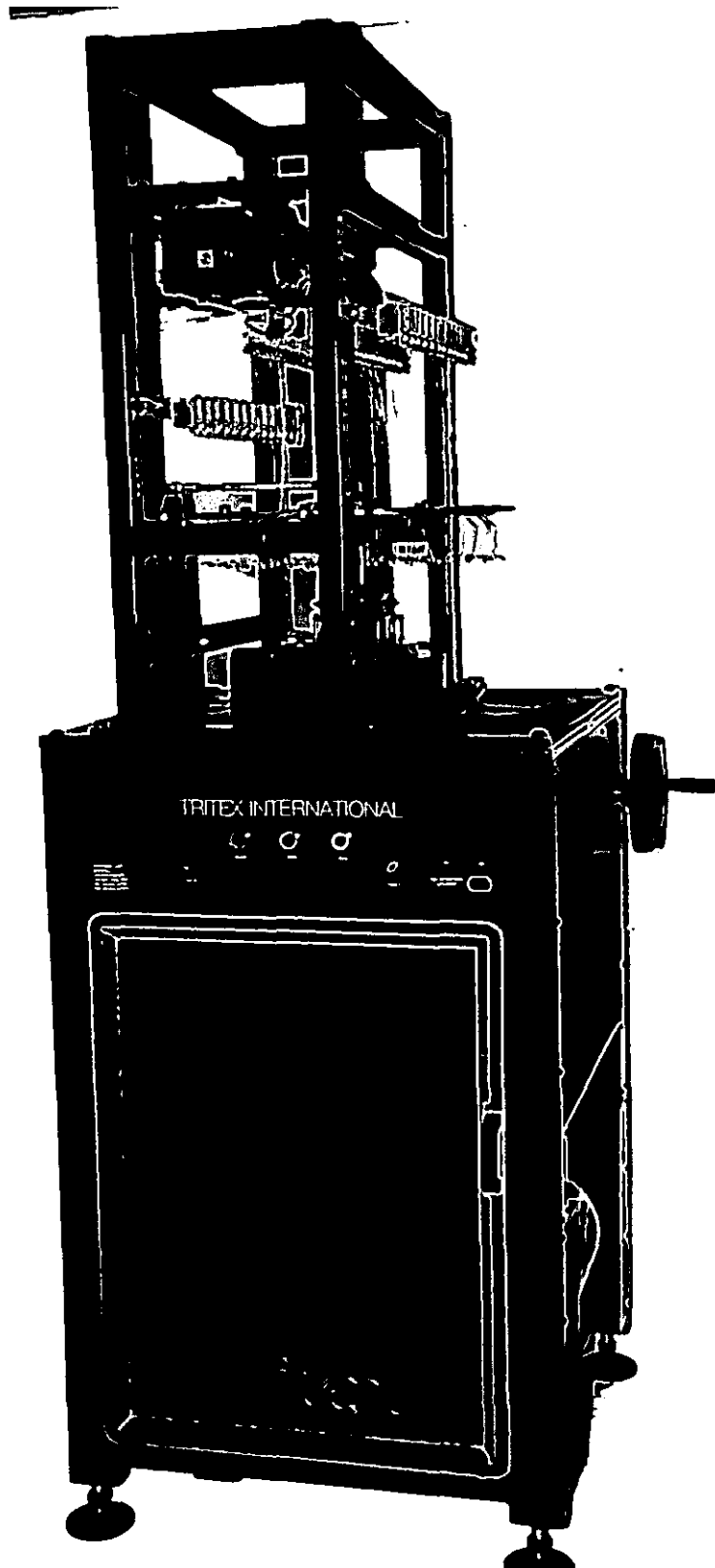


Figure 9-1. Mechanical Patterning Circular Warp Knitting Machine

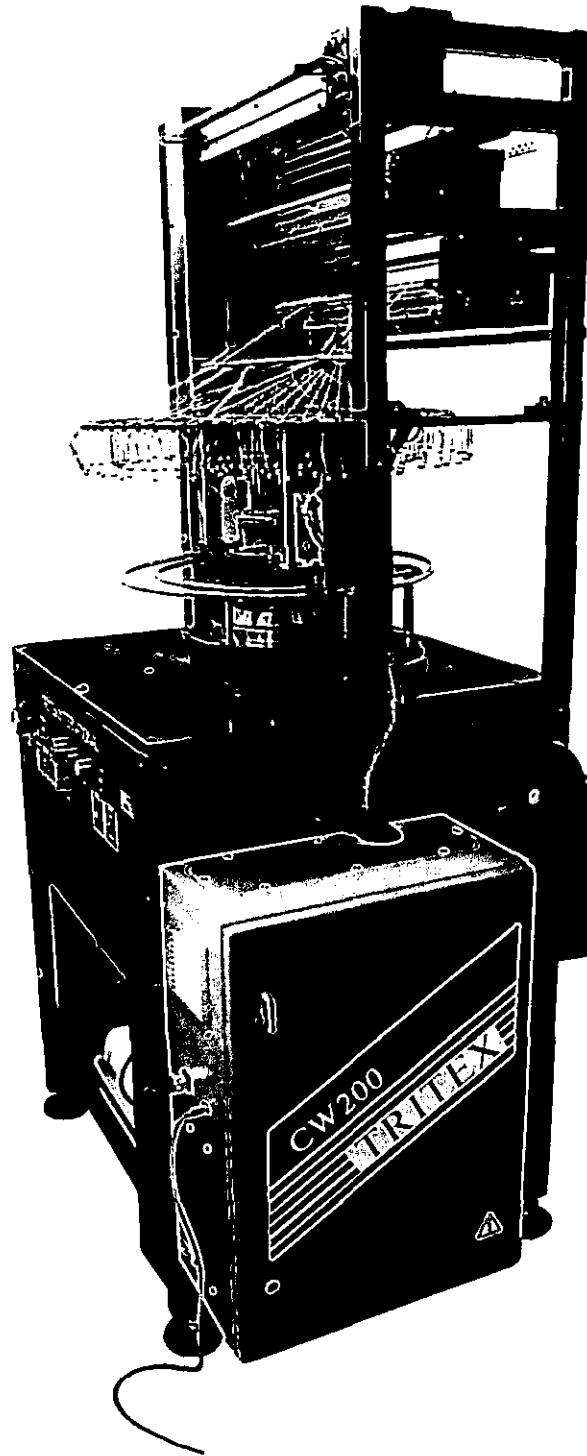


Figure 9-2. Electronically Controlled Circular Warp Knitting Machine

References

- ¹ RAZ S., *Warp Knitting Production*, 1987, Melliand Textilberichte GmbH, Heidelberg, Germany.
- ² WRAY G. R., *Developments in Textile Machinery*, The Chartered Mechanical Engineer, Sept 1973, Volume 20, No 8.
- ³ ANAND, S. *Contributions of Knitting to Current and Future Developments in Technical Textiles*. May 1988. Industrial, Technical and Engineering Textiles Group. The Textile Institute. Inaugural Conference, Manchester, UK
- ⁴ EUROSTAT Intra and Extra European Union Statistics (94-95)
- ⁵ REICHMAN C. *Advanced Knitting Principles*. 1964 National Knitted Outerwear Association. New Jersey, USA.
- ⁶ GROSBERG P., *An Introduction to Textile Mechanisms*, 1968, Ernest Benn Ltd., London, UK.
- ⁷ PALING D. *Warp Knitting Technology*. 1965. Columbine Press (Publishers) Ltd., Manchester, UK, Second Edition.
- ⁸ REISFELD A., *Warp Knitting Engineering*, 1966, National Knitted Outerwear Association, U.S.A.
- ⁹ SPENCER, D.J., *Knitting Technology*, Second edition, 1989, Pergamon Press, UK.
- ¹⁰ LYON, R.H., MALININ, L.M. (1995) 'Needle Fatigue Analysis For High-Speed Knitting Machines', *Design Engineering* Vol. 83, Design Engineering Technical Conferences, Volume 2, ASME 1995.
- ¹¹ SMITH D.E., BURNS N.D. & WRAY G.R., "The frictional Forces between yarns and weft knitting elements". *Journal of the Textile Institute*. Volume 65. No. 7. July 1974.
- ¹² WRAY G.R. and BURNS N.D., "Dynamic Forces in Weft Knitting. Part III: Yarn Tensions During the Loop Forming Process". *Journal of the Textile Institute*. Volume 67. No. 5. May 1976.
- ¹³ VENKATRAJ, R.(1997) 'Double Needle Bar Warp Knitted Patterns', *The Indian Textile Journal* (March):

-
- ¹⁴ MARY, C., MAROIS, Y., KING, M.W. et al. (1997) 'In Vitro And In Vivo Studies Of A Polyester Arterial Prosthesis With A Warp-Knitted Sharkskin Structure', *Journal Of Biomedical Materials Research*, (June 15), Vol. 35, Part 4, Pp 459-72
- ¹⁵ ANAND, S. "New Developments in Warp Knitted Elastic Fabrics". Karl Mayer Textile Machinery Co. 1991.
- ¹⁶ ANAND, S., "Warp Knitted Structures in Composites" Bolton Institute of Higher Education, Bolton, UK.
- ¹⁷ ANAND, S. "Karl Mayer Warp Knitting Equipment at Itma'95 in Milan". Bolton Institute of Higher Education, Bolton, UK.
- ¹⁸ DAVID RIGBY ASSOCIATES (1997), *The World Technical Textile Industry and its Markets. Propects to 2005.*, Messe Frankfurt Gmbh, Germany.
- ¹⁹ PORAT, I., GREENWOOD, A., EREN, R. ROY, A.K. (1994) 'Development Of Hybrid Type Warp Let-Off Systems For Weaving And Warp Knitting', *Indian Journal Of Fibre & Textile Research*, Vol. 19, (September), Pp 114-124.
- ²⁰ XUNWEI, F., GUANGTING, HAN, (1993) 'Optimal Setting-Up Of Knitting Elements And Its Effect On Tension Variation', *Journal Of China Textile University - English Edition-*, (September), Vol. 10, Part 3, Pp. 23-27.
- ²¹ ENDOU, Y., YAMASHITA N., KAWASHIMA, Y., (1994) ' Control Of Yarn Tension And Yarn Speed In Circular Knitting Machine', *Journal Of The Textile Machinery Society Of Japan*, (August), Vol. 47, Part 8, Pp. T205-9.
- ²² KANNON, W.R., DIAS, T. and XIE, P. "A Novel Positive Yarn-feed System for Flat-bed Knitting Machines", *The Journal of the Textile Institute*, Part 3, 2000. Textile Institute, Manchester, UK.
- ²³ HALLOS and SUN "The Analysis and Comparisons of Three Prediction Methods for Run-in in Raschel Warp Knitting". *The journal of the Textile Institute*. Volume 88. 1997. Part 1: Fibre Science and Textile Technology. Number 3. The Textile Institute, Manchester, UK.
- ²⁴ ZHUO, N.J., LEAF, G.A.V. and HARLOCK, S.C. "The Geometry of Weft-Inserted Warp-Knitted Fabrics. Part I: Models of the Structures". *The journal of the Textile Institute*. Volume 82. 1991
The Textile Institute, Manchester, UK
- ²⁵ ZHUO, N.J., LEAF, G.A.V. and HARLOCK, S.C., "The Geometry of Weft-Inserted Warp-Knitted Fabrics. Part II: Experimental Validation of the theoretical Models". *The journal of the Textile Institute*. Volume 82. 1991. The Textile Institute, Manchester, UK
-

-
- ²⁶ ROY, A. K., PORAT, I. and GROSBERG, P. "Reduction of Within-cycle Tension Variations in Warp Knitting". The journal of the Textile Institute. Volume 86. 1995. The Textile Institute, Manchester, UK.
- ²⁷ GRISHANOV, S.A., CASSIDY, T. and SPENCER, D. J., (1996) 'Loop Formation. A Mathematical Model Of Loop Forming On The Knitting Machine', *Textile Horizons*, (February) Vol. 16, Part 1.
- ²⁸ MIYAZAKI, T., SHIMAJIRI, Y., YAMADA, M., SEKI, H., and ITOH, H., (1995), 'A Knitting Pattern Recognition And Stitch Symbol Generating System For Knit Designing', *Computers And Industrial Engineering*. (September) Vol. 29, Part 1-4, Pp. 669 - 673.
- ²⁹ DEMIROZ, A. and DIAS, T. "A Study of the Graphical Representation of Plain Knitted Structures. Part I: Stitch Model for the Graphical Representation of Plain Knitted Structures" The Journal of the Textile Institute, 2000, 91 Part 1, No. 4. Textile Institute, Manchester, UK.
- ³⁰ *International Textile Bulletin. Yarn And Fabric Forming*, (1994 - 2nd Quarter), Vol. 40, Part 2, Pp. 61-68. Based On A Paper Given By Hans-Joachim Stoke On 23.3.94 At The University Of Textiles, Shanghai, China.
- ³¹ BUGAO XU, "Identifying Fabric Structures with Fast Fourier Transform Techniques." *Textile Research Journal*. Volume 66. 1996.
- ³² POURDEYHIMI, B., RAMANATHAN, D and DENT, R. "Measuring Fiber orientation in Nonwovens. Part 1. Simulation". *Textile Research Journal*. Volume 66. 1996.
- ³³ I-SHOU TSAI, CHUNG-HUA LIN and JENG-JONG LIN. "Applying an Artificial Neural Network to Pattern Recognition in Fabric Defects". *Textile Research Journal*. Volume 65. 1995.
- ³⁴ SEEGER, M., VOGEL, C., HERRMANN, U., SCHAFFER, W., (1996) 'Speed Meter and Measurement on Thread Velocity of Warp Knitting Machines', *International Textile Bulletin - Yarn And Fabric Forming*, 3rd Quarter, Pp. 36-40.
- ³⁵ BORENSTEIN M., *Rundstrickmaschine*, European Patent Application, 0 200 094, Filed 05.11.86, Tel-Aviv, Israel.
- ³⁶ VYACHESLAVOVICH RAGOSA, I., *Circular Warp Knitting Machine*, UK Patent Application 2 039 544 A, Filled 20 November 1990.
- ³⁷ European Patent Application EP 0 511 580. LIBA MASCHINENFABRIK GMBH. November 4, 1992. Germany.
- ³⁸ UK Patent Application No. GB 2 290 310 A. KARL MAYER TEXTILMASCHINENFABRIK GMBH. May 1995. Obertshausen, Germany.
-

-
- ³⁹ European Patent Application No. EP 0583631 A1. KARL MAYER TEXTILMASCHINENFABRIK GMBH. February 23, 1994. Germany.
- ⁴⁰ World Patent Application No. WO 9504179 A1. NIPPON MAYER CO. February 9, 1995. Nosaka, Japan.
- ⁴¹ European Patent Application EP 0 457 322. LIBA MASCHINENFABRIK GMBH. November 21, 1991. Germany.
- ⁴² European Patent Application EP 0 457 323. LIBA MASCHINENFABRIK GMBH. November 21, 1991. Germany.
- ⁴³ European Patent Application EP 0 561 710 A1. LABOUREAU, JACQUES-PHILIPPE. September 22, 1993. France.
- ⁴⁴ European Patent Application EP 0 630 997 A1. MARUMIYA SHOKO KABUSHIKI KAISHA. December 28, 1994. Japan.
- ⁴⁵ World Patent Application WO 9424510 A1. BARRACUDA TECHNOLOGIES AB. October 27, 1997.
- ⁴⁶ World Patent Application WO 9504178 A1. LOHMANN GMBH & CO. February 9, 1995. Austria.
- ⁴⁷ European Patent Application EP 0 474 660. MORTON, PETER. March 18, 1992. Great Britain.
- ⁴⁸ SHIGLEY, J.M. & UICKER, J.J., *Theory of Machines and Mechanisms*, McGraw-Hill Book Co, USA, 1989.
- ⁴⁹ ERDMAN, A.G. & SANDOR G.N., *Mechanism Design. Analysis and Synthesis*. Second Edition, Prentice Hall, 1991.
- ⁵⁰ DE SILVA, CLARENCE W., *Vibration: Fundamentals and Practice*, CRC Press, Washington, 1999.
- ⁵¹ SHIGLEY, J.E. and UICKER, J.J. *Theory of Machines and Mechanisms*. 1st Spanish Edition, Mexico: McGraw-Hill, 1983.
- ⁵² FAROUKI, R.T. and MANJUNATHAIAH, J., 'Design of Rational Cam Profiles with Pythagorean-hodograph Curves', *Mechanism and Machine Theory*, Vol 33, Issue 6, August 1998, pp 669-682.
- ⁵³ YU, Q. and LEE, H. P., 'Size optimisation of cam mechanisms with translating roller followers', *Proceedings of the Institute of Mechanical Engineers*, Vol. 212 Part C, (1998), pp. 381-386, IMechE.
- ⁵⁴ WANG, L.T. and YANG, Y. 'Computer Aided Design of Cam Motion Programs', *Computers in Industry*, 28 (1996) 151-161, Elsevier Science Ltd.

-
- ⁵⁵ YAO, Y. et al, 'Motion control of Cam Mechanisms', *Mechanisms and Machine Theory*, Volume 35, Issue 4, April 2000, pp 593-607. Elsevier Science Ltd.
- ⁵⁶ KYRALA, A. *Theoretical Physics: Applications of Vectors, Matrices, Tensors and Quaternions*. W.B. Saunders Company, London, 1967. Page. 35.
- ⁵⁷ BORENSTEIN M (1986), *Rundstrickmaschine*, *European Patent*, Pat No. 0 200 094, Filed 05.11.1986 Tel Aviv, Israel.
- ⁵⁸ RAGOSA I VYACHESLAVOVICH (1990), *Circular Warp Knitting Machine*, UK Patent, No. 2 039 544 A, 20 November, 1990.
- ⁵⁹ BORENSTEIN M (1986), *Rundstrickmaschine*, *European Patent*, Pat No. 0 200 094, Filed 05.11.1986 Tel Aviv, Israel.
- ⁶⁰ RAGOSA I VYACHESLAVOVICH (1990), *Circular Warp Knitting Machine*, UK Patent, No. 2 039 544 A, 20 November, 1990.
- ⁶¹ YAO, YAN-AN et al (2000), "Motion Control of Cam Mechanisms", *Mechanisms and Machine Theory*, Volume 35, Issue 4, April 2000, PP 593-607.
- ⁶² IWASAKI T. et al (1996), Auto-Tuning of two-Degree-of-Freedom Motor Control for High-Accuracy Trajectory Motion, *Control Eng. Practice*, Vol. 4, No. 4, pp. 537-544, Pergamon 1996.
- ⁶³ BEAVEN R. W., et al (1995), *The application of Setpoint Gain Scheduling to High-Speed Independent Drives*. *Control Eng. Practice*, Vol. 3, pp 1581-1585, Pergamon 1995.

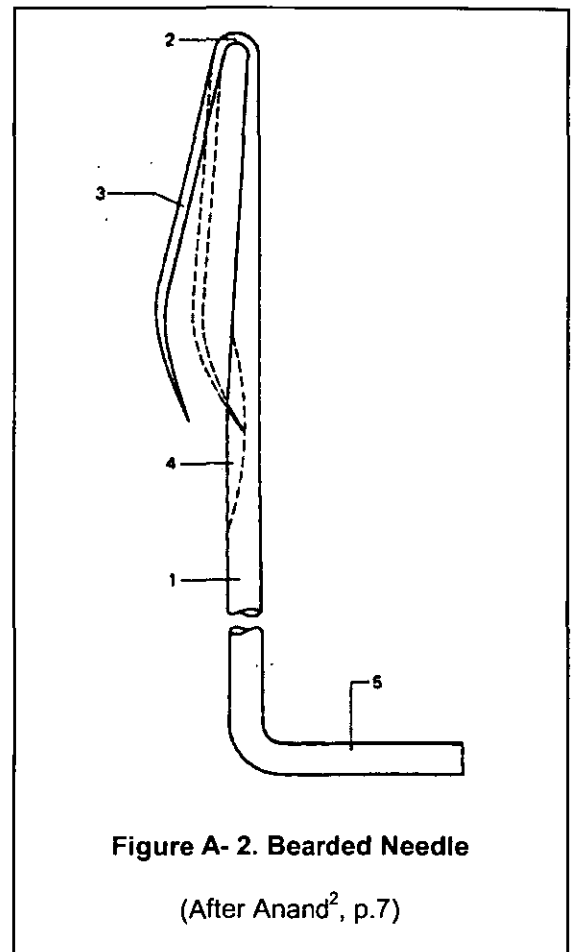
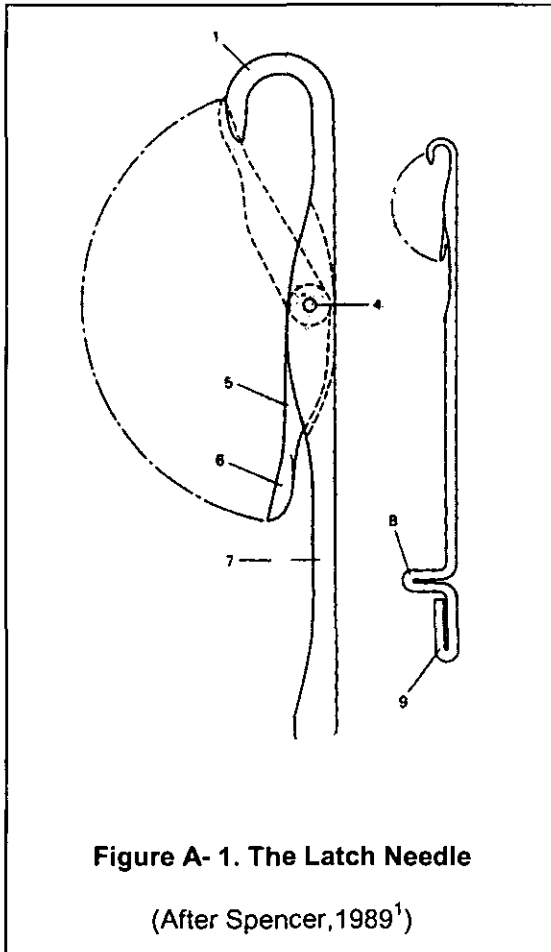
Appendix A. Warp Knitting Terminology.

A.1 Knitting Elements.

Needles

A needle must have some method of closing its hook to retain the new loop and exclude the old loop.

The most common types of needles are; bearded needles (Figure A- 2), latch needles (Figure A- 1) and compound needles (Figure A- 3). In all cases the fabric draw off will be from the side remote from their hooks and a variation of the depth of descent will alter the loop length.



¹ SPENCER D. J., *Knitting Technology*, Second Edition 1989, Pergamon Press, UK.

² ANAND, S. *Principles of Warp Knitting Course*. Bolton Institute of Higher Education, Bolton, UK.

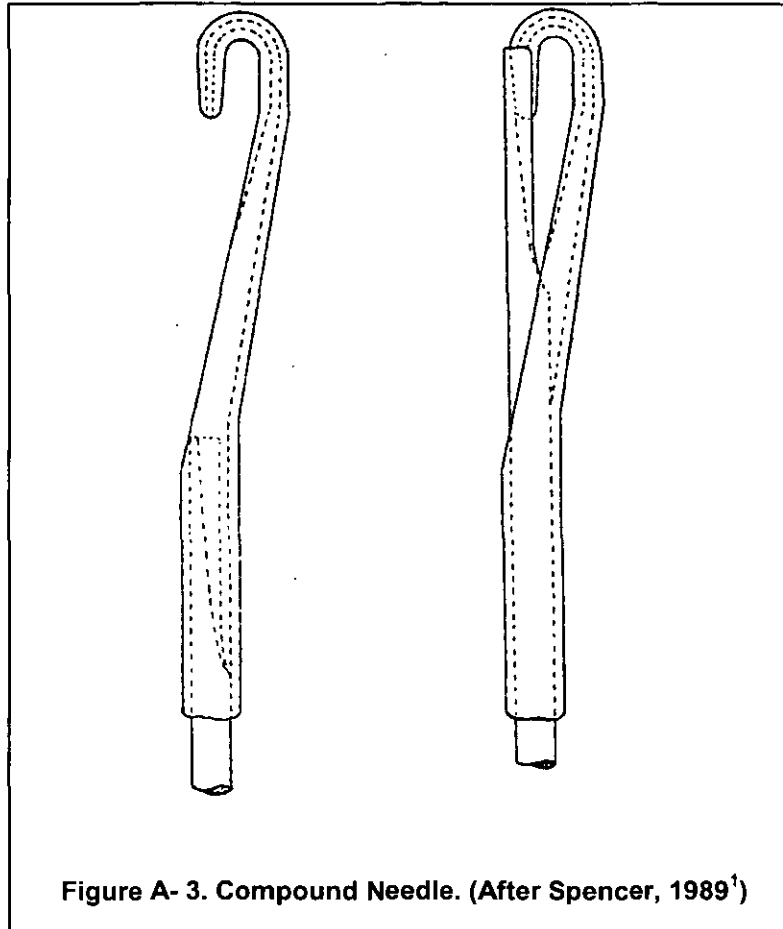
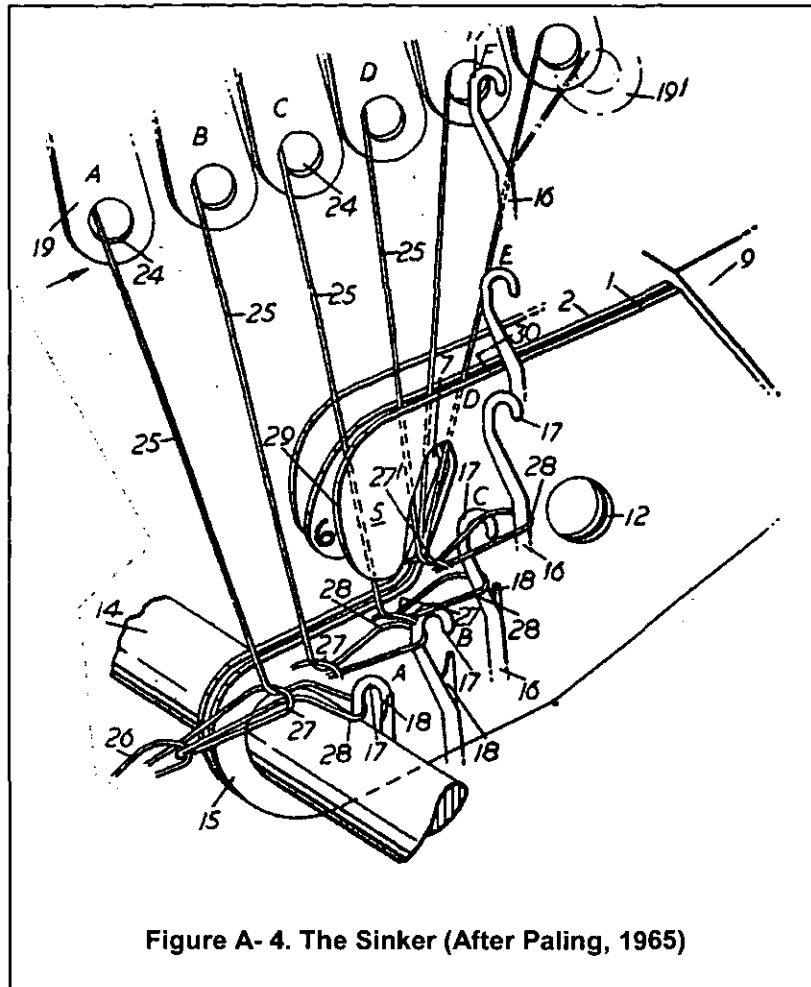


Figure A- 3. Compound Needle. (After Spencer, 1989¹)

Latch needles are self acting while bearded needles need a force F on their hook and compound ones need separate tongue and stem motions in order to produce a new loop. However, latch needles are more prone to making needle lines.

In the case of latch needles, a variation of height of reciprocation can produce missing, tucking or knitting.

Other needles include specially designed ones to facilitate rib loop transfer by selective lifting and double sided purl needles, that can knit from opposing beds by sliding through the old loops and knitting with each side of the needle alternatively.



Sinkers

A sinker (see Figure A- 4) can perform up to three different functions;

- i. Loop formation; only on bearded needle weft knitting.
- ii. Holding down; which enables to produce tighter structures, improved appearance, minimum draw-off tension and knitting can be commenced on empty needles. It is not necessary when knitting on two-bed machines.
- iii. Knocking over; when the sinker holds the fabric while the new loop is being formed. On latch needle machines this function is performed by the verge.

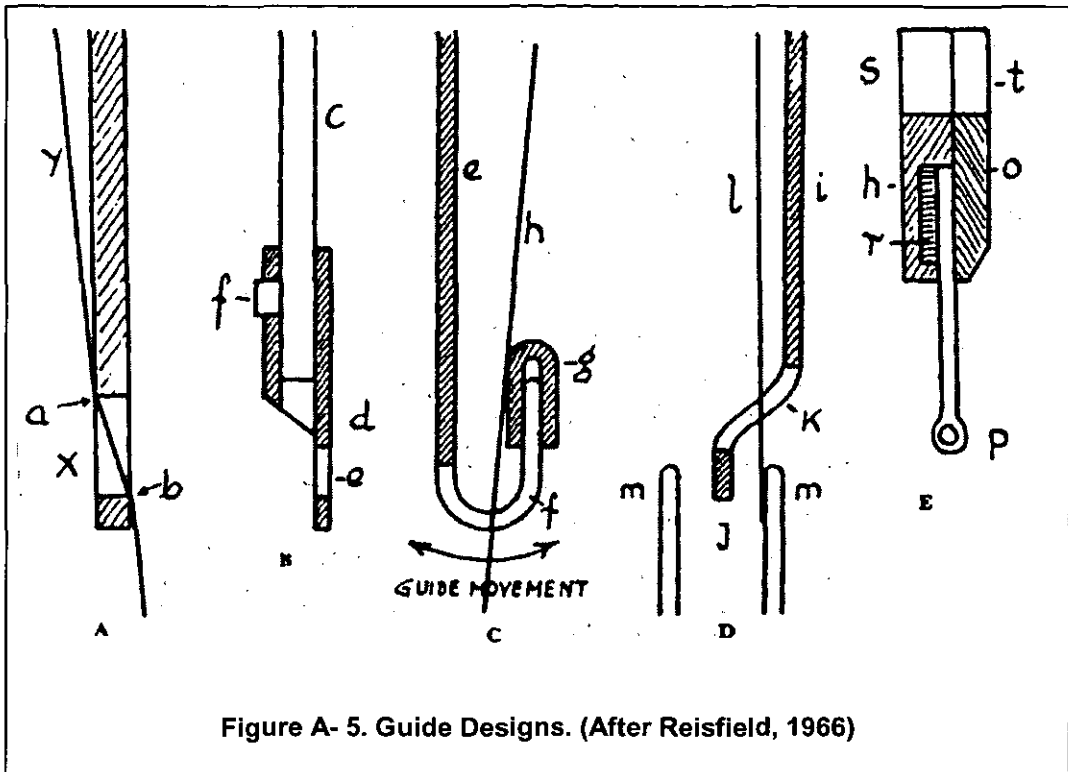


Figure A- 5. Guide Designs. (After Reisfield, 1966)

Guides

The knitting elements that position the threads on and around the needles. Figure A- 5 shows different designs.

Jacks

A secondary weft knitting element. It is placed in the same trick as the needle and its separate butt enables the needle to be controlled directly or indirectly.

Trick Plate

A grooved plate supporting the needles in Raschel machines.

A.2 Loops

Overlap

The motion of the guide bars across the open side of the needle hook during the forming of a new loop; it is normally limited to one needle space.

Underlap

The patterning motion of the guides when the needles are down. The number of needle spaces of the underlap is only restricted by the patterning mechanism characteristics.

Open Loop

Knitted loops whose legs do not cross; the overlap and the next underlap must be performed in the same direction in order to produce it.

Closed Loop

Loops where the overlap and underlap are in opposite directions.

A.3 Yarns and Fabric Delivery**Fabric Take-up or Takedown**

The mechanism for maintaining a constant fabric tension at the needles. The take-up rate, the speed at which the mechanism rotates, is calculated from the courses per inch (cpi) of fabric.

Let-off

The mechanism to feed yarn to the knitting elements in a warp knitting machine at the required rate.

Run-in

The length of yarn used in a RACK (480 courses) of a given fabric.

A.4 Warp and Weft Knitting

The main difference between warp and weft knitting is that in warp knitting every needle being used is supplied with at least a yarn end. Ends supplied by the same warp sheet normally have identical lapping movements. These movements are timed and configured by the patterning mechanism in the form of overlaps and underlaps.

Advantages of Warp over Weft;

- i. Almost any type of fabric can be produced, while weft is restricted to only one type of product.
- ii. In warp, special attachments for pattern work are not necessarily required.
- iii. No need for reduction of speed when patterning.
- iv. It is easier to maintain consistent quality because all elements receive a collective movement and yarn feeding is under control.
- v. The number of stitch possibilities and combinations is unlimited.
- vi. It allows to construct fabrics with predetermined physical properties, run-resist characteristics and texture merely by varying the stitch set up.

Advantages of weft over warp knitting

- i. Semi complete garment length of products.
- ii. The cost of setting up a machine is much lower.
- iii. Tubular form of fabric is an advantage in finishing (Assuming that most warp knitting machines are flat).

Scope of Warp Knitting

Warp knitting is capable of turning out a host of fabrics, nets, laces and other products in a variety of weights from veilings to coarse rugs, and including underwear, elastic foundation cloths, meshes for curtains, shoes, mosquitoes and fishing nets, hammocks, various types of laces, trims, strapping, tapes, bands, fabrics for gloves, bed sheets linens, drapes backing, quilting.

In a general, when classifying the Warp Knitting industry and its products, two major sectors can be defined; the fine gauge tricot fabrics (light apparel and furnishings such as lingerie, shirts, sheets and linings) and the lace and elastic nets group (decorative laces, mesh curtains, power nets for

foundation garments). Other minor groups include the coarse gauge field, whose growth is stimulated by the addition of weft-insertion mechanisms.

A.5 Warp Knitting Machine Types

Raschel Knitting

Raschel warp knitting machines can be defined as those with latch needles. Raschels make laces, plain nets or elastic nets. Those designed for unpatterned nets run at the higher speeds, since, invariably, increasing the patterning complexity reduces the speed. Lace machines generally differ from plain-net ones in the number of warps; the former having very few needles, while the latter having up to 48.

In Raschel machines, warp knitting machines, fabric drawn off is done parallel to the needle stem and sinkers are not necessary to perform the knitting cycle.

Tricot Machines

Tricot fabrics are generally the lighter of the apparel and furnishing fields. They include those made using bearded or compound needles.

Fabric drawn-off on bearded needle machine is generally perpendicular to the needle stem.

A.6 Classification of Warp Knitted products

Most warp knitted products fall into one or more of the following categories;

- i. Single faced; made on a machine with one needle bar
- ii. Double faced; made on a machine with two needle bars. Loop structure on both sides.
- iii. Tubular; requires a minimum of three needle bars if a flat machine is used.

- iv. Solid. Any construction not featuring definite holes, pores or other openings. Solid fabrics can be further divided into Plain, Patterned, Fancy (two or more colours) and Raised.
- v. Openwork, with holes and pores. Solid fabrics can be further divided into Plain, Patterned and Fancy.
- vi. Narrow, when a large number of fabrics is produced at the same time on a machine.

Appendix B. Patents Subclass Index

D 04 BRAIDING; LACE-MAKING; KNITTING; TRIMMINGS; NON-WOVEN FABRICS**D 04 B KNITTING**Notes

- (1) In this subclass, groups designating machines, apparatus, devices, or implements include Processes characterised by, or dependent on, their use, and the products of such processes.
- (2) Knitted products, i.e. fabrics, articles, are classified in this subclass only if they have constructional features which are of interest from the knitting aspect.

Subclass Index**WEFT KNITTING AND MACHINES THEREFOR**

General processes or knitted articles	1/00
Hand tools or implements; knitting apparatus or machines for domestic use	3/00; 5/00, 7/08
Flat-bed knitting machines: with independently-movable needles; with fixed needles	7/00; 11/00
Circular knitting Machines: with independently-movable needles; with fixed spring or bearded needles.....	9/00; 13/00
Details or auxiliary devices incorporated in the machines	15/00; 35/00

WARP KNITTING AND MACHINES THEREFOR

General processes or knitted articles	21/00
Machines flat-bed; other types	23/00; 25/00
details or auxiliary devices incorporated in the machines.....	27/00; 35/00

AUXILIARY APPARATUS USED WITH KNITTING MACHINES..... 37/00**CROCHETING AND APPARATUS THEREFOR**

Processes; tools or implements	31/00; 33/00
Details or auxiliary devices incorporated in the apparatus.....	35/00

REPAIRING; UNRAVELLING 17/00; 19/00**PROCESSES AND KNITTING MACHINES NOT OTHERWISE PROVIDED FOR..... 37/00**

Weft knitting; Machines therefor**1/00 Weft knitting processes for the production of fabrics or articles not dependent on the use of particular machines; Fabrics or articles defined by such processes**

- 1/02 Pile fabrics or articles having similar surface features
- 1/04 characterised by thread material
- 1/06 Non-run fabrics or articles
- 1/08 characterised by thread material
- 1/10 Patterned fabrics or articles
- 1/12 characterised by thread material
- 1/14 Other fabrics or articles characterised primarily by the use of particular thread materials
- 1/16 synthetic threads
- 1/18 elastic threads
- 1/20 crimped threads
- 1/22 specially adapted for knitting goods of particular configuration
- 1/24 wearing apparel
- 1/26 stockings
- 1/28 gloves

3/00 Hand tools or implements

- 3/02 Needles
- 3/04 Finger protectors, Thread tensioners
- 3/06 Ball holders or receptacles

5/00 Knitting apparatus or machines without needles for domestic use (with needles 7/08)**7/00 Flat-bed knitting machines with independently-movable needles (straight-bar machines with fixed needles 11/00)**

- 7/02 with one set of needles
- 7/04 with two sets of needles
- 7/06 for purl work or Links-Links loop formation
- 7/08 for domestic use
- 7/10 with provision for narrowing or widening to produce fully-fashioned goods
- 7/12 with provision for incorporating pile threads
- 7/14 with provision for incorporating internal threads in laid-in fabrics
- 7/16 for producing fabrics consisting of, or incorporating, elastic threads
- 7/18 incorporated as weft or inlaid threads
- 7/20 with provision for changing the fabric construction, e.g. from plain to rib-loop fabric
- 7/22 with special provision for commencing goods, e.g. with non-run edges
- 7/24 for producing patterned fabrics
- 7/26 with colour patterns
- 7/28 with stitch patterns
- 7/30 specially adapted for knitting goods of particular configuration
- 7/32 tubular goods
- 7/34 gloves

9/00 Circular knitting machines with independently-movable needles (with fixed spring or bearded needles 13/00)

- 9/02 with one set of needles
- 9/04 with spring or bearded needles
- 9/06 with needle cylinder and dial for ribbed goods
- 9/08 for interlock goods
- 9/10 with two needle cylinders for purl work or for Links-Links loop formation
- 9/12 with provision for incorporating pile threads
- 9/14 with provision for incorporating loose fibres, e.g. in high-pile fabrics
- 9/16 with provision for incorporating internal threads in laid-in fabrics
- 9/18 with provision for splicing by incorporating reinforcing threads

- 9/20 with provision for narrowing or widening; with reciprocatory action, e.g. for knitting of flat portions
- 9/22 with provision for changing the fabric construction, e.g. from plain to rib-loop fabric
- 9/24 with special provision for commencing goods, e.g. with non-run edges
- 9/26 for producing patterned fabrics
- 9/28 with colour patterns
- 9/30 by striping
- 9/32 by wrap striping
- 9/34 by plating
- 9/36 Intarsia work obtained by reciprocatory action
- 9/38 with stitch patterns
- 9/40 with provision for transfer of knitted goods from one machine to another
- 9/42 specially adapted for producing goods of particular configuration
- 9/44 elongated tubular articles of small diameter, e.g. coverings for cables (sheathing electric cables H 01 B 13/22)
- 9/46 stockings, or portions thereof
- 9/48 non-run stockings
- 9/50 micromesh stockings
- 9/52 surgical stockings
- 9/54 welts, e.g. double or turned welts
- 9/56 heel or toe portions
- 9/58 gloves
- 11/00 Straight-bar knitting machines with fixed needles (flat-bed machines with independently-movable needles 7/00)**
- 11/02 with one set of needles
- 11/04 with two sets of needles
- 11/06 with provision for narrowing or widening to produce fully-fashioned goods
- 11/08 with provision for incorporating pile threads
- 11/10 with provision for incorporating internal threads in laid-in fabrics
- 11/12 for producing fabrics from, or incorporating, elastic threads
- 11/14 with provision for changing the fabric construction, e.g. from plain to rib-loop fabric
- 11/16 with special provision for commencing goods, e.g. with non-run edges
- 11/18 for producing patterned fabrics
- 11/20 with colour patterns
- 11/22 with stitch patterns
- 11/24 with provision for transfer of knitted goods from one machine to another
- 11/26 specially adapted for producing goods of particular configuration
- 11/28 stockings, or portions thereof
- 11/30 non-run stockings
- 11/32 welts, e.g. double or turned welts
- 11/34 heel or toe portions
- 11/36 other wearing apparel
- 13/00 Circular knitting machines with Fixed spring or bearded needles, e.g. loop-wheel machines (with independently-movable needles 9/00)**
- 13/02 with horizontal needles
- 15/00 Details of, or auxiliary devices Incorporated in, weft knitting machines, restricted to machines of this kind (details or auxiliary devices not so restricted 35100)**
- 15/02 Loop-transfer points
- 15/04 for straight-bar knitting machines
- 15/06 Sinkers
- 15/08 Needle latch openers; Brushes
- 15/10 Needle beds
- 15/12 Shogging devices therefor

- 15/14 Needle cylinders
- 15/16 Driving devices for reciprocatory action
- 15/18 Dials
- 15/20 Needle bars
- 15/22 Driving devices therefor
- 15/24 Sinker heads; Sinker bars
- 15/26 Slurcocks
- 15/28 Needle pressers
- 15/30 Driving devices for thread-carrier rods
- 15/32 Cam systems or assemblies for operating knitting instruments
- 15/34 for dials
- 15/36 for flat-bed knitting machines
- 15/38 Devices for supplying, feeding, or guiding threads to needles
- 15/40 Holders or supports for thread packages
- 15/42 Frames for assemblies of two or more reels
- 15/44 Tensioning devices for individual threads
- 15/46 for elastic threads
- 15/48 Thread-feeding devices
- 15/50 for elastic threads
- 15/52 for straight-bar knitting machines
- 15/54 Thread guides
- 15/56 for flat-bed knitting machines
- 15/58 for circular knitting machines, Thread-changing devices
- 15/60 with thread-clamping or -severing devices
- 15/61 arranged within needle circle
- 15/62 with thread knotters
- 15/64 for straight-bar knitting machines
- 15/66 characterised by the knitting instruments used
- 15/70 in flat-bed knitting machines
- 15/72 in straight-bar knitting machines
- 15/74 Pattern drums
- 15/76 Pattern wheels
- 15/78 Electrical devices
- 15/80 characterised by the thread guides used
- 15/82 characterised by the needle cams used
- 15/84 Jacquard cards or mechanisms (stamping apparatus therefor D 03 C)
- 15/86 in flat-bed knitting machines
- 15/88 Take-up or draw-off devices for knitting products
- 15/90 for flat-bed knitting machines
- 15/92 pneumatic
- 15/94 Driving-gear not otherwise provided for
- 15/96 in flat-bed knitting machines
- 15/98 in straight-bar knitting machines
- 15/99 electrically controlled

Repairing or unravelling knitted fabrics

- 17/00 Repairing knitted fabrics by knitting operations
- 17/02 by darning
- 17/04 by picking-up dropped stitches

19/00 Unravelling knitted fabrics**Warp knitting; Machines therefor**

- 21/00 Warp knitting processes for the production of fabrics or articles not dependent on the use of particular machines; Fabrics or articles defined by such processes

- 21/02 Pile fabrics or articles having similar surface features
- 21/04 characterised by thread material
- 21/06 Patterned fabrics or articles (open-work fabrics 21/10)
- 21/08 characterised by thread material
- 21/10 Open-work fabrics
- 21/12 characterised by thread material
- 21/14 Fabrics characterised by the incorporation by knitting, in one or more thread, fleece, or fabric layers, of reinforcing, binding, or decorative threads, Fabrics incorporating small auxiliary elements, e.g. for decorative purposes (pile fabrics; 21/02; non-woven fabrics in general D 04 H)
- 21/16 incorporating synthetic threads
- 21/18 incorporating elastic threads
- 21/20 specially adapted for knitting articles of particular configuration
- 23/00 Flat warp knitting machines**
- 23/02 with two sets of needles
- 23/04 with independently-movable knitting needles
- 23/06 for producing fabrics consisting of, or incorporating, elastic threads
- 23/08 with provision for incorporating pile threads
- 23/10 for knitting through thread, fleece, or fabric layers, or around elongated core material
- 23/12 with provision for incorporating unlooped wefts extending from selvedge to selvedge
- 23/14 with provision for incorporating small auxiliary elements, e.g. for decorative purposes
- 23/16 specially adapted for producing fabrics, or article blanks, of particular form or configuration
- 23/18 with provision for narrowing or widening
- 23/20 for producing stocking blanks
- 23/22 with special thread-guiding means
- 23/24 with cut needle presser arrangements to produce patterns
- 25/00 Warp knitting machines not otherwise provided for**
- 25/02 Tubular machines
- 25/04 Milanese machines
- 25/06 Galloon crocheting machines
- 25/08 for producing pile fabrics
- 25/10 for producing patterned fabrics
- 25/12 with independently-movable weft-thread guides controlled by Jacquard mechanisms
- 25/14 specially adapted for producing articles of particular configuration
- 27/00 Details of, or auxiliary devices incorporated in, warp knitting machines, restricted to machines of this kind (details or auxiliary devices not so restricted 35100)**
- 27/02 Warp-thread guides
- 27/04 Sinkers
- 27/06 Needle bars; Sinker bars
- 27/08 Driving devices therefor
- 27/10 Devices for supplying, feeding, or guiding threads to needles
- 27/12 Tensioning devices for individual threads
- 27/14 Thread tensioning rod arrangements
- 27/16 Warp beams; Bearings therefor
- 27/18 Warp beam braking devices for thread tensioning
- 27/20 Warp beam driving devices
- 27/22 electrically controlled
- 27/24 Thread guide bar assemblies
- 27/26 Shogging devices therefor
- 27/28 with arrangements to reduce the number of members of pattern chains
- 27/30 with driving-gear comprising force-multiplication devices
- 27/32 with independently-movable thread guides controlled by Jacquard mechanisms
- 27/34 Take-up or draw-off devices for knitted products 27/36 . with temples

Crocheting; Apparatus therefor (galloon crocheting machines for warp knitting 25/06)

- 31/00 Crocheting processes for the production of fabrics or articles**
- 31/02 Crocheted strips or threads

- 33/00 Crocheting tools or apparatus**

- 35/00 Details of, or auxiliary devices incorporated in, knitting machines, not otherwise provided for**
- 35/02 Knitting tools or instruments not provided for in group 15/00 or 27/00 (needle manufacture B 21 G 1/00)
- 35/04 Latch needles
- 35/06 Sliding-tongue needles
- 35/08 Spring or bearded needles
- 35/10 Indicating, warning, or safety devices, e.g. stop motions
- 35/12 responsive to thread consumption
- 35/14 responsive to thread breakage
- 35/16 with detectors associated with a series of threads
- 35/18 responsive to breakage, misplacement, or malfunctioning of knitting instruments
- 35/20 responsive to defects, e.g. holes in knitted products
- 35/22 Devices for preparatory treatment of threads
- 35/24 by moistening or lubricating
- 35/26 by beating
- 35/28 Devices for lubricating machine parts (in general F 16 N)
- 35/30 Devices for controlling temperature of machine parts
- 35/32 Devices for removing lint or fluff
- 35/34 Devices for cutting knitted fabrics
- 35/36 Devices for printing, coating, or napping knitted fabrics

- 37/00 Auxiliary apparatus or devices for use with knitting machines (Jacquard cards, pattern chains, apparatus for punching same D 03 C)**
- 37/02 with weft knitting machines
- 37/04 for inserting or adjusting pattern pins or like elements in pattern drums or wheels
- 37/06 with warp knitting machines

- 39/00 Miscellaneous knitting processes, apparatus, or machines, not otherwise provided for**
- 39/02 with work carrier in screw form
- 39/04 adapted for combined weft and warp knitting
- 39/06 adapted for combined knitting and weaving
- 39/08 Sewing machines modified for knitting

Appendix C. PDS Database Records

CONTENTS

1. PATTERNING & FABRIC STRUCTURES.	2
STANDARD AND PATTERN GUIDE BARS.	2
DOUBLE NEEDLE BAR	3
WEFT INSERTION AND OTHERS.	4
JACQUARD.	5
2.KNITTING ELEMENTS	6
COMPOUND NEEDLE:	6
NEEDLES & GAUGES:	6
3. GUIDE BARS	7
STANDARD RASCHEL -FULLY THREADED OR PATTERN-	7
JACQUARD.	8
MULTIAXIAL -DIAGONAL PLACING GUIDE	8
4.PATTERNINGMECHANISMS	9
GENERAL	9
PATTERN CHAINS AND DRUMS, STD RASCHEL MACHINES:	9
ADJUSTABLE:	10
WEFT INSERTION:	10
JACQUARD:	11
PATTERN CONTROL SYSTEM SU;	12
PATTERN CONTROL SYSTEM-EL:	12
5. YARN SUPPLY	13
6. YARNS AND OTHER MATERIALS.	14
GENERAL	14
ELASTIC FABRICS	15
7. TAKE UP MECHANISMS	16
8. DRIVING MECHANISMS OF KNITTING ELEMENTS	17
NEEDLES, HORIZONTAL SWING:	17
NEEDLES, VERTICAL:	17
9. QUALITY CONTROL	18
10.FRAME/ CARCASS	19
11. CONTROL	19

<p>1. Patterning & Fabric Structures.</p> <p>Standard and pattern guide bars.</p>	<p>Fruit Packaging - Nets: <u>Vertical pillar nets:</u> To ensure stability, at least one of the inlays laps over more than one needle space. These nets' wales are generally vertical. Marquisette structures are formed by 2 or 3 fully threaded guide bars, where only the front one is chaining open laps. The other two are inlaying.</p> <p><u>Technical Textiles:</u> <u>Protection Nets,</u> with varying net openings are made in RS 4 N 2 MF. Raschel machines. Prot. against mosquitoes, sand, birds and sun (in green houses). <u>Catching and harvesting nets</u> form a large market for standard Raschel Machines</p>	<p>Stockings: Fish-nets. The basic structure is produced by partly threaded guide bars making a number of pillar stitches. Connections between pillars are made by shogging the guide bars in opposite directions. These net's wales will not remain vertical but take different shapes according to the structure. Generally, two guide bars will knit the structure, while pattern bars will inlay. The fabric diameter is dependant on the depth of the opening and can be several times bigger than the cylinder diameter. Fish-nets are also widely used for flower wrapping.</p>
	<p>Bandages/ Medical: Elasticated fabrics, both plain and net structures are made on Raschel machines with the elastomeric yarn threaded in the back guide bar. It is made in fine gauge, 4-6 guide bars (all half threaded) and a similar str. to fish net. Two bars knit and the other two inlay. 3 u/l max in egs. Mayer's RSE4-6N (Raschel, Compound Needle, Pattern drum) produces elastic fabrics for bandages, in some cases with a structured surface.</p>	<p>Other: Net Curtain structures by inlay are very similar to vertical pillar nets, but use coarser gauges (6 npi in std-18npi in multibar m/cs). One ground base knits open pillars, while two or three more inlay the connections. Tulle net structures have one ground guide bar knitting, one inlaying, and a few pattern guide bars.</p>

<p>1. Patterning & Fabric Structures.</p> <p>Double Needle bar</p>	<p>Fruit Packaging - Nets: Special double-needle-bar machines have been designed for the production of sacks (for coal, potatoes, fruit, beans and rice). The normal sack producing Raschel machine is 170 inches wide and uses a 6npi gauge.</p>	<p>Stockings: Double-needle bar Jacquard machines. By positioning two jacquard bars between the ground bars allows produce complicated tubular fabrics. Patterned panty hose are at present the biggest market. Mayer's HDR 20 EEW (Raschel, latch needle, double needle) m/c produces ladies' elastic tights and briefs. Mayer's HDR 44 SU (Raschel, latch needle, double needle, SU patt.) m/c produces ladies' elastic lace tights.</p>
	<p>Bandages/ Medical: Bandages are made in double needle machines. Mayer's DR6E 2-needle m/c produces tubular elasticated bandages and net wrappings. Branching arteries are made on 2-needle, 16-guide bar, latch needle machines. The lapping movement of the ground structure requires a max. u/l of 3 needles. (2-3/1-0 and 1-0/1-2)</p>	<p>Other: Car upholstery fabric is made in double-needle-bar Plush Raschel machines (6 guide bars). Pile fabrics like these would be very diff. to produce from a circ. machine. Geotextiles, to shape and protect the landscape, generally made on double needle bar machines. E.g. lining for water reservoir, cement sacks for protection of river embankments. Another type of 2-needle jacquard machine is used to produce pile fabrics by the use of a pin bar. (Generally for internal decoration and curtains) Monk Cotton scarf raschel knitting machine is microprocessor controlled to produce plain or lace effect fabric, zig-zag or vertical stripes.</p>

<p>1. Patterning & Fabric Structures.</p> <p><u>Weft insertion and others.</u></p>	<p>Fruit Packaging - Nets:</p>	<p>Stockings:</p>
	<p>Bandages/ Medical: Dialysis filters are made on weft insertion m/cs.</p>	<p>Other: <u>Fabrics for Composite materials.</u> A special Raschel machine was developed by Mayer to produce multiaxial structures. A single guide bar knits the ground structure. Another mislaps to insert a vertical yarn in the fabric. A weft insertion magazine lays a horizontal yarn in the fabric and a diagonal placing element knits one stitch and moves one needle space to one side. Outerwear and upholstery fabrics are produced in Raschel m/cs with weft insertion. (gauge 7-12 npi), using one guide bar knitting and one or two more inlaying, sometimes partly threaded. 4 needle u/l max in egs. The end use is dependant on the weft inserted yarn, since it is the domineering one in the texture and determines the weight of the fabric.</p>

<p>1. Patterning & Fabric Structures.</p> <p><u>Jacquard.</u> In Jacquard raschel machines, ground bars produce a ground net. Each guide can defelect only one needle space, to produce 3 different shading effects. Different lapping movements can be produce according to where the jacquard bar is placed in relation to the other guides. Two individually controlled jacquard bars can also be used to give more patterning possibilities.</p>	<p>Fruit Packaging - Nets:</p>	<p>Stockings: Double-needle bar Jacquard machines. By positioning two jacquard bars between the ground bars allows produce complicated tubular fabrics. Patterned panty hose are at present the biggest market.</p>
	<p>Bandages/ Medical:</p>	<p>Other: Relief patterned elastic fabrics made on Mayer RJSE 3/1. Jacquard patterned elastic fabrics made on RJSE 4F-NE. Other: Another type of 2-needle jacquard machine is used to produce pile fabrics by the use of a pin bar. (generally for internal decoration and curtains)</p>

<p>2. Knitting Elements</p> <p><u>Needles & Gauges:</u></p> <p>Ciconet (IWS) offers gauges from 3npi to 24 npi for the production of Elastic Bandages, patterned stockings and packaging nets. They offer:</p> <p>18 & 22 N for a 50mm Cyl 26, 30 & 34 N for a 63mm Cyl. 68 & 72 N for a 76mm Cyl. Mayer's SU pattern control system uses convertible shogging movements from E14-E24</p>	<p>Fruit Packaging - Nets:</p>	<p>Stockings:</p> <p>The usual gauge used in Double needle, multi guide bar Raschel machines to produce patterned lace panty hose is 18npi. Clothes (sports, lingerie, swimwear) jacquard Mayer m/c uses E28</p>
<p>2. Knitting Elements</p> <p><u>Compound needle:</u></p> <p>-short, simple action without latch or beard inertia. -The short stroke required (5-6mm) and the flat profile of the hook closure contribute vitally to the increased speed.</p>	<p>Bandages/ Medical:</p> <p>The machine to produce blood arteries has a gauge of 16 npi. Rius TC200GE machine to produce tubular sanitary bandages is offered with 15-88 Needles and Cyl. sizes from 15 to 90 mm. (Max m/c gauge = 4.2npi)</p>	<p>Other:</p> <p>Outerwear and upholstery fabrics are produced in Raschel m/cs with weft insertion. (gauge 7-12 npi) Multiaxial m/cs gauges: E10 and E12 Fishing net gauges: 7-32npi for nylon 6 type nets depending on the application. Monk Cotton Raschel 2-needle bar scarf warp knitting m/c is offered in 6 and 10 npi, with latch needles.</p>
	<p>Fruit Packaging - Nets:</p> <p>Needles: Raschel machines manufacturers are now using compound needles. Hook size and needle stroke should be minimised to allow for high speed operation. Gauges should vary from 6 to 32 npi.</p>	<p>Stockings:</p> <p>The number of guide bars varies from 2 to 10. (To increase knitting speeds, only the front guides complete the the O/L movement before the needles go down.). Compound needles are used in the 36 guide bars, 2-needle bar Raschel machines for patterned lace panty hose. (Although some still uses latch needles)</p>
	<p>Bandages/ Medical:</p> <p>Most of the m/cs for elastic fabrics use compound needles (see table 1), except double needle ones, especially where electronic patterning is applied. Its sturdiness makes it ideal for the production of elastic fabrics.</p>	<p>Other:</p> <p>Raschel Weft Insertion machine (RS3EMS) for flat roofings, backlit advertisement sign, awnings, etc uses E-18 compound needles.</p>

<p>3. Guide Bars</p> <p><u>Standard Raschel -Fully Threaded or Pattern-</u></p> <p>Mayer Standard Raschel machines generally have 2 to 10 guide bars and their assy. includes fully threaded ones or a combination of fully threaded with patterns bars nested together.</p>	<p>Fruit Packaging - Nets:</p> <p>In sack-producing machines, (flat 2-needle-bar) 4 fully threaded guide bars and 5 pattern guide bars with individual guide fingers are used.</p> <p>Raschel special machines for the production of packing tube include two needle bars and, 4 fully threaded ground guide bars and 4 pattern guide bars (circular could do the same with only two rings), with a max u/l of 3 needles</p>	<p>Stockings:</p> <p>The basic structure of a fishing net is produced by guide bars threaded 1 in, 1 out.</p> <p>Two fully threaded bars knit the ground structure, while 2,4 or 6 more pattern guides will inlay.</p> <p>Special fish-net machines have been developed incorporating a very short needle stroke and a knitting movement which allows only two bars to form loops. Any extra bar will only be able to inlay.</p> <p>Double needle bar, multi guide bars for the production of patterned lace panty hose are equipped with 36 guide bars. Four fully threaded are used to produce front and back ground structures (two in circular but two cylinders would be required?), between them eight pattern bars knit the connections (not required in circular), 12 pattern guides on each side inlaying inside the ground construction or distorting it. (Only one set of twelve pattern bars would be needed in circular.)</p> <p>A more recent development has 44 guide bars (sets of 16 pattern guide bars) and uses an electronically controlled (SU) patterning mech.</p>
	<p>Bandages/ Medical:</p> <p>The machine to produce branching blood arteries is equipped with 16 guide bars. 4 fully threaded will make the ground structure for the two branches and the remaining patterning ones will link the tubes together.</p>	<p>Other:</p> <p>Machines for the production of fishing nets are built with 7 - 16 needles per inch and 6 guide bars.</p> <p>Monk cotton 2- needle bar scarf raschel m/c has only one guide bar.</p>

<p>3. Guide Bars</p> <p><u>Jacquard.</u></p> <p>In jacquard Raschel machines, the guides are long flexible and staggered so that each one, when deflected is place behind or in front of the adjacent one. These machines also require a dropper pin (or displacement pin) bar. The guides can only be deflected by one needle space to each side. A dropper pin is placed between each two guides. The Jacquard bar and dropper pin bar are controlled and shogged independently</p>	<p>Fruit Packaging - Nets:</p>	<p>Stockings:</p> <p>Double needle bar jacquard machines use 4 guide bars to produce the ground structure and two jacquard bars between them to creating the shaded pattern. Another type of double needle bar jacquard machine that produces a 3-D pattern effect uses a pin bar that replaces one of the needle bars, three ground bars and two jacquard bars. This type of machine is used to produce pile fabrics.</p>
<p>3. Guide Bars</p> <p><u>Multiaxial -Diagonal Placing Guide</u></p>	<p>Bandages/ Medical:</p>	<p>Other:</p>
	<p>Bandages/ Medical:</p>	<p>Other:</p> <p>Multiaxial machines have two full set guide bars (the back guide bar constanttly swinging and mislapping to lay the vertical yarn in), a weft insertion magazine, and a diagonal placing guide</p>

<p>4.PatterningMechanisms <u>General</u> The needles and guides should move horizontally relative to each other. The O/L movement is always on needle space, while the U/L one varies with the application. Up to now, most needle shogging mechanisms have been based on pattern drums or chains. Mayer has develop an electronically controlled patterning system (SU) that uses 6-8 eccentric cams to produce U/Ls of upto 47 needle spaces. Mayer has also developed an electronic jaquard patterining device to work in conjunction with a pattern drum/chain mechanism.</p>	<p>Fruit Packaging - Nets: It should allow for a of 3 needle (maximum) underlap. In vertical pillar nets, the shape of th opening is determined by the lapping movement and the tension applied to the yarns.</p>	<p>Stockings:</p>
<p>4. Patterning Mechanisms <u>Pattern chains and drums, std Raschel machines:</u></p>	<p>Bandages/ Medical:</p>	<p>Other:</p>
	<p>Fruit Packaging - Nets: Vertical pillar nets are made on fully threaded std. raschel machines. Marquisette structures with 2-3 fully threaded guide bars</p> <p>Bandages/ Medical: Elasticates fabrics both plain and net structures. The elastomeric yarn is threaded in the back guide bar. Branching arteries are made in double-needle, 16 guide abar latch needle machines. The ground structure uses 2 guide bars (2-3/1-0 and 1-0/1-2) and a max of 3 needle u/l. Raschel Mayer m/cs to prod. elastic badanges (RSE4 - 6N use pattern wheel. Upto 900cpi.</p>	<p>Stockings: Fishnet</p> <p>Other: Net Cutain Structures. Tulle Net structures.</p>

<p>4.PatterningMechanisms</p> <p><u>Adjustable:</u> The guide bar shogging movement depends on the machine gauge. Since the machine should have interchangeable heads (and gauges) the patterning mechanism should be easily adjustable to these changes.</p> <p>Mayer developed a method for one of their pattern drum machines whereby the shog movement is transmitted through a lever, and the amount of leverage can be adjusted according to the gauge required, without having to change the chain links used..</p>	<p>Fruit Packaging - Nets:</p>	<p>Stockings:</p>
	<p>Bandages/ Medical: The pattern control system SU has convertible shogging movements from E14 to E24</p>	<p>Other:</p>
<p>4. Patterning Mechanisms</p> <p><u>Weft insertion:</u> can be mechanical or electronically controlled.</p>	<p>Fruit Packaging - Nets: Not Generally Used</p>	<p>Stockings: Not generally used.</p>
	<p>Bandages/ Medical: Dyalisis Filters are made on Weft Insertion Raschel machines.</p>	<p>Other: Multiaxial fabrics are made using raschel weft insertion and "diagonal Insertion" methods. Outerwear and upholstery fabrics are also made in Rschel m/cs with w/i capabilities.. The thickness of the weft inserted yarn determines the end use, sine it is the dominant yarn in the fabric.Mayer's weft insertion Raschel Machine (RS3EMS) with EBA/EWA system, E-18, produces coating fabric for flat roofings, backlit advertising signs, awnings</p>

<p>4.PatterningMechanisms</p> <p><u>Pattern control system</u> <u>SU:</u> the shogging motions, fed into a microcomputer, are determined using 8 eccentrics. The length of u/l is created by a binary-based system using the eccentrics.</p>	<p>Fruit Packaging - Nets:</p>	<p>Stockings: SU system is used in Mayer HDR 44, ladies' elastic lac tights m/cs.</p>
	<p>Bandages/ Medical: Some Mayer m/cs for elasticated fabrics use this type of pattern control system. They are mostly tricot ones; KS4 (elastic velours, 600 cpi), HKS2/3 (Duo elastic products and "relief-type" elastic fabrics)</p>	<p>Other:</p>
<p>4. Patterning Mechanisms</p> <p><u>Weft insertion:</u> can be mechanical or electronically controlled,</p>	<p>Fruit Packaging - Nets:</p>	<p>Stockings:</p>
	<p>Bandages/ Medical:</p>	<p>Other: EL system has been fitted on KS4 tricot machines to produce elastic velours, an improved speeds from 600 -using SU system- to 900cpi.</p>

<p>4.PatterningMechanisms</p> <p><u>Jacquard:</u> In jacquard machines, the position of the jacquard bar will determine the texture of the fabric: Jacquard bars behind normal guide bars will produce a flatter fabric (the jacquard pattern is inside the ground structure), while one positioned in front will produce a more textured effect on the surface of the fabric. If the jacquard bar is positioned in front of the others, a fall plate mechanism is required. Mayer is now using a jacquardtronic mechanism based on dropper bars moved by computer-controlled solenoids.</p>	<p>Fruit Packaging - Nets:</p> <p>Not generally used.</p>	<p>Stockings:</p> <p>Patterned panty hose (not lace) are the largest market for double needle bar, 2 jacquard bar m/cs</p>
	<p>Bandages/ Medical:</p> <p>Not generally used.</p>	<p>Other:</p> <p>Developments on 2-needle bar, jacquard pile/plush fabrics for curtains or interior design. Jacquardtronic is now used in elastic lace m/cs (RJSE4F-NE), double sided terry m/cs (KSJ4/1FBZ-EBC), double needle bar velvet m/cs and tricot pile velour m/c (KSJP3/2) for automotive and domestic upholstery.</p>
<p>4.PatterningMechanisms</p> <p>Plush Raschel Machines</p>	<p>Fruit Packaging - Nets:</p>	<p>Stockings:</p>
	<p>Bandages/ Medical:</p>	<p>Other:</p> <p>Flat car upholstery is produced in double needle bar machines, and then split through the middle.</p>

<p>5. Yarn Supply</p> <p>The yarn supply system controls the run-in ratio. It should be positive in action in order to maintain consistent quality and adjust stitch length. The use of a warp beam would depend on the number of warp ends needed to produce the fabric. Alternative feeding systems are preferable since the use of a warp beam requires the user to purchase a warping beam. On Jacquard Raschel machines, the jacquard bar must be fed from a creel due to the individual lapping movements of each guide. Negative let off can be used to feed the</p>	<p>Fruit Packaging - Nets:</p> <p>Generally, small number of needles and therefore the yarn supply can be made directly from cones on the knitting head. (Negative)</p>	<p>Stockings:</p> <p>Moorgate machines have 80 needles. This amount would not justify a the use of a warp beam. Mayer specially developed fishing net machines have positively driven warp beams. Double-needle bar, multi-guide bar Raschel machines for patterned lace panty hose use warp beams to supply the fully threaded guides and positively driven pattern beams to supply the light weight bars.</p>
<p>The introduction of the electronic warp let-off system (EBC in Mayer's machines) made it possible to produce intricate patterns and achieve better dimensional stability. Each beam is driven by a separate DC motor and the run-in for each course can be determined independently.</p>	<p>Bandages/ Medical:</p> <p>The latest m/cs to produce elastic fabrics use Mayer's EBC and combine it with electronic take up systems to produce fancy and sculptured patterns. (Positive)</p> <p>Rius TC-200-GE m/c for sanitary bandages uses creels (Negative)..</p>	<p>Other:</p> <p>Tulle net structures (vertical pillar nets) also require positive feed to prevent the ground construction from deforming. Monk cotton double needle scarf Raschel machine uses creels for 144-240 needles and up to 400 courses per minute. (negative).</p>

<p>6. Yarns and other materials.</p> <p><u>General</u></p>	<p>Fruit Packaging - Nets: For vertical pillar nets in standard raschel machines, guides are generally fully threaded. Pillar bar uses yarns usually too fine for the machine gauge. Laying in bars use any yarn.</p> <p>The raw material used in special raschel m/cs for the production of packing tubes is polyethylene in tape form, in widths from 0.5 to 0.8mm. The splitting, heating and stretching system used by Mayer uses 40m thick tape, cuts it into 2mm wide strips and drws them to produce 0.8mmx16m thick tape.</p>	<p>Stockings:</p>
	<p>Bandages/ Medical:</p>	<p>Other: In heavy-gauge machines for producing fishing nets (capable of holding big fish) yarns can exceed 100,000 dtex Outerwear fabrics can be produced using fine polyester yarns(eg 50 dtex) and coarse weft inlay (eg 1666dtex wool) For obtaining high strength in technical fabrics, high tenacity polyester yarn is used (for the wrp ends as well as for weft inserted yarns). Raschel fishing nets using nylon 6 and 66 in 240-9000 denier (polyesters are not used due to their high modulus of elasticity despite having better weathering resistance).</p>

<p>6. Yarns and other materials.</p> <p><u>Elastic fabrics</u></p>	<p>Fruit Packaging - Nets:</p>	<p>Stockings: Ladies' elastic tights and briefs are produced in Mayer's HDR20 EEW. Ladies' elastic lace tight are produced in Mayer's HDR44 SU.(Raschel, Double needle, electronic eccentric pattern control)</p>
	<p>Bandages/ Medical: Plain elastic fabrics and elasticated bandages are made in Mayer's RSE4-6N m/cs (Raschel, Compound needle, pattern wheel) and tubular ones are produced in DR6E (Raschel, double needle)</p>	<p>Other: Tubular elastic nets (meat-nets) are produced in Mayer's DR5SS. (Raschel, Double-needle).</p>

<p>7. Take up Mechanisms</p> <p>The choice of take up mechanism depends on the let off used. In most tricot machines -using positive let off systems- the take up should only affect the shape of the loop and the yarn tensions. The quality is largely determined by the set run in. On the other hand, when negative let off are used (gen. Raschel), the loop forming process depends greatly on a high take up tension.</p> <p>If a negative let off is used, the take up system should be assembled as close as possible to the knitting point and the angle of the fabric coming out should be as near as possible to 180° from the needle cylinder. Should a positive let-off be used, the take up mech. can be positioned further away from the knitting point and the fabric can come out almost perpendicular to the cylinder.</p>	<p>Fruit Packaging - Nets:</p> <p>Net fabrics have been traditionally manufactured by the Raschel industry. In vertical pillar nets, the shape of the opening is determined by the lapping movement and the tension applied to the yarns.</p>	<p>Stockings:</p> <p>Double-needle bar, multi-guide bar Raschel machines for patterned lace panty hose use electronically controlled take up to vary the fabric quality and therefore produce varying diameters in the stocking (narrower at the toe and wider at the thigh.). This type of mech. is also used for double needle jacquard machines.</p>
	<p>Bandages/ Medical:</p>	<p>Other:</p>

<p>8. Driving Mechanisms of Knitting Elements</p> <p><u>Needles, vertical:</u></p> <p>Eccentrics are used to drive high speed Raschel machines with a low number of guide bars, while pot cams (Mayer) are used when a more complicated movement is required.</p> <p>A combination of the two is also possible.</p> <p>Double eccentric systems can also be used when dwelling periods are required.</p> <p>Traditional methods include single cams and cam-counter cam (to reduce bouncing effect) and single eccentrics systems.</p>	<p>Fruit Packaging - Nets:</p>	<p>Stockings:</p>
	<p>Bandages/ Medical:</p>	<p>Other:</p>
<p>8. Driving Mechanisms of Knitting Elements</p> <p><u>Needles, Horizontal swing:</u></p> <p>Some Mayer Raschel machines have a horizontal counter-movement to the swing of the guide bars in order to increase its speed. They use the vertical movement derived from the pot-cam to produce a horizontal swinging movement.</p> <p>In Jacquard Raschel machines, although there are only a few guide bar used, the swinging motion must be carried out by the needle bar.</p>	<p>Fruit Packaging - Nets:</p>	<p>Stockings:</p>
	<p>Bandages/ Medical:</p>	<p>Other:</p>

<p>9. Quality Control</p> <p>The machine should ensure a consistent fabric quality is obtained. Run-in and let off tension for each guide bar as well as the take up tension should be constantly controlled. Positive let off mechanisms are more suitable for high speed machine and improve the uniformity of the loops. The let off mechanism should also compensate for the fluctuations in tension during the knitting cycle.</p> <p>*Negative let offs - tension controlled: Cord let off mechanism, brake let off mechanism.</p>	<p>Fruit Packaging - Nets:</p>	<p>Stockings:</p>
<p>*Negative/Positive: brake let-off + delivery rollers.</p> <p>*Positive Mechanical: (most common), self-regulating using measuring rollers to compare the actual running speed with the required one, set in a control gear box.</p> <p>*Positive Electronic: (Mayer EBC) for warp beam feeding. By inputting information about the beam and the number of warping revolution, a sequence of run-ins can be programmed. It has a tension rail fitted on as well to compensate for rapid fluctuations in tension during the knitting cycle</p>	<p>Bandages/ Medical:</p>	<p>Other:</p>

<p>10.Frame/ Carcass</p> <p>The frame should support the main knitting head, and the take up and let off mechanisms.</p> <p>It should also hold the control panel.</p>	<p>Fruit Packaging - Nets:</p> <p>Sizes The frame sizes should fit from 1/2" to 6" in Diameter of interchangeable knitting heads</p>	<p>Stockings:</p> <p>Sizes The frame size should fit a fixed head of 4" Diameter of the knitting head</p>
	<p>Bandages/ Medical:</p> <p>Sizes: As in weft knitting machines, three frame sizes cover cylinders from 1/2" to 15 1/4"</p>	<p>Other:</p>
<p>11. Control</p> <p>The machine should have a user interface in which any pattern can be fed in directly or programmed in advance.</p> <p>The user should be able to select the number needle underlaps, and the direction of the underlap and overlap for each course in the fabric.</p> <p>The machine should also have stop, crawl and run buttons and a manual handle.</p> <p>When the machine is stopped due to a triggered stop motion, the user interface should warn the operator about the faults cause.</p>	<p>Fruit Packaging - Nets:</p> <p>The user control system should recognise faulty net patterns before starting to knit.</p> <p>The sytem should calculate the estimated net diameter? and production rate (Using depth of hole, stitch length and gauge)</p>	<p>Stockings</p> <p>The user control system should recognise faulty net patterns before starting to knit.</p>
	<p>Bandages/ Medical:</p> <p>The system should calculate the estimated production rate.</p>	<p>Other:</p>

**Appendix D. Program for Piecewise Polynomials
Case Study No 2.**

Worked Example of Piecewise Polynomials (without optimising)

No of breakpoints

```

> n:=4;
                                     n := 4
No of equations including displacement and derivatives
> T:=4;
                                     T := 4
Order of the polynomial given by T and the conditions imposed on them in this
case Boundary and continuity
> k:=8;
                                     k := 8
Initialise matix for coefficients of the polynomial equations
> b:=array(1..(n-1),1..k);
                                     b := array(1..3,1..8,[])
> betadeg:=array(1..n,[0,90,180,360]);
                                     betadeg := [0,90,180,360]
> for i to n do beta[i]:=
  evalf(convert(betadeg[i]*degrees,radians)) od;
                                      $\beta_1 := 0.$ 
                                      $\beta_2 := 1.570796327$ 
                                      $\beta_3 := 3.141592654$ 
                                      $\beta_4 := 6.283185308$ 
> beta:=array(1..n);
Define the equations for displacement and its derivatives
y[i] is the displacement if beta[i]<=theta<=beta[i+1],
> for i to (n-1) do
>
  y[i]:= (sum('b[i,j]*(theta-beta[i])^(j-1)', 'j'=1..k)
  );
>       dy[i]:= (diff(y[i],theta)) ;
>       ddy[i]:= (diff(dy[i],theta)) ;
>       dddy[i]:= (diff(ddy[i],theta)) ;
>       dddy[i]:= (diff(dddy[i],theta)) ;
> od;

$$y_1 := b_{1,1} + b_{1,2} \theta + b_{1,3} \theta^2 + b_{1,4} \theta^3 + b_{1,5} \theta^4 + b_{1,6} \theta^5 + b_{1,7} \theta^6 + b_{1,8} \theta^7$$


$$dy_1 := b_{1,2} + 2 b_{1,3} \theta + 3 b_{1,4} \theta^2 + 4 b_{1,5} \theta^3 + 5 b_{1,6} \theta^4 + 6 b_{1,7} \theta^5 + 7 b_{1,8} \theta^6$$


$$ddy_1 := 2 b_{1,3} + 6 b_{1,4} \theta + 12 b_{1,5} \theta^2 + 20 b_{1,6} \theta^3 + 30 b_{1,7} \theta^4 + 42 b_{1,8} \theta^5$$


$$dddy_1 := 6 b_{1,4} + 24 b_{1,5} \theta + 60 b_{1,6} \theta^2 + 120 b_{1,7} \theta^3 + 210 b_{1,8} \theta^4$$


$$ddddy_1 := 24 b_{1,5} + 120 b_{1,6} \theta + 360 b_{1,7} \theta^2 + 840 b_{1,8} \theta^3$$


```

$$y_2 := b_{2,1} + b_{2,2} (\theta - 1.570796327) + b_{2,3} (\theta - 1.570796327)^2 \\ + b_{2,4} (\theta - 1.570796327)^3 + b_{2,5} (\theta - 1.570796327)^4 \\ + b_{2,6} (\theta - 1.570796327)^5 + b_{2,7} (\theta - 1.570796327)^6 \\ + b_{2,8} (\theta - 1.570796327)^7$$

$$dy_2 := b_{2,2} + 2 b_{2,3} (\theta - 1.570796327) + 3 b_{2,4} (\theta - 1.570796327)^2 \\ + 4 b_{2,5} (\theta - 1.570796327)^3 + 5 b_{2,6} (\theta - 1.570796327)^4 \\ + 6 b_{2,7} (\theta - 1.570796327)^5 + 7 b_{2,8} (\theta - 1.570796327)^6$$

$$ddy_2 := 2 b_{2,3} + 6 b_{2,4} (\theta - 1.570796327) + 12 b_{2,5} (\theta - 1.570796327)^2 \\ + 20 b_{2,6} (\theta - 1.570796327)^3 + 30 b_{2,7} (\theta - 1.570796327)^4 \\ + 42 b_{2,8} (\theta - 1.570796327)^5$$

$$ddd_2 := 6 b_{2,4} + 24 b_{2,5} (\theta - 1.570796327) + 60 b_{2,6} (\theta - 1.570796327)^2 \\ + 120 b_{2,7} (\theta - 1.570796327)^3 + 210 b_{2,8} (\theta - 1.570796327)^4$$

$$dddd_2 := 24 b_{2,5} + 120 b_{2,6} (\theta - 1.570796327) \\ + 360 b_{2,7} (\theta - 1.570796327)^2 + 840 b_{2,8} (\theta - 1.570796327)^3$$

$$y_3 := b_{3,1} + b_{3,2} (\theta - 3.141592654) + b_{3,3} (\theta - 3.141592654)^2 \\ + b_{3,4} (\theta - 3.141592654)^3 + b_{3,5} (\theta - 3.141592654)^4 \\ + b_{3,6} (\theta - 3.141592654)^5 + b_{3,7} (\theta - 3.141592654)^6 \\ + b_{3,8} (\theta - 3.141592654)^7$$

$$dy_3 := b_{3,2} + 2 b_{3,3} (\theta - 3.141592654) + 3 b_{3,4} (\theta - 3.141592654)^2 \\ + 4 b_{3,5} (\theta - 3.141592654)^3 + 5 b_{3,6} (\theta - 3.141592654)^4 \\ + 6 b_{3,7} (\theta - 3.141592654)^5 + 7 b_{3,8} (\theta - 3.141592654)^6$$

$$ddy_3 := 2 b_{3,3} + 6 b_{3,4} (\theta - 3.141592654) + 12 b_{3,5} (\theta - 3.141592654)^2 \\ + 20 b_{3,6} (\theta - 3.141592654)^3 + 30 b_{3,7} (\theta - 3.141592654)^4 \\ + 42 b_{3,8} (\theta - 3.141592654)^5$$

$$ddd_3 := 6 b_{3,4} + 24 b_{3,5} (\theta - 3.141592654) + 60 b_{3,6} (\theta - 3.141592654)^2 \\ + 120 b_{3,7} (\theta - 3.141592654)^3 + 210 b_{3,8} (\theta - 3.141592654)^4$$

$$dddd_3 := 24 b_{3,5} + 120 b_{3,6} (\theta - 3.141592654) \\ + 360 b_{3,7} (\theta - 3.141592654)^2 + 840 b_{3,8} (\theta - 3.141592654)^3$$

dy, ddy, ... are the displacement derivatives

```

Initialise arrays containing values for breakpoint angles and boundary
conditions (i.e. Disp[i] is the displacement at beta[i],etc)
beta:=array(1..n);
[ > Disp:=array(1..n) :
[ > Vel:=array(1..n) :
[ > Accel:=array(1..n) :
[ > Jerk:= array(1..n) :
[ > s:=array(1..n) :
Define Boundary conditions in terms of the equations above
> with(student) :
> Bouny:= seq(powsubs
(theta=beta[i],y[i])=Disp[i],i=1..(n-1));
> Boundy:= seq(powsubs
(theta=beta[i],dy[i])=Vel[i], i=1..(n-1));
> Bounddy:= seq(powsubs
(theta=beta[i],ddy[i])=Accel[i],i=1..(n-1));
> Boundddy:= seq(powsubs
(theta=beta[i],ddd[i])=Jerk[i],i=1..(n-1));
> Boundddd:= seq(powsubs
(theta=beta[i],dddd[i])=s[i],i=1..(n-1));
      Bouny:= b1,1 = Disp1, b2,1 = Disp2, b3,1 = Disp3
      Boundy:= b1,2 = Vel1, b2,2 = Vel2, b3,2 = Vel3
      Bounddy:= 2 b1,3 = Accel1, 2 b2,3 = Accel2, 2 b3,3 = Accel3
      Boundddy:= 6 b1,4 = Jerk1, 6 b2,4 = Jerk2, 6 b3,4 = Jerk3
      Boundddd:= 24 b1,5 = s1, 24 b2,5 = s2, 24 b3,5 = s3
Boundary conditions ensuring continuity in displacement and three of its
derivatives
> Conty :=seq (powsubs
(theta=beta[i+1],y[i])=powsubs(theta=beta[i+1],y[i+
1]),
i=1..(n-2)), powsubs(theta=beta[n],y[n-1])=powsubs(t
heta=beta[1],y[1]);
Conty:= b1,1 + 1.570796327 b1,2 + 2.467401101 b1,3 + 3.875784587 b1,4
+ 6.088068193 b1,5 + 9.563115156 b1,6 + 15.02170616 b1,7
+ 23.59604086 b1,8 = b2,1, b2,1 + 1.570796327 b2,2 + 2.467401101 b2,3
+ 3.875784587 b2,4 + 6.088068193 b2,5 + 9.563115156 b2,6
+ 15.02170616 b2,7 + 23.59604086 b2,8 = b3,1, b3,1 + 3.141592654 b3,2
+ 9.869604404 b3,3 + 31.00627669 b3,4 + 97.40909108 b3,5
+ 306.0196850 b3,6 + 961.3891943 b3,7 + 3020.293231 b3,8 = b1,1
> Contdy :=seq (powsubs
(theta=beta[i+1],dy[i])=powsubs
(theta=beta[i+1],dy[i+1]),

```

```

i=1..(n-2)), powsubs (theta=beta [n], dy [n-1])=powsubs (
theta=beta [1], dy [1]);
Contdy := b1,2 + 3.141592654 b1,3 + 7.402203303 b1,4 + 15.50313835 b1,5
+ 30.44034096 b1,6 + 57.37869094 b1,7 + 105.1519431 b1,8 = b2,2, b2,2
+ 3.141592654 b2,3 + 7.402203303 b2,4 + 15.50313835 b2,5
+ 30.44034096 b2,6 + 57.37869094 b2,7 + 105.1519431 b2,8 = b3,2, b3,2
+ 6.283185308 b3,3 + 29.60881321 b3,4 + 124.0251068 b3,5
+ 487.0454554 b3,6 + 1836.118110 b3,7 + 6729.724360 b3,8 = b1,2
> Contddy := seq (powsubs
(theta=beta [i+1], ddy [i])=powsubs (theta=beta [i+1], d
y [i+1]), i=1..(n-2)), powsubs
(theta=beta [n], ddy [n-1])=powsubs (theta=beta [1], ddy [
1]);
Contddy := 2 b1,3 + 9.424777962 b1,4 + 29.60881321 b1,5
+ 77.51569174 b1,6 + 182.6420458 b1,7 + 401.6508366 b1,8 = 2 b2,3, 2 b2,3
+ 9.424777962 b2,4 + 29.60881321 b2,5 + 77.51569174 b2,6
+ 182.6420458 b2,7 + 401.6508366 b2,8 = 2 b3,3, 2 b3,3 + 18.84955592 b3,4
+ 118.4352528 b3,5 + 620.1255338 b3,6 + 2922.272732 b3,7
+ 12852.82677 b3,8 = 2 b1,3
> Contdddy := seq (powsubs
(theta=beta [i+1], dddy [i])=powsubs (theta=beta [i+1], d
ddy [i+1]), i=1..(n-2)), powsubs
(theta=beta [n], dddy [n-1])=powsubs (theta=beta [1], ddd
y [1]);
Contdddy := 6 b1,4 + 37.69911185 b1,5 + 148.0440661 b1,6
+ 465.0941504 b1,7 + 1278.494321 b1,8 = 6 b2,4, 6 b2,4 + 37.69911185 b2,5
+ 148.0440661 b2,6 + 465.0941504 b2,7 + 1278.494321 b2,8 = 6 b3,4, 6 b3,4
+ 75.39822370 b3,5 + 592.1762642 b3,6 + 3720.753203 b3,7
+ 20455.90913 b3,8 = 6 b1,4
> Contddddy := seq
(powsubs (theta=beta [i+1], ddddy [i])=powsubs
(theta=beta [i+1], ddddy [i+1]), i=1..(n-2)), powsubs
(theta=beta [n], ddddy [n-1])=powsubs
(theta=beta [1], ddddy [1]);
Contddddy :=
24 b1,5 + 188.4955592 b1,6 + 888.2643964 b1,7 + 3255.659053 b1,8 =
24 b2,5, 24 b2,5 + 188.4955592 b2,6 + 888.2643964 b2,7 + 3255.659053 b2,8
= 24 b3,5

```



```

24 b3,5 + 376.9911185 b3,6 + 3553.057585 b3,7 + 26045.27242 b3,8 =
24 b1,5
> for i to n-1 do Conty[i] od;
b1,1 + 1.570796327 b1,2 + 2.467401101 b1,3 + 3.875784587 b1,4
+ 6.088068193 b1,5 + 9.563115156 b1,6 + 15.02170616 b1,7
+ 23.59604086 b1,8 = b2,1
b2,1 + 1.570796327 b2,2 + 2.467401101 b2,3 + 3.875784587 b2,4
+ 6.088068193 b2,5 + 9.563115156 b2,6 + 15.02170616 b2,7
+ 23.59604086 b2,8 = b3,1
b3,1 + 3.141592654 b3,2 + 9.869604404 b3,3 + 31.00627669 b3,4
+ 97.40909108 b3,5 + 306.0196850 b3,6 + 961.3891943 b3,7
+ 3020.293231 b3,8 = b1,1
to solve the set of eqs, they need to be listed;
Wang uses Boundary and continuity conditions for displacemnt, Velocity,
Acceleration and s;
> eqs := Bouny , Boundy , Bounddy , Bounddddy, Conty
, Contdy , Contddy, Contddddy:
[ > bs := {seq( (seq(b[i,j], i=1..(n-1))), j=1..k)}:
Solve the set of equations listed above and generate expressions for each of the
coeffiecents (b's) in terms of the specifiable values for boundary conds.
[ > sols := solve( {eqs}, bs):
Assign the solution to each of the b's, filling the matrix initialised at the start.
> for i to (n-1) do for j to k do b[i,j] := subs(sols,
b[i,j]) od; od;
>
> for i to (n-1) do for j to k do print (b[i,j]) od;
od;
>

Disp1
Vel1
.5000000000 Accel1
- .7427230743 Accel1 - 1.756233874 Vel1 - 1.806085958 Disp1
- .004363323325 s2 + 1.806085958 Disp2 - .01745329194 s1
+ .2122065966 Accel2 - 1.080759315 Vel2
.04166666667 s1
- .03713615428 s1 + 1.806812914 Vel1 + .5160245611 Accel1
+ 2.195937214 Disp1 + .01061032984 s2 - 2.195937214 Disp2
- .3870184220 Accel2 + 1.642557196 Vel2

```

$$\begin{aligned}
& -1.115396681 \text{ Vel}_1 - .3011354862 \text{ Accel}_1 - 1.397977050 \text{ Disp}_1 \\
& \quad - .009006327632 s_2 + 1.397977050 \text{ Disp}_2 + .01463528267 s_1 \\
& \quad + .2737595326 \text{ Accel}_2 - 1.080540535 \text{ Vel}_2 \\
& .2542799520 \text{ Disp}_1 + .1997110074 \text{ Vel}_1 + .002150102332 s_2 \\
& \quad - .2542799520 \text{ Disp}_2 - .002150102406 s_1 + .05228421955 \text{ Accel}_1 \\
& \quad - .05228421937 \text{ Accel}_2 + .1997110072 \text{ Vel}_2 \\
& \qquad \qquad \qquad \text{Disp}_2 \\
& \qquad \qquad \qquad \text{Vel}_2 \\
& \qquad \qquad \qquad .5000000000 \text{ Accel}_2 \\
& .2122065966 \text{ Accel}_3 - 1.756233874 \text{ Vel}_2 - .7427230743 \text{ Accel}_2 \\
& \quad - 1.806085958 \text{ Disp}_2 - .004363323325 s_3 + 1.806085958 \text{ Disp}_3 \\
& \quad - .01745329194 s_2 - 1.080759315 \text{ Vel}_3 \\
& \qquad \qquad \qquad .04166666667 s_2 \\
& -.03713615428 s_2 + 1.806812914 \text{ Vel}_2 + .5160245611 \text{ Accel}_2 \\
& \quad + 2.195937214 \text{ Disp}_2 + .01061032984 s_3 - 2.195937214 \text{ Disp}_3 \\
& \quad - .3870184220 \text{ Accel}_3 + 1.642557196 \text{ Vel}_3 \\
& -1.115396681 \text{ Vel}_2 - .3011354862 \text{ Accel}_2 - 1.397977050 \text{ Disp}_2 \\
& \quad - .009006327632 s_3 + 1.397977050 \text{ Disp}_3 + .01463528267 s_2 \\
& \quad + .2737595326 \text{ Accel}_3 - 1.080540535 \text{ Vel}_3 \\
& .2542799520 \text{ Disp}_2 + .1997110074 \text{ Vel}_2 + .002150102332 s_3 \\
& \quad - .2542799520 \text{ Disp}_3 - .002150102406 s_2 + .05228421955 \text{ Accel}_2 \\
& \quad - .05228421937 \text{ Accel}_3 + .1997110072 \text{ Vel}_3 \\
& \qquad \qquad \qquad \text{Disp}_3 \\
& \qquad \qquad \qquad \text{Vel}_3 \\
& \qquad \qquad \qquad .5000000000 \text{ Accel}_3 \\
& .1061032976 \text{ Accel}_1 - .4390584670 \text{ Vel}_3 - .3713615365 \text{ Accel}_3 \\
& \quad - .2257607438 \text{ Disp}_3 - .008726646556 s_1 + .2257607438 \text{ Disp}_1 \\
& \quad - .03490658402 s_3 - .2701898274 \text{ Vel}_1 \\
& \qquad \qquad \qquad .04166666667 s_3 \\
& .005305164885 s_1 + .1129258065 \text{ Vel}_3 + .06450306986 \text{ Accel}_3 \\
& \quad + .06862303758 \text{ Disp}_3 - .06862303758 \text{ Disp}_1 - .01856807709 s_3 \\
& \quad - .04837730249 \text{ Accel}_1 + .1026598242 \text{ Vel}_1
\end{aligned}$$

```

-.03485614611 Vel3 - .01882096780 Accel3 - .02184339130 Disp3
  - .002251581897 s1 + .02184339130 Disp1 + .003658820654 s3
  + .01710997070 Accel1 - .03376689153 Vel1
.001986562114 Disp3 + .003120484474 Vel3 + .0002687627905 s1
  - .001986562114 Disp1 - .0002687627993 s3 + .001633881852 Accel3
  - .001633881847 Accel1 + .003120484471 Vel1

```

The Matrix becomes....

```
> evalm(b) :
```

■ Use this section only if NOT Optimising.

```

> condeqs := Disp[1]=0, Disp[2]=100, Disp[3]=100,
Disp[4]=0, Vel[1]=0, Vel[2]=0, Vel[3]=0, Vel[4]=0,
Accel[1]=0, Accel[2]=0,
Accel[3]=0, Accel[4]=0, s[1]=0, s[2]=0, s[3]=0, s[4]=
0;
condeqs := Disp1 = 0, Disp2 = 100, Disp3 = 100, Disp4 = 0, Vel1 = 0,
Vel2 = 0, Vel3 = 0, Vel4 = 0, Accel1 = 0, Accel2 = 0, Accel3 = 0, Accel4 = 0,
s1 = 0, s2 = 0, s3 = 0, s4 = 0
[ > with (linalg) :
> for i to rowdim(b) do
>   for j to coldim(b) do
>     b[i,j] := subs({condeqs}, b[i,j]);
>   od;
> od;
> evalm(b) ;
[0, 0, 0., 180.6085958, 0., -219.5937214, 139.7977050,
-25.42799520]
[100, 0, 0., 0., 0., 0., 0., 0.]
[100, 0, 0., -22.57607438, 0., 6.862303758, -2.184339130,
.1986562114]
> for i to n-1 do
>   y[i];
> od;
180.6085958 θ3 - 219.5937214 θ5 + 139.7977050 θ6 - 25.42799520 θ7
100.
100. - 22.57607438 (θ - 3.141592654)3
+ 6.862303758 (θ - 3.141592654)5 - 2.184339130 (θ - 3.141592654)6

```

```

+ .1986562114 (θ - 3.141592654)7

```

Plots included in Figure 6-1.

```

> ppy:=
  piecewise(theta<beta[2],y[1],theta<beta[3],y[2],theta<beta[4],y[3]):
> plot(ppy, theta=beta[1]..beta[4],
  title=Displacement);

> ppdy:=
  piecewise(theta<beta[2],dy[1],theta<beta[3],dy[2],theta<beta[4],dy[3]):
> plot(ppdy, theta=beta[1]..beta[4], title=Velocity);

> ppddy:=
  piecewise(theta<beta[2],ddy[1],theta<beta[3],ddy[2],theta<beta[4],ddy[3]):
> plot(ppddy, theta=beta[1]..beta[4],
  title=Acceleration);

> ppddy:=
  piecewise(theta<beta[2],ddy[1],theta<beta[3],ddy[2],theta<beta[4],ddy[3]):
> plot(ppddy, theta=beta[1]..beta[4], title=Jerk);

> ppddy:=
  piecewise(theta<beta[2],ddy[1],theta<beta[3],ddy[2],theta<beta[4],ddy[3]):
> plot(ppddy, theta=beta[1]..beta[4], title=s):

```

■ End of Example

**Appendix E. Program for Cam Optimisation
Case Study No 3.**

Initial Piecewise Polynomials and Definitions

```

[ > Digits:=10;
                                     Digits := 10
No of breakpoints
[ > n:=3;
                                     n := 3
[ No of equations including displacement and derivatives
  > T:=4;
                                     T:= 4
[ Order of the polynomial given by T and the conditions imposed on them in this
  case Boundary and continuity
  > k:=2*T;
                                     k:= 8
[ Initialise matrix for coefficients of the polynomial equations
  > b:=array(1..(n-1),1..k);
                                     b := array(1..2,1..8,[ ])
[ > betadeg:=array(1..n,[0,180,360]);
                                     betadeg := [0,180,360]
[ > beta:=array(1..n);
                                     β := array(1..3,[ ])
[ Use above if not defining values for betas and below if defining values
  > for i to n do beta[i]:=
    evalf(convert(betadeg[i]*degrees,radians)) od;
                                     β1 := 0
                                     β2 := 3.141592654
                                     β3 := 6.283185308
[ Define the equations for displacement and its derivatives
  y[i] is the displacement if beta[i]<=theta<=beta[i+1],
  > for i to (n-1) do
  >
    y[i] := (sum('b[i,j]*(theta-beta[i])^(j-1)', 'j'=1..k)
    );
  >     dy[i] := (diff(y[i],theta)) ;
  >     ddy[i] := (diff(dy[i],theta)) ;
  >     dddy[i] := (diff(ddy[i],theta)) ;
  >     dddy[i] := (diff(dddy[i],theta)) ;
  > od;
    y1 := b1,1 + b1,2 θ + b1,3 θ2 + b1,4 θ3 + b1,5 θ4 + b1,6 θ5 + b1,7 θ6 + b1,8 θ7
    dy1 := b1,2 + 2 b1,3 θ + 3 b1,4 θ2 + 4 b1,5 θ3 + 5 b1,6 θ4 + 6 b1,7 θ5 + 7 b1,8 θ6
    ddy1 := 2 b1,3 + 6 b1,4 θ + 12 b1,5 θ2 + 20 b1,6 θ3 + 30 b1,7 θ4 + 42 b1,8 θ5
    dddy1 := 6 b1,4 + 24 b1,5 θ + 60 b1,6 θ2 + 120 b1,7 θ3 + 210 b1,8 θ4

```

$$ddddy_1 := 24 b_{1,5} + 120 b_{1,6} \theta + 360 b_{1,7} \theta^2 + 840 b_{1,8} \theta^3$$

$$y_2 := b_{2,1} + b_{2,2} (\theta - 3.141592654) + b_{2,3} (\theta - 3.141592654)^2$$

$$+ b_{2,4} (\theta - 3.141592654)^3 + b_{2,5} (\theta - 3.141592654)^4$$

$$+ b_{2,6} (\theta - 3.141592654)^5 + b_{2,7} (\theta - 3.141592654)^6$$

$$+ b_{2,8} (\theta - 3.141592654)^7$$

$$dy_2 := b_{2,2} + 2 b_{2,3} (\theta - 3.141592654) + 3 b_{2,4} (\theta - 3.141592654)^2$$

$$+ 4 b_{2,5} (\theta - 3.141592654)^3 + 5 b_{2,6} (\theta - 3.141592654)^4$$

$$+ 6 b_{2,7} (\theta - 3.141592654)^5 + 7 b_{2,8} (\theta - 3.141592654)^6$$

$$ddy_2 := 2 b_{2,3} + 6 b_{2,4} (\theta - 3.141592654) + 12 b_{2,5} (\theta - 3.141592654)^2$$

$$+ 20 b_{2,6} (\theta - 3.141592654)^3 + 30 b_{2,7} (\theta - 3.141592654)^4$$

$$+ 42 b_{2,8} (\theta - 3.141592654)^5$$

$$ddd_2 := 6 b_{2,4} + 24 b_{2,5} (\theta - 3.141592654) + 60 b_{2,6} (\theta - 3.141592654)^2$$

$$+ 120 b_{2,7} (\theta - 3.141592654)^3 + 210 b_{2,8} (\theta - 3.141592654)^4$$

$$dddd_2 := 24 b_{2,5} + 120 b_{2,6} (\theta - 3.141592654)$$

$$+ 360 b_{2,7} (\theta - 3.141592654)^2 + 840 b_{2,8} (\theta - 3.141592654)^3$$

dy, ddy, ... are the displacement derivatives

Initialise arrays containing values for breakpoint angles and boundary conditions (i.e. Disp[i] is the displacement at beta[i], etc)

```
beta:=array(1..n);
```

```
> Disp:=array(1..n);
```

```
Disp:=array(1..3,[])
```

```
> Vel:=array(1..n);
```

```
Vel:=array(1..3,[])
```

```
> Accel:=array(1..n);
```

```
Accel:=array(1..3,[])
```

```
> Jerk:=array(1..n);
```

```
Jerk:=array(1..3,[])
```

```
> s:=array(1..n);
```

```
s:=array(1..3,[])
```

Define Boundary conditions in terms of the equations above

```
> with(student):
```

```
> Bouny:=seq(powsubs
(theta=beta[i],y[i])=Disp[i],i=1..(n-1));
```

```
> Boundy:=seq(powsubs
(theta=beta[i],dy[i])=Vel[i],i=1..(n-1));
```

```
> Bounddy:=seq(powsubs
(theta=beta[i],ddy[i])=Accel[i],i=1..(n-1));
```

```

> Boundddy:= seq(powsubs
  (theta=beta [i] , dddy [i])=Jerk [i] , i=1.. (n-1));
> Boundddy:= seq(powsubs
  (theta=beta [i] , dddy [i])=s [i] , i=1.. (n-1));
Warning, new definition for D
      Bouny := b1,1 = Disp1, b2,1 = Disp2
      Boundy := b1,2 = Vel1, b2,2 = Vel2
      Bounddy := 2 b1,3 = Accel1, 2 b2,3 = Accel2
      Boundddy := 6 b1,4 = Jerk1, 6 b2,4 = Jerk2
      Boundddd := 24 b1,5 = s1, 24 b2,5 = s2
Boundary conditions ensuring continuity in displacement and three of its
derivatives
> Conty :=seq (powsubs
  (theta=beta [i+1] , y [i])=powsubs (theta=beta [i+1] , y [i+
  1]) ,
  i=1.. (n-2)) , powsubs (theta=beta [n] , y [n-1])=powsubs (t
  heta=beta [1] , y [1]) ;
>
> Contdy :=seq (powsubs
  (theta=beta [i+1] , dy [i])=powsubs
  (theta=beta [i+1] , dy [i+1]) ,
  i=1.. (n-2)) , powsubs (theta=beta [n] , dy [n-1])=powsubs (
  theta=beta [1] , dy [1]) ;
>
> Contddy :=seq (powsubs
  (theta=beta [i+1] , ddy [i])=powsubs (theta=beta [i+1] , dd
  y [i+1]) , i=1.. (n-2)) , powsubs
  (theta=beta [n] , ddy [n-1])=powsubs (theta=beta [1] , ddy [
  1]) ;
>
> Contddd :=seq (powsubs
  (theta=beta [i+1] , dddy [i])=powsubs (theta=beta [i+1] , d
  ddy [i+1]) , i=1.. (n-2)) , powsubs
  (theta=beta [n] , dddy [n-1])=powsubs (theta=beta [1] , ddd
  y [1]) ;
> Contddd :=seq
  (powsubs (theta=beta [i+1] , dddy [i])=powsubs
  (theta=beta [i+1] , dddy [i+1]) , i=1.. (n-2)) , powsubs
  (theta=beta [n] , dddy [n-1])=powsubs
  (theta=beta [1] , dddy [1]) ;
Conty:= b1,1 + 3.141592654 b1,2 + 9.869604404 b1,3 + 31.00627669 b1,4
      + 97.40909108 b1,5 + 306.0196850 b1,6 + 961.3891943 b1,7
      + 3020.293231 b1,8 = b2,1, b2,1 + 3.141592654 b2,2 + 9.869604404 b2,3
      + 31.00627669 b2,4 + 97.40909108 b2,5 + 306.0196850 b2,6

```



```

+ 961.3891943 b2,7 + 3020.293231 b2,8 = b1,1
Contdy := b1,2 + 6.283185308 b1,3 + 29.60881321 b1,4 + 124.0251068 b1,5
+ 487.0454554 b1,6 + 1836.118110 b1,7 + 6729.724360 b1,8 = b2,2, b2,2
+ 6.283185308 b2,3 + 29.60881321 b2,4 + 124.0251068 b2,5
+ 487.0454554 b2,6 + 1836.118110 b2,7 + 6729.724360 b2,8 = b1,2
Contddy := 2 b1,3 + 18.84955592 b1,4 + 118.4352528 b1,5
+ 620.1255338 b1,6 + 2922.272732 b1,7 + 12852.82677 b1,8 = 2 b2,3, 2 b2,3
+ 18.84955592 b2,4 + 118.4352528 b2,5 + 620.1255338 b2,6
+ 2922.272732 b2,7 + 12852.82677 b2,8 = 2 b1,3
Contddd := 6 b1,4 + 75.39822370 b1,5 + 592.1762642 b1,6
+ 3720.753203 b1,7 + 20455.90913 b1,8 = 6 b2,4, 6 b2,4 + 75.39822370 b2,5
+ 592.1762642 b2,6 + 3720.753203 b2,7 + 20455.90913 b2,8 = 6 b1,4

```

```
Contddddy :=
```

```

24 b1,5 + 376.9911185 b1,6 + 3553.057585 b1,7 + 26045.27242 b1,8 =
24 b2,5, 24 b2,5 + 376.9911185 b2,6 + 3553.057585 b2,7 + 26045.27242 b2,8
= 24 b1,5

```

to solve the set of eqs, they need to be listed;

Wang uses Boundary and continuity conditions for displacement, Velocity, Acceleration and s;

```
> equs := Bouny , Boundy , Bounddy , Bounddddy, Conty
, Contdy , Contddy , Contddddy;
```

```
> bs := {seq( (seq(b[i,j], i=1..(n-1)), j=1..k))};
```

```
bs := {b1,1, b1,2, b1,3, b1,4, b1,5, b1,6, b1,7, b1,8, b2,1, b2,2, b2,3, b2,4, b2,5, b2,6,
b2,7, b2,8}
```

Solve the set of equations listed above and generate expressions for each of the coefficients (b's) in terms of the specifiable values for boundary conds.

```
> sols := solve( {equs}, bs);
```

Assign the solution to each of the b's, filling the matrix initialised at the start.

```
> for i to (n-1) do for j to k do b[i,j] := subs(sols,
b[i,j]) od; od;
```

The Matrix becomes....

```
> evalm(b);
```

```

[Disp1, Vel1, .5000000000 Accel1, -.3713615365 Accel1
-.03490658402 s1 - .4390584670 Vel1 - .2257607438 Disp1
-.008726646556 s2 + .1061032976 Accel2 - .2701898274 Vel2
+.2257607438 Disp2, .04166666667 s1, -.01856807709 s1
+.1129258065 Vel1 + .06450306986 Accel1 + .06862303758 Disp1

```

```

+ .005305164885 s2 - .04837730249 Accel2 + .1026598242 Vel2
- .06862303758 Disp2 , -.03485614611 Vel1 - .01882096780 Accel1
+ .003658820654 s1 - .02184339130 Disp1 - .002251581897 s2
+ .01710997070 Accel2 - .03376689153 Vel2 + .02184339130 Disp2 ,
.001986562114 Disp1 + .003120484474 Vel1 + .001633881852 Accel1
- .0002687627993 s1 + .0002687627905 s2 - .001633881847 Accel2
+ .003120484471 Vel2 - .001986562114 Disp2]
[Disp2 , Vel2 , .5000000000 Accel2 , -.3713615365 Accel2
- .03490658402 s2 - .4390584670 Vel2 - .2257607438 Disp2
- .008726646556 s1 + .1061032976 Accel1 - .2701898274 Vel1
+ .2257607438 Disp1 , .04166666667 s2 , -.01856807709 s2
+ .1129258065 Vel2 + .06450306986 Accel2 + .06862303758 Disp2
+ .005305164885 s1 - .04837730249 Accel1 + .1026598242 Vel1
- .06862303758 Disp1 , -.03485614611 Vel2 - .01882096780 Accel2
+ .003658820654 s2 - .02184339130 Disp2 - .002251581897 s1
+ .01710997070 Accel1 - .03376689153 Vel1 + .02184339130 Disp1 ,
.001986562114 Disp2 + .003120484474 Vel2 + .001633881852 Accel2
- .0002687627993 s2 + .0002687627905 s1 - .001633881847 Accel1
+ .003120484471 Vel1 - .001986562114 Disp1]
> for i to (k*(n-1)) do 'bs' , n, i, bs[i] od;
      bs, 3, 1, Disp1
      bs, 3, 2, Disp2
      bs, 3, 3, Vel1
      bs, 3, 4, Vel2
bs, 3, 5, -.3713615365 Accel1 - .03490658402 s1 - .4390584670 Vel1
- .2257607438 Disp1 - .008726646556 s2 + .1061032976 Accel2
- .2701898274 Vel2 + .2257607438 Disp2
      bs, 3, 6, .04166666667 s1
bs, 3, 7, -.01856807709 s1 + .1129258065 Vel1 + .06450306986 Accel1
+ .06862303758 Disp1 + .005305164885 s2 - .04837730249 Accel2
+ .1026598242 Vel2 - .06862303758 Disp2
bs, 3, 8, .001986562114 Disp2 + .003120484474 Vel2

```

```

+ .001633881852 Accel2 - .0002687627993 s2 + .0002687627905 s1
- .001633881847 Accel1 + .003120484471 Vel1 - .001986562114 Disp1
bs, 3, 9, .001986562114 Disp1 + .003120484474 Vel1
+ .001633881852 Accel1 - .0002687627993 s1 + .0002687627905 s2
- .001633881847 Accel2 + .003120484471 Vel2 - .001986562114 Disp2
bs, 3, 10, -.03485614611 Vel2 - .01882096780 Accel2 + .003658820654 s2
- .02184339130 Disp2 - .002251581897 s1 + .01710997070 Accel1
- .03376689153 Vel1 + .02184339130 Disp1
bs, 3, 11, -.03485614611 Vel1 - .01882096780 Accel1 + .003658820654 s1
- .02184339130 Disp1 - .002251581897 s2 + .01710997070 Accel2
- .03376689153 Vel2 + .02184339130 Disp2
bs, 3, 12, -.01856807709 s2 + .1129258065 Vel2 + .06450306986 Accel2
+ .06862303758 Disp2 + .005305164885 s1 - .04837730249 Accel1
+ .1026598242 Vel1 - .06862303758 Disp1
bs, 3, 13, -.3713615365 Accel2 - .03490658402 s2 - .4390584670 Vel2
- .2257607438 Disp2 - .008726646556 s1 + .1061032976 Accel1
- .2701898274 Vel1 + .2257607438 Disp1
bs, 3, 14, .5000000000 Accel2
bs, 3, 15, .04166666667 s2
bs, 3, 16, .5000000000 Accel1

```

Optimisation

Define an array w containing all the specifiable boundary values... make sure that those actually specified are at the beginning and the ones to be determined at the end.

```

> xx:=seq(Disp[gg], gg=1..(n-1)), seq(Vel[gg], gg=1..(n-1)), seq(Accel[gg], gg=1..(n-1)), seq(s[gg], gg=1..(n-1));

```

```

xx := Disp1, Disp2, Vel1, Vel2, Accel1, Accel2, s1, s2

```

```

> for i to n-1 do
>   Contddy[i];
> od;

```

```

-1.35456448 Disp1 + 1.35456448 Disp2 - 1.6211390 Vel1 - 2.6343508 Vel2
- .63661982 Accel1 + 2.228169226 Accel2 + .05235990 s1 + .2094395087 s2

```

```

= -2.228169219 Accel2 - .2094395041 s2 - 2.634350802 Vel2
- 1.354564463 Disp2 - .05235987934 s1 + .6366197856 Accel1
- 1.621138964 Vel1 + 1.354564463 Disp1
1.35456448 Disp1 - 1.35456448 Disp2 - 2.634350764 Vel1
- 1.62113904 Vel2 + 2.22816923 Accel1 - .63661982 Accel2
+ .2094395087 s1 + .05235990 s2 = -2.228169219 Accel1 - .2094395041 s1
- 2.634350802 Vel1 - 1.354564463 Disp1 - .05235987934 s2
+ .6366197856 Accel2 - 1.621138964 Vel2 + 1.354564463 Disp2
[ > with (linalg):
[ > with(student):
[ Warning, new definition for D
[ > for i to (n-1) do
[ >   cjvec[i]:=genmatrix([Contdddy[i]], [xx]):
[ > od:
[ > AA:=array(1..(n-1), 1..coldim(cjvec[1]));
[   AA:=array(1..2, 1..8, [])
[ > for i to n-1 do
[ >   for j to coldim(cjvec[1]) do
[ >     AA[i,j]:=cjvec[i][1,j];
[ >   od;
[ > od;
[ > evalm(AA);
[-2.709128943, 2.709128943, -.36 10-7, .2 10-8, -1.273239606,
  4.456338445, .1047197793, .4188790128]
[ 2.709128943, -2.709128943, .38 10-7, -.76 10-7, 4.456338449,
  -1.273239606, .4188790128, .1047197793]
[ > condeqs:=
Disp[1]=0, Disp[2]=100, Disp[3]=0, Vel[1]=0, Vel[2]=0, V
el[3]=0;
  condeqs := Disp1 = 0, Disp2 = 100, Disp3 = 0, Vel1 = 0, Vel2 = 0, Vel3 = 0
[ > ms:=4;
[   ms := 4
[ > xxs:=vector(ms);
[   xxs := array(1..4, [])
[ > xxd:=vector(coldim(cjvec[1])-ms);
[   xxd := array(1..4, [])
[ > for i to ms do
[ >   xxs[i]:=subs({condeqs}, xx[i]);
[ > od;
[   xxs1 := 0
[   xxs2 := 100

```

```

                                 $xxs_3 := 0$ 
                                 $xxs_4 := 0$ 
[ > evalm(xxs);
                                [0, 100, 0, 0]
[ > for i to coldim(cjvec[1]) - ms do
[ >    $xxd[i] := xx[i+ms]$ ;
[ > od;
                                 $xxd_1 := Accel_1$ 
                                 $xxd_2 := Accel_2$ 
                                 $xxd_3 := s_1$ 
                                 $xxd_4 := s_2$ 
[ > AAs:=array(1..(n-1), 1..ms);
                                AAs:=array(1..2, 1..4, [])
[ > AAd:=array(1..(n-1), 1..(coldim(cjvec[1]) - ms));
                                AAd:=array(1..2, 1..4, [])
[ > for i to (n-1) do
[ >   for j to ms do
[ >      $AAs[i, j] := AA[i, j]$ ;
[ >   od;
[ > od;
[ > evalm(AAs);
                                [
                                [-2.709128943  2.709128943   $-0.36 \cdot 10^{-7}$    $.2 \cdot 10^{-8}$ ]
                                [2.709128943  -2.709128943   $.38 \cdot 10^{-7}$    $-.76 \cdot 10^{-7}$ ]
                                ]
[ > for i to (n-1) do
[ >   for j to coldim(cjvec[1]) - ms do
[ >      $AAd[i, j] := AA[i, j+ms]$ ;
[ >   od;
[ > od;
[ > evalm(AAd);
                                [
                                [-1.273239606  4.456338445  .1047197793  .4188790128]
                                [4.456338449  -1.273239606  .4188790128  .1047197793]
                                ]
[ > BB:=multiply(AAs, xxs);
[ > BBneg:=vector(n-1);
[ > for i to (n-1) do
[ >    $BBneg[i] := BB[i] * (-1)$ ;
[ > od;
                                 $BBneg_1 := -270.9128943$ 
                                 $BBneg_2 := 270.9128943$ 
[ > with(linalg):
[ > AAdsys:=concat(AAd, BBneg);
AAdsys:=
                                [-1.273239606, 4.456338445, .1047197793, .4188790128, -270.9128943

```

```

]
[ 4.456338449, -1.273239606, .4188790128, .1047197793, 270.9128943]
> AAusys := ( gausselim(AAdsys, 'r', 'd'));
AAusys :=
[ 4.456338449, -1.273239606, .4188790128, .1047197793, 270.9128943]
[ 0, 4.092555686, .2243995018, .4487989509, -193.5092072]
> AAdu := submatrix(AAusys, 1..(n-1), 1..(n-1));
AAdu := 
$$\begin{bmatrix} 4.456338449 & -1.273239606 \\ 0 & 4.092555686 \end{bmatrix}$$

> AAdv := submatrix(AAusys, 1..(n-1),
(n-1+1)..coldim(cjvec[1]) - ms);
AAdv := 
$$\begin{bmatrix} .4188790128 & .1047197793 \\ .2243995018 & .4487989509 \end{bmatrix}$$

> BBap := submatrix(AAusys, 1..(n-1),
coldim(cjvec[1]) - ms + 1..coldim(cjvec[1]) - ms + 1);
BBap := 
$$\begin{bmatrix} 270.9128943 \\ -193.5092072 \end{bmatrix}$$

> GG := multiply(inverse(AAdu), AAdv);
> for i to rowdim(GG) do
>   GG := mulrow(GG, i, -1);
> od;
> evalm(GG);

$$\begin{bmatrix} -.1096622709 & -.05483114195 \\ -.05483114196 & -.1096622710 \end{bmatrix}$$

> rowdim(GG); coldim(GG);
2
2
> BBu := multiply(inverse(AAdu), BBap);
BBu := 
$$\begin{bmatrix} 47.28321905 \\ -47.28321911 \end{bmatrix}$$

> with(student):
Warning, new definition for D
> for i to (n-1) do
>   jvec[i] := genmatrix([dddy[i]], [xx]);
> od;
jvec1 :=
[4.117382255  $\theta^2$  - 1.354564463 - 2.621206956  $\theta^3$  + .4171780439  $\theta^4$ ,
1.354564463 - 4.117382255  $\theta^2$  + 2.621206956  $\theta^3$  - .4171780439  $\theta^4$ ,
-4.182737533  $\theta^3$  + .6553017395  $\theta^4$  - 2.634350802 + 6.775548390  $\theta^2$ ,
-4.052026984  $\theta^3$  - 1.621138964 + .6553017389  $\theta^4$  + 6.159589452  $\theta^2$ ,

```

```

-2.228169219 + .3431151889  $\theta^4$  - 2.258516136  $\theta^3$  + 3.870184192  $\theta^2$  ,
-2.902638149  $\theta^2$  + .6366197856 - .3431151879  $\theta^4$  + 2.053196484  $\theta^3$  ,
-1.114084625  $\theta^2$  - .2094395041 - .05644018785  $\theta^4$  + .4390584785  $\theta^3$ 
+ 1.000000000  $\theta$  ,
.3183098931  $\theta^2$  - .05235987934 + .05644018601  $\theta^4$  - .2701898276  $\theta^3$ ]
jvec2 :=
[-4.117382255 ( $\theta - 3.141592654$ )2 + 1.354564463
+ 2.621206956 ( $\theta - 3.141592654$ )3 - .4171780439 ( $\theta - 3.141592654$ )4 ,
-1.354564463 + 4.117382255 ( $\theta - 3.141592654$ )2
- 2.621206956 ( $\theta - 3.141592654$ )3 + .4171780439 ( $\theta - 3.141592654$ )4 ,
-4.052026984 ( $\theta - 3.141592654$ )3 + .6553017389 ( $\theta - 3.141592654$ )4
- 1.621138964 + 6.159589452 ( $\theta - 3.141592654$ )2 , -2.634350802
+ .6553017395 ( $\theta - 3.141592654$ )4 - 4.182737533 ( $\theta - 3.141592654$ )3
+ 6.775548390 ( $\theta - 3.141592654$ )2 , 2.053196484 ( $\theta - 3.141592654$ )3
+ .6366197856 - 2.902638149 ( $\theta - 3.141592654$ )2
- .3431151879 ( $\theta - 3.141592654$ )4 , -2.228169219
+ 3.870184192 ( $\theta - 3.141592654$ )2 - 2.258516136 ( $\theta - 3.141592654$ )3
+ .3431151889 ( $\theta - 3.141592654$ )4 , -.2701898276 ( $\theta - 3.141592654$ )3
+ .05644018601 ( $\theta - 3.141592654$ )4 + .3183098931 ( $\theta - 3.141592654$ )2
- .05235987934 , -.05644018785 ( $\theta - 3.141592654$ )4 - 3.351032158
+ .4390584785 ( $\theta - 3.141592654$ )3 + 1.000000000  $\theta$ 
- 1.114084625 ( $\theta - 3.141592654$ )2]
> for i to (n-1) do
>
EEE[i] := array(1..coldim(jvec[1]), 1..coldim(jvec[1])
);
> od;

EEE1 := array(1..8, 1..8, [])
EEE2 := array(1..8, 1..8, [])
> for m to (n-1) do
>   for i to coldim(jvec[1]) do for j to
coldim(jvec[1]) do EEE[m][i,j] :=
int(jvec[m][1,i]*jvec[m][1,j], theta=beta[m]..beta[m
+1]) od od;
> od;
[ > EE:= matrix (coldim(jvec[1]), coldim(jvec[1]), 0) :
[ > for i to n-1 do
[ >   EE:=matadd(EE, EEE[i]) :

```

```

[ > od:
[ > evalm(EE);
[4.940550110, -4.940550110, .00244158, .007143271, 4.059926609,
  -4.065368053, -.0316367756, .0318354477]
[-4.940550110, 4.940550110, -.00244158, -.007143271, -4.059926609,
  4.065368053, .0316367756, -.0318354477]
[.00244158, -.00244158, 12.96926523, 11.40411488, .00294215,
  -.004253114, -.000902609, -.0010623174]
[.007143271, -.007143271, 11.40411488, 12.97796608, -.00274467,
  .006115934, -.001578378, -.0001074070]
[4.059926609, -4.059926609, .00294215, -.00274467, 5.91298715,
  -2.044588661, -.044844001, .0078199680]
[-4.065368053, 4.065368053, -.004253114, .006115934, -2.044588661,
  5.909233828, .0077442200, -.0443899159]
[-.0316367756, .0316367756, -.000902609, -.001578378, -.044844001,
  .0077442200, .0195870541, .01117180780]
[.0318354477, -.0318354477, -.0010623174, -.0001074070, .0078199680
  , -.0443899159, .01117180780, .01980826452]
[ > ee21:=submatrix(EE, ms+1..coldim(cjvec[1]), 1..ms);
  ee21 :=
  [ 4.059926609  -4.059926609  .00294215  -0.00274467
    -4.065368053  4.065368053  -0.004253114  .006115934
    -0.0316367756  .0316367756  -0.000902609  -0.001578378
    .0318354477  -0.0318354477  -0.0010623174  -0.0001074070 ]
[ > rowdim(ee21);
  4
[ > coldim(ee21);
  4
[ > ee22:=submatrix(EE, ms+1..coldim(cjvec[1]),
  ms+1..coldim(cjvec[1]));
  ee22 :=
  [ 5.91298715  -2.044588661  -0.044844001  .0078199680
    -2.044588661  5.909233828  .0077442200  -0.0443899159
    -0.044844001  .0077442200  .0195870541  .01117180780
    .0078199680  -0.0443899159  .01117180780  .01980826452 ]
[ > rowdim(ee22);
  4
[ > coldim(ee22);
  4

```



```

[ > phi:=multiply(ee21,xxs);
  phi:=[-405.9926609,406.5368053,3.163677560,-3.183544770]
[ > type(phi,array);
  true
[ > BBux:=extend(BBu,(coldim(cjvec[1])-ms-(n-1)),0,
0);
  BBux:=

$$\begin{bmatrix} 47.28321905 \\ -47.28321911 \\ 0 \\ 0 \end{bmatrix}$$

[ > rowdim(BBux);
  4
[ > coldim(BBux);
  1
[ > tempmat3:=multiply(ee22,BBux);
  tempmat3:=

$$\begin{bmatrix} 376.2598004 \\ -376.0823314 \\ -2.486540373 \\ 2.468651380 \end{bmatrix}$$

[ > convert(phi,vector);
[ > tempmat:=matadd(phi,tempmat3);
[ > GGap:=stackmatrix(GG,diag(1,1));
  GGap:=

$$\begin{bmatrix} -0.1096622709 & -0.05483114195 \\ -0.05483114196 & -0.1096622710 \\ 1 & 0 \\ 0 & 1 \end{bmatrix}$$

[ > phiv:=multiply(transpose(GGap),tempmat);
  phiv:=

$$\begin{bmatrix} 2.267856608 \\ -2.424313465 \end{bmatrix}$$

[ > tempmat2:=multiply(ee22,GGap);
[ > Qv:=multiply(transpose(GGap),tempmat2);
  Qv:=

$$\begin{bmatrix} .09285967213 & .05470891860 \\ .05470891860 & .09293913139 \end{bmatrix}$$

[ > Xdv:=multiply(inverse(Qv),phiv);
[ > for i to rowdim(Xdv) do
[ >   Xdv:=mulrow(Xdv,i,-1);
[ > od:

```

```

> evalm(Xdv);
      [-60.91717035]
      [61.94404761]
> Xdu:=matadd((multiply(GG,Xdv)),BBu);
      Xdu:= [50.56707142]
            [-50.73598603]
> for i to coldim(cjvec[1])-ms do
>   xxd[i]:=stackmatrix(Xdu,Xdv)[i,1]:
> od:
> evalm(xxd);
      [50.56707142, -50.73598603, -60.91717035, 61.94404761]
>
> deseqs:=Accel[1]=xxd[1], Accel[2]=xxd[2], s[1]=xxd[3]
, s[2]=xxd[4];
deseqs:= Accel1 = 50.56707142, Accel2 = -50.73598603, s1 = -60.91717035,
s2 = 61.94404761
> for i to rowdim(b) do for j to coldim(b) do
>   b[i,j]:=subs({condeqs,deseqs}, b[i,j]):
>   od:
> od:
> evalm(b);
[0, 0, 25.28353571, .12 10-6, -2.538215431, .313635826, .002169576,
-.0001184602]
[100, 0, -25.36799302, -.107 10-6, 2.581001984, -.329979087,
-.0004355016, .00011846022]

```

Results and Plots

```

> jdes:=evalf(sum('int(ddd[i]^2,
theta=beta[i]..beta[i+1])', 'i'=1..n-1));
      jdes := 7842.711437
> for i to n-1 do
>   y[i];
> od;
25.28353571 θ2 + .12 10-6 θ3 - 2.538215431 θ4 + .313635826 θ5
+ .002169576 θ6 - .0001184602 θ7
100 - 25.36799302 (θ - 3.141592654)2 - .107 10-6 (θ - 3.141592654)3
+ 2.581001984 (θ - 3.141592654)4 - .329979087 (θ - 3.141592654)5
- .0004355016 (θ - 3.141592654)6 + .00011846022 (θ - 3.141592654)7

```

Plots included as figure 6-3

```

> ppy:=
  piecewise(theta<beta[2],y[1],theta<=beta[3],y[2]):
> plot(ppy, theta=beta[1]..beta[3],
  title=Displacement);

> ppdy:=
  piecewise(theta<beta[2],dy[1],theta<beta[3],dy[2]):
> plot(ppdy, theta=beta[1]..beta[3], title=Velocity);

> ppddy:=
  piecewise(theta<beta[2],ddy[1],theta<=beta[3],ddy[2]
  ):
> plot(ppddy, theta=beta[1]..beta[3],
  title=Acceleration);

> ppddy:=
  piecewise(theta<beta[2],ddy[1],theta<=beta[3],ddy[2]
  ):
> plot(ppddy, theta=beta[1]..beta[3], title=Jerk);

> ppddy:=
  piecewise(theta<beta[2],ddydy[1],theta<=beta[3],ddydy[2]
  ):
> plot(ppddy, theta=beta[1]..beta[3], title=s);

```

■ Proof of minimum: Trying different values for the dependent design variables (boundary conditions)

```

[ > b:=array(1..(n-1),1..k):
  Define the equations for displacement and its derivatives
  y[i] is the displacement if beta[i]<=theta<=beta[i+1],
  > for i to (n-1) do
  >
    y[i]:= (sum('b[i,j]*(theta-beta[i])^(j-1)', 'j'=1..k)
    ):
  >
    dy[i]:= (diff(y[i],theta)) :
  >
    ddy[i]:= (diff(dy[i],theta)) :
  >
    dddy[i]:= (diff(ddy[i],theta)) :
  >
    dddydy[i]:= (diff(dddy[i],theta)) :
  > od:
  dy, ddy, ... are the displacement derivatives
  Initialise arrays containing values for breakpoint angles and boundary
  conditions (i.e. Disp[i] is the displacement at beta[i],etc)
  beta:=array(1..n);
  > Disp:=array(1..n):
  > Vel:=array(1..n):
  > Accel:=array(1..n):
  > Jerk:= array(1..n):

```

```

| > s:=array(1..n):
| Define Boundary conditions in terms of the equations above
| > with(student):
| >   Bouny:= seq(powsubs
|   (theta=beta[i],y[i])=Disp[i],i=1..(n-1)):
| >   Boundy:= seq(powsubs
|   (theta=beta[i],dy[i])=Vel[i], i=1..(n-1)):
| >   Bounddy:= seq(powsubs
|   (theta=beta[i],ddy[i])=Accel[i],i=1..(n-1)):
| >   Boundddy:= seq(powsubs
|   (theta=beta[i],ddd[i])=Jerk[i],i=1..(n-1)):
| >   Boundddy:= seq(powsubs
|   (theta=beta[i],ddd[i])=s[i],i=1..(n-1)):
| Warning, new definition for D
| Boundary conditions ensuring continuity in displacement and three of its
| derivatives
|
| > Conty :=seq (powsubs
|   (theta=beta[i+1],y[i])=powsubs(theta=beta[i+1],y[i+
|   1]),
|   i=1..(n-2)),powsubs(theta=beta[n],y[n-1])=powsubs(t
|   heta=beta[1],y[1]):
| >
| > Contdy :=seq (powsubs
|   (theta=beta[i+1],dy[i])=powsubs
|   (theta=beta[i+1],dy[i+1]),
|   i=1..(n-2)),powsubs(theta=beta[n],dy[n-1])=powsubs(
|   theta=beta[1],dy[1]):
| >
| > Contddy :=seq (powsubs
|   (theta=beta[i+1],ddy[i])=powsubs(theta=beta[i+1],dd
|   y[i+1]), i=1..(n-2)),powsubs
|   (theta=beta[n],ddy[n-1])=powsubs(theta=beta[1],ddy[
|   1]):
| >
| > Contddy :=seq (powsubs
|   (theta=beta[i+1],ddy[i])=powsubs(theta=beta[i+1],d
|   ddy[i+1]), i=1..(n-2)),powsubs
|   (theta=beta[n],ddd[n-1])=powsubs(theta=beta[1],ddd
|   y[1]):
| > Contddy :=seq
|   (powsubs(theta=beta[i+1],ddd[i])=powsubs
|   (theta=beta[i+1],ddd[i+1]), i=1..(n-2)),powsubs
|   (theta=beta[n],ddd[n-1])=powsubs
|   (theta=beta[1],ddd[1]):
| to solve the set of eqs, they need to be listed;
| Wang uses Boundary and continuity conditions for displacemnt, Velocity,
| Acceleration and s;
| > eqs:= Bouny , Boundy , Bounddy , Boundddy, Conty
|   , Contdy , Contddy , Contddy:
| > bs:={seq( (seq(b[i,j], i=1..(n-1)), j=1..k))}:

```

```

[ Solve the set of equations listed above and generate expressions for each of the
  coefficients (b's) in terms of the specifiable values for boundary conds.
  > sols := solve( {equs}, bs) :
[ Assign the solution to each of the b's, filling the matrix initialised at the start.
  > for i to (n-1) do for j to k do b[i,j] := subs(sols,
  b[i,j]) od; od;

```

The Matrix becomes....

```

> evalm(b);
[Disp1, Vel1, .5000000000 Accel1, -.3713615365 Accel1
  -.03490658402 s1 - .4390584670 Vel1 - .2257607438 Disp1
  -.008726646556 s2 + .1061032976 Accel2 - .2701898274 Vel2
  + .2257607438 Disp2, .04166666667 s1, -.01856807709 s1
  + .1129258065 Vel1 + .06450306986 Accel1 + .06862303758 Disp1
  + .005305164885 s2 - .04837730249 Accel2 + .1026598242 Vel2
  -.06862303758 Disp2, -.03485614611 Vel1 - .01882096780 Accel1
  + .003658820654 s1 - .02184339130 Disp1 - .002251581897 s2
  + .01710997070 Accel2 - .03376689153 Vel2 + .02184339130 Disp2,
  .001986562114 Disp1 + .003120484474 Vel1 + .001633881852 Accel1
  -.0002687627993 s1 + .0002687627905 s2 - .001633881847 Accel2
  + .003120484471 Vel2 - .001986562114 Disp2]
[Disp2, Vel2, .5000000000 Accel2, -.3713615365 Accel2
  -.03490658402 s2 - .4390584670 Vel2 - .2257607438 Disp2
  -.008726646556 s1 + .1061032976 Accel1 - .2701898274 Vel1
  + .2257607438 Disp1, .04166666667 s2, -.01856807709 s2
  + .1129258065 Vel2 + .06450306986 Accel2 + .06862303758 Disp2
  + .005305164885 s1 - .04837730249 Accel1 + .1026598242 Vel1
  -.06862303758 Disp1, -.03485614611 Vel2 - .01882096780 Accel2
  + .003658820654 s2 - .02184339130 Disp2 - .002251581897 s1
  + .01710997070 Accel1 - .03376689153 Vel1 + .02184339130 Disp1,
  .001986562114 Disp2 + .003120484474 Vel2 + .001633881852 Accel2
  -.0002687627993 s2 + .0002687627905 s1 - .001633881847 Accel1
  + .003120484471 Vel1 - .001986562114 Disp1]
> xxd[1] := 49;
> xxd[2] := -50.73598605;
> xxd[3] := -60.91717044;

```

```

> xxd[4] := 61.94404762;
                                xxd1 := 49
                                xxd2 := -50.73598605
                                xxd3 := -60.91717044
                                xxd4 := 61.94404762
> deseqs := Accel[1] = xxd[1], Accel[2] = xxd[2], s[1] = xxd[3]
, s[2] = xxd[4];
> for i to rowdim(b) do
>   for j to coldim(b) do
>     b[i,j] := subs({condeqs, deseqs}, b[i,j]);
>   od;
> od;
deseqs :=
  Accel1 = 49, Accel2 = -50.73598605, s1 = -60.91717044, s2 = 61.94404762
> evalm(b);
[0, 0, 24.50000000, .58195018, -2.538215435, .212554912, .031663375
, -.0026788697]
[100, 0, -25.36799303, -.166271542, 2.581001984, -.254168401,
-.0272480465, .00267886974]

```

Results and Plots

```

> jdes := evalf(sum('int(ddd[y[i]^2,
theta=beta[i]..beta[i+1)]', 'i'=1..n-1));
                                jdes := 7858.563232
> for i to n-1 do
>   y[i];
> od;
24.50000000 θ2 + .58195018 θ3 - 2.538215435 θ4 + .212554912 θ5
+ .031663375 θ6 - .0026788697 θ7
100 - 25.36799303 (θ - 3.141592654)2 - .166271542 (θ - 3.141592654)3
+ 2.581001984 (θ - 3.141592654)4 - .254168401 (θ - 3.141592654)5
- .0272480465 (θ - 3.141592654)6 + .00267886974 (θ - 3.141592654)7
Plots included as Figure 6-4
> ppy :=
  piecewise(theta < beta[2], y[1], theta <= beta[3], y[2]);
> plot(ppy, theta = beta[1]..beta[3],
  title = Displacement);
> pppy :=
  piecewise(theta < beta[2], dy[1], theta < beta[3], dy[2]);
> plot(ppdy, theta = beta[1]..beta[3], title = Velocity);

```

```
[
  > ppddy:=
    piecewise(theta<beta[2],ddy[1],theta<=beta[3],ddy[2]
  ):
  > plot(ppddy, theta=beta[1]..beta[3],
    title=Acceleration);

  > ppddy:=
    piecewise(theta<beta[2],ddy[1],theta<=beta[3],ddy
    [2]):
  > plot(ppddy, theta=beta[1]..beta[3], title=Jerk);

  > ppddy:=
    piecewise(theta<beta[2],ddy[1],theta<=beta[3],ddd
    dy[2]):
  > plot(ppddy, theta=beta[1]..beta[3], title=s);
]
```

**Appendix F. Program for Warp Knitting Cam
Optimisation Case Study.**

Initial Piecewise Polynomials and Definitions

```
[ > Digits:=30:
[ > Amp:=1:
No of breakpoints
[ > n:=9:
[ No of equations including displacement and derivatives
[ > T:=4:
[ Order of the polynomial given by T and the conditions imposed on them in this
case Boundary and continuity
[ > k:=2*T:
[ Initialise matix for coefficients of the polynomial equations
[ > b:=array(1..(n-1),1..k):
[ > betadeg:=array(1..n,[0,45,60,90,180,210,225,
270,360]):
[ > beta:=array(1..n):
[ Use above if not defining values for betas and below if defining values
[ > for i to n do beta[i]:=
[   evalf(convert(betadeg[i]*degrees,radians)) od;
[ Define the equations for displacement and its derivatives
y[i] is the displacement if beta[i]<=theta<=beta[i+1],
> for i to (n-1) do
>
>   y[i]:= (sum('b[i,j]*(theta-beta[i])^(j-1)', 'j'=1..k)
>   );
>       dy[i]:= (diff(y[i],theta)) ;
>       ddy[i]:= (diff(dy[i],theta)) ;
>       dddy[i]:= (diff(ddy[i],theta));
>       ddddy[i]:= (diff(dddy[i],theta));
[ > od:
[ dy, ddy, ... are the displacement derivatives

Initialise arrays containing values for breakpoint angles and boundary
conditions (i.e. Disp[i] is the displacement at beta[i],etc)
beta:=array(1..n);
[ > Disp:=array(1..n):
[ > Vel:=array(1..n):
[ > Accel:=array(1..n):
[ > Jerk:= array(1..n):
[ > s:=array(1..n):
[ Define Boundary conditions in terms of the equations above
[ > with(student):
[ >   Bouny:= seq(powsubs
[   (theta=beta[i],y[i])=Disp[i],i=1..(n-1));
[ >   Boundy:= seq(powsubs
[   (theta=beta[i],dy[i])=Vel[i], i=1..(n-1));
[ >   Bounddy:= seq(powsubs
[   (theta=beta[i],ddy[i])=Accel[i],i=1..(n-1));
[ >   Boundddy:= seq(powsubs
```

```

    (theta=beta[i], dddy[i])=Jerk[i], i=1..(n-1));
  > Boundddy:= seq(powsubs
    (theta=beta[i], dddy[i])=s[i], i=1..(n-1));
  [ Boundary conditions ensuring continuity in displacement and three of its
  derivatives

  > Conty :=seq (powsubs
    (theta=beta[i+1], y[i])=powsubs(theta=beta[i+1], y[i+
    1]),
    i=1..(n-2)), powsubs(theta=beta[n], y[n-1])=powsubs(t
    heta=beta[1], y[1]);
  >
  > Contdy :=seq (powsubs
    (theta=beta[i+1], dy[i])=powsubs
    (theta=beta[i+1], dy[i+1]),
    i=1..(n-2)), powsubs(theta=beta[n], dy[n-1])=powsubs(
    theta=beta[1], dy[1]);
  >
  > Contddy :=seq (powsubs
    (theta=beta[i+1], ddy[i])=powsubs(theta=beta[i+1], dd
    y[i+1]), i=1..(n-2)), powsubs
    (theta=beta[n], ddy[n-1])=powsubs(theta=beta[1], ddy[
    1]);
  >
  > Contddy :=seq (powsubs
    (theta=beta[i+1], dddy[i])=powsubs(theta=beta[i+1], d
    ddy[i+1]), i=1..(n-2)), powsubs
    (theta=beta[n], dddy[n-1])=powsubs(theta=beta[1], ddd
    y[1]);
  > Contddy :=seq
    (powsubs(theta=beta[i+1], dddy[i])=powsubs
    (theta=beta[i+1], dddy[i+1]), i=1..(n-2)), powsubs
    (theta=beta[n], dddy[n-1])=powsubs
    (theta=beta[1], dddy[1]));
  [ to solve the set of eqs, they need to be listed;
  Wang uses Boundary and continuity conditions for displacement, Velocity,
  Acceleration and s;
  > eqs:= Bouny , Boundy , Bounddy , Boundddy, Conty
    , Contdy , Contddy , Contddy;
  [ > bs:={seq( (seq(b[i,j], i=1..(n-1)), j=1..k))};
  [ Solve the set of equations listed above and generate expressions for each of the
  coefficients (b's) in terms of the specifiable values for boundary conds.
  [ > sols := solve( {eqs}, bs):
  [ Assign the solution to each of the b's, filling the matrix initialised at the start.
  [ > for i to (n-1) do for j to k do b[i,j]:=subs(sols,
  [ b[i,j]) od; od;
  [ The Matrix becomes....
  [ > evalm(b);
  [ > for i to (k*(n-1)) do 'bs',n,i, bs[i] od;

```

Optimisation

```

Define an array w containing all the specifiable boundary values... make sure
that those actually specified are at the beginning and the ones to be determined
at the end.
> xx:=Disp[1],Disp[2],Disp[4],Disp[5],Disp[7],Disp[8]
  ,Vel[1],Vel[4],Vel[5],Vel[8],Accel[1],Accel[4],Acce
  l[5],Accel[8],s[1],s[4],s[5],s[8],s[2],s[3],s[6],s[
  7],Accel[2],Accel[3],Accel[6],Accel[7],Vel[2],Vel[3
  ],Vel[6],Vel[7],Disp[3],Disp[6];

[ > for i to n-1 do
  >   Contdddy[i];
  > od;
[ > with (linalg):
[ > with(student):
[ > for i to (n-1) do
  >   cjvec[i]:=genmatrix([Contdddy[i]],[xx]);
  > od;
[ > AA:=array(1..(n-1),1..coldim(cjvec[1])):
[ > for i to n-1 do
  >   for j to coldim(cjvec[1]) do
  >     AA[i,j]:=cjvec[i][1,j];
  >   od;
  > od;
[ > evalm(AA);
[ > condeqs:=Disp[1]=Amp*0,Disp[2]=Amp*0.4185,Disp[4]=A
  mp*0.837,Disp[5]=Amp*0.837,Disp[7]=Amp*0.4185,Disp[
  8]=Amp*0,Vel[1]=0,Vel[4]=0,Vel[5]=0,Vel[8]=0,Accel[
  1]=0,Accel[4]=0,Accel[5]=0,Accel[8]=0,s[1]=0,s[4]=0
  ,s[5]=0,s[8]=0;
[ > ms:=18:
[ > xxs:=vector(ms):
[ > xxd:=vector(coldim(cjvec[1])-ms):
[ > for i to ms do
  >   xxs[i]:=subs({condeqs},xx[i]);
  > od;
[ > evalm(xxs):
[ > for i to coldim(cjvec[1])-ms do
  >   xxd[i]:=xx[i+ms];
  > od;
[ > AAs:=array(1..(n-1),1..ms):
[ > AAD:=array(1..(n-1),1..(coldim(cjvec[1])-ms)):
[ > for i to (n-1) do
  >   for j to ms do
  >     AAs[i,j]:=AA[i,j];
  >   od;
  > od;
[ > evalm(AAs);
[

```

```

[ > for i to (n-1) do
[ >     for j to coldim(cjvec[1])-ms do
[ >         AAd[i,j]:=AA[i,j+ms];
[ >     od;
[ > od;
[ > evalm(AAd);
[ > rowdim(AAd);coldim(AAd);
[ >
[ > BB:=multiply(AAs,xxs);
[ > BBneg:=vector(n-1);
[ > for i to (n-1) do
[ >     BBneg[i]:=BB[i]*(-1);
[ > od;
[ > with(linalg):
[ > AAdsys:=concat(AAd,BBneg);
[ > AAusys:=(gausselim(AAdsys,'r','d'));
[ > AAdu:=submatrix(AAusys,1..(n-1),1..(n-1));
[ > AAdv:=submatrix(AAusys,1..(n-1),
[ >     (n-1+1)..coldim(cjvec[1])-ms);
[ > BBap:=submatrix(AAusys,1..(n-1),
[ >     coldim(cjvec[1])-ms+1..coldim(cjvec[1])-ms+1);
[ > GG:=multiply(inverse(AAdu),AAdv);
[ > for i to rowdim(GG) do
[ >     GG:=mulrow(GG,i,-1);
[ > od;
[ > evalm(GG);
[ > rowdim(GG):coldim(GG);
[ > BBU:=multiply(inverse(AAdu),BBap);
[ > with(student):
[ > for i to (n-1) do
[ >     jvec[i]:=genmatrix([dddy[i]],[xx]);
[ > od;
[ > for i to (n-1) do
[ >
[ >     EEE[i]:=array(1..coldim(jvec[1]),1..coldim(jvec[1])
[ >     );
[ > od;
[ > for m to (n-1) do
[ >     for i to coldim(jvec[1]) do for j to
[ >     coldim(jvec[1]) do EEE[m][i,j]:=
[ >     int(jvec[m][1,i]*jvec[m][1,j],theta=beta[m]..beta[m]
[ >     +1) od od;
[ > od;
[ > EE:=matrix(coldim(jvec[1]),coldim(jvec[1]),0);
[ > for i to n-1 do
[ >     EE:=matadd(EE,EEE[i]);
[ > od;
[ > evalm(EE);
[ > ee21:=submatrix(EE,ms+1..coldim(cjvec[1]),1..ms);
[ > rowdim(ee21);
[

```

```

[ > coldim(ee21);
[ > ee22:=submatrix(EE, ms+1..coldim(cjvec[1]),
[   ms+1..coldim(cjvec[1]));
[ > rowdim(ee22);
[ > coldim(ee22);
[ > phi:=multiply(ee21,xxs);
[ > type(phi,array);
[ > BBux:=extend(BBu, (coldim(cjvec[1])-ms-(n-1)),
[   0,0);
[ > rowdim(BBux);
[ > coldim(BBux);
[ > tempmat3:=multiply(ee22,BBux);
[ > convert(phi,vector);
[ > tempmat:=matadd((phi), tempmat3);
[ > GGap:=stackmatrix(GG, diag(1,1,1,1,1,1));
[ > phiv:=multiply(transpose(GGap),tempmat);
[ > tempmat2:=multiply(ee22,GGap);
[ > Qv:=multiply(transpose(GGap),tempmat2);
[ > Xdv:=multiply(inverse(Qv),phiv);
[ > for i to rowdim(Xdv) do
[ >   Xdv:=mulrow(Xdv, i, -1);
[ > od;
[ > evalm(Xdv);
[ > Xdu:=matadd((multiply(GG,Xdv)),BBu);
[ > for i to coldim(cjvec[1])-ms do
[ >   xxd[i]:=stackmatrix(Xdu,Xdv)[i,1];
[ > od;
[ > evalm(xxd);
[ >
[ > deseqs:=s[2]=xxd[1],s[3]=xxd[2],s[6]=xxd[3],s[7]=xx
[   d[4],Accel[2]=xxd[5],Accel[3]=xxd[6],Accel[6]=xxd[7
[   ],Accel[7]=xxd[8],Vel[2]=xxd[9],Vel[3]=xxd[10],Vel[
[   6]=xxd[11],Vel[7]=xxd[12],Disp[3]=xxd[13],
[   Disp[6]=xxd[14];
[ > for i to rowdim(b) do for j to coldim(b) do
[ >   b[i,j]:=subs({condeqs,deseqs}, b[i,j]);
[ >   od;
[ > od;
[ > evalm(b);

```

Results and Plots

```

[ > jdes:=evalf(sum('int(dddy[i]^2,
[   theta=beta[i]..beta[i+1])', 'i'=1..n-1));
[ > for i to n-1 do
[ >   y[i];
[ > od;
[ > ppy:=
[   piecewise(theta<beta[2],y[1],theta<=beta[3],y[2],th

```

```

eta<=beta[4],y[3],theta<=beta[5],y[4],theta<=beta[6
],y[5],theta<=beta[7],y[6],theta<=beta[8],y[7],thet
a<=beta[9],y[8]):
> plot(ppy, theta=beta[1]..beta[9],
title=Displacement);
> ppdy:=
piecewise(theta<beta[2],dy[1],theta<beta[3],dy[2],t
heta<=beta[4],dy[3],theta<=beta[5],dy[4],theta<=bet
a[6],dy[5],theta<=beta[7],dy[6],theta<=beta[8],dy[7
],theta<=beta[9],dy[8]):
> plot(ppdy, theta=beta[1]..beta[9], title=Velocity);
> ppddy:=
piecewise(theta<beta[2],ddy[1],theta<=beta[3],ddy[2
],theta<=beta[4],ddy[3],theta<=beta[5],ddy[4],theta
<=beta[6],ddy[5],theta<=beta[7],ddy[6],theta<=beta[
8],ddy[7],theta<=beta[9],ddy[8]):
> plot(ppddy, theta=beta[1]..beta[9],
title=Acceleration);
> ppddd:=
piecewise(theta<beta[2],ddd[1],theta<=beta[3],ddd[
2],theta<=beta[4],ddd[3],theta<=beta[5],ddd[4],t
heta<=beta[6],ddd[5],theta<=beta[7],ddd[6],theta<
=beta[8],ddd[7],theta<=beta[9],ddd[8]):
> plot(ppddd, theta=beta[1]..beta[9], title=Jerk);
> ppdddd:=
piecewise(theta<beta[2],dddd[1],theta<=beta[3],ddd
dy[2],theta<=beta[4],dddd[3],theta<=beta[5],dddd[
4],theta<=beta[6],dddd[5],theta<=beta[7],dddd[6],
theta<=beta[8],dddd[7],theta<=beta[9],dddd[8]):
> plot(ppdddd, theta=beta[1]..beta[9], title=s);

```

■ Proof of minimum by design variables Plots

■ PP and Boundaries

```

[ > b:=array(1..(n-1),1..k):
  Define the equations for displacement and its derivatives
  y[i] is the displacement if beta[i]<=theta<=beta[i+1],
  > for i to (n-1) do
  >
  y[i]:= (sum('b[i,j]*(theta-beta[i])^(j-1)', 'j'=1.
.k)):
  > dy[i]:= (diff(y[i],theta)) :
  > ddy[i]:= (diff(dy[i],theta)) :
  > dddy[i]:= (diff(ddy[i],theta)):
  > dddd[i]:= (diff(dddy[i],theta)):
  > od:
  dy, ddy, ... are the displacement derivatives
  Initialise arrays containing values for breakpoint angles and boundary
  conditions (i.e. Disp[i] is the displacement at beta[i],etc)

```

```

beta:=array(1..n);
> Disp:=array(1..n):
> Vel:=array(1..n):
> Accel:=array(1..n):
> Jerk:= array(1..n):
> s:=array(1..n):
Define Boundary conditions in terms of the equations above
> with(student):
>     Bouny:= seq(powsubs
(theta=beta[i],y[i])=Disp[i],i=1..(n-1)):
>     Boundy:= seq(powsubs
(theta=beta[i],dy[i])=Vel[i], i=1..(n-1)):
>     Bounddy:= seq(powsubs
(theta=beta[i],ddy[i])=Accel[i],i=1..(n-1)):
>     Boundddy:= seq(powsubs
(theta=beta[i],ddd[i])=Jerk[i],i=1..(n-1)):
>     Boundddd:= seq(powsubs
(theta=beta[i],dddd[i])=s[i],i=1..(n-1)):
Boundary conditions ensuring continuity in displacement and three of its
derivatives
> Conty :=seq (powsubs
(theta=beta[i+1],y[i])=powsubs(theta=beta[i+1],y
[i+1]),
i=1..(n-2)),powsubs(theta=beta[n],y[n-1])=powsub
s(theta=beta[1],y[1]):
>
> Contdy :=seq (powsubs
(theta=beta[i+1],dy[i])=powsubs
(theta=beta[i+1],dy[i+1]),
i=1..(n-2)),powsubs(theta=beta[n],dy[n-1])=powsu
bs(theta=beta[1],dy[1]):
>
> Contddy :=seq (powsubs
(theta=beta[i+1],ddy[i])=powsubs(theta=beta[i+1]
,ddy[i+1]), i=1..(n-2)),powsubs
(theta=beta[n],ddy[n-1])=powsubs(theta=beta[1],d
dy[1]):
>
> Contddd :=seq (powsubs
(theta=beta[i+1],ddd[i])=powsubs(theta=beta[i+1]
],ddd[i+1]), i=1..(n-2)),powsubs
(theta=beta[n],ddd[n-1])=powsubs(theta=beta[1],
ddd[1]):
> Contdddd :=seq
(powsubs(theta=beta[i+1],dddd[i])=powsubs
(theta=beta[i+1],dddd[i+1]),
i=1..(n-2)),powsubs
(theta=beta[n],dddd[n-1])=powsubs
(theta=beta[1],dddd[1]):

```

```

[ to solve the set of eqs, they need to be listed;
Wang uses Boundary and continuity conditions for displacement, Velocity,
Acceleration and s;
[ > eqs:= Bouny , Boundy , Bounddy , Bounddddy,
  Conty , Contdy , Contddy , Contddddy:
[ > bs:={seq( (seq(b[i,j], i=1..(n-1)), j=1..k))}:
[ Solve the set of equations listed above and generate expressions for each of
the coefficients (b's) in terms of the specifiable values for boundary
conds.
[ > sols := solve( {eqs},bs):
[ Assign the solution to each of the b's, filling the matrix initialised at the
start.
[ > for i to (n-1) do for j to k do
  b[i,j]:=subs(sols, b[i,j]) od; od;

```

The Matrix becomes....

```

[ >
[ > evalm(b);

```

■ Optimisation

```

[ Define an array w containing all the specifiable boundary values... make
sure that those actually specified are at the beginning and the ones to be
determined at the end.
[ > xx;
[ >
[ > for i to n-1 do
  > Contdddy[i];
  > od;
[ > with( linalg):
[ > with(student):
[ > for i to (n-1) do
  > cjvec[i]:=genmatrix([Contdddy[i]], [xx]):
  > od:
[ > AA:=array(1..(n-1), 1..coldim(cjvec[1]));
[ > for i to n-1 do
  > for j to coldim(cjvec[1]) do
  > AA[i,j]:= cjvec[i][1,j];
  > od;
  > od;
[ > evalm(AA);
[ > condeqs;
[ > ms;
[ > xxs:=vector(ms);

```



```

[ > xxd:=vector(coldim(cjvec[1])-ms);
[ > for i to ms do
[ >     xxs[i]:=subs({condeqs},xx[i]);
[ > od;
[ > evalm(xxs);
[ >
[ > AAs:=array(1..(n-1),1..ms);
[ > AAd:=array(1..(n-1),1..(coldim(cjvec[1])-ms));
[ > for i to (n-1) do
[ >     for j to ms do
[ >         AAs[i,j]:=AA[i,j];
[ >     od;
[ > od;
[ > evalm(AAs);
[ > for i to (n-1) do
[ >     for j to coldim(cjvec[1])-ms do
[ >         AAd[i,j]:=AA[i,j+ms];
[ >     od;
[ > od;
[ > evalm(AAd);
[ > BB:=multiply(AAs,xxs);
[ > BBneg:=vector(n-1);
[ > for i to (n-1) do
[ >     BBneg[i]:=BB[i]*(-1);
[ > od;
[ > with(linalg):
[ > AAdsys:=concat(AAd,BBneg);
[ > AAusys:=(gausselim(AAdsys,'r','d'));
[ > AAdu:=submatrix(AAusys,1..(n-1),1..(n-1));
[ > AAdv:=submatrix(AAusys,1..(n-1),
[ >     (n-1+1)..coldim(cjvec[1])-ms);
[ > BBap:=submatrix(AAusys,1..(n-1),
[ >     coldim(cjvec[1])-ms+1..coldim(cjvec[1])-ms+1);
[ > GG:=multiply(inverse(AAdu),AAdv);
[ > for i to rowdim(GG) do
[ >     GG:=mulrow(GG,i,-1);
[ > od;
[ > evalm(GG);
[ > rowdim(GG);coldim(GG);
[ > BBu:=multiply(inverse(AAdu),BBap);
[ > with(student):
[ > for i to (n-1) do
[ >     jvec[i]:=genmatrix([dddy[i]],[xx]);
[ > od;
[ > for i to (n-1) do
[ >
[ >     EEE[i]:=array(1..coldim(jvec[1]),1..coldim(jvec[
[ >     1]));
[ > od;
[ > for m to (n-1) do

```

```

>      for i to coldim(jvec[1]) do for j to
coldim(jvec[1]) do EEE[m][i,j]:=
int(jvec[m][1,i]*jvec[m][1,j],theta=beta[m]..bet
a[m+1]) od od;
> od;
[ > EE:= matrix (coldim(jvec[1]),coldim(jvec[1]),0):
[ > for i to n-1 do
[ >      EE:=matadd(EE,EEE[i]):
[ > od:
[ > evalm(EE);
[ > ee21:=submatrix(EE, ms+1..coldim(cjvec[1]),
[ 1..ms);
[ > rowdim(ee21);
[ > coldim(ee21);
[ > ee22:=submatrix(EE, ms+1..coldim(cjvec[1]),
[ ms+1..coldim(cjvec[1]));
[ > rowdim(ee22);
[ > coldim(ee22);
[ > phi:=multiply(ee21,xxs);
[ > type(phi,array);
[ > BBux:=extend(BBu, (coldim(cjvec[1])-ms-(n-1)),
[ 0, 0);
[ > rowdim(BBux);
[ > coldim(BBux);
[ > tempmat3:=multiply(ee22,BBux);
[ > convert(phi,vector):
[ > tempmat:= matadd(phi, tempmat3):
[ > GGap:=stackmatrix(GG, diag(1,1,1,1,1,1));
[ > phiv:=multiply(transpose(GGap), tempmat);
[ > tempmat2:=multiply(ee22,GGap):
[ > Qv:=multiply(transpose(GGap), tempmat2);
[ > Xdv:=multiply(inverse(Qv), phiv):
[ > for i to rowdim(Xdv) do
[ >      Xdv:= mulrow(Xdv, i, -1):
[ > od:
[ > evalm(Xdv);
[ > Xdu:=matadd( (multiply(GG,Xdv)), BBu);

[ > xxdd:=vector(coldim(cjvec[1])-ms);
[ > for i to coldim(cjvec[1])-ms do
[ >      xxdd[i]:=stackmatrix(Xdu,Xdv)[i,1]:
[ > od:
[ > evalm(xxdd);

[ > evalm(xxdd);
[ > exeqs:=s[2]=xxd[1],s[3]=xxd[2],s[6]=xxd[3],s[7]=
xxd[4],Accel[2]=xxd[5],Accel[3]=xxd[6],Accel[6]=
xxd[7],Accel[7]=xxd[8],Vel[2]=xxd[9],Vel[3]=xxd[

```

```

10], Vel[6]=xxd[11], Vel[7]=xxd[12], Disp[3]=xxd[13
], Disp[6]=xxd[14];
> for i to rowdim(b) do for j to coldim(b) do
>     b[i,j]:=subs({condeqs,exeqs},
b[i,j]):
>     od: od:
> evalm(b):
> deseqs:=array(1..coldim(cjvec[1])-ms):
> deseqs[1]:=xxd[2]=xxdd[2], xxd[3]=xxdd[3], xxd[4]=
xxdd[4], xxd[5]=xxdd[5], xxd[6]=xxdd[6], xxd[7]=xxd
d[7], xxd[8]=xxdd[8], xxd[9]=xxdd[9], xxd[10]=xxdd[
10], xxd[11]=xxdd[11], xxd[12]=xxdd[12], xxd[13]=xx
dd[13], xxd[14]=xxdd[14]:
> deseqs[2]:=xxd[1]=xxdd[1], xxd[3]=xxdd[3], xxd[4]=
xxdd[4], xxd[5]=xxdd[5], xxd[6]=xxdd[6], xxd[7]=xxd
d[7], xxd[8]=xxdd[8], xxd[9]=xxdd[9], xxd[10]=xxdd[
10], xxd[11]=xxdd[11], xxd[12]=xxdd[12], xxd[13]=xx
dd[13], xxd[14]=xxdd[14]:
> deseqs[3]:=xxd[1]=xxdd[1], xxd[2]=xxdd[2], xxd[4]=
xxdd[4], xxd[5]=xxdd[5], xxd[6]=xxdd[6], xxd[7]=xxd
d[7], xxd[8]=xxdd[8], xxd[9]=xxdd[9], xxd[10]=xxdd[
10], xxd[11]=xxdd[11], xxd[12]=xxdd[12], xxd[13]=xx
dd[13], xxd[14]=xxdd[14]: deseqs[4]:=xxd[1]=xxdd[1
], xxd[2]=xxdd[2], xxd[3]=xxdd[3], xxd[5]=xxdd[5], x
xd[6]=xxdd[6], xxd[7]=xxdd[7], xxd[8]=xxdd[8], xxd[
9]=xxdd[9], xxd[10]=xxdd[10], xxd[11]=xxdd[11], xxd
[12]=xxdd[12], xxd[13]=xxdd[13], xxd[14]=xxdd[14]:
> deseqs[5]:=xxd[1]=xxdd[1], xxd[2]=xxdd[2], xxd[3]=
xxdd[3], xxd[4]=xxdd[4], xxd[6]=xxdd[6], xxd[7]=xxd
d[7], xxd[8]=xxdd[8], xxd[9]=xxdd[9], xxd[10]=xxdd[
10], xxd[11]=xxdd[11], xxd[12]=xxdd[12], xxd[13]=xx
dd[13], xxd[14]=xxdd[14];
> deseqs[6]:=xxd[1]=xxdd[1], xxd[2]=xxdd[2], xxd[3]=
xxdd[3], xxd[4]=xxdd[4], xxd[5]=xxdd[5], xxd[7]=xxd
d[7], xxd[8]=xxdd[8], xxd[9]=xxdd[9], xxd[10]=xxdd[
10], xxd[11]=xxdd[11], xxd[12]=xxdd[12], xxd[13]=xx
dd[13], xxd[14]=xxdd[14];
> deseqs[7]:=xxd[1]=xxdd[1], xxd[2]=xxdd[2], xxd[3]=
xxdd[3], xxd[4]=xxdd[4], xxd[5]=xxdd[5], xxd[6]=xxd
d[6], xxd[8]=xxdd[8], xxd[9]=xxdd[9], xxd[10]=xxdd[
10], xxd[11]=xxdd[11], xxd[12]=xxdd[12], xxd[13]=xx
dd[13], xxd[14]=xxdd[14];
> deseqs[8]:=xxd[1]=xxdd[1], xxd[2]=xxdd[2], xxd[3]=
xxdd[3], xxd[4]=xxdd[4], xxd[5]=xxdd[5], xxd[6]=xxd
d[6], xxd[7]=xxdd[7], xxd[9]=xxdd[9], xxd[10]=xxdd[
10], xxd[11]=xxdd[11], xxd[12]=xxdd[12], xxd[13]=xx
dd[13], xxd[14]=xxdd[14];
> deseqs[9]:=xxd[1]=xxdd[1], xxd[2]=xxdd[2], xxd[3]=
xxdd[3], xxd[4]=xxdd[4], xxd[5]=xxdd[5], xxd[6]=xxd
d[6], xxd[7]=xxdd[7], xxd[8]=xxdd[8], xxd[10]=xxdd[

```

```

10],xxd[11]=xxdd[11],xxd[12]=xxdd[12],xxd[13]=xx
dd[13],xxd[14]=xxdd[14];
> deseqs[10]:=xxd[1]=xxdd[1],xxd[2]=xxdd[2],xxd[3]
=xxdd[3],xxd[4]=xxdd[4],xxd[5]=xxdd[5],xxd[6]=xx
dd[6],xxd[7]=xxdd[7],xxd[8]=xxdd[8],xxd[9]=xxdd[
9],xxd[11]=xxdd[11],xxd[12]=xxdd[12],xxd[13]=xxd
d[13],xxd[14]=xxdd[14];
> deseqs[11]:=xxd[1]=xxdd[1],xxd[2]=xxdd[2],xxd[3]
=xxdd[3],xxd[4]=xxdd[4],xxd[5]=xxdd[5],xxd[6]=xx
dd[6],xxd[7]=xxdd[7],xxd[8]=xxdd[8],xxd[9]=xxdd[
9],xxd[10]=xxdd[10],xxd[12]=xxdd[12],xxd[13]=xxd
d[13],xxd[14]=xxdd[14];
> deseqs[12]:=xxd[1]=xxdd[1],xxd[2]=xxdd[2],xxd[3]
=xxdd[3],xxd[4]=xxdd[4],xxd[5]=xxdd[5],xxd[6]=xx
dd[6],xxd[7]=xxdd[7],xxd[8]=xxdd[8],xxd[9]=xxdd[
9],xxd[10]=xxdd[10],xxd[11]=xxdd[11],xxd[13]=xxd
d[13],xxd[14]=xxdd[14];
> deseqs[13]:=xxd[1]=xxdd[1],xxd[2]=xxdd[2],xxd[3]
=xxdd[3],xxd[4]=xxdd[4],xxd[5]=xxdd[5],xxd[6]=xx
dd[6],xxd[7]=xxdd[7],xxd[8]=xxdd[8],xxd[9]=xxdd[
9],xxd[10]=xxdd[10],xxd[11]=xxdd[11],xxd[12]=xxd
d[12],xxd[14]=xxdd[14];
> deseqs[14]:=xxd[1]=xxdd[1],xxd[2]=xxdd[2],xxd[3]
=xxdd[3],xxd[4]=xxdd[4],xxd[5]=xxdd[5],xxd[6]=xx
dd[6],xxd[7]=xxdd[7],xxd[8]=xxdd[8],xxd[9]=xxdd[
9],xxd[10]=xxdd[10],xxd[11]=xxdd[11],xxd[12]=xxd
d[12],xxd[13]=xxdd[13];
> bb:=array(1..coldim(cjvec[1])-ms);
> for kkk to (coldim(cjvec[1])-ms) do
>   for i to rowdim(b) do for j to coldim(b) do
>
>   bb[kkk][i,j]:=subs({condeqs,deseqs[kkk]},
>   b[i,j]):
>   od: od:
>   for i to (n-1) do
>
>   y[i]:=sum('bb[kkk][i,j]*(theta-beta[i])^(j-1)',
>   'j'=1..k):
>
>   dy[i]:=diff(y[i],theta):
>   ddy[i]:=diff(dy[i],theta):
>   dddy[i]:=diff(ddy[i],theta):
>   ddddy[i]:=diff(dddy[i],theta):
>   od:
>   jdes:=evalf(sum('int(dddy[h]^2,
>   theta=beta[h]..beta[h+1])','h'=1..n-1)):
>   plot(jdes,xxd[kkk]=-20..20);
> od;

```

Appendix G. Program for Geometric Model of the Shog Movements.

GEOMETRIC MODEL OF SHOG MOVEMENTS

```
> with(geometry):
> with(student);
> with(linalg):
> with(geom3d):
```

Definitions

Radius of the patterning ring:

```
RR := 1.595
```

Verge Radius:

```
> RV:=1.347;
```

Radius of the top of the cylinder:

```
> RN:=1.492;
```

Last needle the underlap will cover:

```
> N:=0;
```

Length of underlap in number of needles:

```
> U:=-4;
```

The last needle at which an overlap was performed, i.e. the needle under which the thread vector will start:

```
> last_stitch_needle:=N-U;
```

Length of overlap, generally 1:

```
> OL:=1;
```

Alpha n, the angle between needles, i.e 360 divided by the number of needles in the cylinder, in radians:

```
> ALPN:=(360/60)*(evalf(Pi)/180);
```

```
> DDH:=.120;
```

```
> DDO:=.1;
```

```
> STEM:=.039;
```

```
> HHO:=.75;
```

```
> HLO:=.2;
```

Incremental variable for iterations

```
> delta:=.01;
```

Length of the needle stroke:

```
> L:=.837;
```

```

Distance between top and bottom of verge.
> S:=.565;
Height of the patterning rings (location)
> H:=.813;
Angle of cone taper
> beta:=15*evalf(Pi)/180;
Radius of the yarn
> yarn_rad:=.02;
Hook length:
> hook_length:= .1;
Width of needle at hook:
> hook_width:=.2;
Distance from the top of the cylinder to the top of the needle at its lowest
position::
> stitch_depth:=.118;
Maximum allowable Overlap/Underlap angle
MAXTH:=90*evalf(Pi)/180;
>

```

Procedure Threadvector

The program starts before performing a Underlap-Overlap cycle. N is the needle at which the underlap is performed (not where it starts) A positive underlap or overlap represents a clockwise direction.

```

> threadvector:= proc (THU,origin_needle) local
  A,B,lp1,lp2,l1_2; global RV, ALPN, S,U, RR, H;
  Define TU using two points on the thread: OJO!!!! needle es N-U para el
vector TU inicial

  >   A := vector(
    3, [RV*cos(ALPN*(origin_needle)),RV*sin(ALPN*(origin_needle)), -
    S] );
  >   B := vector(
    3, [RR*cos((ALPN*(origin_needle))+THU),RR*sin((ALPN*(origin_needle))+THU),H] );
  lp1 = end of vector A; last stitch
  >   point(lp1,A[1],A[2],A[3]);

  lp2= end of vector B; yarn at ring after underlap shog

```

```

> point (lp2,B[1],B[2],B[3]);
> line (l1_2,[lp1, lp2]);
>
> RETURN (l1_2);
> end;

```

Procedure planepN

```

> planepN:= proc (needle) local pp1,pp2,pp3,pN; global RV,
ALPN,RN,beta;
  Define the plane through needle 'needle' with thre points:

  pp1 = Origin:
  > point (pp1,0,0,0);

  pp2 = Bottom of verge
  > point (pp2,RV*cos(ALPN*needle),RV*sin(ALPN*needle),-S);

  pp3 = top of verge
  > point (pp3,RN*cos(ALPN*needle),RN*sin(ALPN*needle),0);
  > plane (pN,[pp1,pp2,pp3]);
  >

  Create a line to represent the back of the needle with two points
  >
  point (lp4,(RN-sin(beta))*cos(ALPN*needle),RN*sin(ALPN*needle),
cos(beta));
  > line (backN,[pp3, lp4]);
  >
  > RETURN (pN,backN);
  > end;

```

```

> There are two possible cases: the underlap and overlap have the same sign (ie are
moving in the same direction) or they have opposites signs.
> if (U*OL)>0 then

```

SAME DIRECTION

Find the minimum angle for which the yarn will get under the right needle or if it will never do.

Define the needle at which the overlap will be performed and create a 3d line at the back of the stem and a plane in which it moves


```

[ >   olneedle:= N+OL;
[ >   olplane:= planeN(olneedle);
[ >   oldist:= DDO+1;
[ >   THO:= 0;
[ >   intz:= 1;
[ >   INOUTH:= false;
[ >   INOUTD:= false;
[ >   testdistold:= false;
[ >   testhtold:= false;

```

The conditions to the while loop represent: while the intersection point is not in the appropriate area for the needle to intercept it on its way down and the intersection point has not gone in and out of either the height or the distance range increase the angle the ring is turning

```

>   while (not( ( (STEM<oldist) and (oldist<DDO) ) and (
  (HLO<intz) and (intz<HHO) ))) and (not(INOUTH)) and
  (not(INOUTD)) do
>     if (OL>0) then

```

If condition ensures that the angle overlap angle is increasing in the right direction.

```

>       THO:= THO + delta;
>       elif (OL<0) then
>         THO:=THO- delta;
>       fi;
>       THO:=THO;
>       olvector:= threadvector(THO,last_stitch_needle);
>       detail(olvector);

       intersection(olyrn,olvector,olplane[1]); form(olyrn);
coordinates(olyrn);
>       oldist:=distance(olyrn,olplane[2]);
>
>       intz:= zcoord(olyrn);

```

Check that the thread has not gone in and out of the height or the distance range

```

>       if testdistold then
>         INOUTD:= not (evalb (STEM<oldist) and
  (oldist<DDO));
>       fi;
>       if testhtold then
>         INOUTH:= not (evalb(HLO<intz) and

```

```

(intz<HHO));
>         fi;
>         testdistold:= evalb ((STEM<oldist) and
(oldist<DDO));
>         testthold:= evalb ((HLO<intz) and (intz<HHO));
>         INOUTD:=INOUTD;
>         INOUTH:=INOUTH;
>     od;

```

■ If neither of the in&out of range conditions ..

If the overlap is possible testdistold and testthold are true, INOUTD and INOUTH are false.

If the overlap is possible; ie if the while loop has not stopped because of one of the in&out of range conditions, then we need to find the angle that would have given us a successful underlap before this overlap.

```

>         if (not (INOUTH) and not(INOUTD)) then
>
>             ulneedle:= N;
>             ulplane := planeP(N(ulneedle);
>             Equation(ulplane[1],[a,b,c]);
>             Equation(ulplane[2],m);
>             THU:=THO;
>             ulolpndist:=oldist;
>             behind_ul_needle:=true;
>             DDH;
>             while ((ulolpndist <DDH) and (behind_ul_needle)) do
>                 evalb (ulolpndist<DDH);
>                 behind_ul_needle;
>                 ulolpndist;
>                 if (U>0) then

```

If condition ensures that the underlap angle is decreasing in the right direction.

```

>                 THU:= THU - delta;
>                 elif (OL<0) then
>                 THU:=THU+delta;
>             fi;
>
>             THU;
>             ulvector:=
threadvector(THU,last_stitch_needle);

```

```

> Equation(ulvector,m);

>
> olneedle:= N+OL;
> olplane:= planepN(olneedle);
> intersection (ulyrnlpn, ulvector,
olplane[1]);
> form (ulyrnlpn);
> coordinates(ulyrnlpn);
> ulolpndist:= distance(ulyrnlpn,
olplane[2]);
>
> Make sure the yarn is at the back of the needle
> with(geom3d):

> Find intersection between underlap vector and underlap needle
plane
>
> intersection(ulyrn,ulvector,ulplane[1]);
> coordinates(ulyrn);
> uldist:=distance(ulyrn,ulplane[2]);
>
> create a plane parallel to xy at the z value of the intersection
point (yrm[z])
>
> plane(pzulyrn,z=zcoord(ulyrn),[x,y,z]);
>
> Equation(pzulyrn,[x,y,z]);detail(pzulyrn);

> Find the intersection between that plane and the needle vector
>
> intersection(ulpnz,ulplane[2],pzulyrn);
> form(ulpnz);
> coordinates(ulpnz);

> make sure that the x value of the new intersection point is greater
(in absolute value) than that of the yarn
>
> behind_ul_needle:=evalb(abs(xcoord(ulpnz))>abs(xcoord(ulyrn)))

```

```

;
>         xcoord(ulpnz);
>         xcoord(ulyrn);
>     od;
>
>         THU;
>     if behind_ul_needle then
>
>         printf("underlap and overlap
possible!! THO=%.2f THU=%.2f",THO, THU);
>     else
>
>         printf("that underlap is not
possible in the same direction as the overlap. The u/l needle
can't clear the yarn");
>         fi;
>
>     elif INOUTH then
>
>         printf ("Overlap not posible in and out of Height
range");
>     else
>
>         print ("Overlap not possible; in and out of
distance range");
>         fi;
[ > elif (U*OL<=0) then

```

OPPOSITE DIRECTIONS

When the overlap and underlap are performed in opposite directions, then we need to 1) find the minimum angle to make the underlap, 2) determine the yarn vector that will wrap at the side of the needle -make sure the yarn will be under the hook for the overlap-, and 3) calculate the overlap angle required. (see separate flowchart for more detail)

The underlap must finish in a position such that the intersection of the u/l yarn vector with the u/l needle plane is at the back of the needle and sufficiently below the needle hook to ensure that when the o/l is performed, the yarn will

wrap around it without touching the hook.

Hence, the intersection should be 1) below an imaginary line (Underlap limit) from the ring thread hole just above the needle to the hook endpoint when the needle is in its highest position; and 2) behind the vector representing the back of the needle.

To define `max_inter_position` vector, two points are required; one on the ring and one on the needle hook point:

```

>
>         with (geom3d) :
>         ulneedle:=0;
>         ulplane := planePN (ulneedle);
>         Equation (ulplane [1], [x, y, z]);
>         Equation (ulplane [2], m);
>
>
>         Point in the ring
>         rpx:=RR*cos (ALPN*(ulneedle));
>         rpy:=RR*sin (ALPN*(ulneedle));
>         rpz:=H;
>
>         with (geom3d) :
>         point (ringpoint, rpx, rpy, rpz);
>
>
>         Point on the end of the needle hook
>         with (linalg) :
>         verge_bottom := vector ([RV*cos (ALPN*ulneedle) ,
RV*sin (ALPN*ulneedle) , -S]);
>         verge_top := vector ([RN*cos (ALPN*ulneedle) ,
RN*sin (ALPN*ulneedle) , 0]);
>         rconst:=(L-stitch_depth-hook_length);
>         nbx:= (-rconst*cos (beta)*cos (ALPN*ulneedle));
>         nby:= (rconst*cos (beta)*sin (ALPN*ulneedle));
>         needleparallel:= vector
([nbx,nby, (rconst*sin (beta))]);
>         needleperp:=
vector ([hook_width*cos (beta)*cos (ALPN*ulneedle), hook_width*cos
(beta)*sin (ALPN*ulneedle), hook_width*sin (beta)]);
>
hook_point_vector:=matadd (verge_top, (matadd (needleparallel, needleperp)));
>         point (hook_end_point,
hook_point_vector [1], hook_point_vector [2], hook_point_vector [3]
);

```

Underlap Limit Line

```

> line(underlap_limit, [hook_end_point, ringpoint]);
> with(geom3d):
> intersection(P, underlap_limit, ulplane[2]);
> form(P);
> coordinates(P);
[ >
> with(geometry):
> point(alt_axes_intersect, [xcoord(P), zcoord(P)]);
> point(alt_axes_ulneedle_verge_top, [RN, 0]);
> point(alt_axes_ulneedle_ring, [RR, H]);
>
line(backulneedle, [alt_axes_intersect, alt_axes_ulneedle_verge_
top]);
>
line(ullimit, [alt_axes_intersect, alt_axes_ulneedle_ring]);
> ec1:=Equation(backulneedle, [u, z]);
ec2:=Equation(ullimit, [u, z]);

```

Create a graph of the acceptable area for the Underlap Intersection Point.

(Acceptable area in red)

```

> with(plots): inequal( {
  lhs(Equation(backulneedle, [u, z])) < 0, lhs(Equation(ullimit, [u, z]
)) < 0 }, u=-3..3, z=-3..3, optionsfeasible=(color=red),
  optionsopen=(color=blue, thickness=2),
  optionsclosed=(color=green, thickness=3),
  optionsexcluded=(color=yellow));

```

```
[ > with(geom3d):
```

```
[ >
```

```
[ >
```

```
[ >
```

```
[ >
```

Note that the radius of the rings should never be defined as less than the radial coordinate of hook end point because otherwise the yarn will never wrap around the needle after an underlap.

```

> minRR= ((hook_point_vector[1])^2
+ (hook_point_vector[2])^2)^(0.5);

```

Initialising Parametes for the While loop:

The starting THU will be taken as that to place the thread exactly above the u/l needle, as an angle smaller than that will certainly not be an adequate u/l.

```

>         THU:=ulneedle;
Touch is the boolean variable used to exit the loop. It only becomes true when
the intersection meets both inequalities (ie is in the red zone inthe graph above)
>         touch:=false;
>         with (geom3d) :
>
>         while (not (touch)) and ((abs(THU))< MAXTH) do
>
>                                     If -then ensures that the
underlap angle is decreasing in the right direction.
>                                     if (U<0) then
>                                         THU:= THU - delta;
>                                     elif (OL>0) then
>                                         THU:=THU+delta;
>                                     fi;
>                                     THU;
>
>                                     Line ul_thread representes the
yarn
>
>         point (last_stitch, [RV*cos (ALPN*last_stitch_needle),
RV*sin (ALPN*last_stitch_needle), -S]);
>
>         point (ul_ring, [RR*cos (THU), RR*sin (THU), H] );
>
>         line (ul_thread, [last_stitch, ul_ring]);
>         detail (ul_thread);
>
>                                     Intersection between the yarn
and the needle plane:
>
>         intersection (ulyrn, ul_thread, ulplane [1] );
>
>         coordinates (ulyrn);
>
>
>
>
>
>
>         bool1:=eval ( lhs (ec1),
{u=xcoord (ulyrn), z=zcoord (ulyrn)} );
>         bool2:=eval ( lhs (ec2),
{u=xcoord (ulyrn), z=zcoord (ulyrn)} );
>

```

```

>         if ((bool1<0)and(bool2<0)) then
>
>             touch:=true;
>             fi;
>
>
>
>
>
>
>         KEY FOR GRAPHS: GREEN= Underlap Limit Line
>
>             MAGENTA= Back of the Needle
>
>             RED= YARN (Changes on each iteration)
>
>
>
>             touch;
>
>
>             with(plots):
>                 spacecurve({ [RV*cos(t) , RV*sin(t) ,
> -S,t=0..2*evalf(Pi),color=pink], [RN*cos(t) , RN*sin(t) ,
> 0,t=0..2*evalf(Pi),color=blue], [RR*cos(t) , RR*sin(t) ,
> H,t=0..2*evalf(Pi),color=cyan], [seq(Equation(underlap_limit,m)
> [i],i=1..3),m=-4..4,color=green], [seq(Equation(ul_thread,m) [i]
> ,i=1..3),m=-4..4,color=red] ,
> [seq(Equation(ulplane[2],m) [i],i=1..3),m=-4..4,color=magenta] }
>
> ,
> axes=FRAME,scaling=UNCONSTRAINED,orientation=[-90,90],style=POI
> INT,symbol=DIAMOND,numpoints=60,labels=[x,y,z]);
>                 spacecurve({ [RV*cos(t) , RV*sin(t) ,
> -S,t=0..2*evalf(Pi),color=pink], [RN*cos(t) , RN*sin(t) ,
> 0,t=0..2*evalf(Pi),color=blue], [RR*cos(t) , RR*sin(t) ,
> H,t=0..2*evalf(Pi),color=cyan], [seq(Equation(underlap_limit,m)
> [i],i=1..3),m=-4..4,color=green], [seq(Equation(ul_thread,m) [i]
> ,i=1..3),m=-4..4,color=red] ,
> [seq(Equation(ulplane[2],m) [i],i=1..3),m=-4..4,color=magenta] }
>
> ,
> axes=FRAME,scaling=UNCONSTRAINED,orientation=[-90,0],style=POI
> NT,symbol=DIAMOND,numpoints=60,labels=[x,y,z]);
>                 spacecurve({ [RV*cos(t) , RV*sin(t) ,
> -S,t=0..2*evalf(Pi),color=pink], [RN*cos(t) , RN*sin(t) ,
> 0,t=0..2*evalf(Pi),color=blue], [RR*cos(t) , RR*sin(t) ,
> H,t=0..2*evalf(Pi),color=cyan], [seq(Equation(underlap_limit,m)
> [i],i=1..3),m=-4..4,color=green], [seq(Equation(ul_thread,m) [i]
> ,i=1..3),m=-4..4,color=red] ,
> [seq(Equation(ulplane[2],m) [i],i=1..3),m=-4..4,color=magenta] }
>
> ,

```



```
axes=FRAME,scaling=UNCONSTRAINED,orientation=[180,90],style=POINT,
symbol=DIAMOND,numpoints=60,labels=[x,y,z]);
>
> od;
>
>
>
[ >
[ > fi;
```

